ANALYSIS OF THE MOLECULAR MECHANISM AND PHYSIOLOGICAL ROLE OF GOLGI STACK FORMATION AND GOLGI BIOGENESIS

by

Yi Xiang

A dissertation submitted in partial fulfillment
of the requirements for the degree of
Doctor of Philosophy
(Molecular Cellular and Developmental Biology)
in the University of Michigan
2011

Doctoral Committee:

Assistant Professor Yanzhuang Wang, Chair
Professor Cunming Duan
Professor Robert S. Fuller
Professor Daniel J. Klionsky
Associate Professor Ursula H. Jakob

Dedication

This dissertation is dedicated to my parents, husband and baby-to-be, for their unconditional love and support, as well as the joy they brought to my life.

Acknowledgements

First, I would like to express my deepest gratitude to my thesis advisor, Dr. Yanzhuang Wang, for his invaluable guidance and training. I have learned a lot from his expertise and persistence in research. I have been and will always be inspired by his passion toward science. I would also like to thank my thesis committee members, Dr. Cunming Duan, Dr. Robert S. Fuller, Dr. Ursula H. Jakob and Dr. Danial J. Klionsky, for their perceptive support and insightful suggestion to my research.

It has been a wonderful time to work together with all the former and current members of the Wang lab. This thesis would not have been possible without their collaboration and support. I would like to thank them for scientific discussion, reagent sharing, and generous assistance during my research, especially Dr. Xiaoyan Zhang, to carry out those experiments for me when I could not make it. Special thanks give to Danming Tang, Youjian Chi, for being passionate colleague and good friends, and sharing pleasures and joys with me.

I began my graduate study with the rotation work with Dr. Anju Kumar, and I really appreciate his guidance and the wonderful time I spent in his lab. It's a pleasure to thank all the faculty and staff members in the Department of MCDB, especially Dr. Laura Olsen, Ms. Mary Carr, for their generous help and support that make my journey much easier. I also want to thank my undergraduate thesis advisor, Dr. Duanqing Pei, at

Tsinghua University, China, for his passionate guidance to science, patient instruction, encouragement to my research and support to my graduate study.

I owe my deepest gratitude to my husband Jiefei Geng, my parents and parents-in-law, for their everlasting love and support. I could never express my gratefulness to them.

Chapter II is reprinted from the *Journal of Cell Biology*, 2010, Volume 188, Yi Xiang, and Yanzhuang Wang. **GRASP55 and GRASP 65 play complementary and essential roles in Golgi cisternal stacking,** page 237-251, Copyright (2010), with minor modifications. Yi Xiang and Dr. Yanzhuang Wang designed the experiments and wrote the paper. Dr. Yanzhuang Wang performed experiments in Fig. 2.S3A, 2.S3E and 2.4B, Yi Xiang contributed to the rest data.

Chapter III is manuscript in preparation by authors: Yi Xiang, Xiaoyan Zhang and Yanzhuang Wang, entitled as **Golgi cisternal stacking acts as a quality control mechanism for cargo sorting and modification.** Yi Xiang and Dr. Yanzhuang Wang designed the experiments, Yi Xiang and Dr. Xiaoyan Zhang together performed experiments in Fig. 3.6 and 3.7B, Yi Xiang contributed to the rest experiments and wrote the paper.

Chapter IV is reprinted from the *Journal of Biological Chemistry*, Volume 282, Yi Xiang, Joachim Seemann, Blaine Bisel, Sukanya Punthambaker and Yanzhuang Wang: **Active ADP-ribosylation factor-1 (ARF1) is required for mitotic Golgi fragmentation,** page 21829-21837, Copyright (2007), with minor modifications. Dr. Yanzhuang Wang designed the research and performed experiments in Fig. 4.1, 4.2, 4.3,

4.4A-F. Dr. Joachim Seemann and Dr. Blaine Bisel contributed to Fig. 4.6. Sukanya Punthambaker performed experiments in Fig. 4.S1. Yi Xiang contributed to the rest data.

Chapter V is a manuscript prepared for *Nature Cell Biology*, Danming Tang*, Yi Xiang*, Stefano De Renzis, Jochen Rink, Gen Zheng, Honghao Zhang, Marino Zerial, and Yanzhuang Wang: **The ubiquitin ligase HACE1 is involved in regulating Golgi membrane dynamics during the cell cycle**. Dr. Yanzhuang Wang designed the research. Yi Xiang performed the experiments in Fig. 5.1F, 5.3, 5.6C, 5.S5. Danming Tang performed the experiments in Fig. 5.6 except 5.6C. Dr. Stefano De Renzis performed the experiments in Fig. 5.1A and 5.1B. Dr. Gen Zheng performed the experiments in Fig. 5.1D, 5.1E, 5.2, 5.4. Dr. Yanzhuang Wang contributed to the rest data and wrote the paper. (* Equal contribution)

Table of Contents

Dedication…...……ii

Acknowledgements…….……..……iii

List of Figures…….....…..vii

Chapter

I. Introduction……..……1

II. GRASP55 and GRASP65 play complementary and essential roles in Golgi cisternal stacking……....43

III. Golgi cisternal stacking acts as a quality control mechanism for cargo sorting and modification…….……..…..85

IV. Active ADP-ribosylation factor-1 (ARF1) is required for mitotic Golgi fragmentation……...118

V. The ubiquitin ligase HACE1 is involved in regulating Golgi membrane dynamics during the cell cycle…….149

VI. Conclusion……...…188

References……200

List of Figures

Figure:

1.1 The electron microscopic images of the mammalian Golgi apparatus 4

1.2 The Golgi apparatus in animals, plants and budding yeasts 5

1.3 The ARF1 GTPase cycle 8

1.4 The vesicle transport model and the cisternal maturation model 11

1.5 The progenitor model of *intra*-Golgi transport 13

1.6 The post-Golgi transport 16

1.7 Golgi disassembly/ reassembly during the cell cycle in mammalian cells 18

1.8 Two models explaining the Golgi fragmentation during mitosis 20

1.9 Illustration of the Golgi disassembly and reassembly process 23

1.10 Comparison of the *rattus norvegicus* GRASP65 and GRASP55 sequences 27

1.11 GRASP65 and GRASP55 structures 30

1.12 Biosynthesis of N-linked glycans 37

2.1 Knockdown of GRASP55 reduces the number of cisternae per stack.....47

2.S1 Depletion of GRASP55 and GRASP65 over time 48

2.2 Effect of GRASP55-depletion on Golgi ribbon linking 51

2.3 Depletion of both GRASP55 and GRASP65 leads to disassembly of the entire Golgi stack 53

2.4 GRASP55 is phosphorylated during mitosis 56

2.S3 GRASP55 phosphorylation, dephosphorylation and oligomerization.....57

2.5 Cell cycle regulated GRASP55 oligomerization is sufficient to link adjacent surfaces 61

2.6 Mapping the domain structure of GRASP55 for oligomerization and mitotic regulation 63

2.7 Over expression of non-regulatable GRASP55 mutants enhances Golgi stack formation in interphase cells.....65

2.S2 Histogram presentation of the number of cisternae per stack in cells with indicated treatments 66

2.S4 Confocal images of HeLa cells expressing GFP-tagged GRASP55 or GRASP65, or/and transfected with indicated siRNA 68

2.S5 Rescue of the Golgi structure in GRASP55-depleted cells by expression of GRASP55 and its mutants 69

2.8 Rescue of Golgi structure by expression of exogenous GRASP55 and GRASP65 in cells with both GRASPs depleted.....70

2.9 Expression of non-phosphorylatable GRASP55 mutants inhibits mitotic Golgi disassembly.....72

3.1 GRASP-depletion accelerates VSV-G trafficking and impairs cathepsin D sorting 91

3.2 Depletion of GRASP results in altered glycosylation pattern on the cell surface 94

3.S1 Golgi unstacking impacts glycosylation of cell surface proteins 95

3.S2 GRASP-depletion does not affect the localization of Golgi enzymes.....95

3.S3 GRASP-depletion does not affect the Golgi localization of the endogenous Galactosyltransferase (GalT) 96

3.3 GRASP-depletion reduces cell attachment.....97

3.4 GRASP-depletion reduces cell migration.....98

3.S4 Depletion of GRASPs does not cause apoptosis 100

3.S5 Depletion of GRASPs does not cause ER stress 100

3.5 Depletion of GRASP65 or both GRASPs causes a reduction of α5 and β1 integrins.....102

3.S6 Glycosidase treatment of α5/β1 integrins 102

3.6 Golgi unstacking reduces α5/β1 integrin synthesis but accelerates their trafficking 104

3.S7 Depletion of GRASPs enhances cell proliferation and total protein synthesis 105

3.7 Depletion of GRASPs enhances cell proliferation and total protein synthesis.....106

4.1 *In vitro* Golgi fragmentation using purified coatomer and ARF1 124

4.2 Association of activated ARF1 with membranes after the budding assay.....126

4.3 ARF1 binds to COPI vesicles 128

4.S1 Purification of myristoylated ARF1 WT and mutant proteins 129

4.4 Fragmentation of Golgi membranes by mitotic cytosol treatment is ARF1-dependent 132

4.5 ARF1 is associated with membranes during mitosis 135

4.S2 ARF1 is associated with membranes in mitotic NRK cells collected by shake-off 135

4.S3 ARF1 is associated with COPI vesicles during mitosis.....136

4.6 Microinjection of ARF1(Q71L) does not block Golgi fragmentation and progression through mitosis.....138

5.1 HACE1 binds to Golgi-associated Rab proteins.....155

5.2 HACE1 is concentrated on the Golgi apparatus 157

5.S1 HACE1 co-localizes with cis-Golgi markers 158

5.S2 HACE1 is a ubiquitin ligase bound to Golgi membranes.....159

5.3 Expression of an inactive Rab1 mutant leads to HACE1 dissociation from the Golgi membranes and Golgi fragmentation.....160

5.4 Expression of HACE1 mutants leads to Golgi fragmentation 162

5.S3 HACE1 is not directly involved in post-mitotic Golgi membrane assembly 165

5.5 HACE1 ubiquitin ligase activity in mitotic Golgi disassembly is required for

p97/p47-mediated post-mitotic Golgi membrane reassembly *in vitro* 166

5.6 Depletion of HACE1 leads to Golgi fragmentation.....169

5.S4 HACE1 protein has a long half-life in the cell 170

5.S5 The Golgi apparatus is fragmented in SK-NEP-1 cells, which have reduced HACE1 expression.....172

5.7 Syntaxin 5 is a target of the ubiquitin ligase HACE1 on the Golgi membrane 174

6.1 GRASP65 and GRASP55 form mitotic regulated oligomers to link adjacent Golgi cisternae together 191

6.2 Golgi cisternal stacking regulates cargo flow through the Golgi 194

Chapter I. Introduction

The Golgi apparatus was discovered by Camillo Golgi, who observed a "basket-like network surrounding the nucleus in Purkinje cells" [1]. The existence of this organelle was confirmed by electron microscopy in 1951 [1]. Afterwards, numerous discoveries have been made about the morphology and function of this organelle, and it is now considered as the central conduit in the secretory pathway [2]. The Golgi apparatus is the biosynthetic station where protein and lipid glycosylation, as well as the assembly of triglyceride with apolipoproteins occur [2, 3]. After posttranslational modification, secretory proteins and lipids are sorted to their ultimate destinations by the *trans*-Golgi network (TGN) [4]. Occupying the central position, the Golgi is also the hub where membrane components from different organelles could be exchanged, thereby provides a crosstalk between exocytosis and endocytosis [3, 5]. It is also involved in various other cellular processes such as apoptosis [6], cell cycle control, cytoskeleton organization [7], etc. In most eukaryotic cells, the Golgi apparatus is comprised of flattened cisternae that are closely arranged together in parallel to form stacks [8], although in *S.cerevisiae* and some protists, the Golgi is comprised of isolated cisternae and tubular networks [3, 9]. In mammalian cells, tens and hundreds of Golgi stacks are laterally linked to form a ribbon-like structure adjacent to the nuclei [2]. The relevance of the unique morphology to its functions is unclear. In addition, the Golgi is a highly dynamic organelle that is able to undergo rapid and reversible reorganization during the cell cycle [2].

Golgi architecture

Golgi stacking

In *S.cerevisiae* and some protists, the Golgi is comprised of discrete cisternae and tubular networks [3, 9]. In most eukaryotic cells, including plants and animals, the Golgi apparatus is composed of a series of flattened cisternae that are closely apposed and aligned in parallel to form a stack [8], which is surrounded by transport vesicles (Fig. 1.1). Cryo-electron microscopic analysis of normal rat kidney cells reveals that all Golgi cisternae within the cells have similar surface area, so are the length of all the cisternae within a stack [3, 8]. Cargo flows through the Golgi could only temporally change the length of cisternae, which rapidly restores to the original size [3, 10]. The lumen of a Golgi cisterna is about 10-20 nm [8]. A canonical Golgi stack is composed of three main compartments: the *cis*-, *medial*- and *trans*-Golgi cisternae, with extensive tubulovesicular networks on each side: the *cis*-Golgi network (CGN) and *trans*-Golgi network (TGN) [2]. The CGN receives biosynthetic cargo from the ER, whereas the TGN sorts post-translationally modified cargo to their final destinations [2]. Vesicles budded from the *cis*- and *medial*- cisternae are COPI coated, whereas vesicles budded from the TGN are exclusively clathrin-coated [3, 8]. Golgi cisternal stacking is a remarkably conserved characteristics within the eukaryotic kingdom, even one of the earliest eukaryotes, the diplomonad *Giardia lamblia* contains stacked Golgi cisternae [11], indicating that the Golgi apparatus arose early in the eukaryotic evolution.

The Golgi is a polarized organelle [3]. The cisternal fenestration decreases towards the *medial* cisternae, while the cisternal thickness decreases from *cis*- to *trans*-side [8]. The glycosylation enzymes are distributed in the stack in accordance with the sequence

they are involved in the glycosylation of cargo proteins [12]. From the *cis*- to the *trans*-side of a Golgi stack, the thickness of lipid bilayer and the concentration of cholesterol increase [13, 14], while the pH within the lumen decreases [3].

The mechanism underling the formation of Golgi stacks has been studied in mammalian cells. Two homologous proteins, the Golgi Reassembly Stacking Protein of 65 kDa (GRASP65) and GRASP55 have been identified as the Golgi stacking factors [15, 16]. Both proteins have been shown to mediate the stacking of Golgi cisternae *in vitro* and *in vivo*, by forming mitotic regulated oligomers that link adjacent cisternae together [15-18]. In addition, the antiparallel dimerization of cytosolic domains of sugar transporters might also participate in Golgi cisternal stacking [3, 19]. However, how the Golgi cisternal stacking regulates its biological functions is unclear.

Golgi ribbon

In plants and lower animal cells, the Golgi apparatus exists as discrete stacks that are dispersed throughout the cytoplasm and localize adjacent to the ER exist sites (Fig. 1.2D) [20]. In mammalian cells, the Golgi stacks are laterally linked by tubular continuities to form a pericentriolar ribbon (Fig. 1.2A) [2]. The formation and localization of the Golgi ribbon at the pericentriolar area depend on multiple players, including Golgi matrix proteins, microtubule and actin cytoskeletons, etc.[7]. Tens of Golgi matrix proteins are involved in the formation of Golgi ribbon. For example, depletion of GM130 [21], or GRASP65/55 [22, 23] leads to disconnected Golgi ribbon in the pericentriolar region, whereas depletion of Golgin-84 [24], Golgin-160 [25], or p115 [26] leads to dispersed ministacks in the cytoplasm. Microtubules play a dual role in the organization of the

pericentriolar Golgi ribbon. First, Golgi stacks are transported to the pericentriolar region along microtubules emanated from centrosomes via minus end-directed motor complex dynein; second, a subset of microtubules that is emanated from the Golgi facilitates the lateral linking of Golgi stacks into a connected ribbon [7]. Actin filaments are also detected at the Golgi complex and are required for the localization of Golgi via actin-based motor proteins [7]. Disruption of cytoskeletons causes Golgi fragmentation (Fig. 1.2B). The Golgi ribbon is oriented towards the cell surface where exocytosis occurs, such as the leading edges of migrating cells [27]. The precise function of the Golgi ribbon is unclear. Several studies reported that the basic functions of the Golgi apparatus, such as membrane trafficking and modification of secretory proteins, are unaffected when the Golgi is fragmented into separate ministacks [24, 25]. Recently, it has been suggested that the Golgi ribbon facilitates lateral diffusion of Golgi enzymes and glycosylation of cargo proteins [22], controls cell polarity [7], functions as a cell cycle check point [28, 29], or is involved in apoptosis [6] or parasite proliferation [30].

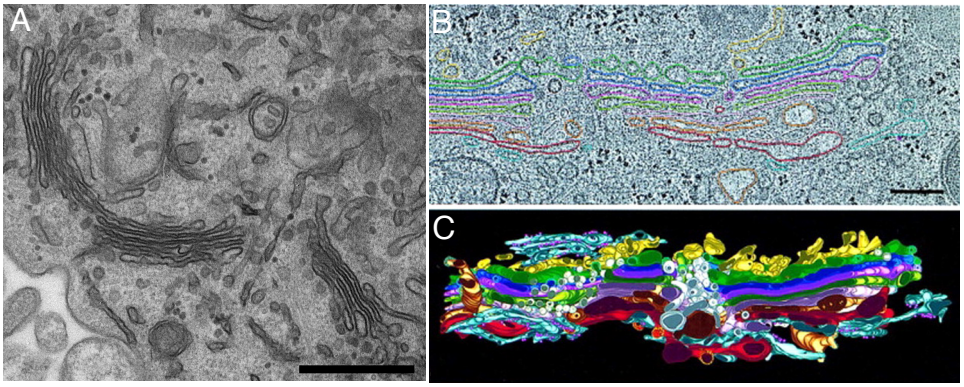

Figure 1.1. The electron microscopic images of the mammalian Golgi apparatus. (A) A Golgi ribbon in HeLa cells is composed of several stacks. Scale bar, 500 nm. **(B)** A Part of the Golgi from a fast frozen, freeze-substitution fixed NRK cell. **(C)** Tomographic reconstruction of the Golgi ribbon. The colors used to represent different components in (B) and (C): ER, blue-gray; ribosomes, small purple spheres; ERGIC, yellow; Golgi cisterna: C1, green; C2, purple; C3, rose; C4, olive; C5, pink; C6, bronze; C7, red. Polymorphic structures in the non-compact region are light pink and gold. Non-clathrin-coated budding profiles on cisternae C1–C6, blue stippling. Clathrin-coated buds on C7, yellow stippling. Bars, 250 nm. (B) and (C) are adopted from [8].

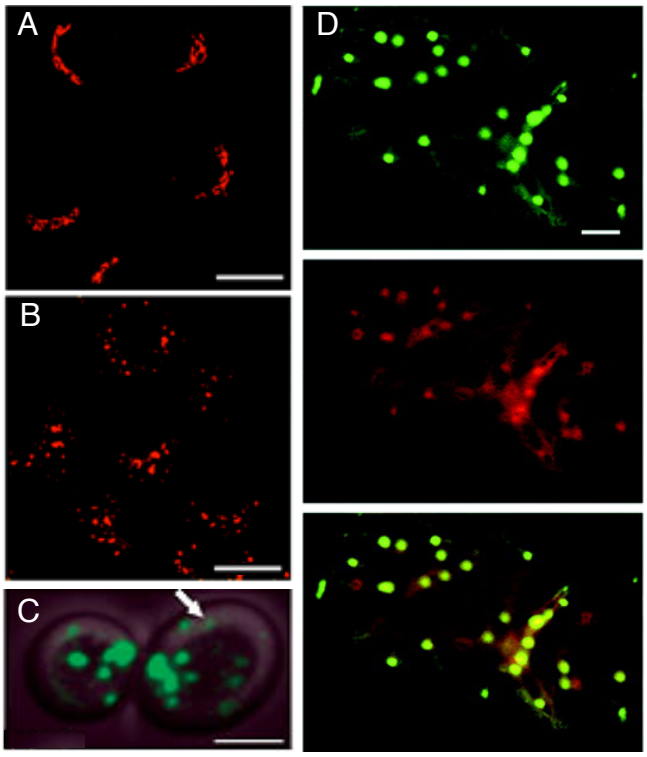

Figure 1.2. The Golgi apparatus in animals, plants and budding yeasts. (A) In animal cells, the Golgi stacks are laterally linked to form a ribbon like structure that localized adjacent to the nucleus. Image shown is the NRK cells immunostained for the Golgi enzyme Mannosidase II. Scale bar, 10 μm. Image is modified from [31] **(B)** The formation of Golgi ribbon depends on microtubules, the disassembly of microtubule network causes the fragmentation of the Golgi ribbon. Image shown is NRK cells treated with nocodazole to disrupt the microtubule network. Scale bar, 10 μm. Image is modified from [31] **(C)** In *S. cerevisiae*, the Golgi does not form stacks, but exists as single cisternae and are dispersed throughout the cell. Image shown are the *S.cerevisiae* cells expressing the Sec7-GFP, arrow indicates a single cisternae. Scale bar, 2 μm. Image is modified from [32]. **(D)** In plant cells, the Golgi stacks are dispersed in the cytoplasm and localized adjacent to ER exit sites. Images shown are tobacco leaf epidermal cells. Upper panel: Golgi marker ERD2-GFP; middle panel: Sar1-YFP; lower panel: colocalization. Note the Golgi and ER exit sites colocalize. Scale bar, 5 μm. Images are modified from [33].

The Golgi apparatus as the crossroad in the secretory pathway

ER-to-Golgi and Golgi-to-ER transport

Biosynthetic cargo proteins are transported from the endoplasmic reticulum (ER) to the Golgi apparatus after they are properly folded. The vesicular coat complex COPII mediates the anterograde ER-to-Golgi transport, while retrograde transport from the Golgi to the ER is mediated by vesicular coat complex COPI [3].

The first step of the ER-to-Golgi transport is the generation of COPII vesicles, which mediates the exit of cargo proteins from the ER [3]. Components of COPII vesicles are involved in the selection and concentration of cargo proteins at the ER and the membrane deformation that generates COPII coated vesicles whose diameters are 60-80nm [34]. In *S. cerevisiae*, COPII vesicles can bud across the entire surface of ER, while in *P. pastoris* and metazoan, COPII vesicles can only bud from distinct ribosome free domains, termed as transitional ER (tER), or ER exit sites (ERES) [35].

In *P. pastoris* and plant cells, the Golgi stacks localize adjacent to the ERES [33], therefore, COPII vesicles can fuse with *cis*-Golgi cisternae [3]. However, in mammalian cells, the Golgi apparatus localizes in the pericentriolar region, which is not necessarily adjacent to ERES [3]. Uncoating of COPII vesicles occurs adjacent to the ERES, which is followed by homotypical fusion to form vesicular tubular clusters (VTCs), or fusion with existing carriers, or membrane structures such as the ER-Golgi-intermediate-compartment (ERGIC) [3, 36]. Those VTCs are transported along microtubules via motor protein dynein to the Golgi apparatus [3]. Docking of VTCs with the *cis*-Golgi depends on p115 and GM130, and the following fusion event involves the SNARE syntaxin 5 [37-39].

The Golgi-to-ER retrograde transport is mainly mediated by COPI vesicles [3]. Cargos transported from the Golgi to the ER include chaperones bearing a KDEL motif that could be recognized by the KDEL receptors [40]. Some other transmembrane proteins, such as the p24 family, bearing the di-lysine signal on the cytoplasmic tail, are also retrieved via COPI vesicles [41].

COPII and COPI vesicles

COPII vesicles mediate the transport from the ER to the Golgi apparatus [3]. COPII vesicles consist of Sar1, Sec23/Sec24, Sec13/Sec31 subunits [42]. The assembly of COPII vesicles is well characterized in *S. cerevisiae* [42]. The ER-integral membrane protein Sec 12 is the guanine nucleotide exchange factor (GEF) for the small GTPase Sar1, and it catalyzes the exchange of GTP for GDP on Sar1 [43]. When it is in the GTP-bound form, the hydrophobic N-terminus of Sar1 extends outward and anchors the protein onto the ER membranes [44]. The membrane-bound Sar1-GTP then recruits the heterodimeric Sec23/Sec24 coat protein complex [44]. Membrane cargo proteins bearing specific sorting sequences in their cytosolic domains that bind to the Sec23/24 complex are recruited and enriched into the budding vesicles [42]. Luminal soluble cargos are recruited to the vesicle by binding to specific receptors [42]. A second heterodimeric coat Sec13/Sec31 complex are recruited to the budding vesicle to form the outer layer and promote membrane deformation [45] . After the budding of the vesicle, the Sec23 coat subunit catalyzes GTP hydrolysis of Sar1, which leads to the disassembly of the coat, so that the uncoated COPII vesicles can fuse with target membranes [34].

The formation of COPI vesicles is initiated by small GTPase ADP-ribosylation factor 1 (ARF1), which recruits coatomer composed of α, β, β', γ, δ, ε, ζ subunits for the assembly of COPI vesicles [46]. ARF1 is myristoylated at its amino terminus, which is critical for its membrane association [47]. Like all small GTPases, guanine nucleotide exchange factors (GEFs) are needed to catalyze the activation of ARF1, while GTPase-activating proteins (GAPs) catalyze its deactivation (Fig. 1.3) [46]. When it is in the GTP-bound or active form, ARF1 binds to the membranes; when the GTP is hydrolyzed to GDP, ARF1 disassociates from the membranes [48]. Two mutant form of ARF1 have been widely used. The Q71L mutant has low GTPase activity and is constitutively active; the T31N mutant preferentially binds GDP and remains inactive [49]. Brefeldin A (BFA) is a chemical that binds to ARF1 GEF, and causes the inactivation of ARF1 GTPase and dissociation of coatomers from the Golgi membranes; the Q71L mutant is insensitive to BFA treatment [49]. The Golgi apparatus quickly merges into the ER via tubular structures when cells are treated with BFA [50].

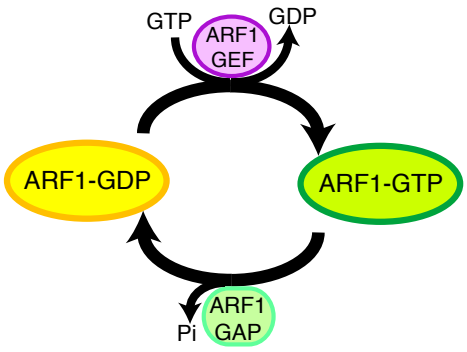

Figure 1.3. The ARF1 GTPase cycle. The GTP-bound ARF1 GTPases is active and associated with the membranes. The intrinsic GTPase activity of the molecule hydrolyzes GTP to GDP, and GDP-bound form is inactive and dissociates from the membranes. GTPase activating proteins (GAPs) enhance GTPase activity and favor the inactive, GDP-bound state. GTP exchange factors (GEFs) catalyze the exchange of GDP with GTP and thus favors the active, GTP-bound state.

Intra-Golgi cargo transport

A long existing debate about the Golgi apparatus is how cargo is transported within the Golgi apparatus. There are four models: (1) the vesicle transport model, (2) the cisternal maturation model [51], (3) the rapid partitioning model [52], and (4) the cisternal progenitor model [53].

The vesicle transport model (Fig.1.4A) proposed that Golgi enzymes are retained in the cisternae while cargo proteins are transported from *cis* to *trans* Golgi via anterograde COPI vesicles [51]. The polarized distribution of Golgi enzymes can be easily explained with this model [51]. It is also conceivable that the Golgi is surrounded by abundant COPI vesicles, since COPI vesicles mediate the transport of cargo proteins [8]. However, the vesicle transport model encountered difficulties in explaining some phenomena. Some of the cargos traversing the Golgi are too large to fit into COPI vesicles (diameter = 60-80 nm), for example, scales in algae and procollagen in mammalian cells [51, 54, 55]. In addition, although the role of COPI vesicles in retrograde transport has been established, evidence for COPI-dependent anterograde transport is lacking [51].

In the scenario of the cisternal maturation model (Fig. 1.4B), new cisternae form at the *cis* side of the stack, cargos are retained in the cisternae while the Golgi resident proteins are recycled from older to younger cisternae via retrograde COPI vesicles, thereby driving the maturation of the cisternae [51]. This model is supported by the morphological observation that cisternae form at the *cis* side and peel off at the *trans* side of the stacks [56], and it has many advantages and is reconciled with most experimental data. First of all, the transport of large cargos can be easily explained. It explains why Golgi resident proteins can be found in multiple adjacent cisternae [51]. The observation

that different cargos, like procollagen and smaller transmembrane protein VSV-G, travel through the Golgi at the same rate supports the cisternal maturation model [57]. Another piece of strong evidence came from two recent independent high resolution live cell video microscopic data showing that one Golgi cisterna was converted to another without change of localization in *S. cerevisiae* [32, 58].

The key issue regarding the two models above is the content of COPI vesicles [51]. Several groups have reported that glycosylation enzymes are concentrated in COPI vesicles [59, 60], while other groups reported conflicting results that COPI vesicles contain cargo proteins like proinsulin and VSV-G, while glycosylation enzymes are depleted from COPI vesicles [61-63]. Different subsets of COPI vesicles have been reported, and it is possible that two or more classes of COPI vesicles may exist to mediate retrograde and anterograde transport, respectively [64, 65]. For example, the GM130-p115-giantin tether binds COPI vesicles that contain the p24 cargo receptor family protein and anterograde cargos, while the CASP-golgin-84 complex binds retrograde transport vesicles containing Golgi enzymes, suggesting the existence of different subpopulations of COPI vesicles [65]. New approaches are needed to address those controversies.

In addition to COPI-mediated transport, tubular connections between different cisternae may provide an alternative mean of transport between Golgi cisternae [10, 66]. It is reported that cargo flow through the Golgi stimulates the formation of intercisternal connections among different Golgi compartments; when cargos exit the Golgi, these connections disappear [10]. However, whether it is the cargo or Golgi resident proteins that are transported through these tubular continuities is unknown.

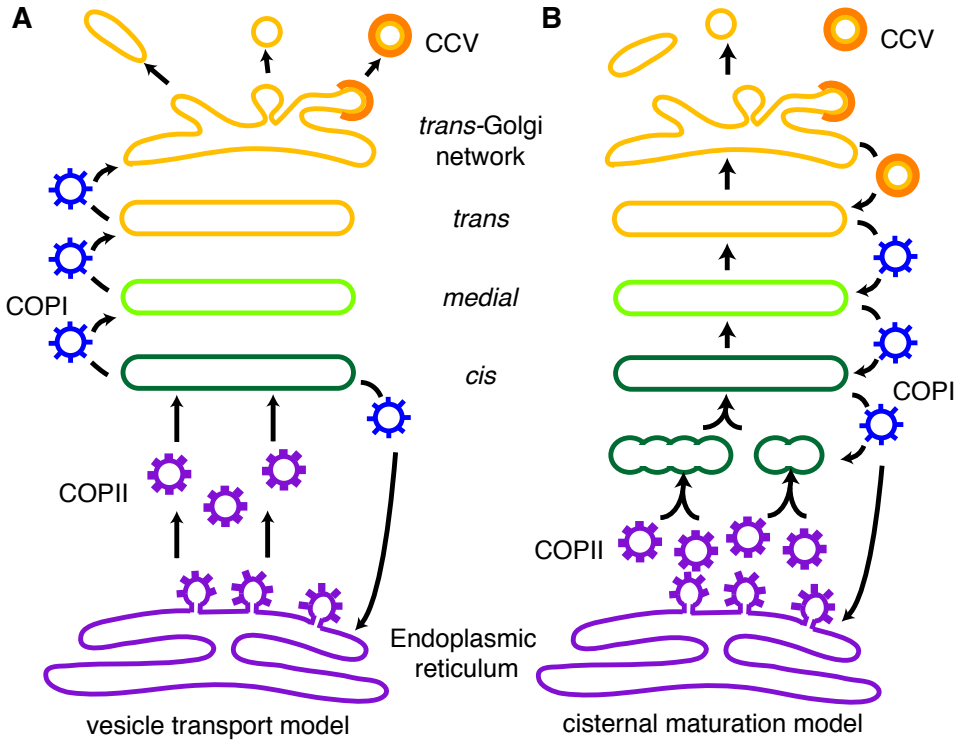

Figure 1.4. The vesicle transport model and the cisternal maturation model [51]. (A) The vesicle transport model. Golgi resident proteins are retained in individual Golgi compartments, whereas cargo proteins are transported from the endoplasmic reticulum (ER) to the Golgi via COPII vesicles. After fusing with the *cis*-Golgi cisternae, the *intra*-Golgi transport is mediated via anterograde COPI vesicles in the *cis*-to-*trans* direction. Finally, cargo proteins exit the TGN in clathrin-coated vesicles (CCV) or secretory carriers. **(B)** The cisternal maturation model. New Golgi cisterna is formed by the fusion of COPII vesicles that carry cargos from the ER, maturates in the *cis*-to-*trans* direction and then breaks down into transport carriers at the TGN. Maturation of the cisternae is driven by retrograde COPI vesicles or CCV vesicles (at TGN) carrying Golgi resident proteins from older cisternae to younger cisternae.

The third model is the rapid partitioning model proposed by Jennifer Lippincott-Schwartz [52]. This model regards the Golgi as a "two-phase membrane system" where cargo proteins are rapidly partitioned into the "processing domains" and "export domains". This model is based on the microscopic result showing that cargo proteins exit the Golgi with exponential kinetics, and they are quickly distributed into different Golgi cisternae upon arrival, but are not enriched in certain cisterna at anytime [52]. However, these experimental data are inconsistent with previous reports that VSV-G is enriched in

given cisternae that maturate along the *cis*-to-*trans* axis, and colocalizes with different Golgi markers at different time points after the temperature release [57].

Recently, Suzanne Pfeffer proposed a fourth model for the *intra*-Golgi transport termed as the cisternal progenitor model [53]. This model is based on two premises. The first premise is that the Golgi "undergoes continual, lateral fission and fusion" [53], which has been widely observed. The second premise is based on the Rab cascade theory that upstream Rab GTPase recruits the guanine nucleotide exchange factor (GEF) for the downstream Rab, therefore recruits and activates the downstream Rab, whereas the downstream Rab recruits the GTPase accelerating protein (GAP) for the upstream Rab and inactivate it [67, 68]. Combining the two premises, Pfeffer proposed that the *cis-, meidal-* and *trans*-Golgi cisternae contain RabA, RabB, and RabC, respectively. Golgi stacking proteins hold the cisternae together. RabA recruits the GEF for RabB, and a RabB subdomain is formed and can be separated from the RabA cisterna by fission (Fig. 1.5A). The RabB subdomain then fuses with the stable RabB cisterna via homotypical fusion, which can transport cargos to the RabB cisternae (Fig. 1.5B). Cargos can also be transported via vesicles from RabA compartment to RabB compartment followed by heterotypic fusion. RabB then recruits the GAP for RabA and displaces RabA from the RabB dominant cisternae (Fig. 1.5C). Golgi resident proteins such as glycosyltransferases are retained in a given compartment probably by interacting with specific Rab effectors [53]. This model accommodates the observation mentioned above that cargo proteins exit the Golgi in an exponential manner [52], which does not fit into the cisternal maturation model. More evidences are needed to support this new model. For example, how the Golgi resident and cargo proteins are segregated into different domains of the cisternae is

unknown. It would be essential to identify the Rabs, GEFs, GAPs, as well as Rab effectors that act within the Golgi apparatus to provide the identity, directionality and polarity of the Golgi.

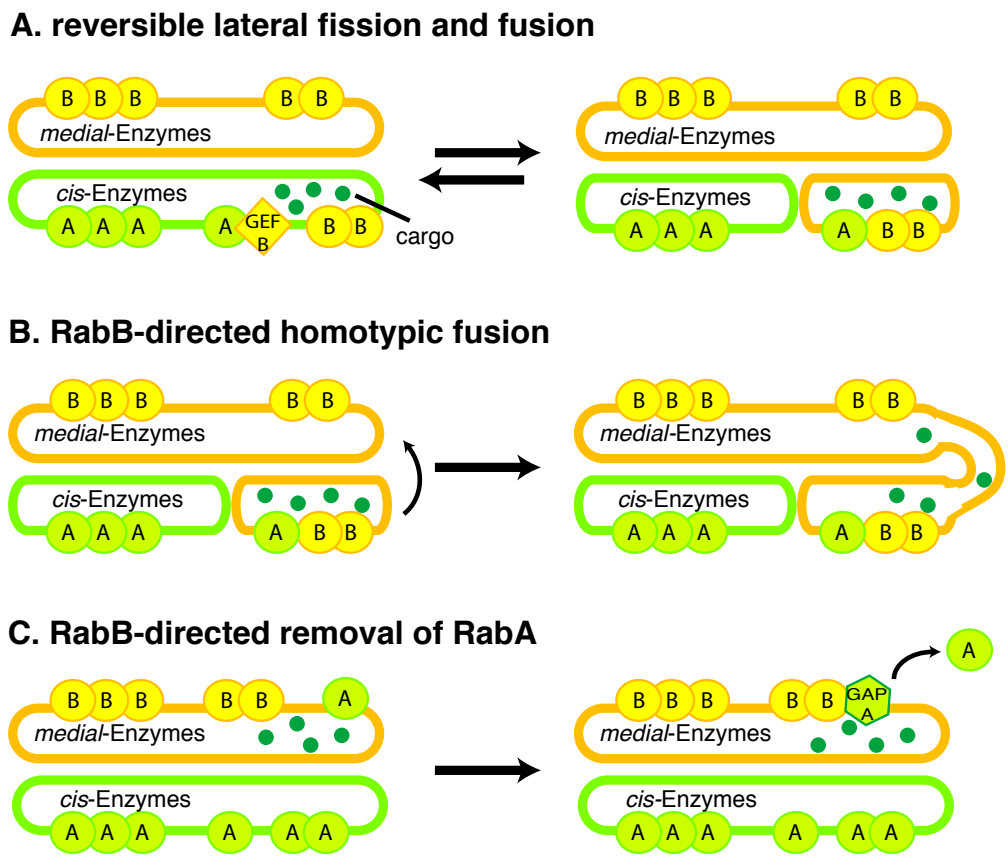

Figure 1.5. The progenitor model of *intra*-Golgi transport [53]. (A) Different Golgi cisternae in a stack are marked with different Rab GTPase (e.g. RabA and RabB) in the *cis*-to-*trans* direction. RabA can recruit the RabB GEF and create a RabB subdomain, which may be segregated by fission. Cargo proteins in this subdomain are thereby separated from the RabA compartment. **(B)** The RabB subdomain can fuse with the stable RabB dominant compartment and transport cargo proteins to a later cisterna, Golgi resident proteins are retained in a given cisterna probably by interacting with other effectors of the dominant Rab GTPase in the cisterna. **(C)** RabB recruits the GAP for RabA and displaces RabA from the RabB dominant domain. Through the reversible lateral fission/fusion and Rab cascade, cargos are transported through the Golgi stacks, whereas Golgi resident proteins are retained in a given cisterna.

Post-Golgi transport

After the cargo proteins have been modified in the *cis*-to-*trans* cisternae of the Golgi apparatus, they are sorted to different destinations via the *trans*-Golgi network (TGN)

[42]. The morphology and biochemical properties of the TGN are different from that of earlier Golgi cisternae [4]. The TGN in most cell types is a tubular network that bound to the *trans*-Golgi cisterna [4]. Membranes of the TGN have high concentration of cholesterol and sphingolipid due to the input from endocytosis [4]. TGN produces clathrin-coated vesicles but not COPI vesicles, while earlier Golgi cisternae produce COPI vesicles [3]. TGN resident proteins contain cytosolic tail with signals for adaptor-mediated retrieval from endosomes, which are different from that of earlier Golgi resident proteins [69]. In plant cells, the TGN is usually physically disconnected from the Golgi stacks [70].

The TGN contains multiple sorting stations (Fig.1.6)[4]. Transport from TGN to late endosomes (LE) and lysosomes (LL) are mediated via clathrin coated vesicles (CCV) and adaptors [51]. For example, lysosomal hydrolases bearing the mannose-6-phosphate signal bind to mannose-6-phosphate receptors (M6PRs) and are transported to LE and LL via CCV. Lysosomal hydrolases dissociate from M6PR at the low pH environment in LE/LL, and the M6PRs recycle back to TGN [42]. Transport from TGN to plasma membrane is mediated through several routes: many secretory proteins are transported via pleiomorphic structures; some mammalian secretory proteins, like VSV-G, pass through recycling endosomes (RE) *en route* to the cell surface; regulated secretory cargoes are condensed and "pinch off" the TGN to form dense-core secretory granules [4]. Only recently, a COPI, COPII like transport carrier, exomer, has been identified to mediate the transport of a subset of secretory proteins from TGN to plasma membranes in yeast [71]. Cargo carriers from the TGN are elongated and transported along microtubules via the interaction with motor complexes [4].

In addition to functioning as the exit site of the Golgi, TGN is also the interface between the Golgi and the endocytotic system. The overall size and lipid content of the TGN, as well as the shape and function of the TGN, are affected by the membrane input from endocytosis, since the input from the plasma membrane-endosomal membranes are rich in cholesterol and sphingolipid, as well as other proteins, which contributes to the tubular morphology of TGN [4].

Endocytosis is the process of internalizing molecules from the cell surface into intracellular compartments [42]. The classical endocytosis depends on adaptor proteins and clathrin coated vesicles (CCVs) [42]. Ligands of clathrin-dependent endocytosis include TGN38 and transferrin receptor (TfR), etc. [3]. After uncoating, CCVs homotypical fuse with each other to form early endosomes (EE) or fuse with existing EE [3]. Membrane proteins in EE, such as TfR, can recycle back to the plasma membrane directly or through the recycling endosomes (RE), while some other membrane proteins, such as receptor-ligand complexes LDLR, EGFR, are sorted to LE/LL for degradation (Fig. 1.6) [3, 4]. TGN38 is delivered from plasma membrane to the TGN via RE, and this route is exploited by some bacteria toxins and viruses, such as cholera toxin, shiga toxin, SV40, to escape from the lysosomal degradation [3, 4].

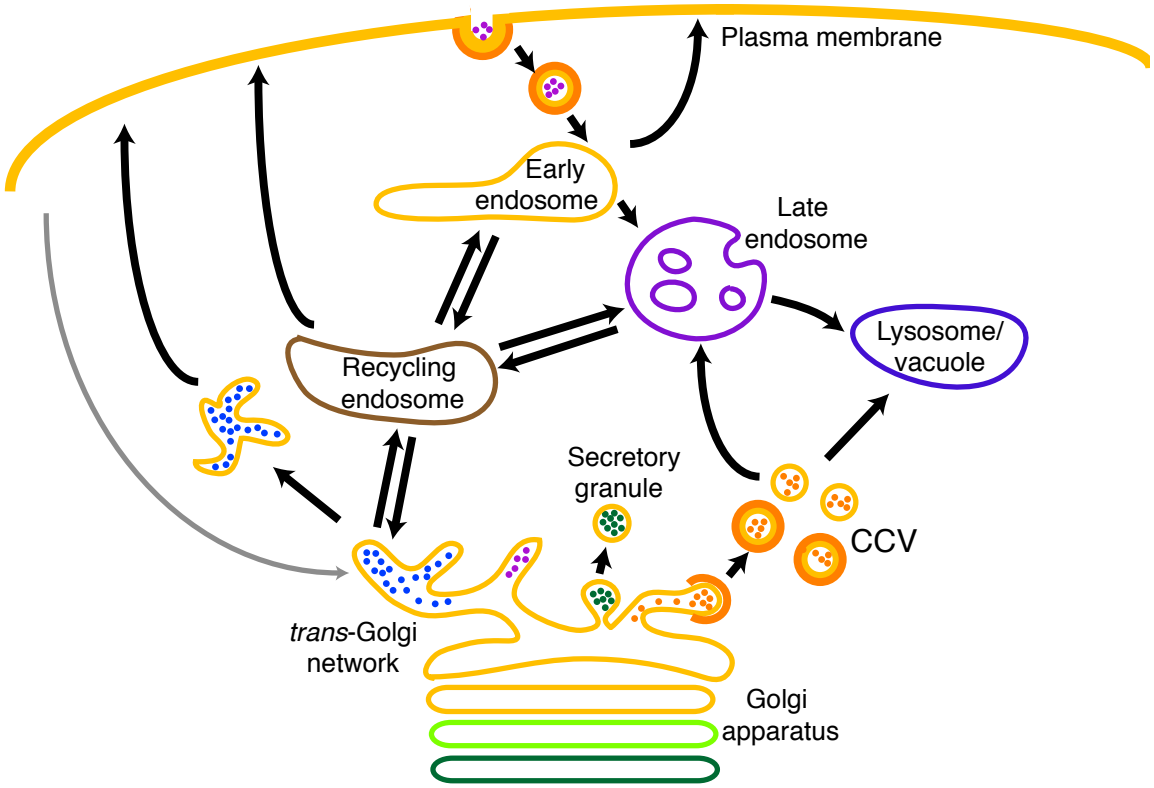

Figure 1.6. The post-Golgi transport [4]. Transport from the TGN to the plasma membrane is mediated through multiple routes. TGN-derived transport carriers can be directly delivered to plasma membrane, or through recycling endosomes. Regulated secretory cargos are condensed in the TGN, pinch off and condensed further to form dense-core secretory granules. Transport from TGN to late endosomes and lysosomes are mediated via clathrin-coated vesicles (CCV). TGN is also the interface of the Golgi stacks and plasma membrane. TGN receives input from plasma membrane and late endosomes via recycling endosomes.

Golgi biogenesis

In many eukaryotic cells, Golgi stacks are closely associated with transitional ER (tER) sites [54]. COPII vesicles fuse homotypically to form new *cis*-Golgi cisternae [72], or heterotypically with formed cisternae [73]. Therefore, tER sites can be regarded as the "birthplace of Golgi cisternae" [51]. In the budding yeast *Pichia pastoris*, Golgi stacks localize adjacent to tER sites and are generated *de novo* along with new tER sites [74]. Similar observation has been made in the protozoan *Trypanosoma brucei* [75]. In addition, the transport of ER membranes into the bud is indispensable for the generation of new Golgi cisternae in *Saccharomyces cerevisiae* [76]. In mammalian cells where the Golgi existed as a ribbon in the pericentriolar region (Fig. 1.7A), the Golgi apparatus undergoes extensive fragmentation during mitosis and reassembles in the two daughter cells after mitosis (Fig. 1.7). The Golgi ribbon first breaks down to individual stacks at G2 phase, which is followed by the unstacking of Golgi cisternae. Isolated Golgi cisternae undergo further disassembly, and the mitotic Golgi fragments are distributed throughout the cell (Fig. 1.7B) and partitioned equally in the two daughter cells [2]. After mitosis, the Golgi remnants reassemble in the two daughter cells (Fig. 1.7C)[77]. The mitotic fragmentation of the Golgi was thought to facilitate the inheritance of this organelle [2]. However, a wide debate regarding to this process exist for a long time. Does the Golgi maintain its separate identity, or merge into the endoplasmic reticulum (ER) during mitosis? It also raises the question whether the Golgi is an independent organelle or a transient intermediate station with enzymes constitutively recycling between the Golgi and the ER [78]. Two models have been proposed to explain the

mitotic fragmentation of the Golgi apparatus: (1) the Golgi-ER recycling model, and (2) the direct Golgi fragmentation model [78].

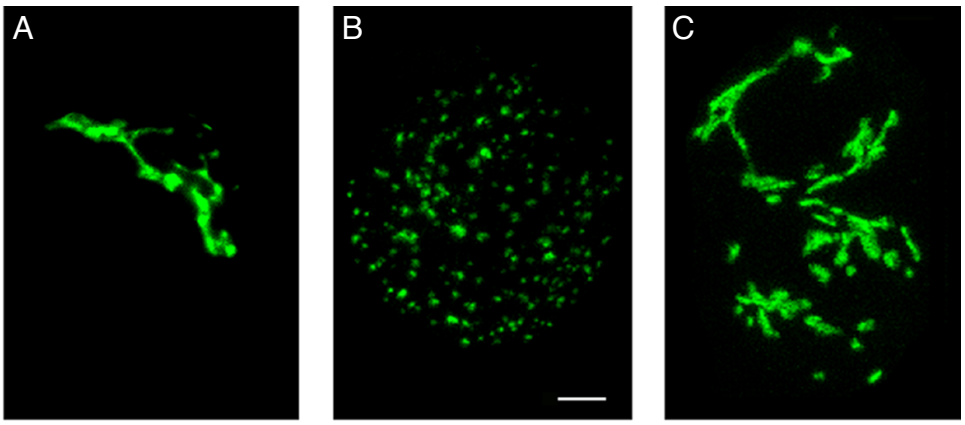

Figure 1.7. Golgi disassembly/ reassembly during the cell cycle in mammalian cells [79]. HeLa cells at different stages of the cell cycle are stained for Golgi marker (A) Interphase, (B) Metaphase, (C) Cytokinesis. Scale Bar, 5 μm. Images are adopted from Dr. David Shima [79].

Two models explaining the mitotic Golgi fragmentation

The Golgi-ER recycling model (Fig. 1.8) proposes that the mitotic Golgi disassembly resembles the phenotype of brefeldin A (BFA)-treated cells, in which the Golgi fuses with the ER due to the inactivation of ARF1 GTPase [80]. This model has been supported by the observation of redistribution of Golgi enzymes into ER by expression of the dominant-negative form of Sar1 GTPase, which blocks the formation of COPII vesicles [81]. Zaal et.al. showed that Golgi enzymes have high diffusion mobility and are recycling between the ER and the Golgi constantly using the microscopy technique and GFP-tagged Golgi enzyme β1,4-galactosyltransferase; at steady state over 30% of the enzyme was found in the ER [82]. However, it is possible that the GFP tag may change the behavior of Golgi enzymes and retain them in the ER.

The Golgi direct fragmentation model (Fig. 1.8) proposes that during mitosis, the COPI vesicles bud from the Golgi continuously without membrane fusion, resulting in a

pool of tubules and vesicles (Golgi "haze") containing Golgi resident proteins [78, 80]. Earlier biochemical studies showed that the Golgi and ER proteins could be separated using sucrose gradient [83, 84]. The mitotic Golgi membranes can be divided into two classes according to the sizes of the fragments, and the major class comprises of vesicles whose diameters are about 60 nm [83]. Mitotic Golgi membranes are morphologically different from mitotic ER membranes. Immunofluorescent images showed that mitotic ER remains as a fine reticulum that is excluded from the spindle-pole region, while mitotic Golgi membranes are distributed throughout the cytoplasm [83], and appeared as clusters or separate vesicles under electron microscope [85]. Surgically generated cytoplasts without the Golgi failed to regenerate Golgi from the ER, nor could they transport cargos to the cell surface, whereas re-introduction of a small quantity of the Golgi reassumed exocytosis significantly, suggesting that the Golgi is an independent organelle [86]. Another piece of evidence was provided by Malhotra's group using a novel trapping assay [87]. The author tagged an ER resident protein, the human invariant chain, and a Golgi enzyme sialytransferase, with a pair of domains that rapidly interact in the presence of rapamycin. While sialytransferase was trapped in the ER after BFA treatment and washout, it was only found in the Golgi after mitosis, suggesting that there is no recycling of Golgi enzymes to the ER at any time of mitosis [87]. Furthermore, Warren's group has studied the dynamic characteristics of the Golgi "haze". They treated the cells with the drug filipin that fragments ER membranes into large but immobilized pieces, and monitored the diffusion pattern of Golgi markers. Although the diffusion of ER proteins was largely reduced, the diffusion of Golgi markers remained unaffected, indicating the Golgi remains independent from the ER during mitosis [88]. In addition,

our previous experiments demonstrated that the small GTPase ARF1 that is required for the generation of COPI vesicles, remains active during mitosis, and its activity is required for mitotic Golgi fragmentation [89]. Our results confirm the role of COPI vesicles in mitotic Golgi disassembly and support the Golgi direct fragmentation model.

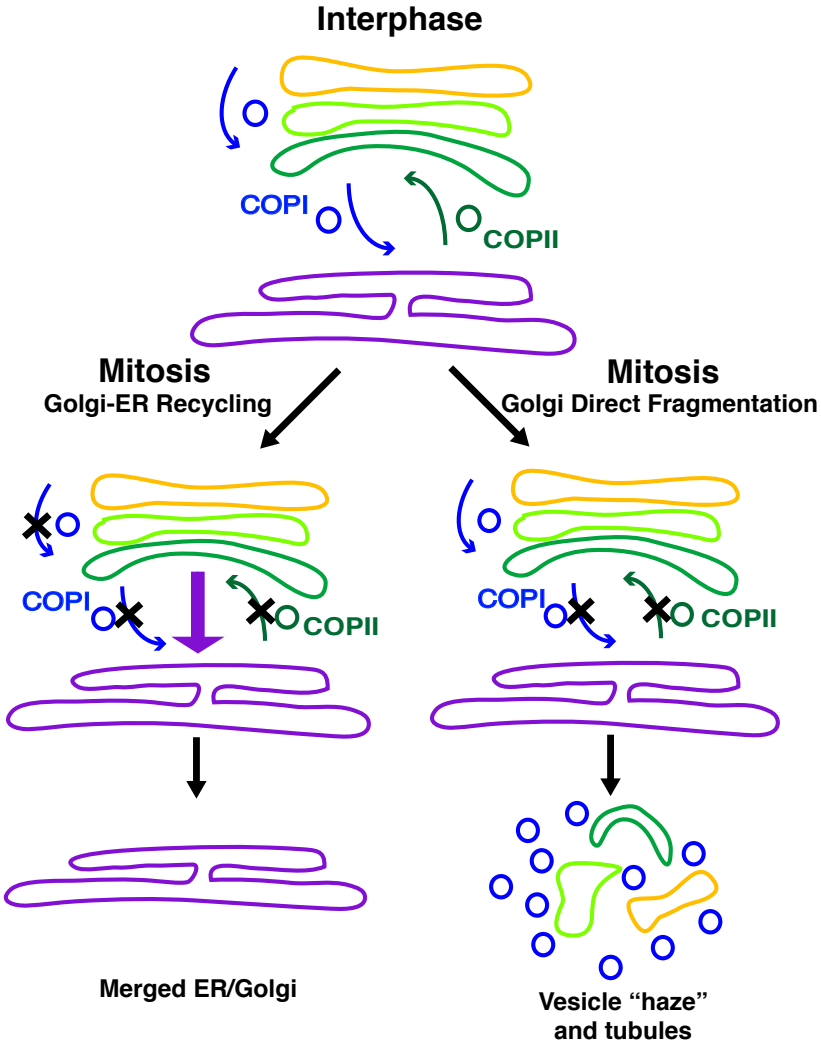

Figure 1.8. Two models explaining the Golgi fragmentation during mitosis [78]. In interphase cells, the Golgi receives cargos from the ER via COPII vesicles. The retrograde transport within the Golgi and from Golgi to ER is mediated by COPI vesicles. Two models have been proposed to explain the fragmentation of the Golgi apparatus in mitosis. The Golgi-ER recycling model hypothesizes that both anterograde and retrograde transport are blocked and Golgi enzymes are redistributed into the ER via tubular structures. The direct fragmentation model states the forward transport by COPII vesicles is blocked, but COPI vesicles continue to bud in the absence of membrane fusion, which generates a pool of tubules and vesicles.

Golgi disassembly/reassembly during the cell cycle

The mitotic Golgi fragmentation is a complicated and multi-step process (Fig. 1.9) [90]. The Golgi ribbon first breaks down to separated stacks in G2 phase, which requires the membrane-fission proteins CtBP3/BARS [91], as well as the activity of the mitogen-activated protein kinase kinase 1 (MEK1) [92]. Once the cell has passed the mitotic checkpoint, the duplicated centrosomes migrate to opposite sides of the nucleus and subsequently, the microtubules are rapidly rearranged to form the mitotic spindle [77]. The elevated Cdk1/cdc2 activity causes Golgi unstacking [77]. The stacking of Golgi cisternae is mediated by two homologous proteins GRASP65 and GRASP55, which form mitotic regulated oligomers to link adjacent Golgi cisternae together. Upon on the phosphorylation by mitotic kinases, the oligomers of GRASP65 and GRASP55 break down, therefore, the Golgi is unstacked [17, 18]. The isolated Golgi cisternae further break down into vesicles and tubules termed as mitotic Golgi fragments (MGF) via COPI mediated budding in the absence of membrane fusion [77].

The Golgi reassembly is a reverse process of disassembly involving cisternal regrowth via membrane fusion and cisternal restacking (Fig. 1.9) [77]. *In vitro* reconstitution assay demonstrated that the membrane fusion depends on two AAA ATPase, N-ethylmaleimide-sensitive factor (NSF) and p97 [93]. NSF is well known as an ATPase that separates SNARE (soluble NSF attachment protein receptor) complexes formed during the membrane fusion, thereby releases them for another round of fusion [94]. NSF functions together with α-SNAP, γ-SNAP, and p115 [93]. However, the ATPase activity of NSF is dispensable for Golgi reassembly [95], whereas the ubiquitin-like protein GATE-16, which regulates SNARE pairing, is involved in this process [96].

In the other pathway, p97 cooperates with its adaptor protein p47, which links it to the t-SNARE, syntaxin-5 [97]. p47 also contains a ubiquitin-associated domain, this UBA domain binds ubiquitin and is required for its activity in Golgi reassembly [98]. Indeed, ubiquitination in mitosis is required for post-mitotic regrowth of Golgi cisternae, and another cofactor of p97, VCIP135, acts as a deubiquitinating enzyme during p97-p47-mediated post-mitotic Golgi reassembly [99]. However, the substrate and E3-ligase of ubiquitination remain unknown. In chapter V, we have identified a potential Golgi localized E3-ligase HACE1 that may regulates this process, and syntaxin-5 as a potential ubiquitination substrate. The initial and transient restacking of cisternae is mediated via p115 by binding to GM130 and giantin that localize on opposite cisternae [100]. After that, the alignment and stacking between cisternae are strengthened by GRASP65 and GRASP55, which are dephosphroylated by protein phosphatase 2A (PP2A) after mitosis [77, 90].

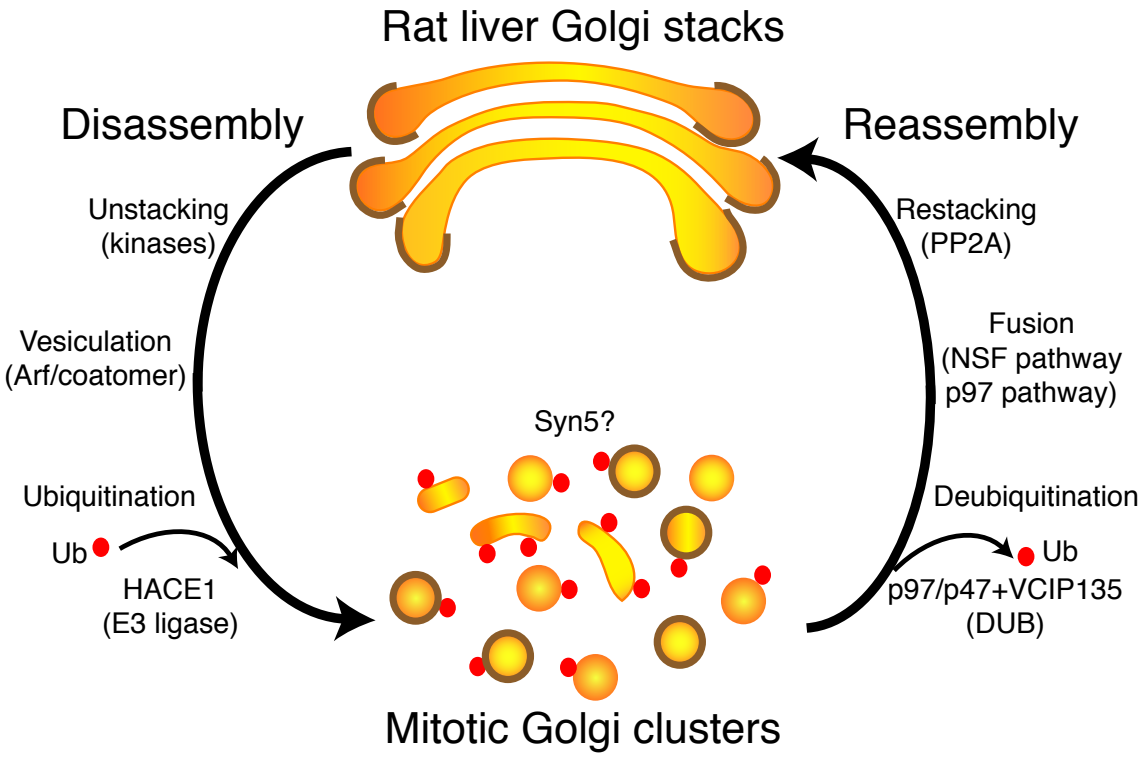

Figure 1.9. Illustration of the Golgi disassembly and reassembly process [90]. Golgi disassembly can be divided into two processes: unstacking and vesiculation. Two mitotic kinases, Cdk1/cdc2 and plk, phosphorylate GRASP65 and thus disrupt GRASP65 oligomers and unstack the Golgi. ARF1 and the coatomer complex are the minimal components needed for the budding of COPI vesicles and thus the vesiculation of Golgi membranes. After mitosis, Golgi reassembly could also be divided into two processes: cisternal regrowth and restacking. Cisternal regrowth mediated by membrane fusion requires two AAA ATPases, p97 and NSF. NSF functions together with syntaxin-5, α-SNAP, γ-SNAP, and p115. p97 cooperates with adaptor proteins p47 and VCIP135. The cisternae regrowth mediated by p97 pathway requires mono-ubiquitination of Golgi membrane proteins during mitosis, and deubiquitination in the reassembly process by VCIP135. Restacking of the cisternae depends on the dephosphorylation of Golgi matrix proteins by protein phosphatase PP2A.

GRASP65 and GRASP55

As mentioned before, in most animal, plant and fungi cells, the Golgi apparatus is consisted of flattened cisternae that are arranged in stacks embedded in a ribosome-free zone, and functions as the hub in the secretory pathway [3]. In animal cells, these Golgi stacks are further connected to form a ribbon-like structure that localizes adjacent to the nuclei, whereas in plant cells and fungi, the Golgi stacks are dispersed throughout the cytoplasm [8, 101]. How the Golgi maintains this unique architecture is far from clear. Early morphological and biochemical studies revealed that there were "proteinaceous cross-bridges" linking adjacent Golgi cisternae [102, 103]. Warren and colleagues isolated a protein complex that was resistant to detergent and salt, and raised the concept of Golgi matrix proteins for the first time [103]. Tens of components of the Golgi matrix have been identified, including GRASPs and golgins, both have major roles in maintaining the structural organization of the Golgi apparatus, and regulating traffic through the Golgi [104].

Golgins

Golgins are a family of Golgi-associated coiled-coil proteins that are necessary for vesicle docking and Golgi integrity. Many Golgins interact with Rab-family small GTPases, and these interactions may recruit golgins to the Golgi or other organelles, or regulate their function [105]. Golgins localize to different compartments of the Golgi apparatus, for example, GM130 is found in the central region of the CGN and *cis*-cisternae [106], whereas Golgin-84 localizes to the rims [107], GMAP210 is a *cis*-Golgi localized golgin [108], and golgin-97 localizes to the *trans*-side [109]. The extended

configuration of the coiled-coil domain makes golgins ideal for tethering membranes over a relative long distance [104]. In addition, spaces between predicted coiled-coil domains allow golgins to make conformational changes, which may be needed to bring two membranes close enough for fusion [104]. Tethering may be followed by membrane fusion, such as membrane traffic, Golgi cisternae formation, and ribbon formation; tethering may occur without fusion, for example, the formation of Golgi stacks [104].

The most well-characterized golgin is GM130. GM130 is *cis*-Golgi localized peripheral membrane protein that form stable complex with GRASP65 [110]. GM130 contains 6 coiled-coil domains and exhibits an extended rod-like configuration [106]. GM130, together with its interacting protein p115, is involved in both anterograde and retrograde transport. p115 is recruited onto COPII-coated vesicles via interaction with Rab1 GTPase to mediate ER-to-Golgi transport [38], or alternatively onto COPI-coated vesicles via interaction with integral golgin giantin [100]. p115 then interacts with GM130 and its interacting partner GRASP65 to link these vesicles to the *cis*-Golgi [110]. In the giantin/p115/GM130 pathway, it has been shown that the tethering precedes and directs the cognate SNARE complex assembly that is necessary for membrane fusion [38, 111]. Consistent with the role in the tethering event, a recent study showed that depletion of GM130 by RNA interference causes fragmentation of Golgi ribbon and aberrant glycosylation of the plasma membrane proteins. It is speculated that knockdown of GM130 inhibits the lateral fusion of Golgi cisternae and disrupts the uniform distribution of Golgi enzymes that are responsible for proper glycosylation of proteins [22]. GM130 also regulates the microtubule cytoskeleton. GM130 recruits γ-tubulin complex to the *cis*-Golgi via A-kinase anchoring protein 450 (AKAP450) and nucleates non-centrosomal

microtubules. These Golgi originated microtubules function in Golgi ribbon formation, cell polarity establishment and directed cell migration [21]. In addition, GM130 controls centrosome organization by binding to a cdc42 GEF, Tuba. Depletion of GM130 results in multiplication of centrosomes, aberrant multi-polar spindles, and improper cell division [112]. Similar to GM130, many golgins have been shown to have functions other than membrane tethering (table 1.1), for instance, the *trans*-Golgi localized GCC-185 also recruits non-centrosomal microtubules via its interaction protein CLASP [113].

GRASPs

GRASPs (Golgi Reassembly Stacking Proteins) are peripheral membrane proteins that attach to the Golgi membranes via the N-terminal myristic acid [15]. Two homologous proteins GRASP65 and GRASP55 (Fig. 1.10), localizing to *cis*- and *medial/trans*-Golgi, respectively, have been identified in mammalian genome [16]. Homologues in other organisms, including yeasts [114], flies [115], Dictyostelium [116], etc. have also been identified and characterized. GRASPs have been shown to participate in Golgi cisternal stack formation, Golgi ribbon formation, unconventional secretion, cargo transport, cell cycle regulation, apoptosis, mitotic spindle formation, cell polarity establishment, etc [15, 18, 22, 29, 117-119].

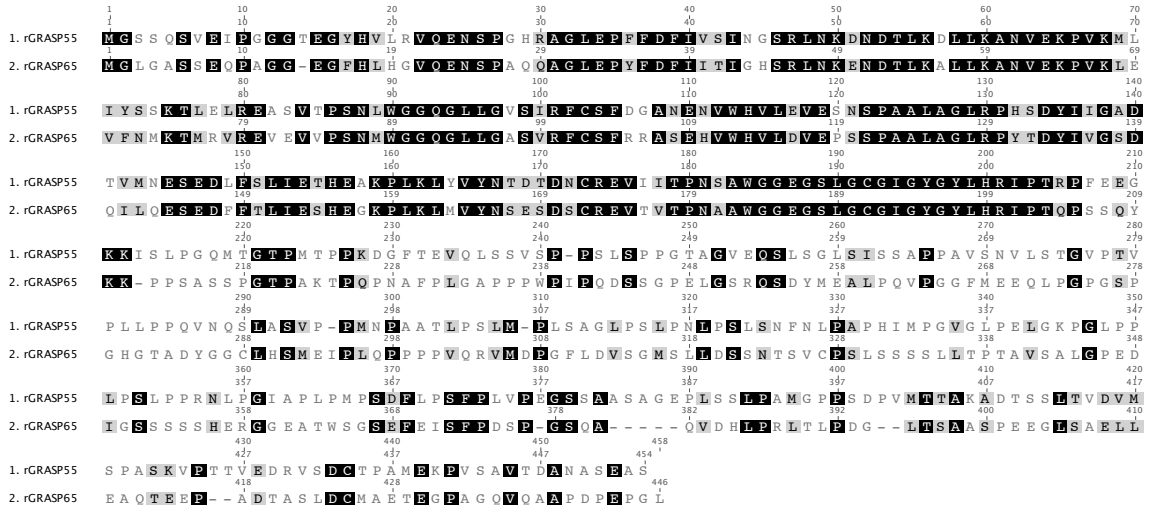

Figure 1.10. Comparison of the *rattus norvegicus* GRASP65 and GRASP55 sequences. Alignment of the GRASP55 (NP_001007721.1) and GRASP65 (NP_062258.2) sequences: black background indicates identity and the shading indicates these residues are conserved.

GRASPs are originally identified as Golgi stacking factors using the *in vitro* Golgi disassembly and reassembly assay [15, 16]. Purified rat liver Golgi can be fragmented upon the incubation of mitotic cytosol extracted from spinner HeLa cells, and these mitotic Golgi fragments (MGF) are able to reassemble to cisternae and Golgi stacks when further incubated with interphase cytosol. Adding antibodies against GRASP65 or GRASP55 or soluble recombinant proteins inhibits the reassembly of Golgi stacks, but not the regrowth of Golgi cisternae, suggesting that GRASP65 and GRASP55 are involved in the formation of Golgi stacks [15, 16]. Microinjection of GRASP65 antibodies into mitotic cells blocks the reassembly of the Golgi apparatus in post-mitotic daughter cells, confirming the *in vitro* results [17]. However, the *in vivo* experiments revealed controversial observations. The initial RNA interference (RNAi) experiment confirmed that GRASP65 is involved in the cisternal stacking process [118], whereas another group reported that GRASP65 participates in the ribbon formation rather than the stack formation [22]. Similar arguments applied to GRASP55, too [23]. We have

performed a systematic electron microscopic analysis of HeLa cells depleted of GRASP65, or GRASP55, or both GRASPs, and found that depletion of a single GRASP protein led to partially unstacking of the Golgi, which could be rescued by the exogenous expression of GFP-tagged RNAi resistant GRASP65 or GRASP55; depletion of both GRASPs resulted in a more complete disassembly of the Golgi stacks; exogenously expressing GRASP65 or GRASP55 could only partially rescue the knockdown effects [18]. We did observe a mild fragmentation of the Golgi ribbon in 22-24% of the cells depleted of GRASP55 [18], suggesting that GRASP55 may be also involved in the Golgi ribbon formation, or the ribbon unlinking is a secondary effect of the unstacking of cisternae.

GRASP65 and GRASP55 form stable dimers, which further form phosphorylation regulated oligomers that link adjacent cisternae into a Golgi stack [17, 18, 120]. Both the dimerization and oligomerization are mediated through the highly conserved N-terminal GRASP domain (Fig. 1.11), which consists of two predicted PDZ domains [17, 18, 120]. The PDZ domain is a common protein module involved in protein-protein interaction, which typically contains two α-helices (α1-2) and five to six β-strands (β1-6). A ligand inserts between the α2 and β2, and form a sheet with β2 and β3 [121]. It is the first PDZ domain in the GRASP domain that mediates the homotypic interaction of GRASP proteins [122]. The C-terminuses of GRASP65 and GRASP55, although less conserved, contain multiple proline-directed serines/threonines, thereby termed the Serine/Proline-rich (SPR) domain (Fig. 1.11) [120]. Both GRASP65 and GRASP55 are phosphorylated during mitosis through the SPR domain, which disrupts the oligomerization of GRASP proteins, and leads to the unstacking of Golgi during mitosis [17, 18, 120]. GRASP65 is a

target of the mitotic kinase Cdk1/cdc2 and polo-like kinase 1 (plk1) [17, 18, 120, 123]. plk1 docks onto GRASP65 after the latter has been phosphorylated by Cdk1/cdc2 [124]. A combination of purified Cdk1/cdc2 and plk1 kinases phosphorylates GRASP65 to the same extend as mitotic cytosol does, and leads to the unstacking of purified rat liver Golgi [17]. Therefore, a combination of the Cdk1/cdc2 and plk is used to mimic the mitotic cytosol to generate the phosphorylated GRASP65. Expression of the C-terminus of GRASP65 delays the mitotic progression, suggesting that the C-terminal SPR domain of GRASP65 may function as a mitotic checkpoint [118]. GRASP55, on the other hand, is phosphorylated by the MAPK ERK2 [125], whereas it is only mildly phosphorylated by Cdk1/cdc2, but not by plk1 [18], suggesting that GRASP65 and GRASP55 are regulated by different signaling pathways.

GRASP65 interacts with the vesicle docking receptor protein GM130 via amino acid 189-201 (Fig. 1.11) [110]. GRASP65 and GM130 were found in a detergent extracts of Golgi membranes under both interphase and mitotic conditions. This interaction is thought to anchor GM130 on the Golgi membrane and participate in the docking of p115 tethered COPII vesicles [110]. It has also been shown that the GM130/GRASP65 complex recycles between the *cis*-Golgi and the late intermediate compartment, the membrane station that dynamically protrudes from the Golgi and undergoes homotypic fusion with intermediate compartments [117]. Similarly, GRASP55 interacts with a Golgi localized coiled-coil protein, golgin-45. Golgin-45 is a Rab2 effector, depletion of golgin-45 disrupts the Golgi structure and inhibits secretory cargo transport [126].

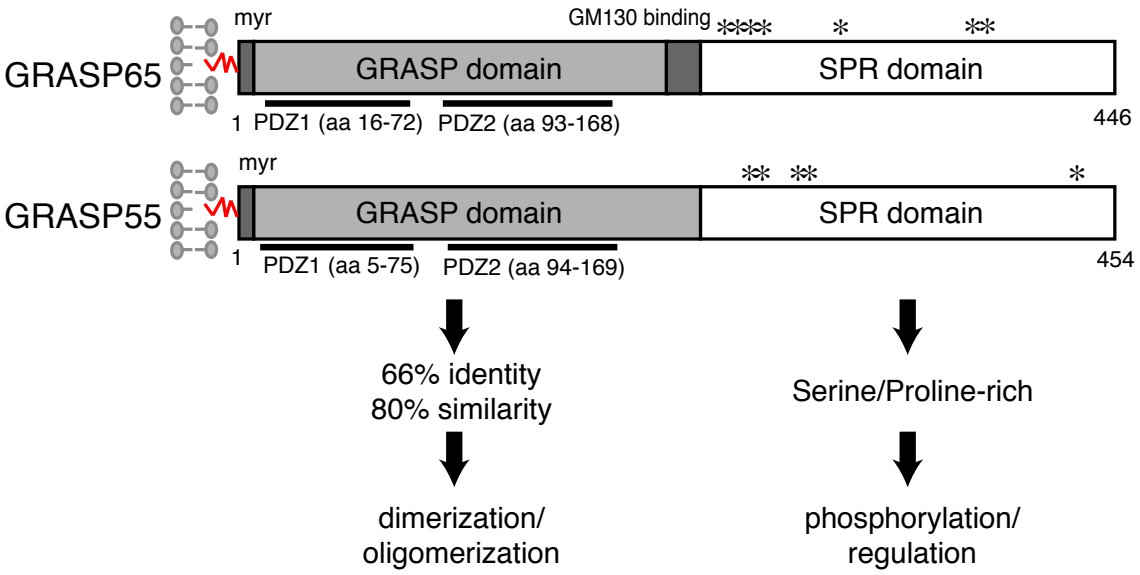

Figure 1.11. GRASP65 and GRASP55 structures. Rat GRASP65 and GRASP55 are composed of the GRASP domain on the N-terminus and the Serine/Proline-rich (SPR) domain on the C-terminus. The GRASP domain of GRASP55 is 66% identical and 80% similar to that of GRASP65, and mediates the dimerization and oligomerizaiton of the proteins. The PDZ domains within the GRASP domain are predicted using the SMART database (http://smart.embl-heidelberg.de/). The SPR domains contain multiple potential phosphorylation sites, as indicated by asterisks, and regulate the oligomerization status of these proteins via phosphorylation. Asterisks: predicted phosphorylation sites, myr: myristoylation site. The phosphorylation sites of GRASP65 are S216/S217/T220/T224/S277/S367/S376; the phosphorylation sites of GRASP55 are T222/T225/S245/S249/T435.

In addition to cisternal stacking and ribbon formation, GRASPs also participate in other cellular processes, such as unconventional secretory pathway [116, 127], specific cargo transport [128-130], apoptosis [131], cell cycle control [119, 131], mitotic spindle formation [118], centrosome orientation [27], etc.

During *Dictyostelium idscoideum* development, prespore cells secrete acyl-CoA binding protein (AcbA). AcbA lacks a signal sequence, thereby it is not secreted via the conventional secretory pathway. Recent studies reported that depletion of the putative GRASP orthologue in *Dictyostelium idscoideum* inhibited the secretion of AcbA [116, 127], suggesting that GRASP is involved in the unconventional secretion, although the mechanism is unclear. This result is supported by the observation that depletion of the

yeast homologue of GRASP, Grh1, also caused the failure of AcbA secretion [127]. In addition, the single drosophila homologue of GRASP65 and GRASP55, dGRASP, mediates the nonconventional integrin secretion that is required for Drosophila epithelial remodeling [132].

GRASP65 and GRASP55 are also involved in specific cargo transport and enzyme retention by binding to their cytosolic domains. Both GRASP65 and GRASP55 interact with p24 cargo receptor family, which is required for the efficient retention of p24 cargo receptors in the Golgi apparatus [133]. GRASP55 interacts with the cytoplasmic domain of the transforming growth factor-alpha (TGF-α) via its first PDZ domain, and this interaction is required for the traffic of TGF-α, as mutation in the GRASP55-binding motif at the C-terminus of TGF-α impairs its transport to the cell surface [130]. D'Angelo et.al. also investigated the role of GRASP65 and GRASP55 in the transport of a specific class of cargos bearing the C-terminal valine, such as CD8α and Frizzled 4, and they found that GRASP65 and GRASP55 both bind to these receptors via the PDZ domains and are required sequentially for their efficient transport to the plasma membranes through the Golgi [129]. Therefore, mutation of the C-terminal valine leads to a dominant form of autosomal human familial exudative vitreoretinopathy [129].

During apoptosis, the Golgi apparatus is fragmented into dispersed clusters of tubulovesicular membranes, and several Golgi matrix proteins are cleaved by caspases [134]. It is reported that GRASP65 cleavage by caspase 3 is required for the Golgi fragmentation during apoptosis, and expression of caspase-resistant mutant partially preserved cisternal stacking and inhibited the breakdown of Golgi ribbon [119, 131].

GRASP65 and GRASP55 also participate in the cell cycle control. Over-expression of the GRASP domain of GRASP65 that is resistant to phosphorylation regulation delays mitotic entry [18], probably by inhibiting the mitotic Golgi fragmentation. Expression of the C-terminal SPR domain of GRASP65, or microinjection of the phosphorylation sites bearing peptides of GRASP55 also inhibit the mitotic progression [29, 118], possibly by sequestering or consuming kinases that are needed for mitotic phosphorylation of other cellular components.

GRASP65 was also reported to participate in the formation of spindles during mitosis, as depletion of GRASP65 resulted in multiple aberrant spindles and defective cell division [118]. Bisel et al. found that the reorientation of centrosome depends on the phosphorylation of GRASP65, and the expression of non-phosphorylatable mutants prevented cells from polarizing and migrating in the wound-healing assay [27], indicating that GRASP65 is a critical factor in the regulation of cell polarity.

Homologues of GRASP65/GRASP55 have been identified in other eukaryote, including flies, yeasts, plants, etc. The single Drosophila homologue of GRASP65/GRASP55, dGRASP, which localizes to both tER sites and Golgi membranes, has been reported to participate in cisternal stacking. Depletion of dGRASP and its interacting protein dGM130, the homologue of GM130, converts the Golgi stacks into clusters of vesicles and tubules in *Drosophila* S2 cells [115]. The yeast homologue of GRASP65/GRASP55, Grh1, lacks the N-terminal myristoylation site; it is targeted to the *cis*-Golgi via the acetylation site on the N-terminal amphipathic helix. Grh1 interacts with the COPII coat component Sec23/24, as well as a coiled-coil protein Bug1. The

Grh1/Bug1 complex is dispensable for traffic and cell growth, it may optimize membrane traffic in the early Golgi [114].

Given the Golgi exhibits as single disks, but not stacks in *S.cerevisiae*, the evolutional conservation of GRASP proteins in the cisternal stacking has been doubted. However, the yeast homologue Grh1 does not contain the first PDZ domain that is required for the oligomerization of GRASP65/GRASP55, nor have yeast the homologue of GRASP65 interacting protein GM130, suggesting the role of Grh1 can be quite different from its mammalian homologue [114].

Table 1.1. Golgi matrix proteins

Names	Features	GTPase	Interaction	Functions and Reference
GRASP65	N-myr		GM130, p24,	• stacking [15, 18, 115, 119] • ribbon formation [22] • apoptosis [131] • cell cycle control [119] • mitotic spindle formation [118] • unconventional secretion [116, 127] • transport of specific cargos [129] • p24 cargo receptor retention [133] • centrosome orientation [27]
GRASP55	N-myr		Golgin-45, p24, TGF-α	• stacking [16, 18] • ribbon formation [23] • cell cycle control [29] • transport of specific cargos [129, 130] • p24 cargo receptor retention [133]
GM130/ golgin-95	P	rab1, rab2, rab33b	p115, GRASP65 [110], syntaxin 5, AKAP450, Tuba	• ER-to-Golgi traffic, COPII vesicle tethering [135, 136] • Golgi ribbon formation [22] • non-centrosomal microtubules organization [137] • centrosome regulation [21, 112] • apoptosis [138] • spindle formation • cell migration [139]
p115	P	rab1	GM130, Giantin, syntaxin 5, GOS-28, Bet1p	• membrane tethering [39, 111, 136, 140, 141] • post-mitotic Golgi reassembly[142] • apoptosis [143] • Nuclear import [144]
Golgin-45	P	rab2	GRASP55	• membrane tethering [126]
Golgin-67/ GM88	TMD*			• uncharacterized [145, 146]
Golgin-84	TMD	rab1	CASP, COG complex	• membrane tethering [65] • Golgi integrity [24] • intra-Golgi retrograde transport [147] • Bacteria infection [148]

Golgin-97/ GOLGA1	GRIP	ARL1/3 [109]	FIP1/RCP	• TGN-to-plasma membrane traffic of E-cadherin [149] • endosome-to-TGN [150, 151] • retrograde transport from recycling endosomes to the trans-Golgi network [152] • poxvirus morphogenesis [153]
Golgin-160/ mea-2/ GCP170	P		GCP60, GCP16, beta1AR, ROMK, PIST	• plasma membrane transport of renal ROMK channel [154] • apoptosis [155-157]
Golgin-230/245/256/GOLGA4	GRIP	ARL1/3		• TGN-to-plasma membrane traffic [158]
Giantin/ GCP372/ macrogolgin	TMD	rab1, rab6	p115, GCP60	• membrane tethering [100, 159-162] • apoptosis [160]
Bicaudal-D	P	rab6	Dynactin, p50-dynamitin	• recruits the dynein–dynactin complex [163] • COPI-independent Golgi-to-ER transport [164]
CASP	TMD		Golgin-84	• membrane tethering [65]
GCC88	GRIP	ARL1/3	CPSF7, FBF1	• trans-Golgi network organization, early endosoms to TGN traffic [165]
GCC185	GRIP	ARL1/3, rab1, rab2, rab6, rab9 [166]	syntaxin 16, CLASP	• membrane tethering [167, 168] • MPR recycle [168] • attachment of non-centrosomal microtubules [169] • Golgi ribbon formation [167]
GCP16	acylation		GCP170	• transport from Golgi to PM[170]
GCP60/ ACBD3	P		Giantin, Golgin-160 [157], Numb	• ER-to-Golgi transport [171] • asymmetric cell division [172] • anti-apoptosis [157]
GCP364				• Golgi ribbon formation and perinuclear localization [173]
CG-NAP			protein kinase PKN, RIIalpha, protein phosphatase 2A (PP2A), protein phosphatase 1	• scaffold protein for kinases/phosphatases [174]
GMAP210/ Trip230	GRAB	ARF1	ITF20, γ-tubulin, thyroid receptor, retinoblastoma protein	• membrane tethering [175] • ER-to-Golgi traffic [176] • ribbon formation [177] • γ-tubulin recruitment [177] • sorting to primary cilia [178] • interacts with thyroid hormone receptor beta [179]
IIGP165	P			• anti-apoptosis [114]
NECC1/2	TMD*			• uncharacterized [180]
SCOCO	P			• uncharacterized [181]
SCYL1BP1	P	rab6	Scyl1	• loss of function causes Gerodermia osteodysplastica [182] [183]
TMP/ ARF160	P	rab6	hSNF2a, hSNF2b, Fer, AR, Stat3	• traffic from early/recycling endosome to TGN, Golgi enzyme retention [104, 184]

N-Myc: N-terminal myristoylation; P: peripheral membrane protein; TMD: transmembrane domain; TMD^{P}: predicted transmembrane domain; GRIP: golgin-97, RanBP2alpha, Imhlp and p230/golgin-245 domain; GRAB: GRIP-related ARF-binding domain.

Function of the Golgi apparatus

Localizing at the central position in the secretory pathway, the Golgi apparatus receives and modifies posttranslationally newly synthesized proteins from the ER, and sorts these proteins to their ultimate destinations [2]. Resident Golgi enzymes conjugate secretory proteins and lipids with various glycans, which are highly diverse compared with glycans added in the ER [185]. The Golgi apparatus is also the major site of sphingolipid biosynthesis and assembly of triglyceride with apolipoproteins within cells [3]. In addition, the Golgi apparatus separates the glycerolipid-rich ER from the cholesterol/sphingolipid-rich plasma membrane. It exchanges membrane components with other organelles, including endosomes, caveosomes, autophagosomes, etc., thereby connects multiple membrane traffic pathways [3]. Other cellular processes involve the Golgi apparatus include apoptosis, cell cycle control, cytoskeleton organization, signaling pathway, transcription, etc.

Glycosylation

Protein glycosylation encompasses N-glycans, O-glycans, and proteoglycans [186]. N-glycans are conjugated onto a subset of asparagine residues within the Asn-X-Ser/Thr motif of proteins, whereas O-glycans are linked to a subset of serines and threonines [42]. While O-glycosylation occurs exclusively in the Golgi, N-glycosylation of proteins is initiated in the ER by the transfer of the 14-residue precursor of N-linked oligosaccharides onto nascent proteins (Fig. 1.12) [42]. Three glucose (Glc) and one mannose (Man) residues are removed from the glycan, and glycoproteins bearing 10-residue oligosaccharides $(Man)_8(GlcNAc)_2$ are transported to *cis*-Golgi [42].

Glycosylation enzymes are sequentially arranged along the *cis*-*trans* axis of the Golgi apparatus [12]. In the *cis*- and *medial*-Golgi, five more mannoses are removed and N-acetylglucosamines are added to the extending glycan; galactoses and sialic acids are added to the N-glygan in the *trans*-Golgi; the number of branches of glycans, as well as the number and identity of carbohydrates conjugated, are variable [42].

The N-glycosylation occurring in the ER is uniform, and mainly functions to facilitate the correct folding of nascent polypeptides, whereas the glycosylation that occurs in the Golgi is much more complicate with elaborate and highly diverse glycans conjugated to glycoproteins [185]. The complexity of glycosylation conferred by Golgi localized glycosyltransferases and glycosidases bestows functional diversification of glycoproteins, including the adaptive and innate immune response [187, 188]. Glycosylation can be regulated by the transcription and intracellular localization of glycosylation enzymes, the synthesis and transport of donor sugar, enzyme accessibility to substrates, proteolysis within the lumen of Golgi, and glycan turnover at the plasma membrane [186]. In chapter III, I studied whether the Golgi cisternal stacking regulates the glycosylation process.

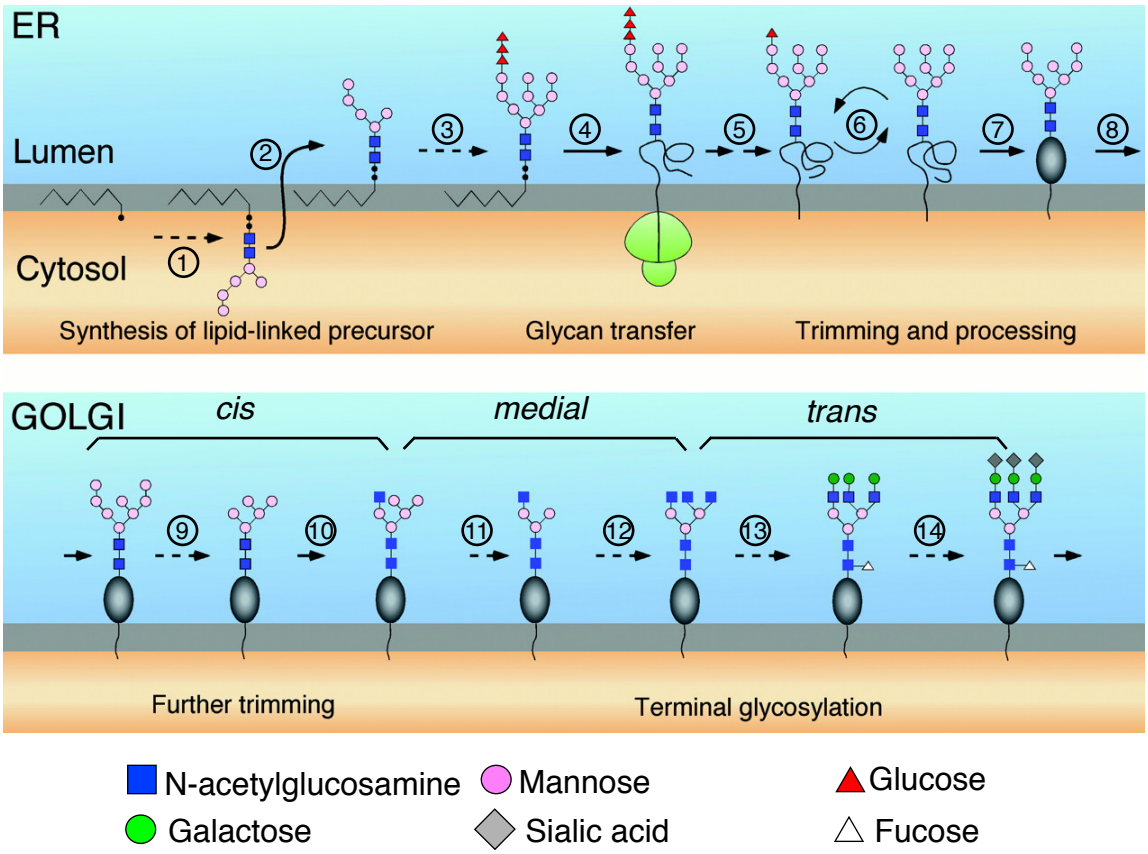

Figure 1.12. Biosynthesis of N-linked glycans [185]. Synthesis starts on the cytosolic surface of the ER membrane by addition of sugars to dolichylphosphate[1]. After N-acetylglucosamine (GlcNAc) and five mannose residues are added, the precursor is flipped to the luminal side of ER membrane[2], and more sugars are added[3]. After the last three Glucoses are added, the oligosaccharide is transferred to the asparagine residues of nascent polypeptide chains by the oligosaccharyltransferase enzyme[4]. The three glucoses are trimmed by glucosidase I and II[5]. The ER localized glucosyltransferase reglucosylate glucose-free chains, and the glucosidase II deglucosylate the sugar chain, until the glycoprotein has folded[6]. A terminal mannose is trimmed by ER localized mannosidases[7], and the folded glycoprotein is transported to the *cis*-Golgi[8], where three additional terminal mannoses are further trimmed[9], followed by the addition of a GlcNAc[10]. Two more terminal mannoses are cleaved in the *medial* Golgi[11], followed by the addition of GlcNAc residues[12]. Galactose, sialic acid, and fucose residues are added to the glycan in the *trans*-Golgi [13,14]. Shown is one of many possible terminal glycosylation pathways; the number of branches, as well as the number and identity of sugars added, varies.

Cell cycle regulation

In mammalian cells, the Golgi apparatus undergoes extensive fragmentation during mitosis: the Golgi ribbon first disassembles into separated stacks in late G2 and prophase, and the Golgi stacks break down to isolated cisternae, which are further fragmented, generating vesicular/tubular membranes [77]. The first step, ribbon unlinking, requires

kinases plk3 [189], MEK1 [92], and the fission protein BARS [28], while the second step, unstacking, depends on mitotic kinase plk1 and Cdk1 [17, 120, 123, 124, 190]. The mitotic disassembly of the Golgi apparatus was originally proposed to facilitate the inheritance of this organelle by equally distributing Golgi fragments into daughter cells [2]. However, recent studies implicate unexpected link between mitotic Golgi fragmentation and cell cycle progression.

First, the breakdown of Golgi ribbon may function as a check point for mitotic progression [7], interfering with mitotic Golgi disassembly by microinjection of the C-terminus of GRASP65 [191] or GRASP55 [29], or blocking the activity of Golgi fission protein BARS [91], results in cell cycle arrest in G2 phase. These inhibitory effects are not caused by the activation of DNA damage check point [91, 191], therefore, it is proposed that the fragmentation of Golgi ribbon is a mitotic check point to ensure the Golgi fragments can migrate to the two poles of dividing cells with spindle microtubules [7]. This Golgi checkpoint may employ a similar mechanism as the spindle check point, that is, by monitoring the attachment of spindle microtubules to individual Golgi stacks after the unlinking of the Golgi ribbon to regulate the entry into mitosis [7].

Recent studies have demonstrated that several Golgi-associated proteins are required for the formation of the bipolar spindles [7], including GRASP65 [118], GM130 [21, 112], poly-ADP ribosyl transferase, tankyrase-1 [192], RINT-1 (spindle checkpoint regulator) [193], and the phosphatidylinositide phosphatase, Sac1 [194]. Depletion of any of these proteins causes aberrant multipolar spindles and mitotic cell death [7]. For example, knockdown of GRASP65 by RNA interference leads to the formation of multipolar spindle and mitotic arrest [118]. Similarly, GM130 controls centrosome

organization by binding to a cdc42 GEF, Tuba; depletion of GM130 results in multiple centrosomes, aberrant multi-polar spindles, and improper cell division [21, 112].

In addition, mitotic Golgi disassembly may regulate mitotic progress by releasing factors from Golgi membranes. Those factors, such as clathrin [195], ACBD3 [172], Rab6A′ [196], are required for cell division [7]. For example, clathrin, which is needed to stabilize mitotic spindle fibers, is released from the Golgi complex and endocytic vesicles and translocated to the spindle pole [195]. The Golgi associated protein ACBD3 is also released during mitotic Golgi fragmentation to activate Numb, and this translocation of ACBD3 is required for asymmetric cell division [172]. Inhibition of translocation of Rab6A′ leads to mitotic arrest via the activation of spindle checkpoint [196]. It is proposed that the pericentriolar localization or the formation of Golgi ribbon may confer some inhibitory effects on cell division, which is relieved by the mitotic Golgi disassembly [172].

Apoptosis

The Golgi apparatus undergoes an extensive fragmentation during apoptosis, the Golgi ribbon is first unlinked and Golgi stacks break down into tubulovesicular clusters, which are morphologically similar to mitotic disassembly of the Golgi complex [134]. Several Golgi matrix proteins are cleaved during apoptosis by caspases, including GRASP65 [131], golgin-160 [155], giantin [160], GM130 [138], vesicle transport protein p115 [143], the t-SNARE syntaxin-5 [160], the intermediate chain of dynein, and the $p150_{Glued}$ subunit of dynactin [197]. Expression of noncleavable mutants of these proteins delays Golgi disassembly after pro-apoptotic stimuli [6]. Cleavage of Golgi matrix

proteins and subsequent disassembly of the Golgi apparatus could simply be the result of the apoptotic process, and is required to pack the remnants of this organelle into apoptotic blebs for disposal [6].

However, recent studies raise intriguing possibilities that the cleavage of Golgi proteins and the disassembly of the Golgi may regulate the apoptotic process [6]. First, the cleavage of Golgi proteins may occur in the upstream of apoptotic signaling events [6]. The expression of the non-cleavable golgin-160 delays response to some apoptotic stimuli that cause ER stress, even when the Golgi was disrupted with drugs before the induction of ER stress [156]. However, this delayed apoptotic response was not observed with other apoptotic stimuli, such as staurosporine treatment, suggesting that the cleavage of golgin-160 may be required for the progression of apoptosis induced by specific stimuli in the secretory pathway [6]. Second, the fragments of Golgi matrix proteins may influence the apoptotic process by regulating gene expression to either alleviate stress, or promote apoptosis [134]. The vesicle transport protein p115 is cleaved by caspase 3 during apoptosis and the C-terminal fragment is translocated and accumulated in the nucleus; over-expression of this fragment promotes both Golgi fragmentation and apoptosis [143]. Similarly, the fragment of golgin-160 generated by caspase 2 cleavage, also translocates and accumulates in the nucleus. Although its role in regulating apoptosis-related gene expression has not been tested, it does contain several sequence motifs conserved in transcription factors [198]. Caspase 2 is partially localized on the cytoplasmic side of the Golgi apparatus and understanding how it regulates apoptotic Golgi disassembly may reveal the role of the Golgi in apoptotic progression [134].

Centrosome orientation and directed transport

In the mammalian cells, the Golgi apparatus localizes adjacent to centrosomes during interphase by interacting with microtubules and microtubule associated motor proteins. Recent studies implicated that this Golgi-centrosome association is important for centrosome positioning and directional protein transport, which are required for cell polarization and migration [7]. The Golgi apparatus may regulate the directional protein transport through two means: (1) centrosome positioning, (2) non-centrosomal microtubules. Both the Golgi apparatus and centrosome undergo repositioning to the leading edge upon stimulation [7]. It is reported that centrosome reorientation requires the phosphorylation of a Golgi matrix protein GRASP65 by MAPK; expression of nonphosphorylatable mutants of GRASP65 prevents Golgi and centrosome reorientation and inhibits cell migration [27]. In addition, non-centrosomal microtubules also contribute to the directional transport [169]. Several Golgi matrix proteins have been reported to nucleate the assembly of Golgi emanating microtubules, including GMAP-210 [25, 199], GCC185 [169], GM130 [137], etc. GMAP-210 recruits γ-tubulin complex to the *cis*-Golgi membrane, which facilitates the formation of the Golgi ribbon [199]. Depletion of GMAP-210 causes Golgi ribbon unlinking and also inhibits directional cell migration [25]. The *trans*-Golgi localized golgin GCC185 interacts with CLASP and is involved in non-centrosomal microtubules polymerization from the TGN. These Golgi-emanating microtubules preferentially orient toward the leading edge in motile cells and contribute to asymmetric cargo transport [169]. GM130 recruits γ-tubulin complex to the *cis*-Golgi via A-kinase anchoring protein 450 (AKAP450) and nucleates non-centrosomal microtubules [137]. These Golgi-originated microtubules play a role in Golgi ribbon

formation and cell polarity establishment. A most recent study reported that two signaling pathways influence Golgi morphology to regulate the polarization of neuronal cells via GM130. The Stk25 kinase may phosphorylate GM130 and promotes a condensed Golgi and axon development, while the Reelin-Dab signaling pathway antagonizes the Stk25 pathway and leads to the extended morphology of the Golgi, subsequently promote dendrite development [200].

Chapter II. GRASP55 and GRASP65 play complementary and essential roles in Golgi cisternal stacking

Abstract

In vitro studies have suggested that Golgi stack formation involves two homologous peripheral Golgi proteins, GRASP65 and GRASP55, which localize to the *cis* and *medial-trans* cisternae, respectively. However, no mechanism has been provided on how these two GRASP proteins work together to stack Golgi cisternae. Here we show that depletion of either GRASP55 or GRASP65 by siRNA reduces the number of cisternae per Golgi stack, while simultaneous knockdown of both GRASP proteins leads to disassembly of the entire stack. GRASP55 stacks Golgi membranes by forming oligomers through its N-terminal GRASP domain. This process is regulated by phosphorylation within the C-terminal serine/proline-rich domain. Expression of non-phosphorylatable GRASP55 mutants enhances Golgi stacking in interphase cells and inhibits Golgi disassembly during mitosis. These results demonstrate that GRASP55 and GRASP65 stack mammalian Golgi cisternae via a common mechanism.

Introduction

The Golgi complex is a membrane-bound organelle that serves as a central conduit for the processing of membrane and secretory proteins in all eukaryotic cells. It comprises stacks of flattened cisternae that are laterally linked to form a ribbon in mammalian cells. Formation of stacks is thought to be significant that it facilitates the accurate localization and function of enzymes that modify N- and O-linked oligosaccharides [201]. However, the mechanism that mediates stacking is poorly understood. GRASP65 (Golgi Reassembly Stacking Protein of 65 kDa), a peripheral Golgi protein that is associated with membranes via N-terminal myristoylation, was identified as the first Golgi stacking factor through the use of an *in vitro* assay that reconstitutes the cell-cycle regulated Golgi disassembly and reassembly process. Adding either GRASP65 antibodies or a soluble GRASP65 mutant inhibited restacking of newly formed Golgi cisternae in this assay [15]. Consistent with this finding, microinjection of anti-GRASP65 antibodies into mitotic cells inhibited subsequent Golgi stack formation in the daughter cells [17]. Knockdown of the sole GRASP protein in Drosophila, dGRASP, and its interacting protein dGM130 led to the disassembly of the Golgi stacks into single cisternae and vesicles [115]. In one study, depletion of GRASP65 in mammalian cells reduced the number of cisternae per stack from 6 to 3 [118], although a separate study reported that knockdown of GRASP65 resulted in unlinking of the Golgi ribbon [22]. Further biochemical studies revealed that GRASP65 forms stable homodimers, and that homodimers residing on adjacent Golgi membranes form oligomers. These *trans*-oligomers are capable of holding the cisternal membranes together into stacks [17, 120]. Oligomerization is regulated by cdc2- and polo-like kinase (plk)-mediated

phosphorylation [90, 202]. Taken together, these results provided strong evidence that GRASP65 is essential for Golgi structure formation. However, as GRASP65 is localized only at the *cis* Golgi [16], the molecular machinery that links *medial-trans* cisternae into stacks remains unknown.

GRASP55, a homolog of GRASP65 primarily localized to the *medial-trans* cisternae, was identified by database searching [16]. As was the case for GRASP65, recombinant GRASP55 and anti-GRASP55 antibodies blocked the stacking of Golgi cisternae *in vitro*. GRASP55 exhibits a high level of sequence identity with GRASP65. Its N-terminal GRASP domain is 80% similar and 66% identical to that of GRASP65 in rat. Its C-terminal Serine/Proline-Rich (SPR) domain, like that of GRASP65, also contains a number of potential phosphorylation sites. The sequence similarity and distinct localizations suggest that two GRASP proteins may contribute to the stacking of different regions of the Golgi [203]. However, whether GRASP55 plays a direct role in stacking *in vivo* and what the underlying mechanism is remain unclear. In this study, we provide evidence that GRASP55 is directly involved in Golgi stacking in a manner similar to GRASP65, in particular that mitotically regulated *trans*-oligomerization of GRASP55 plays a role in *medial-trans* Golgi stack formation. Our results define the mechanism by which GRASP55 functions as a Golgi stacking factor and provide evidence that GRASP65 and GRASP55 function collaboratively to stack Golgi cisternal membranes.

Results

Knockdown of GRASP55 reduces the number of cisternae per stack

To determine the function of GRASP55 *in vivo*, we depleted GRASP55 in HeLa cells using an siRNA strategy published previously [23]. Both Western blotting and immunofluorescence microscopy showed that the knockdown efficiency was time-dependent. It was most efficient (> 98% reduction based on Western blotting) 96 hours (h) after transfection (Fig. 2.S1A-E). GRASP55-depletion had no effect on the expression level of other Golgi proteins, GRASP65, GM130, and Gos28. Using GM130 (Fig. 2.1A, B) and mannosidase II (ManII, not shown) as Golgi markers, no obvious change in Golgi morphology or localization was detected in majority of the cells. As light microscopy lacks the necessary resolution to determine Golgi stacking, we analyzed the cells by electron microscopy (EM). Cells transfected with GRASP55 siRNA exhibited a reduced number of cisternae in individual stacks (Fig. 2.1 F vs. E). The average number of cisternae per stack dropped from 5.7 ± 0.2 in cells transfected with control siRNA to 3.7 ± 0.1 in GRASP55-depleted cells (Fig. 2.1J). Most of the stacks in GRASP55-depleted cells contained 3-4 cisternae, a significant reduction from 5-6 in cells treated with control siRNA (Fig. 2.1K). Taken together, these results suggest that GRASP55 is involved in Golgi stacking *in vivo*.

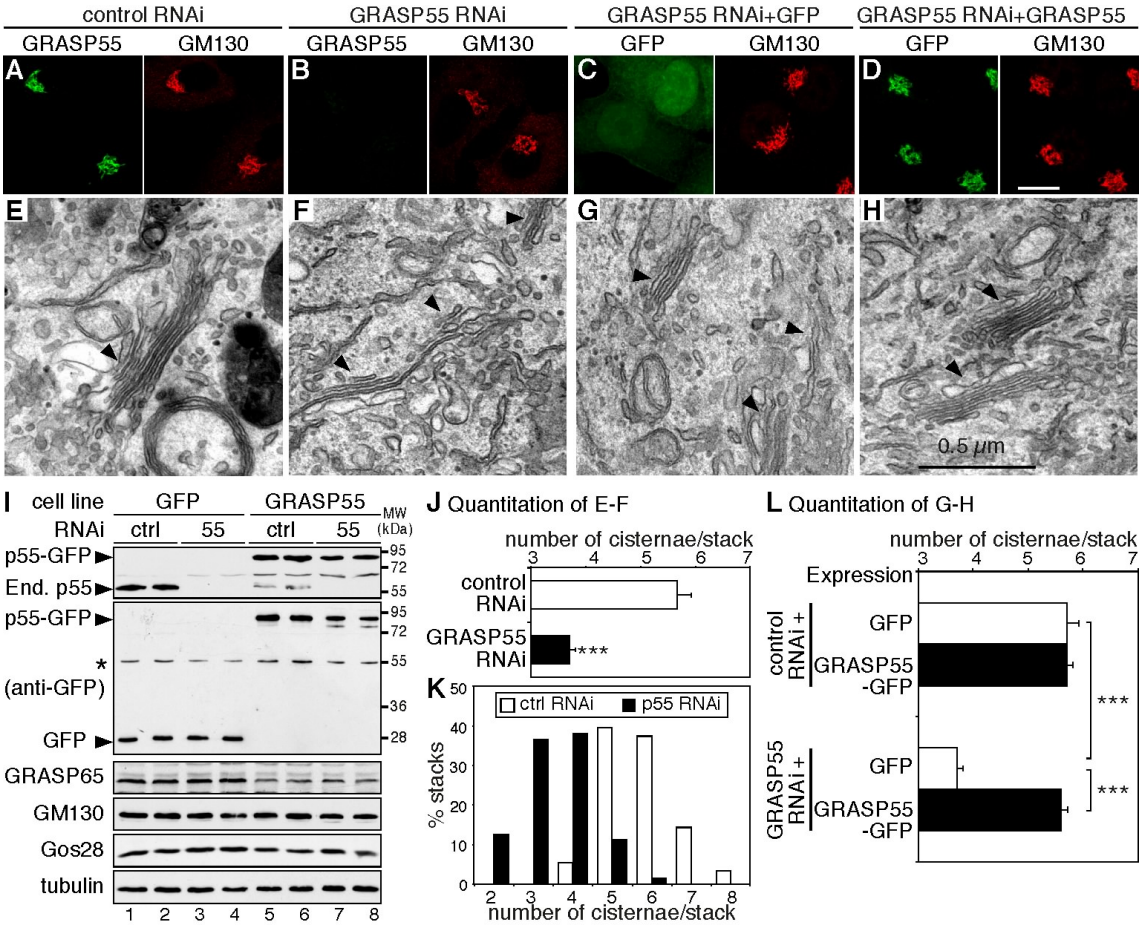

Figure 2.1. Knockdown of GRASP55 reduces the number of cisternae per stack. (A-B) Confocal fluorescence images of GRASP55 knockdown cells. HeLa cells transfected with indicated siRNA were fixed after 96 h and immunostained for GRASP55 and GM130. **(C-D)** Fluorescence images of HeLa cells in which endogenous GRASP55 was replaced by exogenous GRASP55. HeLa cells expressing GFP or rat GRASP55-GFP using an inducible retroviral expression system were transfected with control siRNA or siRNA specific for human GRASP55. Doxycycline was added 48h after transfection. Cells were fixed and stained for GM130. **(E-H)** Representative EM micrographs of cells described in A-D. Arrowheads indicate Golgi stacks. Note that the number of cisternae in the stacks was reduced in GRASP55 knockdown cells (F), which was restored by the expression of rat GRASP55 (H), but not by GFP (G). **(I)** Immunoblots of cells described in C-D. Duplicate samples were loaded; * indicates a non-specific band. End. p55, endogenous GRASP55. **(J)** Quantitation of the EM images in E-F from 3 sets of independent experiments. Results expressed as the mean ± SEM. **(K)** The numbers of cisternae per stack from one representative experiment were presented in a histogram format. Note that most stacks contained 5-6 cisternae in control RNAi cells, which was reduced to 3-4 in GRASP55 RNAi cells. **(L)** Quantitation of G-H. Note that GRASP55 knockdown significantly reduced the number of cisternae per stack, while expression of rat GRASP55 restored it. ***, $p<0.001$.

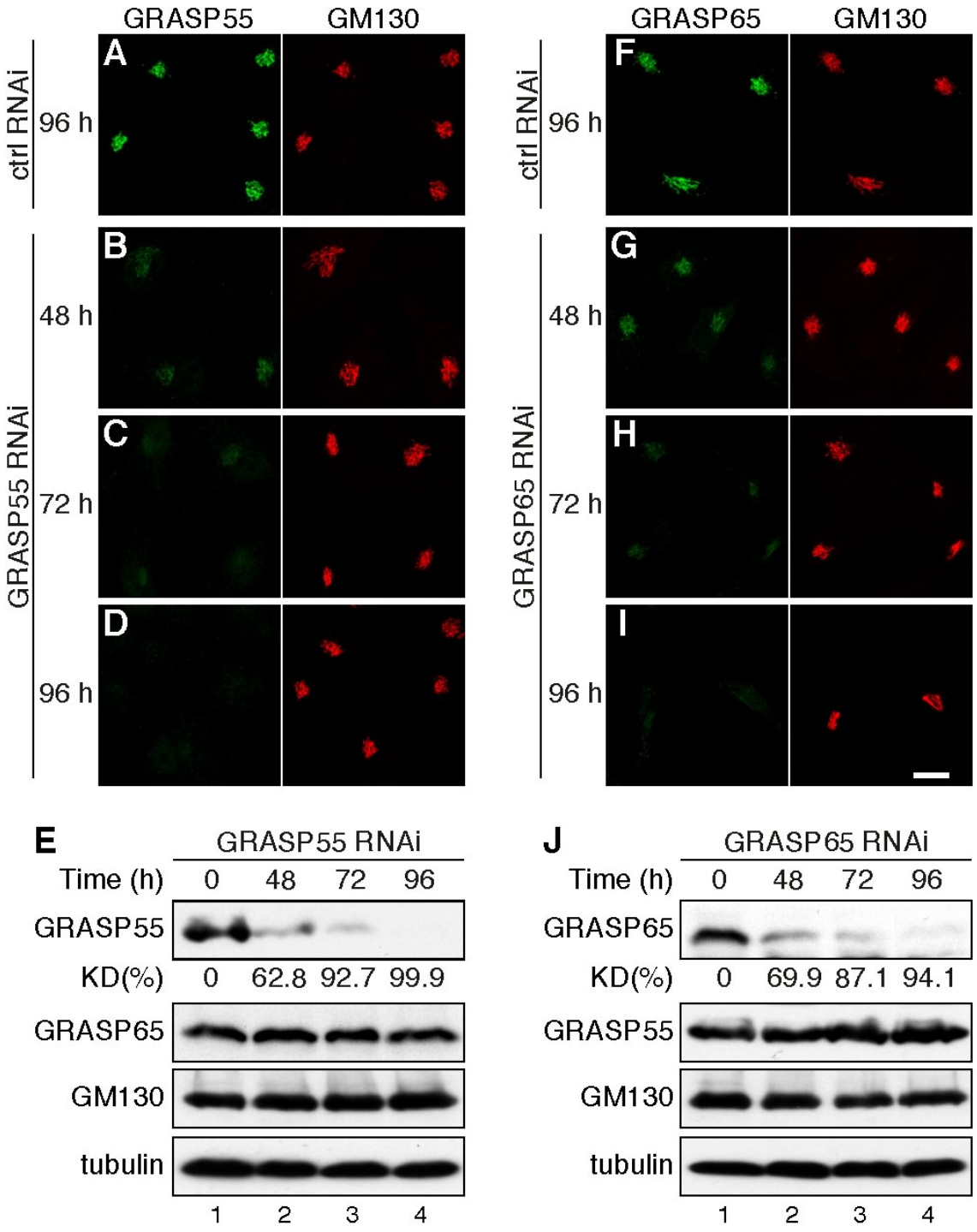

Figure 2.S1. Depletion of GRASP55 and GRASP65 over time. (A-D) Confocal fluorescence images of GRASP55 knockdown cells at different time points. HeLa cells transfected with control or GRASP55 siRNA were fixed at indicated time and immunostained for GRASP55 and GM130. **(E)** Immunoblot of HeLa cells transfected with GRASP55 siRNA for indicated time. The numbers below the GRASP55 blot indicate the percentage of protein depleted after siRNA transfection. **(F-I)** As in A-D, but with control or GRASP65 siRNA, and stained for GRASP65 and GM130. **(J)** As in E, with cells transfected with GRASP65 siRNA.

The effect of GRASP55 knockdown was rescued by expression of exogenous GRASP55

To ensure that the observed effects of GRASP55 siRNA on Golgi stacking were directly caused by GRASP55 depletion, we expressed rat GRASP55 in HeLa cells in which endogenous GRASP55 was depleted. We generated HeLa cell lines that stably expressed GFP-tagged rat GRASP55 using an inducible retroviral expression system [204]. This allowed us to control the expression time and the level of the exogenous protein and to avoid possible effects of continuous over-expression of this protein (or its mutants) on cell growth [29]. In addition, this approach ensured that all cells expressed rat GRASP55, thus permitting EM analysis. These cells were transfected with control or GRASP55 siRNA, and 48 h later, doxycycline was added to induce expression of rat GRASP55. In the presence of control siRNA, cells expressing rat GRASP55 showed little change in the expression of other Golgi markers, such as GM130 and Gos28, although the levels of endogenous GRASP55 and GRASP65 were reduced. The total GRASP55 in the cell line was about 2-fold that of endogenous GRASP55 in the GFP cell line (Fig. 2.1I). After transfection with siRNA targeted to human but not rat GRASP55, the endogenous GRASP55 was efficiently knocked down (> 98% depletion), while both rat GRASP55-GFP and GFP were well expressed (Fig. 2.1I). When examined under a confocal microscope, GRASP55-GFP colocalized with GM130, while GFP was cytosolic. Overall Golgi morphology was not significantly affected in cell lines expressing either GFP or rat GRASP55, with or without endogenous GRASP55 (Fig. 2.1C, D). When examined by EM, depletion of GRASP55 in the GFP cell line significantly reduced stacking (Fig. 2.1G). Expression of GRASP55-GFP restored the

average number of cisternae per stack to 5.6 ± 0.2 (Fig. 2.1H, L). These results confirmed that the reduced Golgi stacking was caused by GRASP55 depletion.

Effects of GRASP55-depletion on Golgi ribbon formation

Recently it was shown that GRASP55-depletion led to fragmentation of the Golgi ribbon [23], although this effect was not observed in a similar study by a different group [29]. To address this discrepancy, we carefully analyzed Golgi morphology in GRASP55-depleted cells by fluorescence microscopy. We divided the cells into 3 groups according to Golgi morphology (Fig. 2.2 A-C): 1) intact, with all the membranes linked in a compact structure; 2) mildly fragmented, with mini Golgi elements less connected, but still clustered and adjacent to the nucleus; and 3) scattered, with Golgi elements dispersed in the cytoplasm, as previously observed [23]. Using GM130, GRASP65 and Gos28 as Golgi markers, most cells treated with control siRNA (96-97%) had intact Golgi, with a small number of cells containing either mildly fragmented (~1%) or scattered (~1%) Golgi (Fig. 2.2D). Depletion of GRASP55 led to mild fragmentation of the Golgi in 22-24% of the cells (Fig. 2.2D). However, a majority (~75%) of the cells had intact Golgi, and the number of cells with scattered Golgi (1-2%) did not increase, indicating a mild effect of GRASP55-depletion on Golgi ribbon formation. To determine more precisely whether GRASP55-depletion affects the continuity of Golgi membranes, we performed fluorescence recovery after photobleaching (FRAP) analysis [23, 29]. HeLa cells were transfected with ManII-GFP 72 h after the initial siRNA transfection and analyzed 24 h later. A region of the Golgi was bleached with an argon laser at maximal intensity, and the recovery of fluorescence in this area was recorded for 480 s by time-

lapse imaging. As shown in Fig. 2.2 E-G, cells treated with GRASP55 siRNA exhibited a reduced recovery rate compared to cells treated with control siRNA. It is necessary to note that significant variation existed among cells with different Golgi morphologies (Fig. 2.2 A-C). Nevertheless, this experiment demonstrated that GRASP55-depletion affected the continuity of the Golgi membranes, indicating a role for GRASP55 in Golgi ribbon linking, which may be directly or indirectly caused by Golgi unstacking.

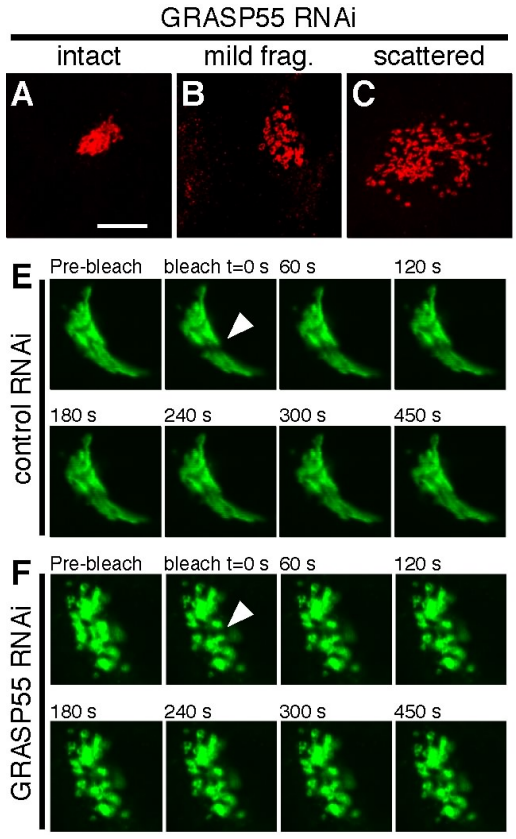

D % of cells with indicated Golgi morphology

RNAi	marker	intact	mild frag	scattered
control	GM130	97.4±0.1	1.2±0.1	1.3±0.2
	GRASP65	97.9±0.4	0.9±0.2	1.1±0.2
	Gos28	96.3±1.1	2.1±0.7	1.6±0.4
GRASP55	GM130	74.2±3.7	24.2±3.4	1.6±0.4
	GRASP65	75.2±2.3	23.2±2.3	1.6±0.1
	Gos28	76.3±1.5	21.9±1.8	1.6±0.4

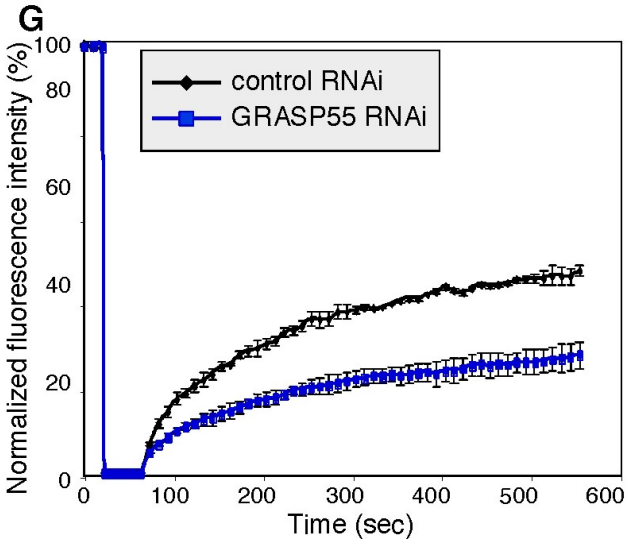

Figure 2.2. Effect of GRASP55-depletion on Golgi ribbon linking. (A-C) Enlarged confocal fluorescence images of the Golgi with classified morphology in GRASP55 knockdown cells stained for GM130. Bar = 10 µm. mild frag., mildly fragmented. **(D)** Quantitation (mean ± SEM) of classified Golgi morphology in HeLa cells treated with control or GRASP55 siRNA from 3 independent experiments. GM130, GRASP65 and Gos28 were used as Golgi markers and 300 cells were counted. **(E-F)** FRAP analysis of ManII-GFP-expressing HeLa cells transfected with indicated siRNAs. The indicated regions (arrows) were photobleached with laser pulses and fluorescence recovery was recorded. Representative images at indicated times are shown. Bar, 5 µm. **(G)** Quantitation of FRAP results. Fluorescence recovery was represented by the ratio of GFP fluorescence intensity in the bleached area to that of the entire Golgi. Normalization was set between the values before bleaching and the first time point after bleaching. Results represent mean ± SEM from two independent experiments, with more than 17 cells quantified in each case.

Knockdown of both GRASP55 and GRASP65 leads to disassembly of the entire Golgi stack

Because GRASP55 and GRASP65 localize to different compartments of the Golgi, we suspected that the two homologues might stack different parts of the Golgi, and therefore, knockdown of both proteins might lead to complete unstacking of the Golgi. To test this, we transfected HeLa cells with siRNAs for both GRASP55 and GRASP65. Both fluorescence microscopy (Fig. 2.3A, B) and Western blotting (Fig. 2.3C, F) showed that depletion of both proteins was efficient (~95%). We also noticed that the level of GM130 was reduced when both GRASPs were depleted, while Gos28 was unaffected (Fig. 2.3C). Using Gos28 (Fig. 2.3A, B) and GM130 (Fig. 2.S4K) as Golgi markers, simultaneous depletion of both GRASP proteins had only minor effects on organization and localization of the Golgi ribbon at the level of fluorescence microscopy, much as was seen with depletion of GRASP55 alone.

Strikingly, however, EM analysis showed that simultaneous depletion of GRASP55 and GRASP65 led to complete disassembly of the Golgi stacks (Fig. 2.3 D-E), an effect much more dramatic than depletion of GRASP55 or GRASP65 alone (Fig. 2.3F). The Golgi membranes were transformed into single cisternae (Fig. 2.3D, arrowheads) and tubulovesicular or dilated structures. There were no detectable normal Golgi stacks in most (>80%) cells that were examined. The effects of GRASP55/65 double depletion could be partially rescued by expression of GRASP55 (or its mutants) or GRASP65, as described later (Fig. 2.8). These data provide strong evidence that GRASP55 and GRASP65 play complementary and essential roles in Golgi cisternal stacking.

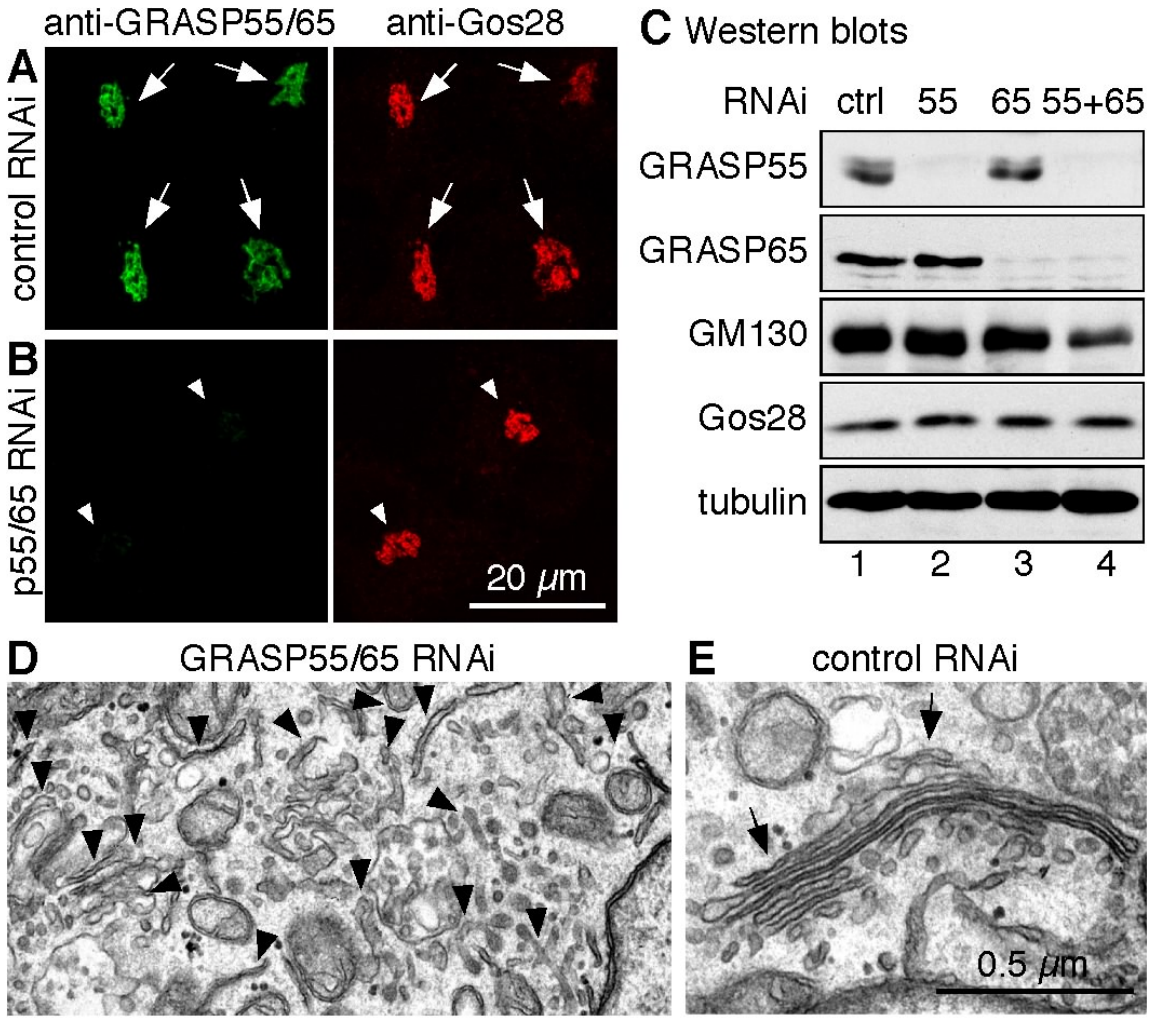

F Quantitation of knockdown efficiency and effects on Golgi stacking

RNAi	control	GRASP55	GRASP65	GRASP55 GRASP65
GRASP55 KD efficiency	—	98.4 ± 0.3%	—	95.5 ± 0.8%
GRASP65 KD efficiency	—	—	96.2 ± 2.9%	94.8 ± 4.1%
cisternal number/stack	5.7 ± 0.2	3.7 ± 0.1 *p<0.005*	3.8 ± 0.1 *p<0.005*	*

Figure 2.3. Depletion of both GRASP55 and GRASP65 leads to disassembly of the entire Golgi stack. **(A-B)** Confocal fluorescence images of GRASP55 and GRASP65 double knockdown cells. HeLa cells were transfected with a mixture of GRASP55 and GRASP65 siRNA (B) or with control siRNA (A). Cells were fixed and immunostained for both GRASP55 and GRASP65 (anti-GRASP55/65), and for Gos28. **(C)** Immunoblots of HeLa cells transfected with indicated siRNA. **(D-E)** Representative EM micrographs of cells transfected with indicated siRNAs. Arrowheads in D indicate single cisternae and Golgi fragments. Arrows in E indicate normal Golgi stacks. **(F)** Quantitation (mean ± SEM) of GRASP55 and GRASP65 knockdown efficiency and effects on Golgi stacking from 3 independent experiments. Statistical significance was assessed by comparison with the control siRNA cells. *, double knockdown cells were not quantified due to the complete disassembly of the Golgi stacks.

GRASP55 is phosphorylated by MAP kinase during mitosis

We next addressed the molecular mechanisms of GRASP55 function in Golgi stacking. We hypothesized that, as in the case of GRASP65, cell cycle-regulated GRASP55 phosphorylation may be essential for Golgi disassembly during mitosis and reassembly in telophase and cytokinesis. Phosphorylation of GRASP55 in the cell cycle was first confirmed by [γ-^{32}P] ATP labeling (Fig. 2.S3A). We then developed a band-shift assay to analyze GRASP55 phosphorylation. When Golgi membranes were treated with mitotic cytosol (MC), GRASP55 exhibited a sharp decrease in mobility on SDS-PAGE. This shift was caused by phosphorylation, because treatment of mitotic Golgi fragments (MGF) with calf intestine alkaline phosphatase (CIP), a non-specific protein phosphatase, largely restored the original SDS-PAGE mobility. The mobility shift was abolished by adding β-glycerophosphate, a general phosphatase inhibitor (β-GP, Fig. 2.4B). Unlike GRASP65 [17, 123], GRASP55 was not phosphorylated by plk and was only slightly phosphorylated by cdc2 (Fig. 2.4C). Treatment of Golgi membranes with a combination of mitogen-activated protein kinase ERK2 and constitutively active MEK1 (Mitogen-activated protein kinase kinase 1) shifted GRASP55 to a similar extent as MC, consistent with previous reports that GRASP55 is phosphorylated by ERK2 [125]. Phosphorylation of GRASP55 by ERK2 was confirmed using both recombinant GRASP55 and endogenous GRASP55 in cell lysates (Fig. 2.S3 B-D). In addition, GRASP55 phosphorylation was inhibited by the MEK1 inhibitor U0126 and was reversed when mitotic Golgi fragments were treated with interphase cytosol (Fig. 2.S3 C-E). These data suggest that GRASP55 is subjected to phosphorylation and dephosphorylation during the cell cycle.

The phosphorylation sites on GRASP55 are located in the C-terminal SPR-domain

GRASP55 contains an N-terminal GRASP domain (aa1-212) and a C-terminal SPR domain (aa213-454) (Fig. 2.4A). To identify the phosphorylation sites, recombinant GRASP55 fragments were treated with mitotic or interphase cytosol and analyzed by the band-shift assay. As shown in Fig. 2.4D, no mobility shift was observed for the GRASP domain when treated with MC, while the SPR domain exhibited a sharp band shift. In addition, deletion of a portion of the SPR domain, aa213-231, significantly reduced the molecular weight shift (Fig. 2.4D), indicating that this segment contains a majority of the phosphorylation sites, or that it may function as a prerequisite for phosphorylation of other sites.

To map more precisely the phosphorylation sites in the SPR domain, potential phosphorylation sites, T222, T225, S245, T249 and T435, some of which were previously identified [29, 125], were mutated to alanines, either individually or in combination. As shown in Fig. 2.4E, phosphorylation of GRASP55 by mitotic cytosol was largely abolished when T222 and T225 were mutated, and further mutation of S245 or T249 almost completely abolished the phosphorylation. Mutation of T435 had no detectable effect on GRASP55 phosphorylation. These data suggest that S245, T249, and particularly T222 and T225, are the key phosphorylation sites on GRASP55 during mitosis. As shown below, a T222A/T225A/S245A mutant was constructed to probe GRASP55 function *in vitro* and *in vivo*. In addition, T222 and T225 were also mutated to glutamates to mimic the phosphorylated state of the protein (Fig. 2.4E).

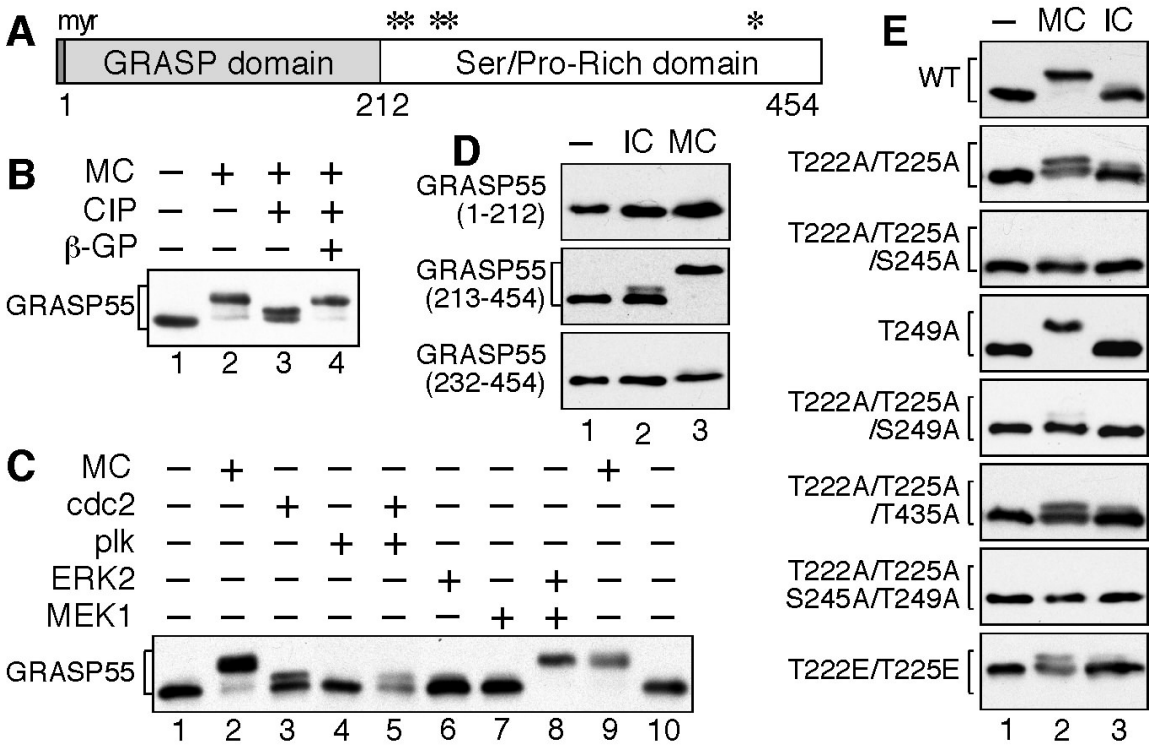

Figure 2.4. GRASP55 is phosphorylated during mitosis. (A) GRASP55 schematic with phosphorylation sites indicated. Predicted phosphorylation sites (T222, T225, S245, T249, T435) are indicated by asterisks. myr: myristoylated N-terminal glycine. **(B)** Detection of GRASP55 phosphorylation using a band-shift assay. Golgi membranes were either treated with buffer (lane 1) or mitotic cytosol (MC, lanes 2-4). Membranes were re-isolated and further treated with calf intestine alkaline phosphatase (CIP) in the absence (lane 3) or presence (lane 4) of a general phosphatase inhibitor, β-glycerophosphate (β-GP). Note the increase in molecular weight of GRASP55 under mitotic conditions was reversed by CIP. **(C)** GRASP55 phosphorylation by ERK2. Golgi membranes were incubated with indicated proteins followed by Western blotting. Note that ERK2 /MEK1 phosphorylated GRASP55 to a similar extent as MC. **(D)** The mitotic phosphorylation sites of GRASP55 are in the SPR domain. GST-tagged GRASP55 constructs were incubated with buffer (lane 1), or interphase (IC, lane 2) or mitotic (MC, lane 3) cytosol and analyzed by immunoblotting. Note that the SPR domain (213-454), but not the GRASP domain (1-212), exhibited a band shift after MC treatment, while deletion of aa213-231 largely abolished the phosphorylation. **(E)** Mapping the phosphorylation sites of GRASP55. Potential sites (asterisks in A) in His-GRASP55 were mutated to alanines or glutamates and the purified proteins were analyzed as in D.

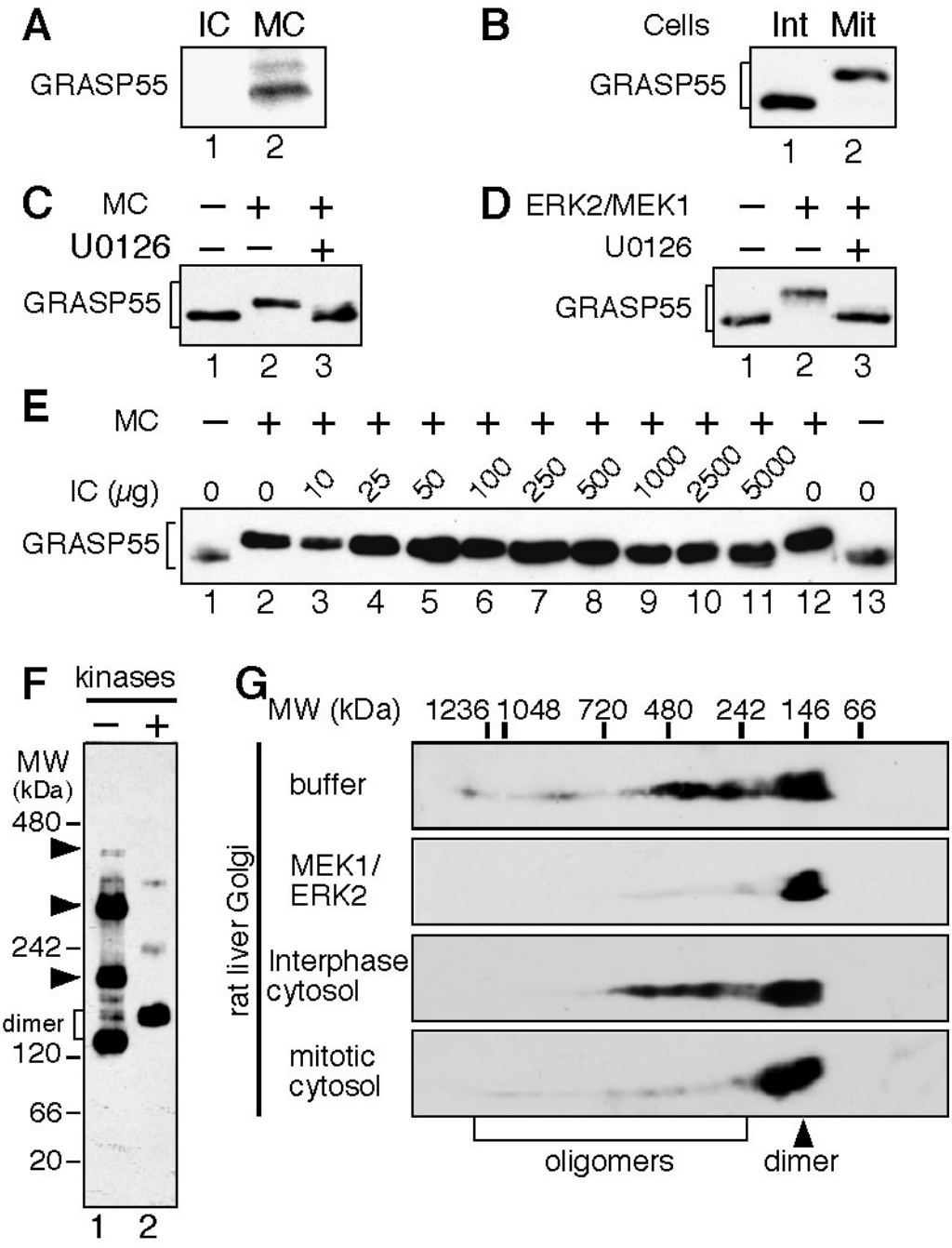

Figure 2.S3. GRASP55 phosphorylation, dephosphorylation and oligomerization. (A) Phosphorylation of native GRASP55 by mitotic cytosol. Purified Golgi membranes were incubated in the presence of [γ-32P]ATP with either interphase (IC, lane 1) or mitotic cytosol (MC, lane 2). GRASP55 was immunoprecipitated from solubilized membranes and analyzed by SDS-PAGE and autoradiography. **(B)** GRASP55 phosphorylation in mitotic cells. Interphase (non-synchronized) or mitotic HeLa cells synchronized by nocodozole were analyzed by Western blotting. **(C)** Inhibition of GRASP55 phosphorylation by U0126. Purified Golgi membranes were incubated with buffer (lane 1) or MC in the absence (lane 2) or presence (lane 3) of U0126. **(D)** Inhibition of GRASP55 phosphorylation by MAPK with U0126. Purified Golgi membranes were incubated with buffer (lane 1) or ERK2/MEK1 in the absence (lane 2) or presence (lane 3) of U0126. **(E)** Dephosphorylation of endogenous GRASP55. Purified Golgi membranes (4 μg) were first treated with MC (400 μg) as indicated. Membranes were reisolated by

centrifugation through a 0.4 M sucrose cushion and further incubated with increasing amount of interphase cytosol (IC) and immunoblotted for GRASP55. Note the downshift of the GRASP55 band after the treatments. **(F)** Longer time exposure of Figure 5B of a non-reducing gel probed for GRASP55. **(G)** Two dimensional gels to analyze oligomerization of native GRASP55. Purified Golgi membranes were treated as indicated and solubilized. Samples were analyzed by first dimensional non-denaturing gels followed by second dimensional denaturing gels and Western blotting for GRASP55. Note that the high molecular weight structures can be seen with no treatment or interphase incubation, but not with mitotic cytosol or kinase treatment.

GRASP55 forms higher order oligomers in a cell cycle-dependent manner

In analogy to GRASP65, we hypothesized that the stacking activity of GRASP55 might involve dimerization and oligomerization [17, 120]. To test whether GRASP55 interacts with itself, MBP-GRASP55 and His-GRASP55 recombinants were separately purified, mixed and incubated with either buffer or mitotic cytosol. Protein complexes were isolated using nickel beads for His-GRASP55, or amylose beads for MBP-GRASP55, and analyzed by SDS-PAGE and immunoblotting for GRASP55. As shown in Fig. 2.5A, the two tagged forms co-purified under control conditions, but this was abolished by treatment with mitotic cytosol, regardless of the beads that were used, indicating that GRASP55 interacts with itself and that this interaction is abolished by mitotic cytosol.

Oligomerization of GRASP55 was also analyzed by electrophoresis on non-denaturing gels. As shown in Fig. 2.5B, His-GRASP55 exhibited four bands, with apparent molecular weights of 130, 194, 288 and 418 kDa, respectively (lane 1, arrowheads). These bands were more visible after longer exposure (Fig. 2.S3F). Because the apparent molecular weight of the most rapidly migrating band was twice that of GRASP55 on denaturing gels (64 kDa), this result suggested that GRASP55 formed both homodimers and higher oligomers. After kinase treatment, His-GRASP55 exhibited only one major band (139 kDa), most likely representing the phosphorylated dimer. All

of these bands were shown by analysis on second dimensional denaturing gels to correspond to GRASP55 rather than contaminants (data not shown). Similar experiments showed that the endogenous GRASP55 in Golgi membranes formed oligomers under interphase conditions, but remained as dimers when the Golgi membranes were treated with ERK2/MEK1 or mitotic cytosol (Fig. 2.S3). Further analysis by gel filtration and protein cross-linking also confirmed this conclusion (data not shown). Taken together, these results demonstrate conclusively that GRASP55 forms phosphorylation-regulated oligomers.

Trans-oligomerization of GRASP55 is sufficient to link surfaces together

We then used an established bead assay [17] to test whether GRASP55 oligomers could link adjacent Golgi cisternae. Purified GRASP55, or bovine serum albumin (BSA), was covalently linked to the surface of magnetic Dynal beads. After treatment with BSA solution (control), interphase cytosol (IC) or mitotic cytosol (MC), beads were placed on glass slides and observed under bright-field illumination. As shown in Fig. 2.5C, GRASP55-coated beads aggregated after BSA treatment (27.7 ± 1.5%). Aggregation was enhanced upon IC treatment (85.7 ± 5.5%), but inhibited by MC (2.4 ± 1.4%). In contrast, BSA-coated beads did not aggregate regardless of the treatment (Fig. 2.5C, E). To test whether the aggregation was regulated by phosphorylation, we sequentially treated GRASP55-coated beads with IC followed by MC (IC→MC) or purified ERK2/MEK1 kinases (IC→K). Both treatments led to disaggregation of the beads (22.6 ± 8.3% and 14.1±12.9%, respectively, Fig. 2.5D, E).

To determine the effect of GRASP55 phosphorylation on stacking of Golgi membranes, we treated purified Golgi stacks with these kinases (Fig. 2.5F) and quantified the EM images. 47.4 ± 2.6% of the cisternae were found in stacks when Golgi membranes were treated with buffer alone. Treatment with either ERK2 or MEK1 slightly reduced the percentage of cisternae in stacks (30.6 ± 2.2 % for ERK2; 33.1 ± 7.5% for MEK1). This reduction may result from the weak kinase activity of wild type ERK2, or the activation of membrane-bound ERK kinase by the addition of constitutively active MEK1 [92, 205]. When Golgi membranes were incubated with both ERK2 and MEK1 together, the percentage of cisternae in stacks dropped to 10.6 ± 2.5%, a level similar to cdc2/plk treatment (14.8 ± 3.0%) that resulted in GRASP65 phosphorylation [17]. When the four kinases were all included in the reaction, the percentage of cisternae in stacks was reduced to 8.6 ± 2.3% (Fig. 2.5F). It is necessary to note that the effects of ERK2/MEK1 treatment may also be partially due to GRASP65 phosphorylation, as ERK2 also phosphorylates GRASP65, at least on S277 [27, 206]. Nevertheless, these results show that phosphorylation of Golgi proteins such as GRASP55 by ERK2/MEK1 leads to Golgi membrane unstacking.

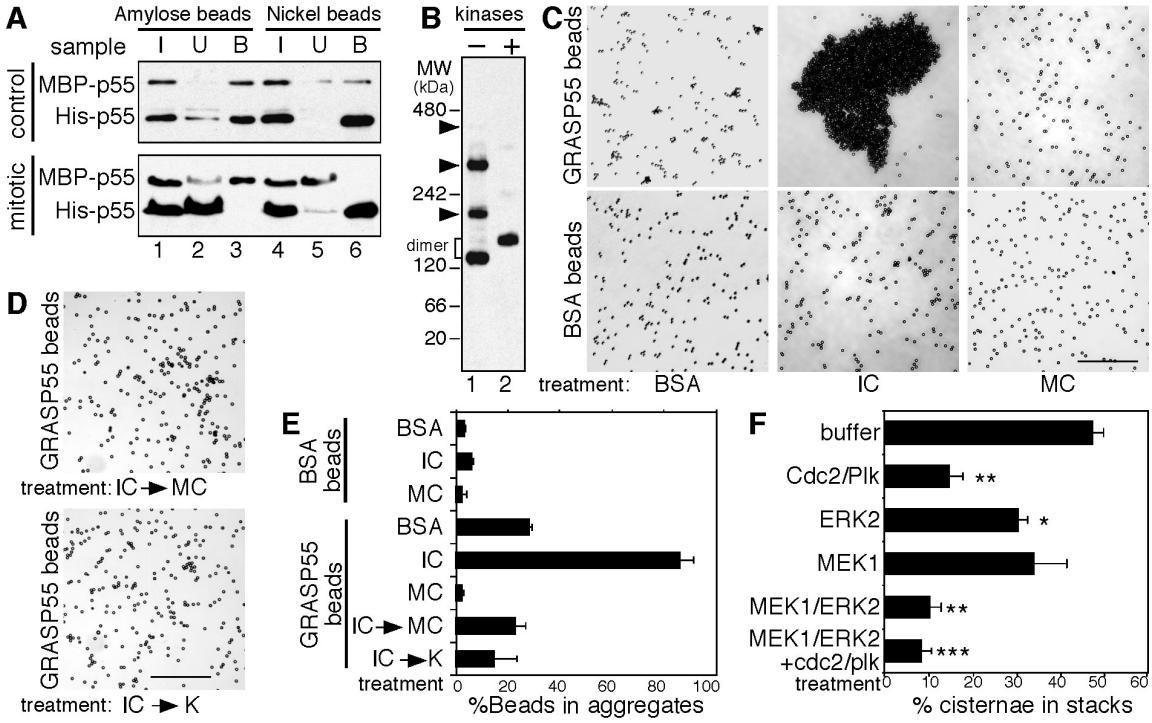

Figure 2.5. Cell cycle regulated GRASP55 oligomerization is sufficient to link adjacent surfaces. (A) Co-purification of MBP-GRASP55 and His-GRASP55. Differently tagged proteins were separately purified, mixed and incubated in the presence of buffer (control) or mitotic cytosol (mitotic). The protein complex was isolated using either amylose (lanes 1-3) or nickel beads (lanes 4-6). Equal proportions of input (I), unbound (U) or bound (B) fractions were analyzed by immunoblotting for GRASP55. Note the co-purification of the two proteins under control but not mitotic conditions. **(B)** Analysis of GRASP55 oligomerization by non-denaturing gels. His-GRASP55 was incubated in the absence (–, lane 1) or presence (+, lane 2) of ERK2/MEK1 kinases followed by non-denaturing electrophoresis and Western blotting. Molecular weight standards are indicated on the left. Note that the higher molecular weight bands in lane 1 (arrowheads) diminished after kinase treatment. **(C)** Aggregation of GRASP55 coated beads. Purified His-GRASP55 or BSA was covalently coupled to the surface of magnetic Dynal beads and incubated with bovine serum albumin (BSA), interphase cytosol (IC), or mitotic cytosol (MC). After incubation the beads were placed on glass slides and random fields photographed. A representative image of each condition is shown. Note that GRASP55 coated beads aggregated slightly in the presence of BSA; this was enhanced by IC, but inhibited by MC. **(D)** As in (C) except that GRASP55 beads were first aggregated using IC and then treated with either MC (IC→MC) or with purified ERK2/MEK1 kinases (IC→K). Note that aggregates were reversibly disassembled by MC and kinases. Bar, 100 μm. **(E)** Quantitation (mean ± SEM) of C-D, n=3. **(F)** Treatment of Golgi membranes with purified kinases leads to cisternal membrane unstacking. Purified Golgi stacks were treated with either buffer or indicated kinases, and analyzed by EM. Shown are the quantitation results from a representative experiment. Statistical significance was assessed by comparison of kinase treatment with buffer treatment. *, $p \leq 0.05$; **, $p \leq 0.01$; ***, $p \leq 0.001$.

Mapping the domain structure of GRASP55 for oligomerization and mitotic regulation

To map the domain of GRASP55 required for oligomerization, purified GRASP domain (aa1-212, His-tagged) was coupled to the surface of Dynal magnetic beads and

sequentially treated with interphase cytosol (IC) and mitotic cytosol (MC). These beads aggregated extensively upon IC treatment (70.6 ± 3.2%), but the aggregates were not dispersed by MC (79.4 ± 4.7%, Fig. 2.6A, E). Further experiments using gel filtration confirmed that the GRASP domain alone could form oligomers (data not shown). In addition, when a soluble form of the GRASP domain, or full-length GRASP55 (FL), was added into the reaction, it inhibited aggregation of beads coated with full length GRASP55. The percentage of aggregated beads dropped from 76.3 ± 6.1% to 20.6 ± 3.6% with FL-GRASP55 and to 20.5 ± 7.6% with the GRASP domain. In contrast, the SPR domain (aa213-454) had no significant effect (67.5 ± 8.0%, Fig. 2.6D, G). These results demonstrate that the GRASP domain alone is sufficient for oligomerization and that its oligomerization is not mitotically regulated.

We then determined the phosphorylation sites that regulate GRASP55 oligomerization. Beads coated with the non-phosphorylatable T222A/T225A/S245A mutant formed aggregates upon IC treatment (83.5 ± 6.0%), and the aggregates largely remained after further treatment with MC (80.3 ± 5.7%, Fig. 2.6B, E). In contrast, beads coated with the T222E/T225E mutant aggregated slightly when treated with IC (28 ± 10.2%), a level significantly reduced compared to beads coated with wild type GRASP55 (85.7 ± 5.5%, Fig. 2.6C, F). Taken together, these data demonstrate that the GRASP domain of GRASP55 is both necessary and sufficient for oligomerization, while the SPR domain plays a role in mitotic regulation.

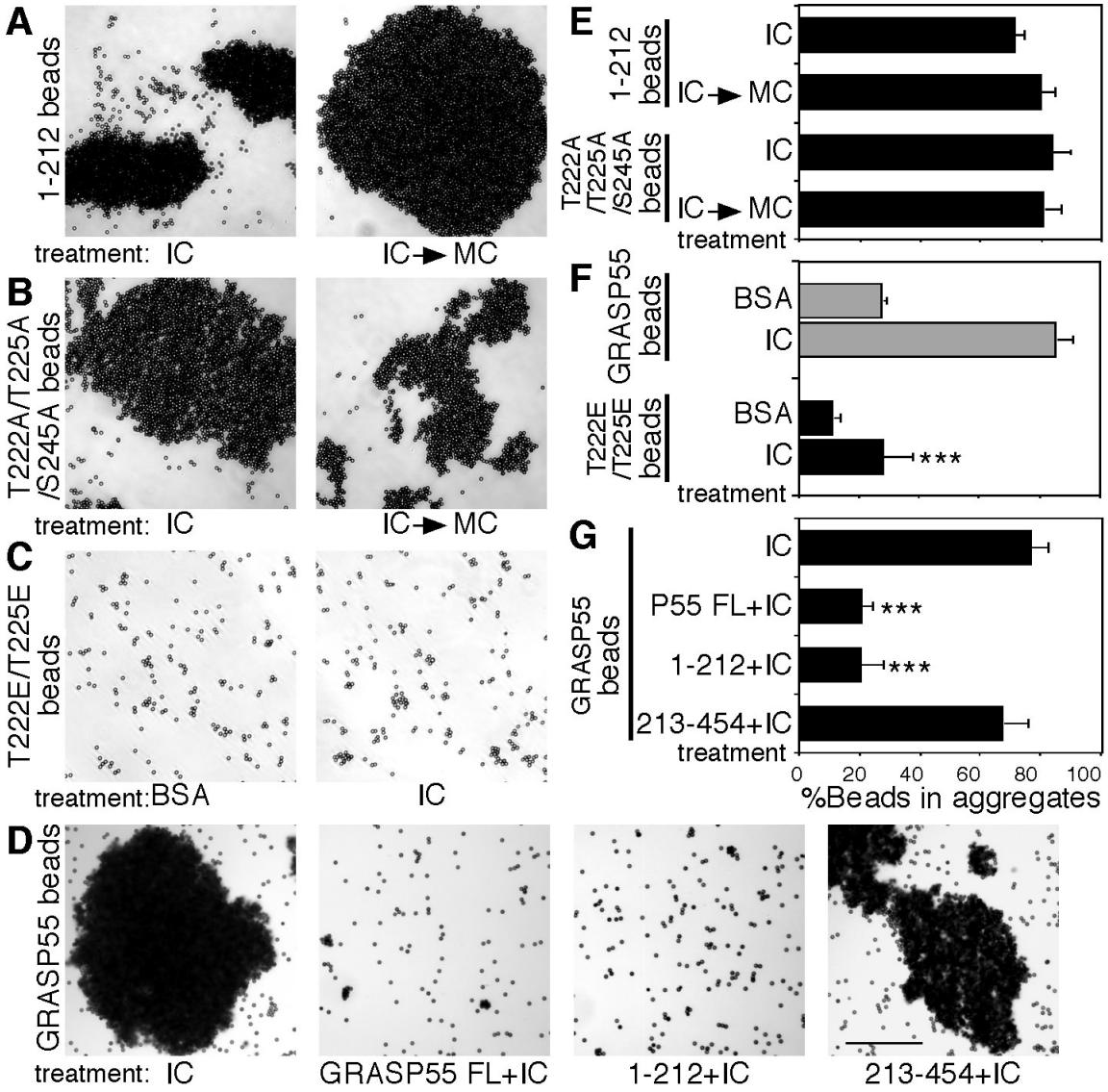

Figure 2.6. Mapping the domain structure of GRASP55 for oligomerization and mitotic regulation. **(A)** Purified His-tagged GRASP domain (1-212) was coupled to Dynal beads and sequentially incubated with interphase cytosol (IC) and mitotic cytosol (IC→MC). Note that aggregates of beads formed by IC treatment were not dispersed by MC. **(B)** As in (A) using the T222A/T225A/S245A mutant. Beads aggregated under both conditions. **(C)** Beads coated with the T222E/T225E mutant were incubated with BSA or IC. Note that beads did not aggregate after IC treatment. **(D)** Wild type GRASP55-coupled beads were incubated with IC in the presence of soluble full length (FL) GRASP55, the GRASP domain (1-212), or the SPR domain (213-454) recombinants. Bar, 100 µm. Note that the aggregation was suppressed by the soluble full length protein and the GRASP domain, but not by the SPR domain. **(E)** Quantitation of A-B from 3 independent experiments (mean ± SEM). **(F)** Quantitation of C. Aggregation of the beads coupled with the T222E/T225E mutant was significantly reduced compared to those coated with wild type GRASP55 when treated with interphase cytosol (IC). **(G)** Quantitation of D. **, $p \leq 0.01$; ***, $p \leq 0.001$.

Expression of non-phosphorylatable GRASP55 mutants enhances Golgi stack formation in interphase cells

To test the function of GRASP55 *in vivo*, we generated HeLa cell lines that stably expressed various rat GRASP55 constructs using an inducible promoter [204]. Western blot analysis showed that each of the constructs was expressed at relatively equivalent levels upon doxycycline induction (Fig. 2.7H). Fluorescence microscopy showed that the GFP-tagged wild type GRASP55, the GRASP domain, and the T222A/T225A/S245A and the T222E/T225E mutants localized to the Golgi in interphase cells, as shown by co-staining for GRASP65 (Fig. 2.S4, A-F) and GM130 (data not shown). The SPR domain lacked a Golgi localization signal and was largely cytoplasmic. Expression of GRASP55 and its mutants did not significantly affect the overall organization of the Golgi as judged by fluorescence microscopy.

When examined by EM, however, alignment of the cisternal membranes was improved in cells expressing the GRASP domain or the non-phosphorylatable T222A/T225A/S245A mutant compared to cells expressing GFP alone (Fig. 2.7, C and D vs. A). The number of cisternae per stack increased from 5.7 ± 0.2 in cells expressing GFP to 6.9 ± 0.1 and 6.7 ± 0.1 in cells expressing the GRASP domain or the T222A/T225A/S245A mutant, respectively (Fig. 2.7G). Expression of wild type GRASP55 (5.7 ± 0.1), the T222E/T2225E mutant (5.5 ± 0.1) or the SPR domain (5.5 ± 0.1) did not significantly affect the number of cisternae per stack.

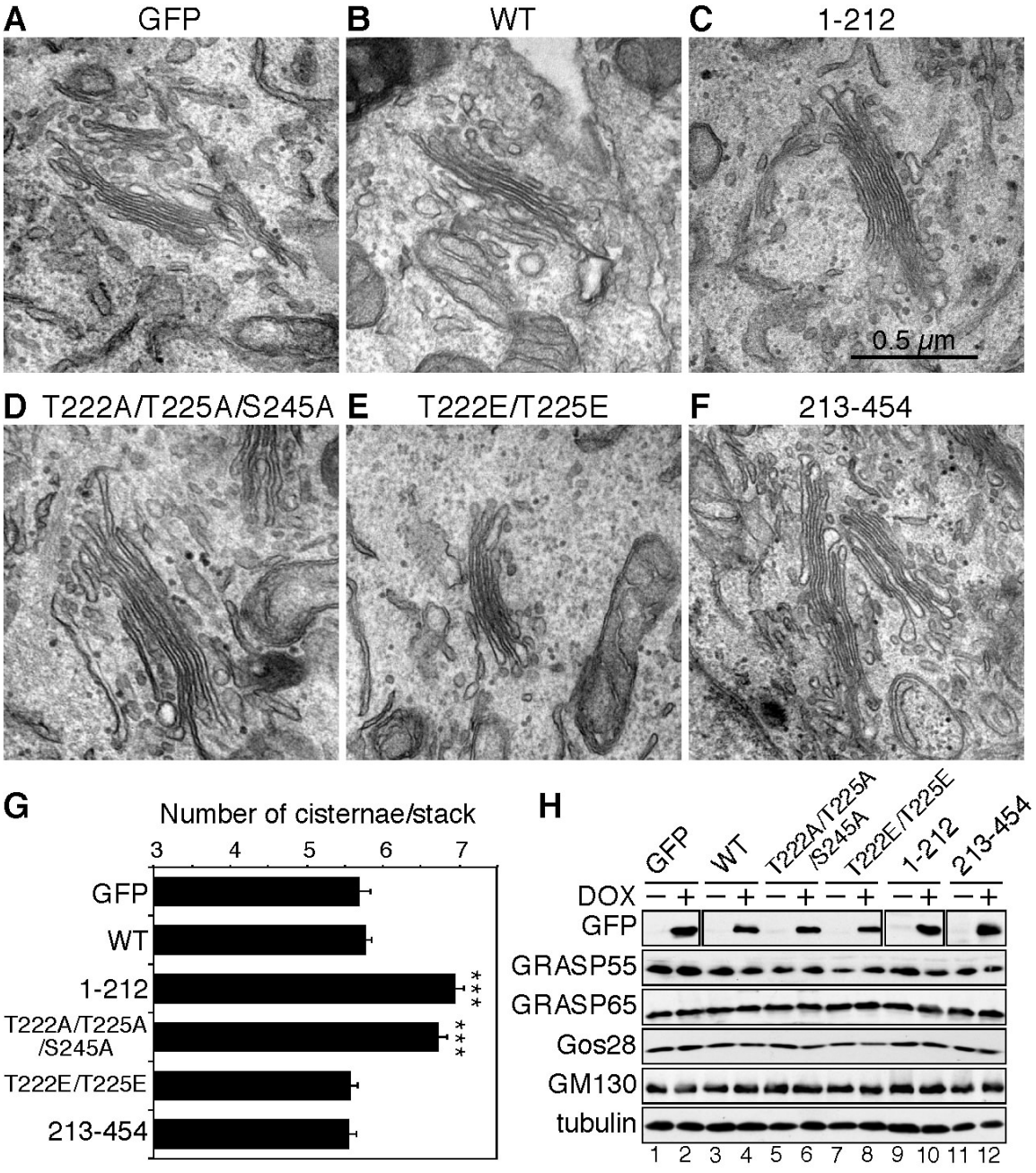

Figure 2.7. Over expression of non-regulatable GRASP55 mutants enhances Golgi stack formation in interphase cells. (A-F) Representative EM images of interphase cells expressing indicated GRASP55 constructs. Bar, 0.5 µm. Note that the Golgi structures in cells expressing the GRASP domain (C) and the T222A/T225A/S245A mutant (D) are better organized than those in the GFP cell line (A). **(G)** Quantitation (mean ± SEM) of 20 cells from conditions indicated in A-F. Statistical significance was assessed by comparison to the GFP cell line. ***, *p<0.001*. **(H)** Cells in A-F were lysed in SDS-buffer and analyzed by Western blotting.

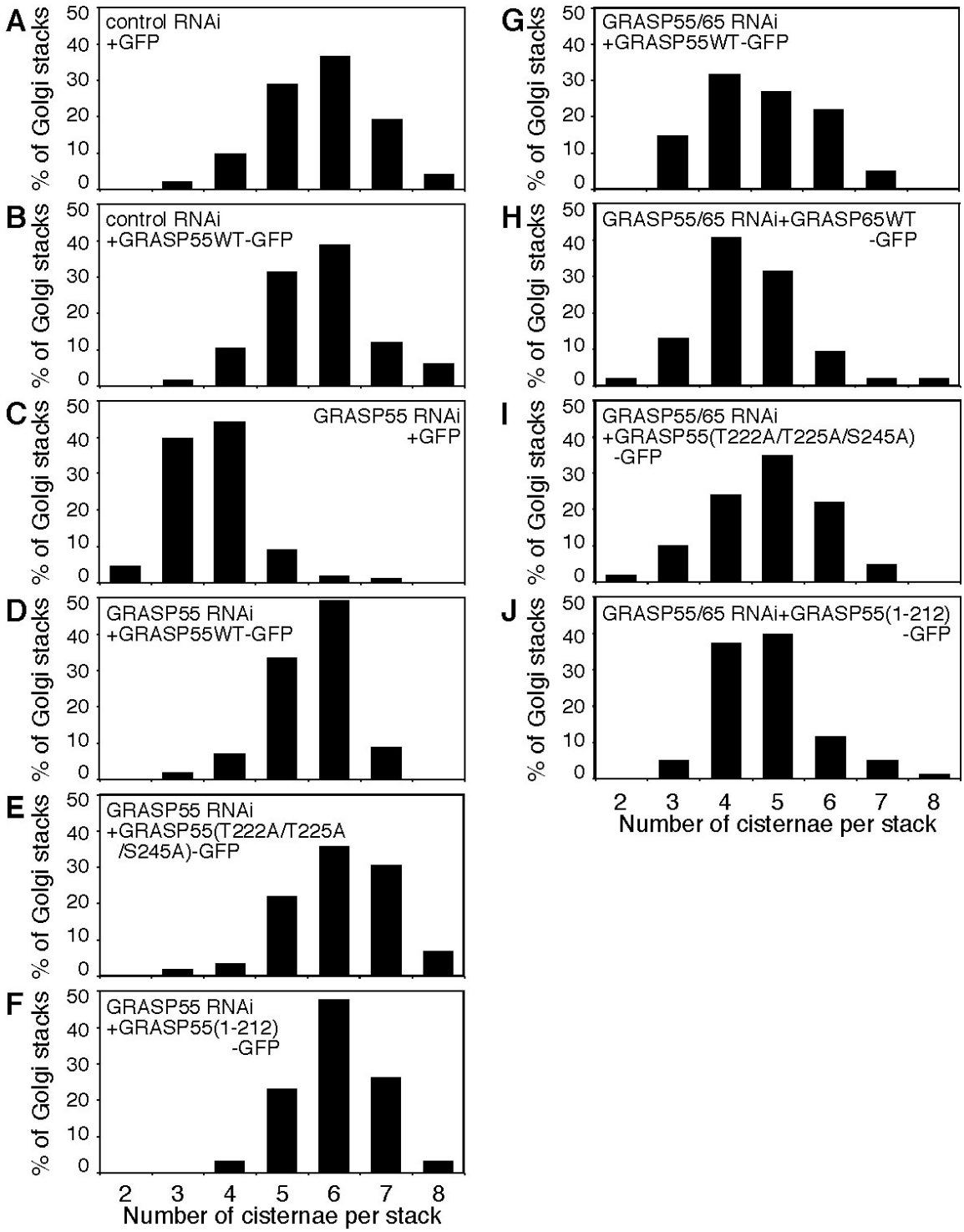

Figure 2.S2. Histogram presentation of the number of cisternae per stack in cells with indicated treatments. (A-F) HeLa cell lines were transfected with control or GRASP55 siRNA for 48 h followed by 48 h induction to express the indicated proteins. Cells were processed for EM and quantitation of the EM results for the number of cisternae in the stacks was expressed in the histograms. **(G-J)** As in A-F, but with both GRASP55 and GRASP65 depleted.

Rescue of the Golgi structure in GRASP55 and GRASP65-depleted cells by expression of wild type or mutant GRASP55 and GRASP65

Further experiments showed that Golgi structure in GRASP55-depleted cells could be rescued by expressing GRASP55 or its mutants (Fig. 2.S5). Expression of the GRASP domain or the T222A/T225A/S245A mutant increased the average number of cisternae per stack to 6.0 ± 0.1 and 6.1 ± 0.1, respectively, slightly higher than expression of wild type GRASP55 (5.6 ± 0.1).

To understand whether GRASP55 and GRASP65 have redundant functions in Golgi stacking, we tested whether expression of a single GRASP protein (or its mutant) could rescue Golgi structure in cells with both GRASPs depleted. By fluorescence microscopy, all the exogenous GRASP constructs were localized at the Golgi in the absence of endogenous proteins (Fig. 2.S4, K-O). When examined by EM, Golgi stacks were observed in most cells expressing exogenous GRASP proteins, but not in cells expressing GFP. The number of cisternae per stack was 4.7 ± 0.2 and 4.5 ± 0.2 in cells expressing wild type GRASP55 and GRASP65, respectively (Fig. 2.8), suggesting that expression of a single GRASP protein can only partially rescue the phenotype caused by the depletion of both endogenous GRASP proteins. Expression of the GRASP domain (5.2± 0.2) and the T222A/T225A/S245A mutant (4.9 ± 0.2) of GRASP55 rescued Golgi stacking to a greater extent than expression of the wild type protein, but rescue was still incomplete. These results indicate that the GRASP proteins have complementary functions in Golgi stacking in mammalian cells.

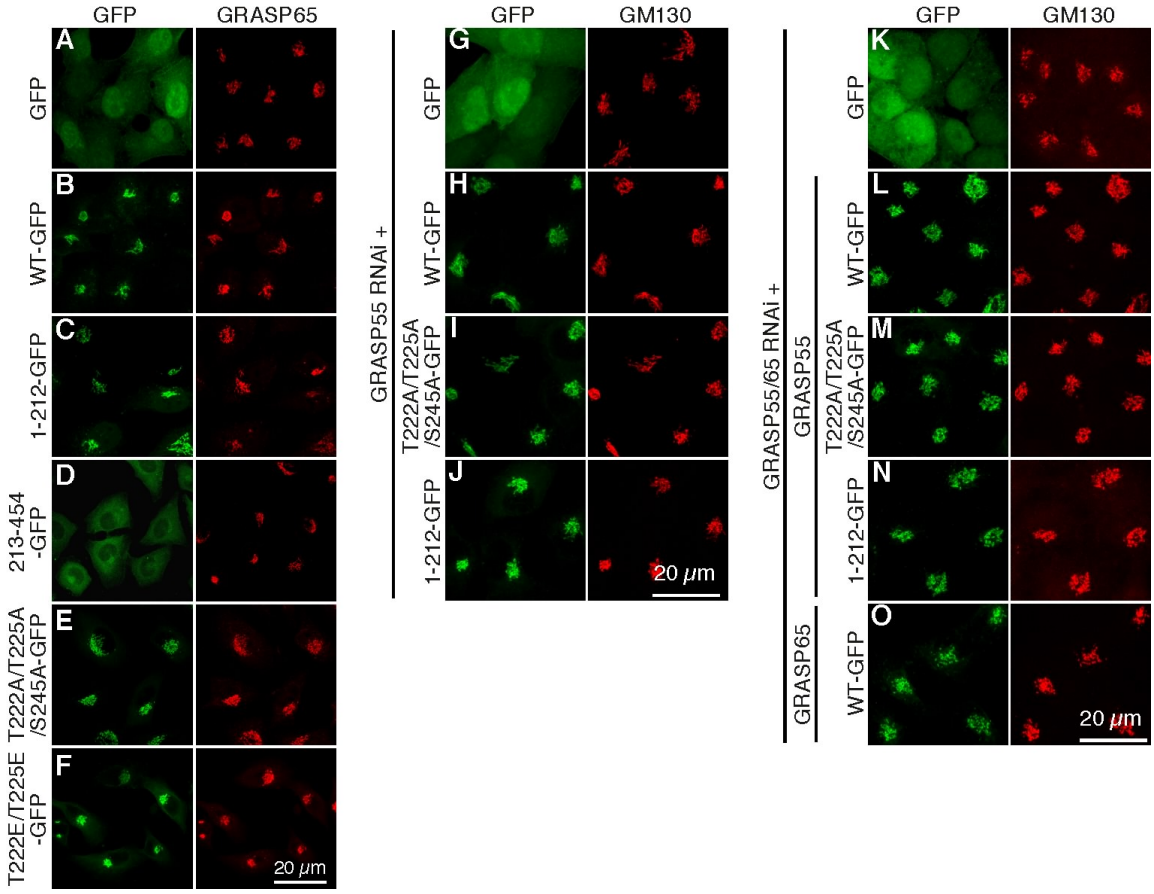

Figure 2.S4. Confocal images of HeLa cells expressing GFP-tagged GRASP55 or GRASP65, or/and transfected with indicated siRNA. (A-F) Expression of GRASP55 and its mutants does not affect Golgi morphology. Interphase HeLa cells stably expressing indicated GRASP55 constructs using an inducible retroviral expression system were treated with 1 μg/ml doxycycline for 48 h. Cells were fixed, stained for GRASP65 and observed by confocal microscopy. Note that the expressed GRASP55 constructs, except the SPR domain, are localized on the Golgi membranes. Scale bar, 20μm. **(G-J)** Expression of GFP-tagged GRASP55 and its mutants in GRASP55-depleted HeLa cells. Cells were stained for GM130. **(K-O)** Expression of GFP-tagged GRASP55 and its mutants or GRASP65 in HeLa cells with both endogenous GRASP55 and GRASP65 depleted. WT, wild type.

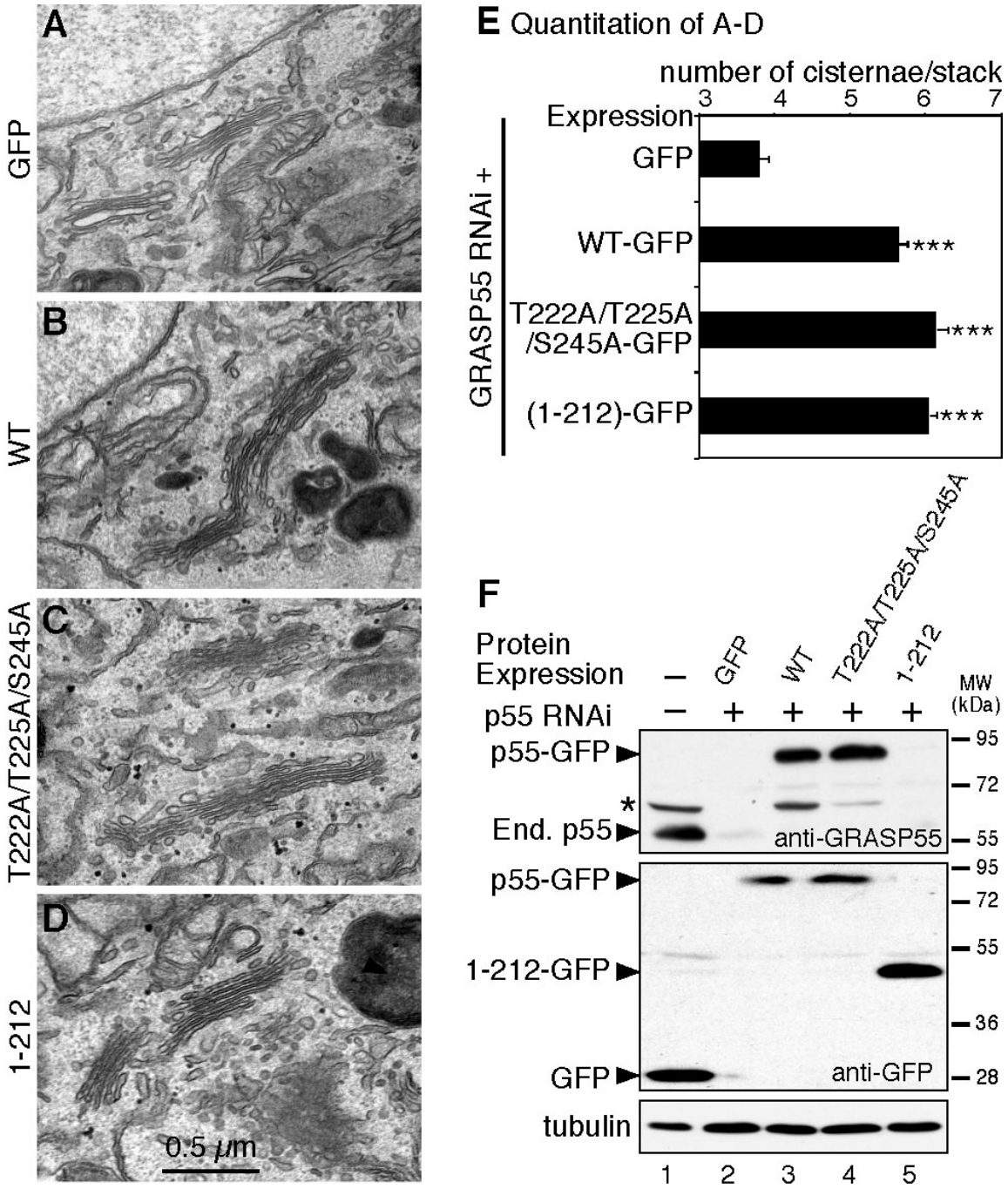

Figure 2.S5. Rescue of the Golgi structure in GRASP55-depleted cells by expression of GRASP55 and its mutants. (A-D) EM images of HeLa cells expressing GFP (A), GFP-tagged wild type (WT) GRASP55 (B), the T222A/T225A/S245A mutant (C), or the GRASP domain (1-212) (D) transfected with GRASP55 siRNA. **(E)** Quantitation of A-D. 20 cells are examined in each condition. Results are expressed as mean ± SEM. Statistical significance was assessed by comparison to the GFP cell line. ***, $p<0.001$. **(F)** Immunoblot of cells from A-D. * indicates a non-specific signal. End. p55, endogenous GRASP55.

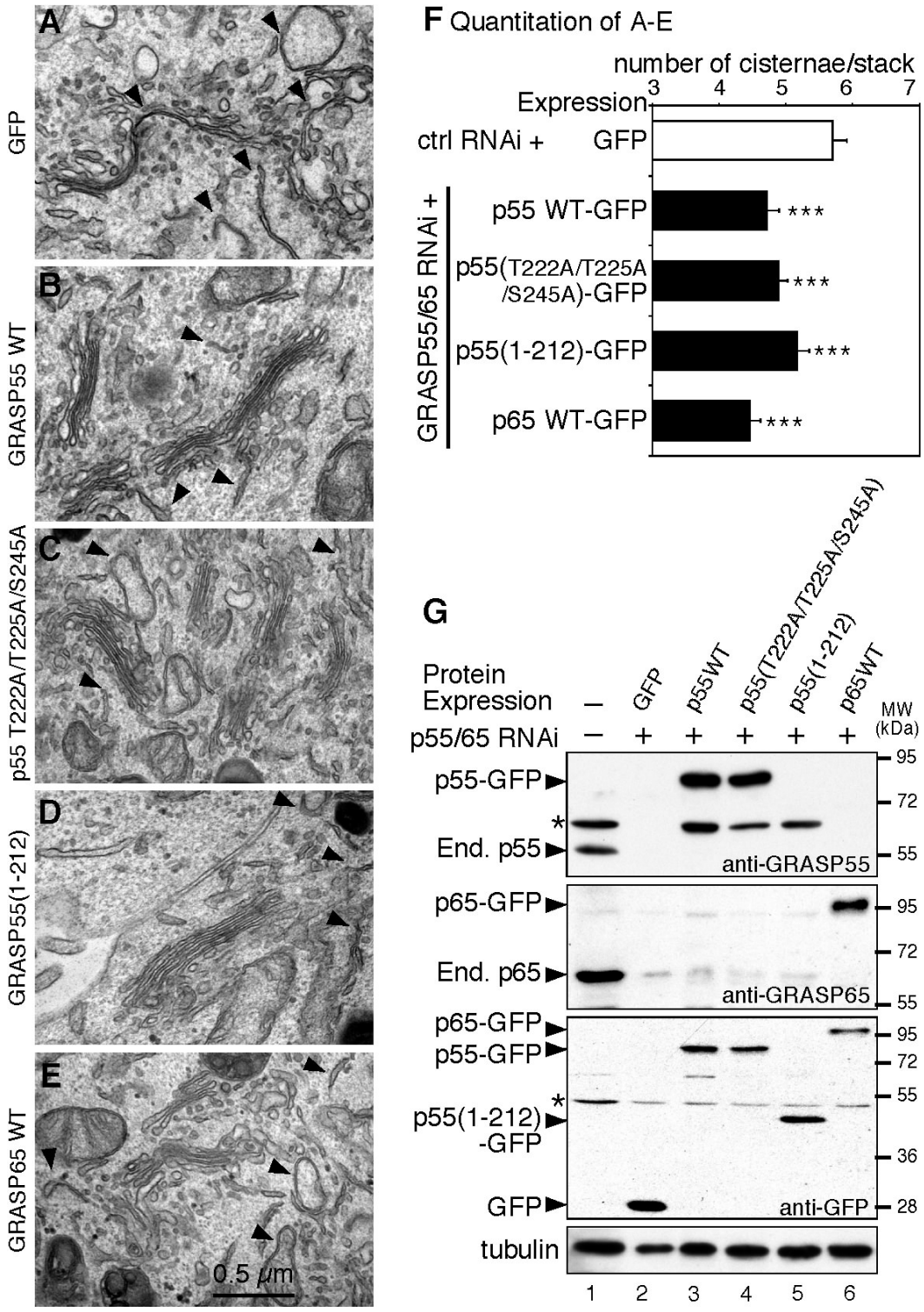

Figure 2.8. Rescue of Golgi structure by expression of exogenous GRASP55 and GRASP65 in cells with both GRASPs depleted. (A-E) EM images of HeLa cell lines transfected with a mixture of GRASP55 and GRASP65 siRNAs and induced to express indicated protein. **(F)** Quantitation of 20 cells in panels B-E. Statistical significance was assessed by comparison to the GFP-cell line treated with control siRNA. ***, *p<0.001*. **(G)** Western blots of cells in A-E. End.p55, endogenous p55; End. p65, endogenous GRASP65. * indicates a non-specific band.

Expression of non-phosphorylatable GRASP55 mutants inhibits mitotic Golgi fragmentation

Because the non-phosphorylatable GRASP55 mutants form oligomers that are resistant to mitotic regulation, these mutants were expected to inhibit Golgi disassembly at the onset of mitosis. To test this, Golgi structure in mitotic cells was analyzed. By confocal microscopy, exogenous GRASP55 co-localized with GRASP65 (Fig. 2.9B-E) and other Golgi markers, such as GM130 (not shown), on the mitotic clusters, whereas GFP alone (Fig. 2.9A) was evenly distributed throughout cells. Interestingly, mitotic cells expressing the GRASP domain or the T222A/T225A/S245A mutant increased in number and size of mitotic clusters compared to those expressing wild type GRASP55, the SPR domain, or GFP alone (Fig. 2.9A-D). Notably, the Golgi in cells expressing the T222E/T225E mutant exhibited more extensive fragmentation than that in GFP-expressing cells (Fig. 2.9E).

When observed by EM, a considerable amount of Golgi membranes in cells expressing the GRASP domain or the T222A/T225A/S245A mutant remained as Golgi remnants (e.g. mini stacks, short cisternae and tubular structures) (Fig. 2.9F-I). Some membranes were vesiculated, but these vesicles were presumably held together by non-phosphorylatable GRASP55 proteins, which remain oligomeric during mitosis. Quantitation of EM images showed that the number of Golgi clusters in each profile for mitotic cells expressing the GRASP domain (7.5 ± 0.9) and the T222A/T225A/S245A mutant (6.9 ± 0.8) was at least three times greater than the number in cells expressing wild type GRASP55 (1.9 ± 0.3), the T222E/T225E mutant (1.7 ± 0.3), the SPR domain (1.9 ± 0.3), or GFP (1.6 ± 0.2) (Fig. 2.9J). These results substantiate the *in vitro* data

(Fig. 2.6), suggesting that the lack of mitotic regulation of GRASP55 prevents the breakdown and dispersal of Golgi membranes during mitosis. Taken together, these results provide strong evidence that GRASP55 functions together with GRASP65 to link Golgi membranes into stacks and outline a molecular mechanism for GRASP55 function.

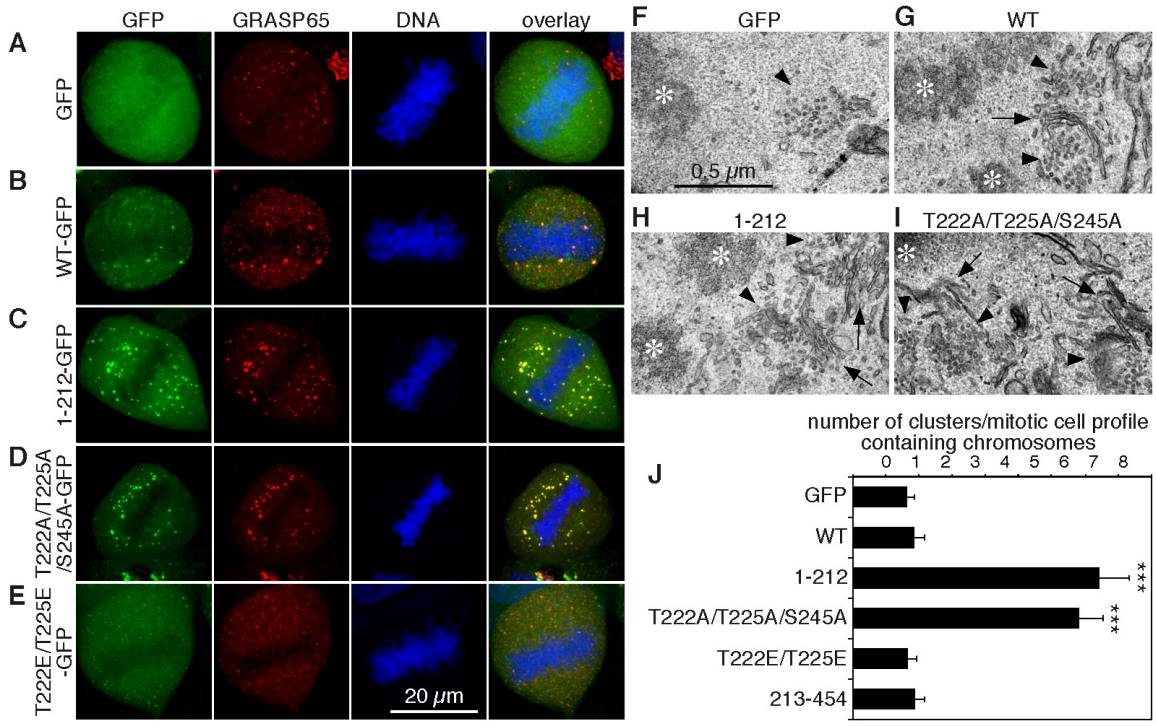

Figure 2.9. Expression of non-phosphorylatable GRASP55 mutants inhibits mitotic Golgi disassembly. (A-E) Confocal images of mitotic cells of indicated HeLa cell lines stained for DNA and GRASP65. Note that cells expressing the GRASP domain (C) and the T222A/T225A/S245A mutant (D) had more mitotic clusters, while Golgi fragmentation in cells expressing the T222E/T225E mutant (E) was more complete compared to that in GFP-expressing cells (A). Bar, 20 μm. **(F-I)** Representative EM images of mitotic cells expressing indicated GRASP55 constructs. Mitotic cells were collected by shake-off after release from a double-thymidine block and processed for EM. Bar, 0.5 μm. Note the remaining Golgi cisternal membranes or stacks (arrows) and vesicle clusters (arrowheads) in the GRASP domain- (H) and the T222A/T225A/S245A mutant- (I) expressing cells. Asterisks indicate condensed chromosomes. **(J)** Quantitation of the number of Golgi clusters in mitotic cells expressing indicated proteins. 20 cells were examined in each case. Results expressed as the mean ± SEM. Statistical significance was assessed by comparison to the GFP cell line. ***, $p<0.001$.

Discussion

The role of GRASP55 in Golgi stack formation was first indicated by an *in vitro* Golgi reconstitution assay [16]. However, siRNA-based depletion experiments in other studies led to inconsistent conclusions [23, 29]. To address these discrepancies, we performed systematic EM analysis of GRASP55-depeleted cells. Our results showed that GRASP55 knockdown significantly reduced the number of cisternae per stack and that this effect was rescued by the expression of exogenous rat GRASP55 or its mutants. When GRASP55 was depleted, GRASP65 expression and Golgi targeting were not affected, and vice-versa, indicating that the two homologues might function and target to the Golgi independently. Strikingly, simultaneous depletion of both GRASP proteins led to the disassembly of the entire Golgi stack, an effect that was partially rescued by the expression of GRASP55 or GRASP65. Given that GRASP55 and GRASP65 localize to different parts of the Golgi stack, these results strongly suggest that GRASP55 and GRASP65 play complementary and essential functions in Golgi stacking.

It has been reported that GRASP55 depletion results in scattered Golgi and therefore that GRASP55 plays a role in Golgi-ribbon linking [23]. In our study, however, the majority of the cells with depletion of GRASP55 contained intact Golgi as judged by fluorescence microscopy, only 22-24% cells had partially fragmented Golgi. The heterogeneity of Golgi morphology may account for the inconsistent observation made by the other studies [23, 29]. FRAP analysis confirmed that the Golgi ribbon was affected by GRASP55-depletion, suggesting that either GRASP55 is directly involved in Golgi-ribbon linking, or the observed effect is caused by Golgi unstacking. The mechanism for Golgi ribbon formation is so far unclear, but disruption of many factors

can potentially affect the Golgi ribbon. For example, depletion of the cargo receptors Surf4 and ERGIG53, p25, golgin 84, or the microtubule-binding protein CLASP all lead to Golgi fragmentation [24, 113, 207]. In addition, it has been shown that Golgi disassembly affects protein trafficking [208], which may indirectly affect ribbon formation. Therefore, whether GRASP55 plays a direct role in Golgi ribbon formation in addition to stacking requires further investigation.

Further biochemical experiments demonstrated that GRASP55 formed oligomers in a mitotically regulated fashion, and that these oligomers are sufficient to link Golgi membranes together, a mechanism shared with GRASP65 [17, 120]. GRASP65 is phosphorylated by cdc2 and plk during mitosis, while GRASP55 is mainly phosphorylated by MAPK. This difference may allow for accurate regulation of the alternating oligomeric status of the two proteins to fulfill physiological functions. For example, it has been shown that expression of a S277A mutant of GRASP65 in tissue culture cells inhibited Golgi orientation towards the leading edge in a would healing assay [27]. A similar mechanism may exist for GRASP55 to allow cells to react to different conditions. Indeed, phosphorylation sites on GRASP55 responsible for mitotic regulation were identified in this and previous studies, and phosphorylation at these sites is required for mitotic Golgi disassembly and cell cycle progression [29, 125].

When expressed in cells, the non-phosphorylatable mutants of GRASP55 (i.e., the GRASP domain and the T222A/T225A/S245A mutant) enhanced Golgi stacking in interphase cells and inhibited Golgi unstacking and disassembly at the onset of mitosis, consistent with the biochemical and knockdown results. Mitotic disassembly of the Golgi in those cells was clearly not complete, as Golgi remnants (short cisternae and

stacks) were often seen in mitotic cells by EM. In addition, the Golgi remnants in those cells were clustered, presumably reflecting tethering by the exogenous GRASP55 mutant proteins. Overall Golgi disassembly was not blocked, consistent with a previous report [23], and possibly due to the fact that other Golgi structural proteins such as GRASP65 still responded to mitotic regulation. Taken together, the results in this study demonstrate that GRASP55, like GRASP65, plays a critical role in Golgi stacking and that the two proteins function collaboratively to maintain cisternal membranes stacking through a common mechanism, by forming mitotically-regulated trans-oligomers. Future studies will determine how differential targeting of the two GRASP proteins leads to the establishment of the polarized structure of the Golgi stack.

Important unanswered questions remain concerning the mechanism of Golgi structure formation. For example, it is unclear why the budding yeast *Saccharomyces cerevisiae* has a GRASP homologue but lacks Golgi stacks, while plants have Golgi stacks but no GRASP proteins. First, different organisms may have evolved different mechanisms for Golgi structure formation. Because the organization of the secretory pathway in plant differs from that in mammalian cells, e.g., there is no ERGIC, no Golgi ribbon and no mitotic Golgi fragmentation, it is possible that an alternative mechanism for Golgi stacking may have developed [209]. Alternatively, plant cells may have evolved highly divergent and as yet undiscovered GRASP-related proteins. Indeed, plant golgins have been found only in the last a few years [20, 210, 211]. A second possibility is that GRASP has gained different functions during evolution. In addition to stacking, other functions have been reported for GRASP55, GRASP65 and their homologues, including roles in protein trafficking in budding yeast [114] and mammals [126, 129, 130,

133], unconventional secretion in *Dictyostelium* [116] and noncanonical secretion in *Drosophila* [132] and Golgi ribbon linking [22, 23, 122], as well as cell cycle regulation [29, 118, 191, 206] in mammals. The sole GRASP protein in the budding yeast, Grh1p, lacks the first PDZ domain that mediates the oligomerization of mammalian GRASP [16, 114, 122]. Therefore, it is possible that GRASPs may have gained different functions in yeast and animal cells. Third, the proposed functions are not mutually exclusive; some of these functions may be related to Golgi stack formation. For example, GRASP oligomerization may mediate either stacking or ribbon linking depending on whether it is localized on the flat region or on the rims of the Golgi cisternae. Furthermore, the Golgi in budding yeast forms stacks under special conditions [212], and the role of the yeast GRASP homolog has not been tested under such conditions. These questions could be answered only through further experiments. For example, it will be interesting to test whether the Golgi structure in GRASP55/65-depleted HeLa cells could be rescued by the expression of yeast or fly GRASP proteins.

Materials and methods

Reagents

All reagents were from Sigma Co., Roche or Calbiochem, unless otherwise stated. The following antibodies were used: monoclonal antibodies against α-actin (Sigma), Gos28 and GM130 (Transduction Laboratories), GRASP65 (G. Warren), and α-tubulin (K. Gull); polyclonal antibodies against ERK2 (Upstate), green fluorescence protein (GFP, J. Seemann), GM130 (N73, J. Seemann), human GRASP55 (Proteintech Group, Inc.), rat GRASP55 (Susan, against rat GARSP55 aa1-212; Rich, against rat GRASP55 aa232-454; both from J. Seemann), human GRASP65 (J. Seemann), rat GRASP65 [120], α-Mannosidase II (K. Moremen), and MEK1 (Upstate).

Preparation of kinases, cytosol, Golgi membranes and GRASP55 fusion proteins

Golgi membranes [213], constitutively active cdc2 and polo-like kinase [17], and interphase (IC) and mitotic (MC) cytosol [214] were prepared as previously described. cDNA constructs for wild type ERK2 and constitutively active MEK1 (S218E/S222D/ΔN3) were provided by K. Guan. GRASP55 cDNAs (provided by J. Seemann, GenBank accession # NM_001007720.1) were cloned into pMAL-c2X (New England Biolabs), pET30a, pET23a (Novagen) or pGEX (GE Healthcare) vectors by PCR or restriction digestion and confirmed by DNA sequencing. GRASP55 point mutations were introduced using the QuikChange mutagenesis kit (Stratagene) and confirmed by DNA sequencing. Proteins were expressed in BL21-CodonPlus(DE3)RILP bacteria and purified on amylose (New England Biolabs), nickel (Qiagen), or glutathione-Sepharose (GE Healthcare) beads.

Phosphorylation assay

Five μg of purified Golgi membranes, or 500 ng of recombinant GRASP55, were mixed with 500 μg of mitotic HeLa cell cytosol or with 1 μg ERK2 and 1 μg MEK1, and an ATP-regenerating system (10 mM creatine phosphate, 0.1 mM ATP, 20 μg/ml creatine kinase, 20 μg/ml cytochalasin B) was added in MEB buffer (50 mM Tris-HCl, pH7.4, 0.2 M sucrose, 50 mM KCl, 20 mM β-glycerophosphate, 15 mM EGTA, 10 mM $MgCl_2$, 2 mM ATP, 1 mM GTP, 1 mM glutathione, and protease inhibitors), for a final volume of 50 μl. In some reactions, MEK inhibitor U0126 (200 μM, Promega) was included. Similar reactions were carried out with interphase cytosol in KHM buffer (20 mM Hepes-KOH, pH7.0, 0.2 M sucrose, 60 mM KCl, 5 mM $Mg(OAc)_2$, 2 mM ATP, 1 mM GTP, 1 mM glutathione, protease inhibitors) to determine GRASP55 dephosphorylation. Phosphorylation of GRASP55 was analyzed by a band-shift assay. To ensure that the band-shift was caused by phosphorylation, 5 μg of mitotic cytosol-treated Golgi membranes were further treated with 20 U of calf alkaline phosphatase (CIP, Invitrogen) in the absence or presence of a phosphatase inhibitor, ß-glycerophosphate (50 mM) for 60 min at 37˚C; the membranes were then analyzed by immunoblotting. For [γ-^{32}P] ATP labeling, 0.5 μCi/μl of [γ-^{32}P] ATP and 5 μM ATP were used. After 60 min incubation at 37˚C, the membranes were pelleted through 0.4 M sucrose at 55,000 rpm for 30 min in a TLA55 rotor (Beckman). Samples were analyzed by immunoprecipitation, SDS-PAGE and autoradiography.

GRASP55 dimerization and oligomerization

To measure GRASP55 oligomerization, recombinant MBP-GRASP55 and His-GRASP55 were separately expressed in bacteria and purified, and mixed followed by treatment with mitotic cytosol or buffer as described for the phosphorylation assay. The protein complex was isolated using amylose beads or nickel beads and analyzed by immunoblotting for GRASP55. For non-denaturing electrophoresis, purified His-GRASP55 was incubated with purified ERK2 and MEK1, or buffer, at 37˚C for 60 min. Non-denatured samples were loaded onto a 4-12% NuPAGE Novex Bis-Tris mini gel (Invitrogen) [215]. After electrophoresis, the gel was soaked with 0.1% SDS followed by immunoblotting.

Golgi disassembly assay and aggregation of GRASP55-coated beads

Purified rat liver Golgi membranes were treated with kinases at 37˚C for 20 min. For a reaction using 20 μg Golgi membranes, the amounts of the kinases used were equivalent to the activity found in 2 mg mitotic cytosol. Normally about 20 μg cdc2 and 30 μg plk were used, based on the quality of preparation. For MEK1 and ERK2 activity, we have determined the protein amount in the cytosol by Western blotting using purified kinase as the standard. Normally there are about 4 μg MEK1 and 2 μg ERK2 in 2 mg interphase or mitotic cytosol. Accordingly, we used 4 μg MEK1 and 2 μg ERK2 to treat 20 μg purified Golgi membranes. After the treatment, the membranes were collected by centrifugation and processed for EM. At least 10 random regions were photographed for each condition and membrane profiles were quantified using the intersection method [214].

His-tagged, full-length GRASP55, the GRASP domain, or bovine serum albumin (BSA, Invitrogen) were cleared by centrifugation and cross-linked to Dynal beads (M500, Invitrogen) following the manufacturer's instructions [17, 120]. The beads (8 x 10^6) were incubated for 60 min at 37˚C with 0.5 mg (25 µl) cytosol or kinase mixture (ERK2/MEK1, 2 µg each) in the presence of 4 µg/ml nocodazole in a 50 µl reaction system and observed under a bright field microscope. In some experiments, beads were sequentially treated with interphase and mitotic cytosol or kinases [17, 120]. For quantitation of the beads, 15 random phase contrast digital images of each reaction were captured with a 20X lens and a Spot Slider2 Camera (Diagnostic Instruments). Images were analyzed using MATLAB7.4 software to determine the surface area of objects, which was used to calculate the number of beads in the clusters. Aggregates were defined as those with ≥ 6 beads. For large aggregates, only visible surface beads were counted; therefore, the number of beads in these aggregates was underestimated. Results were expressed as the mean ± SEM from 3 independent experiments; statistical significance was assessed using Student's *t*-test.

Cell culture, transfection and microscopy

HeLa cells transfections were performed using published siRNAs for human GRASP55 (AACTGTCGAGAAGTGATTATT, Ambion) [23] and GRASP65 (CCTGAAGGCACTACTGAAAGCCAAT, Invitrogen) [118]. Lipofectamine RNAiMAX was used according to the manufacturer's recommendations (Invitrogen). Control non-specific siRNAs were purchased from Ambion. Assays were performed 96 h after transfection. To establish stable cell lines, GFP cDNA was first cloned into

pRevTRE2 vector using HindIII and NotI sites. GRASP55 cDNA was then inserted at the N-terminus of GFP using BamHI and HindIII sites. To generate retroviral particles, HEK293 cells were transfected with pRevTRE2-rGRASP55-GFP, viral DNA pV Pack GP and pV Pack Eco, using lipofectamine 2000. 36 h after transfection, the virus supernatant was collected and filtered via MILLEX ® GV (0.45 μm) and the undiluted supernatants were used to infect rtTA HeLa m2 cells, a tet-on cell line [204]. Infected cells were selected with 500 μg/ml hygromycin for 2 weeks, and GRASP55-GFP positive cells were sorted by flow cytometry. The expression of GRASP55-GFP was induced with 1 μg/ml doxycycline (DOX) for 48 h, and protein expression was determined by immunoblotting for GRASP55 and/or GFP. For the gene replacement experiment, GRASP55- or GFP-expressing cell lines were transfected with siRNA for 48 h followed by induction with doxycycline for 48 h. Immunofluorescence microscopy and collection of mitotic cells were previously described [89]. Pictures were taken with a Leica SP5 confocal laser-scanning microscope using a 100X oil lens. Each image was a maximum projection from a z-stack. Pictures were assembled in Adobe Photoshop.

For EM analysis, Golgi stacks and clusters were identified using morphological criteria and quantified using standard stereological techniques [120]. For interphase cells, the profiles had to contain a nuclear profile with an intact nuclear envelope; only stacked structures with 2 or more cisternae were counted. For mitotic cells, the profile had to contain one or more profiles of condensed chromosomes lacking a nuclear envelop. Quite often, multiple condensed chromosomes were aligned at the center of the cell. A low magnification (normally 1600x) image and a series of higher magnification images were taken to cover the entire cell. More than 20 cells were quantified for each reaction.

Fluorescence recovery after photobleaching (FRAP)

HeLa cells were first transfected with siRNA. After 48 h, the cells were trypsinized and plated on chambered coverglasses (Thermo Scientific Nunc Lab-Tek II). After 24 h incubation, cells were transfected with a ManII-GFP cDNA using lipofectamine 2000 and further cultured for 24 h until they were used for FRAP analysis. FRAP was performed using an OLYMPUS FluoView^{TM}FV500/IX Laser Scanning Confocal Microscope equipped with an environmental control system set to 37˚C and 5% CO2. Cells were cultured in phenol red-free Opti-MEM (Invitrogen) with 10% FBS and visualized using the argon laser line (488nm) with a 60X, 1.0 numerical aperture water immersion objective. Images were taken every 10 s for 30 s (2% laser power) and the selected area of the Golgi was bleached using 15 laser pulses of the 488-nm laser line at maximal intensity. Fluorescence images were then recorded every 10 s for 480 s. After background correction, the recovery of the fluorescence was calculated as the ratio of the average intensity of the bleached region to that of the entire Golgi. Normalization was set between the values before bleaching and the first time point after bleaching. More than 17 cells were quantified in each experiment. The average of two independent experiments is shown (Fig. 2. 2).

Acknowledgements

We thank Xiao-Wei Chen, David Ginsburg, Kun-Liang Guan, Martin Lowe, Joachim Seemann and Graham Warren for antibodies and cDNA constructs, Hebao Yuan and Blanche Schwappach for help with the retroviral vector and the rtTA HeLa cell line. We also thank Timothy Welliver for technical help with the FRAP assay, Danming Tang and Guoping Ren for technical help with gel filtration, Majan Varedi and Xiaoxia Lin for developing the Matlab program to quantify beads in aggregates, Danming Tang and other members of the Wang Lab for suggestions and reagents, Joachim Seemann and James Bardwell for critical reading, and Robert Fuller for editing of the manuscript. This work was supported by the Pardee Cancer Research Foundation, the National Institute of Health (GM087364), American Cancer Society (RGS-09-278-01-CSM), a University of Michigan Rackham Faculty Research Grant, the NIH-funded Michigan Alzheimer's Disease Research Center (P50 AG08761) and an anonymous donation to Y. Wang.

Abbreviations

BSA, bovine serum albumin; CIP, calf intestine alkaline phosphatase; EM, electron microscopy; GRASP55, Golgi Reassembly Stacking Protein of 55 kDa; GRASP65, Golgi Reassembly Stacking Protein of 65 kDa; IC, interphase cytosol; MAPK, mitogen-activated protein kinase; MC, mitotic cytosol; MEK1, Mitogen activated protein kinase kinase 1; MGF, mitotic Golgi fragments; plk, polo-like kinase, siRNA, small interference RNA

Chapter III. Golgi cisternal stacking acts as a quality control mechanism for cargo sorting and modification

Abstract

A unique feature of the Golgi apparatus is the formation of Golgi stacks, however, the biological significance of cisternal stacking has not been tested due to the lack of molecular tools to control Golgi stacking. Previous work showed that the Golgi stacking proteins GRASP65 and GRASP55 play complementary and essential roles in Golgi cisternal stacking by forming mitotically regulated *trans*-oligomers. In this study, we demonstrate that Golgi unstacking by the depletion of GRASP65/55 accelerates protein trafficking, which impairs protein sorting and alters the glycosylation of cell surface proteins. Subsequently, cell adhesion and migration are attenuated when the Golgi is unstacked, which is probably the result of reduced α5/β1 integrin expression. Furthermore, total protein synthesis and proliferation of cells with unstacked Golgi are enhanced. Our results demonstrate that Golgi cisternal stacking regulates protein transport and modification, which are important for cell attachment, migration and proliferation.

Introduction

The Golgi complex is a membrane-bound organelle that plays a central role in the processing of membrane and secretory proteins, in the endocytic pathway, as well as in multiple recycling routes in all eukaryotic cells. It is comprised of stacks of flattened cisternae in almost all eukaryotic cells, and these stacks are laterally linked to form a perinuclear ribbon-like structure in mammalian cells [8]. Previous studies have explored the mechanism of the stack formation. Two homologous peripheral proteins GRASP65 (Golgi Reassembly Stacking Protein of 65 kDa) and GRASP55, which associate with the Golgi membranes via N-terminal myristoylation, were first identified as the Golgi stacking factors using an *in vitro* assay that reconstitutes the cell cycle regulated Golgi disassembly and reassembly process [15, 16]. Antibodies against GRASP65 or GRASP55 or soluble recombinant proteins inhibited stacking of newly formed cisternae in the *in vitro* assay [15, 16]. Consistently, microinjection of anti-GRASP65 antibody into mitotic cells inhibited subsequent Golgi stack formation in the daughter cells [17]. Depletion of GRASP65 or GRASP55 by small interference RNA (siRNA) in mammalian cells reduced the number of cisternae per stack [18, 118, 119], and simultaneous depletion of both GRASP65 and GRASP55 resulted in complete disassembly of Golgi stacks [18]. Consistent observation was made in fly that depletion of the sole GRASP protein dGRASP and its interacting protein dGM130 in *Drosophila* S2 cells led to the disassembly of the Golgi stacks into single cisternae and vesicles [115]. Biochemical studies revealed that both GRASP65 and GRASP55 form stable homodimers, and those dimers from adjacent cisternae form *trans*-oligomers to link the cisternae into stacks [17, 18]. Both dimerization and oligomerization are mediated via the N-terminal GRASP

domain, which is highly conserved between GRASP65 and GRASP55. Oligomerization of GRASP65 and GRASP55 is regulated by mitotic phosphorylation. GRASP65 is phosphorylated by the Polo-like kinase Plk1 and Cdk1 [17, 123], while GRASP55 is phosphorylated by ERK2 and Cdk1 [18, 125]. As GRASP65 and GRASP55 localize to the *cis*- and *medial-to-trans* Golgi, respectively [16], both are required for the formation of the polarized stacked structure [18, 203].

Although stack formation is a conserved feature in most eukaryotic cells, its physiological role remains elusive. It has been speculated that cisternal stacking improves the efficiency of vesicular transport because the close spatial arrangement of cisternae in a Golgi stack minimizes the distance that vesicles have to travel [140]. In addition, tethering complexes hold the vesicles to the target cisternae and enhances membrane fusion [216]. However, the exact role of Golgi stacking has not been tested due to the lack of molecular tools to manipulate Golgi stack formation. Previously we have shown that microinjection of GRASP65 antibodies inhibits Golgi stack formation, which results in an increased rate of protein transport due to the acceleration of vesicle formation from unstacked cisternae, suggesting that cisternal stacking regulates the cargo flow through the Golgi [208]. This study used an artificial marker, CD8, to monitor protein trafficking, therefore additional proteins especially endogenous ones are needed to test this hypothesis.

Protein glycosylation is one of the main functions of the Golgi apparatus. The Golgi harbors various glycosyltransferases and glycosidases in different compartments, and cargos are modified sequentially as they travel through the Golgi complex. Protein glycosylation encompasses N-glycans, O-glycans, and glycosaminoglycans. Most

secreted and cell surface proteins such as the cell adhesion molecule, integrins, are glycosylated. By binding to lectins and other interaction molecules, cell surface carbohydrates participate in a variety of cellular activities, including cell adhesion and migration, cell-cell communication, signal transduction, protein folding and stability, molecular trafficking and clearance, as well as endocytosis [186]. Therefore, aberrant glycosylation could affect multiple cellular functions and serve as pathological markers. It is known that glycosylation can be regulated by multiple factors, including the transcription and intracellular localization of glycosyltransferases and glycosidases, the synthesis and transport of nucleotide sugar donors to the endoplasmic reticulum (ER) and Golgi, etc [186]. An interesting unknown question is whether the Golgi cisternal stacking is required for proper glycosylation of cargo molecules, since different carbohydates are added to the growing glycan chain in the same sequence as the oligosaccharide processing enzymes localized in different Golgi cisterane.

In this study, we have manipulated Golgi stacking by the depletion of GRASP55, GRASP65, or both proteins with siRNA to determine the biological significance of Golgi stacking. Our results showed that Golgi unstacking increased the rate of cargo transport, altered the glycosylation pattern on the cell surface, and caused missorting of lysosomal proteins. In addition, other cellular functions, such as cell adhesion, migration, and proliferation were subsequently affected. Our results implicate that cisternal stacking regulates cargo flux through the Golgi and functions as a quality control machinery for protein sorting and modifications.

Results

Golgi unstacking accelerates VSV-G transport

To determine the effect of Golgi unstacking on protein trafficking, we monitored the transport of vesicular stomatitis virus glycoprotein (VSV-G) temperature-sensitive mutant (ts045). This mutant is unfolded at 39.5ºC and thus is blocked in the ER; upon the reduction of the temperature to 32ºC, the protein is released from the ER and travel through the secretory pathway. A HeLa cell line that stably expressed the GFP-tagged VSV-G using an inducible retroviral expression system [18] was generated and the Golgi membranes were unstacked by the depletion of GRASP55, GRASP65 or both [18]. These cells were then induced by doxycycline to express the VSV-G protein at 40.5 ˚C for 16 h and then shifted to 32 ˚C in the presence of cycloheximide to allow the release of VSV-G from the ER. The VSV-G on the cell surface was labeled with an antibody against the extracellular domain of VSV-G, while total VSV-G level was indicated by the intensity of GFP signal. The intensity of total cellular VSV-G and surface-bound VSV-G were assessed by flow cytometry 2 h after release. As shown in Fig. 3.1A, the ratio of surface-to-total VSV-G was increased in the cells depleted of GRASP55, GRASP65 or both, suggesting that VSV-G transport to the plasma membrane is accelerated upon Golgi unstacking. This result is consistent with previous observation that the CD8 trafficking is accelerated in NRK cells with unstacked Golgi [208].

Golgi unstacking leads to cathepsin D secretion

To determine the effect of Golgi unstacking on protein sorting, we monitored the sorting and processing of the lysosomal hydrolase cathepsin D. Cathepsin D is synthesized in the

ER as a polypeptide precursor of 53 kDa; it is transported through the Golgi to the lysosomes, where the precursor is converted to a 47 kDa intermediate and then a 31 kDa mature form [217, 218]. It has been shown previously that the precursor of cathepsin D was missorted to the extracellular space when the Golgi structure was disrupted by depletion of the actin-depolymerizing factor (ADF)/cofilin [219]. Therefore, cathepsin D was used as a marker for protein sorting in this study. Cells treated with control or GRASP siRNAs were incubated within serum-free media for 2 h, and cathepsin D in the cell lysate and media were analyzed by western blot. As shown in Fig. 3.1B, 3 bands of cathepsin D were detected in the cell lysate, with the 31 kDa mature form as the major band; while only the 53 kDa immature form was detected in the media. In the control cell lysate, the ratio between the intermediate and the immature form was about 2, while this ratio increased to 3-4 when the Golgi was unstacked by GRASP-depletion (Fig. 3.1B, 1C). As cathepsin D processing occurs in the lysosomes, these results showed that the transport from TGN to endosomes/lysosomes is accelerated when the Golgi is unstacked. In addition, the total protein amount of cathepsin D in the cell also reduced to 35-55% upon the depletion of GRASPs, especially in GRASP55 knockdown cells (Fig. 3.1B, 1D). When both GRASP55 and GRASP65 were depleted, the amount of immature cathepsin D in the medium increased to 2 folds, compared to that of control cells (Fig. 3.1B, 1E). The increase of cathepsin D in the medium of GRASP-knockdown cells was not due to cell lysate contamination, as β-actin was not detected in the medium of these cells. These results suggest that Golgi unstacking leads to the missorting of cathepsin D to the extracellular space instead of the endosomes/lysosomes.

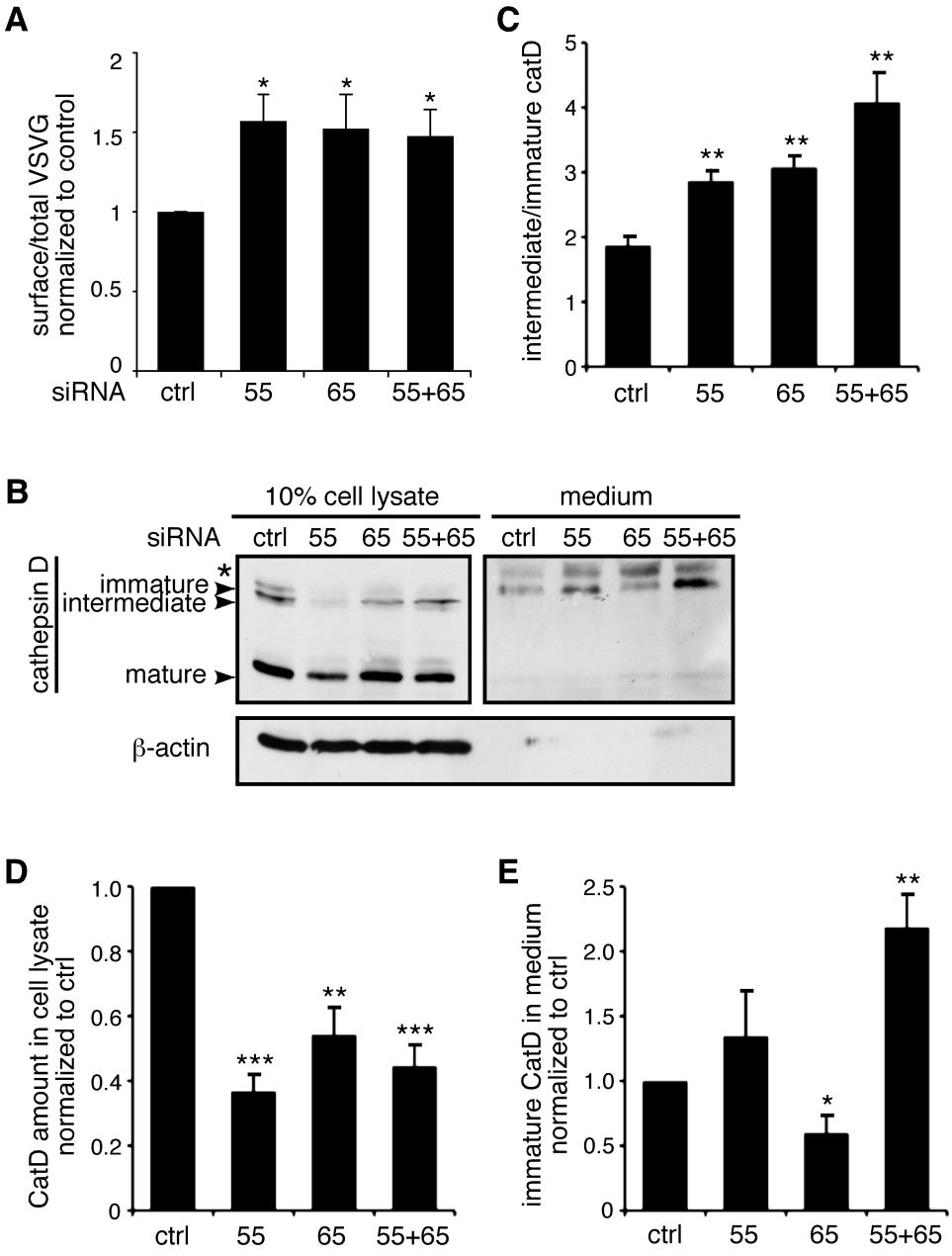

Figure 3.1. GRASP-depletion accelerates VSV-G trafficking and impairs cathepsin D sorting. (A) GRASP-depletion accelerates VSV-G trafficking. HeLa cells stably expressing VSV-G-ts045-GFP under an inducible promoter were transfected with control (ctrl), GRASP55 (55), GRASP65 (65), or both GRASP55 and GRASP65 (55+65) siRNAs. 80 h after transfection the cells were incubated at 40.5˚C for 16 h in the presence of doxycycline to induce VSV-G expression. Cells were then treated with 100 mM cycloheximide at 40.5˚C for 1 h and shifted to 32˚C for 120 min to release the VSV-G from the ER. The VSV-G on the surface was stained with an antibody against the extracellular domain of VSV-G followed by incubation with fluorescently labeled secondary antibodies. Total VSV-G and surface-bound VSV-G were assessed by flow cytometry. Shown are the ratios of surface-to-total VSV-G normalized against control cells (mean±SEM). **(B)** Missorting of cathepsin D in cells with unstacked Golgi. HeLa cells transfected with indicated siRNAs were washed with PBS and incubated in serum-free DMEM for 2 h. The secreted proteins in the medium were TCA precipitated and normalized according to the total protein amount in the cell lysate. Equal proportion of the cell lysate and medium were analyzed by SDS-PAGE

followed by western blot for cathepsin D. Immature form: 53 kDa; intermediate form: 47 kDa; mature form: 31 kDa. Asterisk indicates a nonspecific band. **(C)** Ratio of intermediate vs. immature cathepsin D in cells transfected with indicated siRNAs. **(D)** The amount of cathepsin D in the cell lysate, normalized to the cells transfected with control siRNA. **(E)** The amount of immature cathepsin D in the medium, normalized to the cells transfected with control siRNA. Bar in all the panels represents the average of four independent experiments. Error bar = SEM. *, $p<0.05$, **, $p<0.01$, ***, $p<0.001$.

Golgi unstacking alters cell surface glycosylation pattern

As glycosylation occurs in the Golgi in a sequential manner, we determined whether unstacking affects protein glycosylation by assessing the glycosylation pattern on the surface of HeLa cells depleted of GRASP55, GRASP65 or both using fluorescently labeled lectins. *Maackia amurensis* (MAA) binds to α (2,3) sialic acids, one of the terminal carbohydrates found in glycoproteins [220], while *Erythrina cristagalli* (ECA) binds to terminal β-galactose, a glycan structure that is rarely found in properly modified surface glycoproteins [220]. When the cells were stained with these lectins before fixation, the intensity of MAA staining decreased in cells depleted of GRASP55, GRASP65, or both, compared with cells treated with control siRNA (Fig. 3.2, A-C vs. D). In contrast, the ECA signal increased (Fig. 3.2E-H). In addition, the cell surface signal for *Wheat germ agglutinin* (WGA), a lectin that selectively binds to N-Acetyl glucosamine (GlcNAc) groups and sialic acid, was significantly reduced in GRASP-depeleted cells compared to those transfected with control siRNA (Fig. 3.S1). These results suggest that unstacking causes incomplete glycosylation of cell surface proteins. To assess the glycosylation pattern quantitatively, cells were stained with fluorescently labeled lectins without permeabilization and analyzed by flow cytometry. Consistent with the microscopy result, the MAA staining decreased when GRASP55, GRASP65 or both were depleted (Fig. 3.2I), while the ECA staining increased (Fig. 3.2K). The staining of another sialic acid binding lectin, *Sambucus nigra* (SNA), which specifically binds to α

(2,6) sialic acids [220], also decreased (Fig. 3.2J). The staining pattern of *Maclura pomifera* (MPA) that binds to galactose and N-acetyl-D-galactosamine did not change (Fig. 3.2L). The effects of GRASP-depletion on protein glycosylation were not due to the deprivation or displacement of the glycosylation enzymes from the Golgi membranes, since the exogenous expressing Mannosidase II (ManII, Fig. 3.S2A), galactosyltransferase I (GalT, Fig. 3.S2B), and the endogenous galactosyltransferase I (GalT, Fig. 3.S3) were correctly localized to the Golgi apparatus.

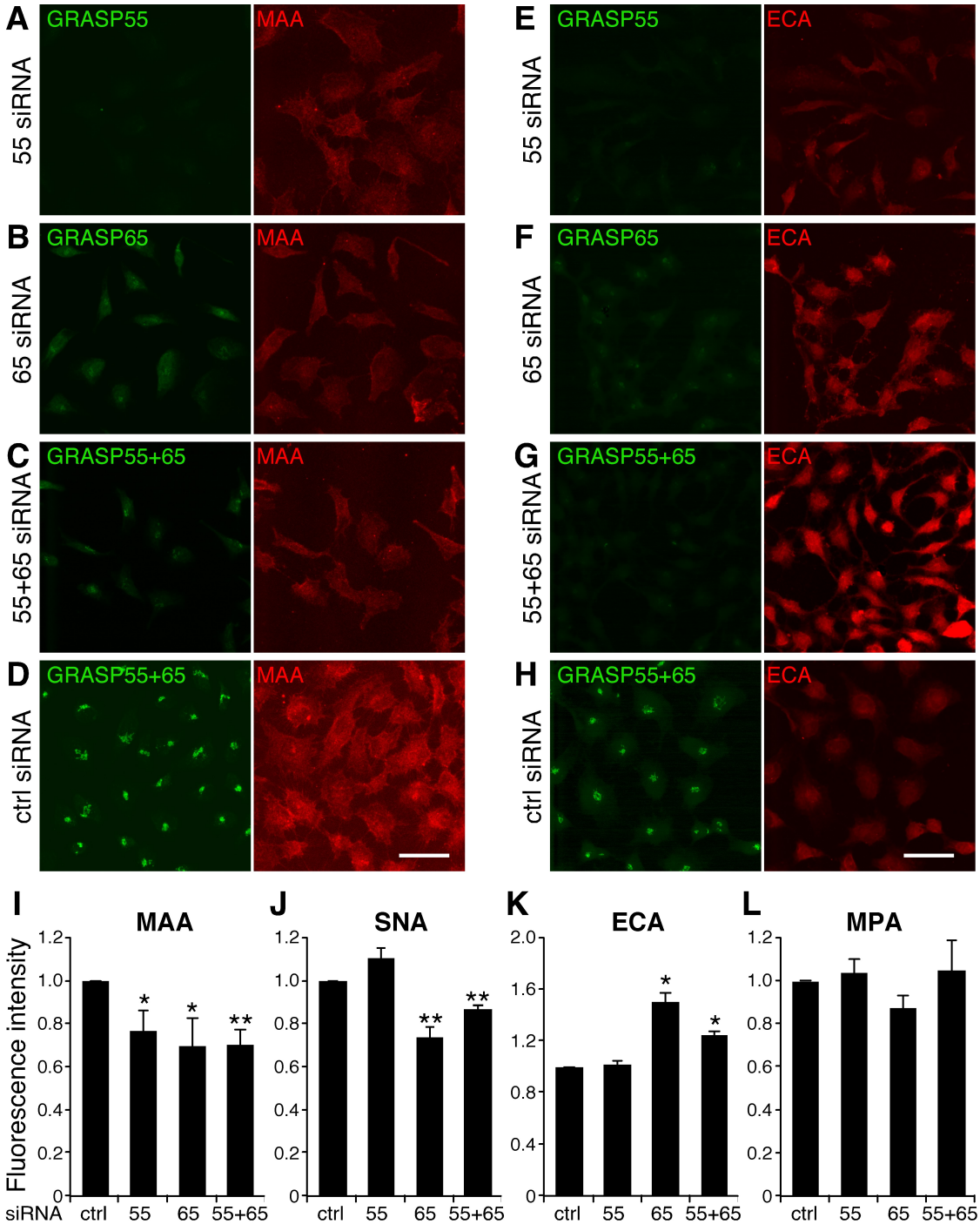

Figure 3.2. Depletion of GRASP results in altered glycosylation pattern on the cell surface. (A-D) Surface staining of fluorescence-conjugated lectin MAA, specific for α (2,3) sialic acid, was reduced upon the depletion of GRASPs. Non-permeabilized HeLa cells treated with indicated siRNAs were exposed to TRITC-conjugated MAA. The cells were then fixed, stained with GRASP antibodies, and visualized with confocal microscope. Scale bar, 50 μm. **(E-H)** Surface staining of fluorescence conjugated lectin ECA that is specific for terminal β-galactose. **(I-L)** Lectin staining on the plasma membrane of cells treated with indicated siRNAs was determined with flow cytometry. The result was normalized against control siRNA treated cells, and represents the mean±SEM of three independent experiments. *, $p<0.05$; **, $p<0.01$. Note that MAA, SNA staining decreased, while ECA staining increased upon the depletion of GRASPs.

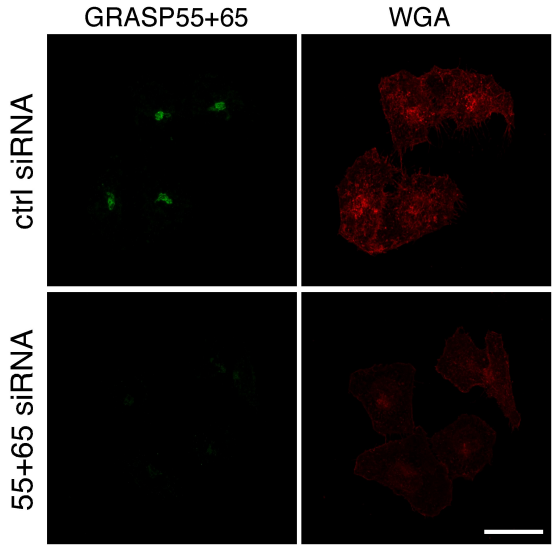

Figure 3.S1. Golgi unstacking impacts glycosylation of cell surface proteins. HeLa cells transfected with control siRNA and with siRNAs for GRASP65 and 55 were stained for GRASP65, GRASP55 (green) and WGA (red). Scale bar, 20 μm.

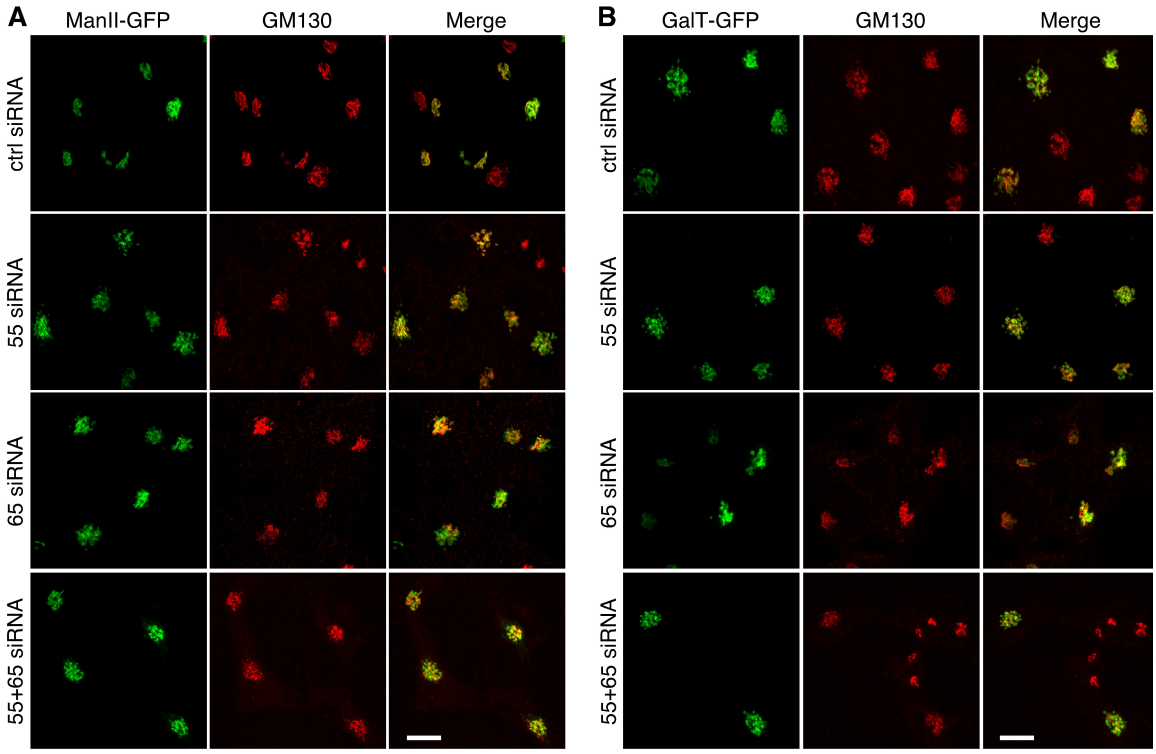

Figure 3.S2. GRASP-depletion does not affect the localization of Golgi enzymes. (A) Mannosidase II (ManII)-GFP localizes on the Golgi in GRASP-depleted cells. HeLa cells treated with indicated siRNAs were transfected with a ManII-GFP plasmid and analyzed by immunofluorescence microscopy for GM130. Note that ManII-GFP colocalized with GM130 in all cells. **(B)** Galactosyltransferase (GalT)-GFP localizes on the Golgi in GRASP-depleted cells. Scale bars in (A) and (B), 10 μm.

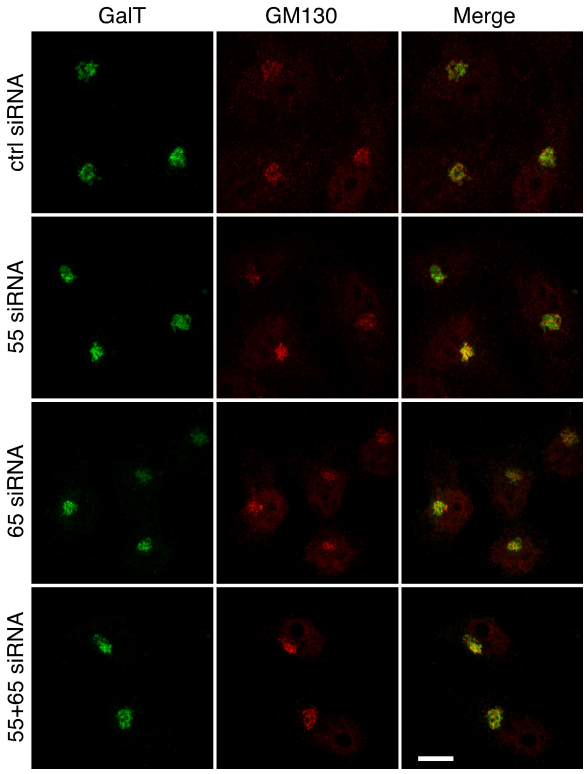

Figure 3.S3. GRASP-depletion does not affect the Golgi localization of the endogenous Galactosyltransferase (GalT). HeLa cells treated with indicated siRNAs were stained for GalT1 and GM130. Scale bar, 10 μm

Golgi unstacking reduces cell attachment and migration

Proper glycosylation of cell surface proteins is important for cell adhesion and migration. When examined under the phase contrast microscope, we noticed that cells transfected with GRASP65 or both GRASP55 and GRASP65 siRNAs spread less well on the dish compared with cells transfected with control or GRASP55 siRNAs, they appeared to be rounder and formed clusters (Fig. 3.3C, D vs. 3A, B). To further assess the effect of GRASP-depletion on cell adhesion, we detached HeLa cells with EDTA and placed the cells on fibronectin-coated plates. After incubation with serum-free medium at 37˚C for 30 min, attached cells were counted. Compared to the control cells of which 55±4% were attached to the dish, only 38±1% cells depleted of GRASP55 and 31±3% of

those depleted of GRASP65 bound to the dish (Fig. 3.3E). When both GRASP55 and GRASP65 were depleted, the percentage of cell attachment was reduced to 22±4% (Fig. 3.3E). This effect was rescued by expression of EGFP-tagged GRASP65 or GRASP55, but not by EGFP alone (Fig. 3.3, F and G). These results demonstrate that Golgi unstacking decreases cell adhesion.

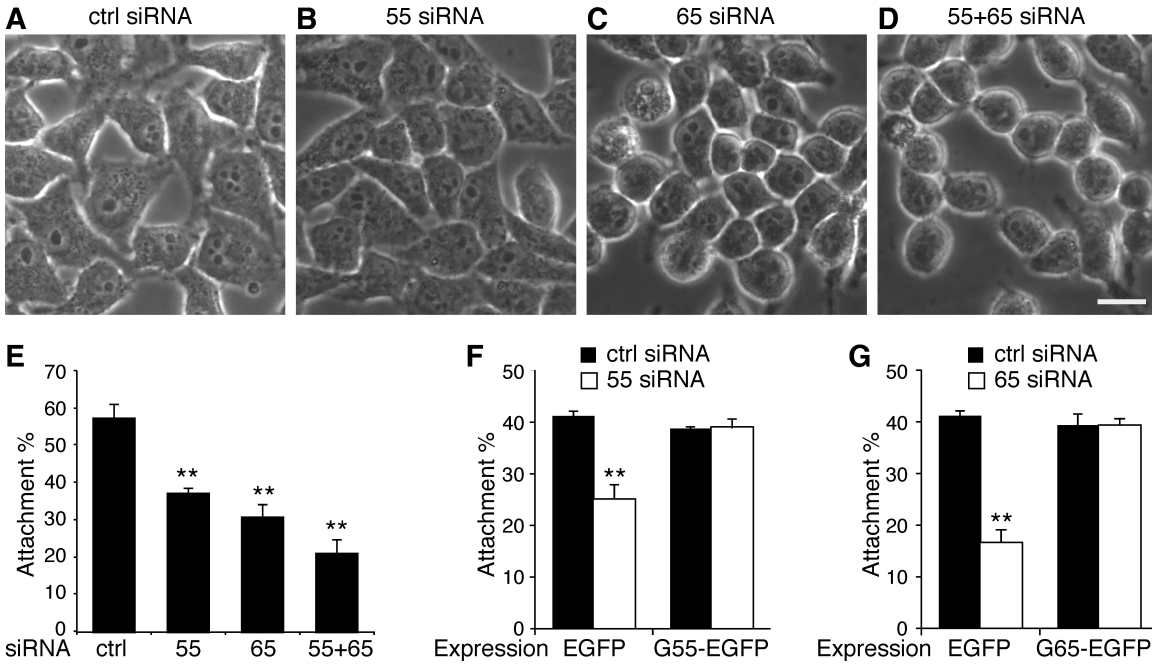

Figure 3.3. GRASP-depletion reduces cell attachment. (A-D) Phase contrast images of HeLa cells transfected with indicated siRNAs. Scale bar, 20 μm. Note that GRASP-depleted cells are generally rounder than control siRNA treated cells. **(E)** The attachment of cells on fibronectin coated plate was reduced upon GRASP-depletion. 300,000 siRNA-treated cells were seeded on fibronectin coated plates and incubated in serum-free medium for 30 min. After the removal of unbound cells, the attached cells were collected and counted. Each bar represents the mean of three independent experiments, error bar = SEM. **, $p<0.01$. **(F)** The reduced attachment of GRASP55-depleted cells could be rescued by expressing GRASP55-EGFP but not by EGFP alone. As in (E), except that HeLa cells transfected with indicated siRNA were induced to express EGFP or GRASP55-EGFP. The result represents the average of two independent experiments, error bar = SEM. **, $p<0.01$. **(G)** The reduced attachment of GRASP65-depleted cells depleted could be rescued by expressing GRASP65-EGFP.

We then determined the effect of Golgi unstacking on cell migration using the well-developed wound-healing assay [221]. The human breast tumor cell line MDA-MB-231 was used in the study. Both GRASP55 and GRASP65 were readily depleted when transfected with siRNAs in this cell line (Fig. 3.4A). 72 h after siRNA transfection, fully

confluent MDA-MB-231 cells were starved within serum-free DMEM for 24 h. A scratch was made with a 200 μl pipet tip, and the cells were cultured in complete growth medium for another 20 h to allow the cells to migrate into the wound region. When examined under a microscope, cells transfected control siRNA almost completely covered the wound region, while GRASP-depleted cells only covered part of the wound region (Fig. 3.4B). Control siRNA treated cells migrated at about 39±1 μm per hour, while cells depleted of GRASP55, GRASP65, or both, migrate at about 33±1, 25±2, and 19±2 μm per hour, respectively, significantly slower than that of the control cells (Fig. 3.4C). These results showed that Golgi unstacking reduces cell migration.

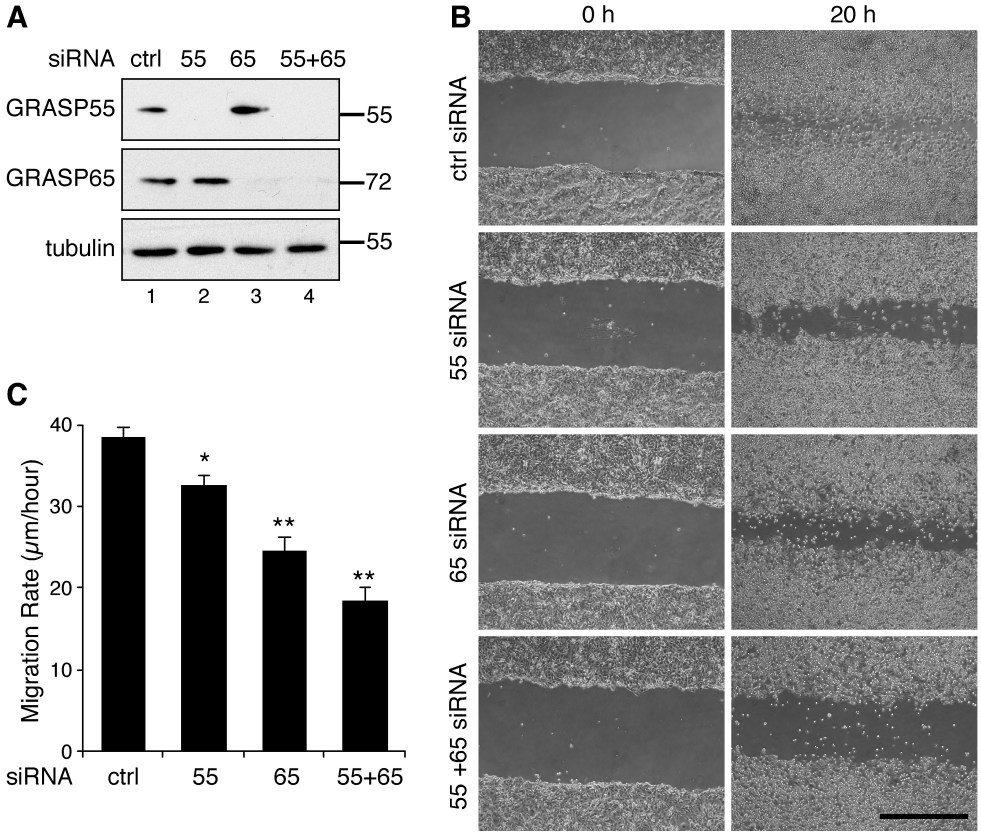

Figure 3.4. GRASP-depletion reduces cell migration. (A) Western blot analysis of MDA-MB-231 cells transfected with indicated siRNAs. **(B)** GRASP-depletion reduces MDA-MB-231 cell migration. Cells transfected with indicated siRNAs were analyzed with wound assay. Images shown were taken at 0 h and 20 h after the scratch. Scale bar, 600 μm. **(C)** The migration rate is calculated using images obtained from the experiment described in (B). The result is derived from three independent experiments, error bar = SEM. *, $p<0.05$; **, $p<0.01$.

GRASP depletion did not cause apoptosis and ER stress

To determine whether the effects above were caused by apoptosis, we stained the non-permeabilized cells with annexin V-GFP that binds to phosphatidylserine, a phospholipid that is translocated from the inner leaflet of the plasma membrane to the outer leaflet at early stage apoptosis [222, 223]. As shown in Fig. 3.S4A, cells treated GRASP siRNA lacked annexin V staining, while cells treated with staurosporine, a known apoptosis inducer, were readily stained (Fig. 3.S4B). Furthermore, no fragmentation of the nuclei was observed of GRASP-depleted cells, although they are slightly smaller than control siRNA cells, possibly because these cells are relatively rounder on the dish (Fig. 3.4). In addition, cleaved caspase 3, another widely used apoptotic marker [224], was detected in staurosporine-treated cells but not GRASP-depleted cells (Fig. 3.S4C). Finally, GRASP-depleted cells were not stained by the TUNEL apoptosis-detection kit (data not shown). Taken together, these results showed that that depletion of GRASP protein did not cause apoptosis in this study.

We have also determined whether GRASP-depletion causes ER stress by probing the cell lysate with the anti-Bip antibody [225]. Bip expression level was increase by tharpsigargin treatment that is known to induce ER stress, but not by GRASP-depletion (Fig. 3.S5). This result excludes the possibility that Golgi unstacking leads to ER stress.

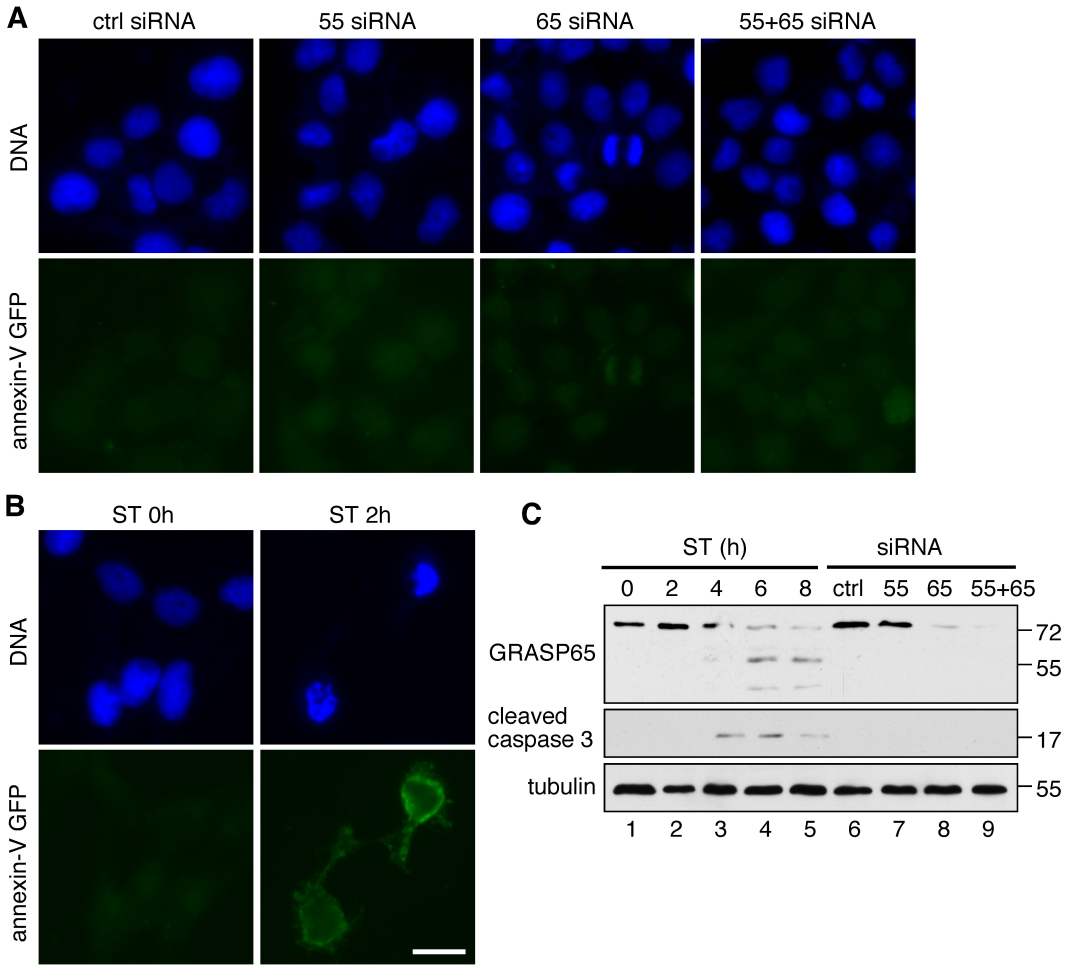

Figure 3.S4. Depletion of GRASPs does not cause apoptosis. (A) HeLa cells transfected with indicated siRNAs were stained with annexin V-GFP before fixation. Note that no obvious annexin V staining was observed on GRASP-depleted cells. **(B)** HeLa cells treated with 2 μM staurosporine (ST) for 0 h or 2 h were stained with annexin V-GFP before fixation. Note cells treated with staurosporine were stained by annexin V-GFP. **(C)** HeLa cells transfected with indicated siRNAs, or treated with staurosporine (ST) were analyzed by western blot. Note that the cleaved caspase 3 was detected after 4 h staurosporine treatment, but not upon the depletion of GRASPs.

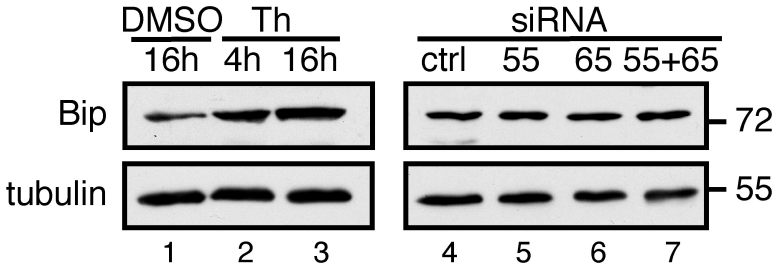

Figure 3.S5. Depletion of GRASPs does not cause ER stress. HeLa cells transfected with indicated siRNAs, or treated with DMSO or 2 μM tharpsigargin for 4h or 16h to induce ER stress, were analyzed by SDS-PAGE and western blot. Note the protein level of Bip increased after tharpsigargin treatment but not by GRASP depletion.

Golgi unstacking reduces integrin level in the cell

The fact that Golgi unstacking reduces cell adhesion and migration (Fig. 3.3 and 3.4) suggests that it may affect cell adhesion molecules such as integrins. Integrins are heterodimers consisted of α and β subunits, both are type I transmembrane proteins with a small cytosolic tail and a large extracellular domain. Integrins are major carriers of N-glycans; 18 α and 8 β integrins have been identified in human and mouse genome [226]. The best characterized integrin is α5/β1 integrin, which mediates cell adhesion by binding to fibronectin, which requires proper N-glycosylation of the integrins [227, 228]. Peptidase N-glycosidase F (PNGase F) that cleaves between the innermost N-Acetylglucosamine (GlcNAc) and asparagine residues from a N-linked glycoprotein blocked the formation of the α5/β1 complex and its interaction with fibronectin, suggesting that the presence of N-glycans on integrins is critical for their functions [229]. Western blot analysis of HeLa cell lysate using an antibody against the C-terminal cytosolic tail of β1 integrin detected two bands of about 130 kDa and 110 kDa (Fig. 3.5A). Both bands were glycosylated, as the treatment of PNGase F reduced both bands to 95 kDa (Fig. 3.S6). The cell lysates have also been treated with Endoglycosidase H (Endo H), an enzyme that cleaves within the chitobiose core of high mannose oligosaccharides from N-linked glycoproteins, a conversion that occurs in the *medial* Golgi region. The 130 kDa band was resistant to the treatment of Endo H, suggesting that it is the mature form of β1 integrin. The lower 110 kDa band was downshifted by Endo H treatment, indicating that it is the immature ER form (Fig. 3.S6). Similarly, α5 integrin also existed as the mature form of 150 kDa and a precursor form of 135 kDa (Fig. 3.S6).

The protein levels of α5/β1 integrin in cells depleted of GRASPs were assessed by western blot. When GRASP65 or both GRASP55 and GRASP65 were depleted, the protein levels of α5 and β1 integrins reduced to about 50% compared to control siRNA treatment; while other surface proteins such as insulin-like growth factor receptor (IGF R) did not change significantly (Fig. 3.5). This result is consistent with the conclusion that Golgi unstacking reduces cell attachment and migration.

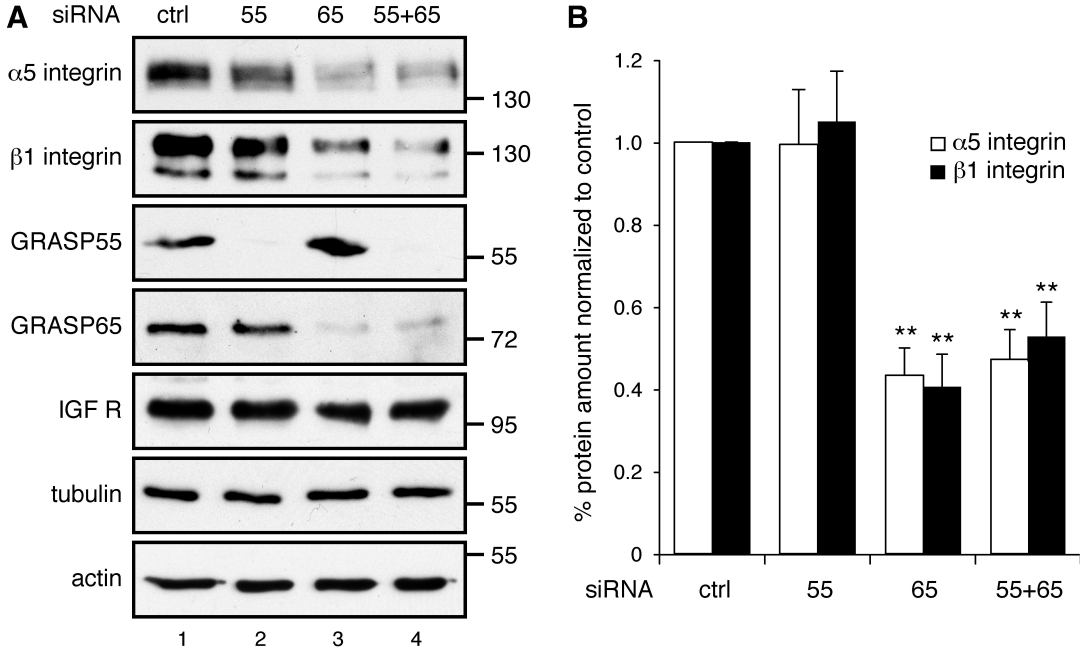

Figure 3.5. Depletion of GRASP65 or both GRASPs causes a reduction of α5 and β1 integrins. (A) Western blot analysis of HeLa cells transfected with indicated siRNAs. Note the reduction of both α5 and β1 integrins. **(B)** Quantitation of (A), normalized with α-tubulin. Error bar = SEM, n=3. **, *p<0.01*.

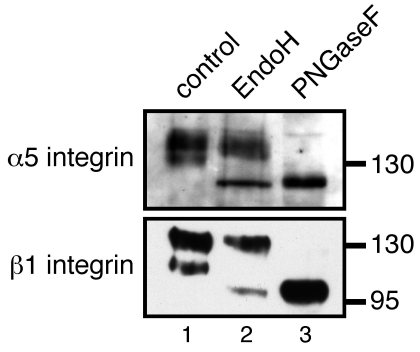

Figure 3.S6. Glycosidase treatment of α5/β1 integrins. HeLa cell lysates treated with EndoH or PNGase F were analyzed by western blot. Note that the two bands of α5/β1 integrins detected at steady state were both cleaved by PNGase F, while only the lower bands were sensitive to EndoH treatment.

The synthesis of α5/β1 integrins is reduced in cells with unstacked Golgi

To determine whether the reduction of integrin protein level was due to decreased protein synthesis, we assessed integrin synthesis using a pulse-chase assay. Cells transfected with control or GRASP siRNAs were incubated within medium containing ^{35}S-labeled methionines and cysteines for 1 h, and α5 and β1 integrins were immunoprecipitated and analyzed by SDS-PAGE followed by autoradiography. The newly synthesized α5 and β1 integrin existed as a single band of 135 kDa and 110 kDa, respectively (Fig. 3.6A), corresponding to the immature ER forms. Notably, the amounts of α5 and β1 integrins were reduced by about 50% upon GRASP-depletion (Fig. 3.6A, 6B), consistent with the observation that α5 and β1 integrin protein levels were reduced in GRASP-depletion cell in steady state (Fig. 3.5A, 5B).

We then tested integrin glycosylation and trafficking. siRNA treated cells were label by ^{35}S-labeled methionines and cysteines for 1 h as described above followed by a chase for different time periods. Integrins were then immunoprecipitated and analyzed by autoradiography. At 0 h chase, all cells had both α5 and β1 integrins as a single immature form (Fig. 3.6C). After 2 h chase, the mature form of α5 and β1 integrin began to appear. About 40% of α5 integrin existed as the mature form in the cells treated with control siRNA, while the mature form increased to 80 % in cells depleted of GRASP55, GRASP65, or both (Fig. 3.6C, 6D), suggesting that α5 integrin glycosylation in the Golgi apparatus is accelerated when the Golgi is unstacked. At 4 h and 6 h chases, detectable amounts of α5 integrin existed as the immature form in control cells; while almost all α5 integrin had matured in GRASP-depleted cells (Fig. 3.6C). The maturation of β1 integrin is also faster in cells depleted of GRASP65. After 2 h chase, 50 % β1 integrin has

matured to the fully glycosylated form in GRASP65 knockdown cells compared with 30 % in control cells (Fig. 3.6C, 6E). After 4 h chase, 80 % mature form of β1 integrin was found in GRASP65 knockdown cells compared with 60 % in control cells (Fig. 3.6C, 6E), although this effect was less significant in cells depleted of GRASP55, or both GRASPs (Fig. 3.6C, 6E). The degradation of α5 and β1 integrins was also assessed using the same pulse/chase method. The amount of integrins immunoprecipitated after 24 h and 48 h chases were compared with that at 12 h, when both integrins existed as the single mature form. All cells showed similar trend in the reduction of the signals (Fig. 3.S7).

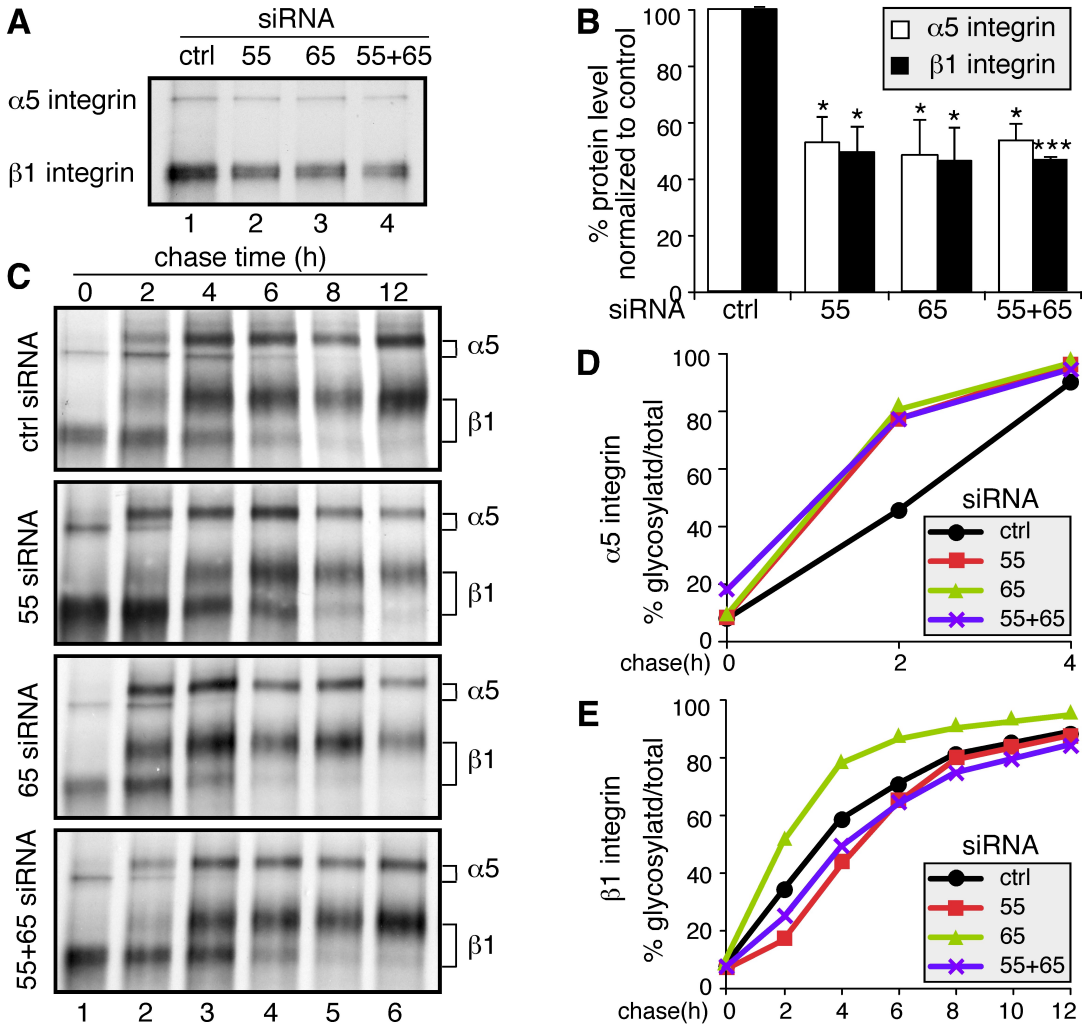

Figure 3.6. Golgi unstacking reduces α5/β1 integrin synthesis but accelerates their trafficking. (A) GRASP-depletion reduces α5/β1 integrin synthesis. HeLa cells transfectd with indicated siRNA were

labeled by 250μCi/ml TRANS ^{35}S-LABEL [^{35}S] for 1 hour and lyzed. Both α5 and β1 integrin were immunoprecipitated and analyzed with SDS-PAGE and autoradiography. **(B)** Quantitation of (A) from two independent experiments. *, *p<0.05,* ***, *p<0.001*. **(C)** GRASP-depletion increases α5/β1 integrin trafficking. As in (A) but with a chase for indicated time periods. Note that mature form of α5/β1 integrin appeared faster in GRASP-depleted cells. **(D)** Quantitation of the ratio of the mature form vs. total α5 integrin at indicated chase time of one representative result out of three independent experiments. Note that the maturation rate of α5 integrin increased in GRASP-depleted cells. **(E)** Quantitation of the ratio of the mature form vs. total β1 integrin at indicated chase time. Note that the maturation rate of β1 integrin increased in GRASP65-depleted cells

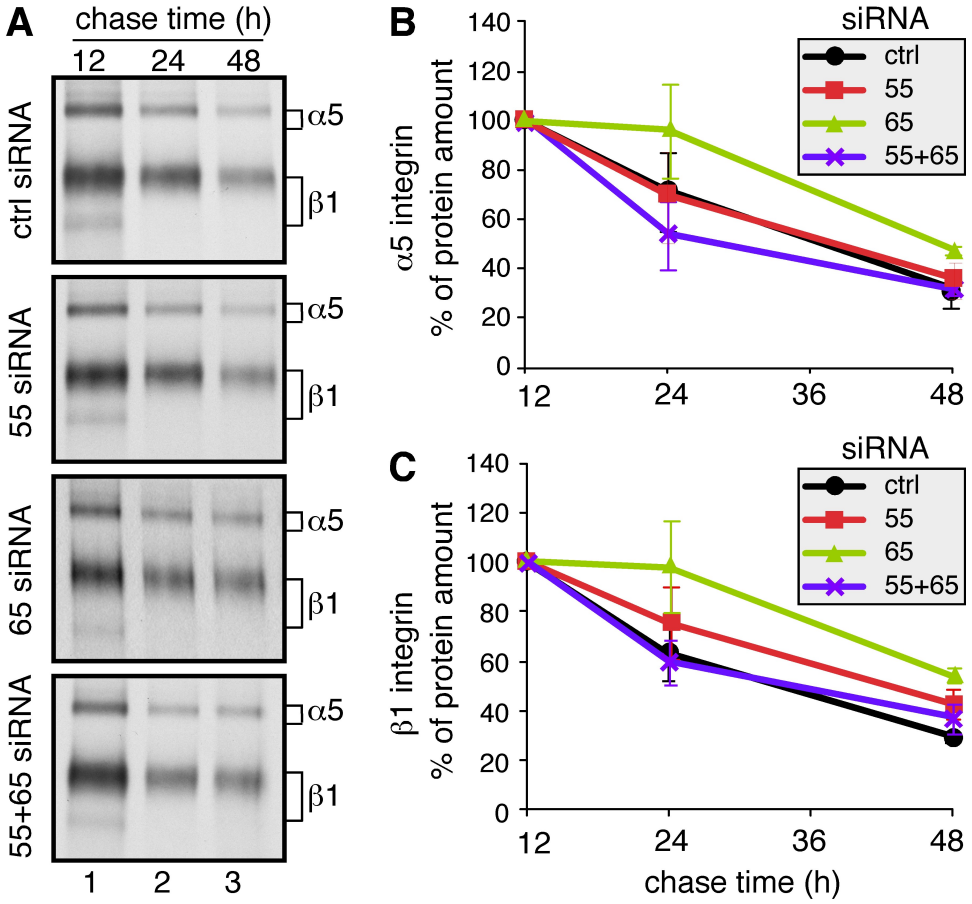

Figure 3.S7. Golgi unstacking does not affect α5/β1 integrin degradation. (A) HeLa cells transfected with indicated siRNAs were labeled with TRANS ^{35}S-LABEL [^{35}S] for 1 hour and lyzed at indicated chase time. Both α5 and β1 integrin were immunoprecipitated and analyzed by SDS-PAGE and autoradiography. Error bar = SEM, n=3. **(B)** Quantification of the amount of α5 integrin, normalized to the protein amount at 12 h chase. Result represents the average of three independent experiments. **(C)** Quantification of the amount of β1 integrin.

Golgi unstacking enhances total protein synthesis and cell growth

To determine how Golgi unstacking affect cell proliferation, we examined the growth rate of GRASP-depleted cells using the established crystal violet assay [119]. The

cells were transfected with indicated control or GRASP siRNAs, and seeded to 24 well plates 24 h after transfection. After 24 h incubation, the number of cells was assessed for 6 successive days. As shown in Fig. 3.7A, the increase of the cell number was significantly higher in cells treated with GRASP siRNAs in comparison with those treated with control siRNA. We then determined total protein synthesis in these cells. Cells treated with control or GRASP siRNAs were labeled by ^{35}S-labeled methionines and cysteines for 1 h and lysed in detergent. Equal amount of total proteins were TCA precipitated and total radioactivity incorporation was measure in a scintillation counter. As shown in Fig. 3.7B, total protein synthesis increased when GRASPs were depleted compared to control siRNA treated cells. This result is consistent with the observation that Golgi unstacking increases cell growth, suggesting a link between protein synthesis, trafficking, modifications and cell growth.

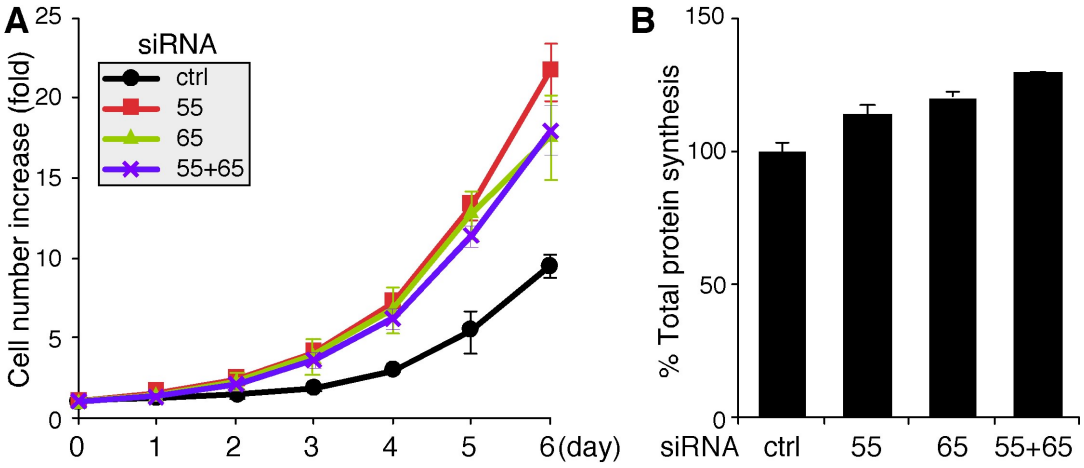

Figure 3.7. Depletion of GRASPs enhances cell proliferation and total protein synthesis. (A) Growth rates of HeLa cells transfected with indicated siRNAs, measured using crystal violet staining. The measurement starts 48 hours after transfection. Shown are the averages of three independent experiments. **(B)** Total protein synthesis is enhanced in GRASP-depleted cells. HeLa cells transfected with indicated siRNA were labeled with TRANS ^{35}S-LABEL [^{35}S] for 1h. Equal amount of total proteins were precipitated by TCA and [^{35}S]-methinonine/ cysteine incorporation was assessed with scintillation counting.

Discussion

Golgi stacking is a pronounced feature of the vast majority of eukaryotic organisms [230], however, whether it has any biological relevance on protein trafficking and modifications is unclear. On one hand, the close spatial arrangement of cisternae in stacks minimizes the distance the molecules have to travel, which may improve the efficiency of cargo transport. On the other hand, Golgi stacking may limit the area of membranes for vesicle formation and fusion to the Golgi rims. Therefore it was unclear how Golgi stacking affects the rate of protein trafficking through the Golgi stack. In this study, we use GRASP65 and GRASP55 RNA interference as the tool to manipulate Golgi stack formation and determined the biological roles for Golgi stacking in protein trafficking, sorting and glycosylation as well as cell attachment, migration and growth. Our results demonstrated that cisternal stacking slows down protein trafficking and thus ensures proper glycosylation of cargo proteins as they travel through the stack.

How Golgi cisternal stacking affects protein trafficking has been a long-standing question in cell biology. In our earlier study, we inhibited Golgi stacking by microinjection of GRASP65 antibodies into mitotic cells and monitored the transport of CD8 in post-mitotic daughter cells. We showed that CD8 arrived at the plasma membrane faster in cells with unstacked Golgi [208]. However, the microinjection technique did not allow us to perform biochemical and cell biology experiments to determine protein glycosylation, sorting and other cellular activities. In this study, we inhibited Golgi stacking by the depletion of the Golgi stacking factors GRASP65 and GRASP55, and showed that Golgi unstacking increased the trafficking of VSV-G and α5/β1 integrins, using flow cytometry and radioactive pulse/chase labeling, respectively. Notably, at

earlier time points of the VSV-G experiment, the differences of VSV-G on the cell surface was less significant among control and GRASP siRNA treated cells; while at 120 min after the release, the difference became more obvious, and this effect was gradually diminished after longer chase. This may explain why the earlier studies did not detect the effect of GRASP65 or GRASP55 depletion on VSV-G transport [29, 118]. A plausible explanation for the increased trafficking is that when the Golgi cisterane are fully stacked, vesicles can only form and fuse at the rims; Once the cisternae unstack, more membrane area becomes accessible, thereby increasing the rate of vesicle budding and cargo transport through the Golgi [208]. Consistently, *in vitro* budding assay revealed that unstacking increased the rate of COPI vesicle formation from the Golgi membranes [208].

Using fluorescence-conjugated lectins, we demonstrated that GRASP-depletion led to a decrease of sialic acid and an increase of terminal β-galactose on the cell surface, especially when GRASP65 was knocked down (Fig. 3.2). Our results are in agreement with the speculation that stacking ensures efficient and accurate post-translational modifications of cargo proteins by the resident glycosylation enzymes [187]. These enzymes are distributed across the stack in the order by which they operate [201, 231]. Each cisterna corresponds to a different reaction compartment in which specific enzymes are concentrated. Unlike the ER that contains a high concentration of soluble chaperones and folding enzymes, where improperly modified cargos are retained or degraded, the Golgi apparatus lacks a rigorous system to control the fidelity for its biosynthetic processes [185]. Even when the glycosidases or glycotransferases are inhibited or mutated, membrane and secretory glycoproteins carrying defective glycans are still

readily exported [232]. In addition, the concentration of cargo proteins inside the Golgi apparatus is considerably higher than that in the ER, since the Golgi resident enzymes are mostly transmembrane proteins. Therefore, a controlled slow cargo flow through the Golgi apparatus could be critical for cells in which correct glycosylation is important. In higher multicellular organisms such as vertebrates, particularly in mammals, accurate glycosylation of cell surface proteins such as receptors and cell adhesion molecules is essential for their cellular functions. Therefore, improper glycosylation could results in significant consequences. Aberrant glycosylation is a hallmark of many cancers, and Golgi fragmentation has been observed in some tumor cell lines [233] and tumor tissues (unpublished data), although the causality between the two is undetermined. On the other hand, Golgi stacking may not be required for protein trafficking as cells without proper Golgi stacks survive. In the budding yeast *S. cerevisiae*, as one rare exception in which Golgi membranes do not form stacks under normal growth conditions, N-glycosylation in the Golgi, which only involves the addition of mannoses, is much simpler [234]. Therefore, Golgi stacking may be a gained feature during evolution to improve the accuracy of protein modifications.

In addition to proper glycosylation, Golgi stacking is also essential for protein sorting and higher cellular activities. Our results showed that unstacking resulted in missorting of cathepsin D precursor to the extracellular space instead of endosomal/lysosomal system. Similar observation has been reported in human mammary cancer cells upon the induction of estrogen [235]. It is possible that stack formation ensures that sorting of cargo molecules only occurs in the TGN but not other cisternae. In addition, the ratio between the intermediate form and the precursor in cells with GRASP-

depletion increased, implicating that the hydrolase was sorted to the endosomal/lysosomal system faster when the Golgi was unstacked, consistent with the conclusion that the cisternal stacking functions as the flux regulator.

The reduction of cell adhesion and migration of the cells with unstacked Golgi may be attributed to the alteration of the glycosylation on the cell surface and the reduction of α5/β1 integrins. In multicellular environment, the glycans on the cell surface are usually the first molecules to contact with other cells and extracellular environment, and they are known to contribute to cell adhesion, migration and communication [186]. Altered expression of cell surface N-linked oligosaccharides, for example, elevated 6GlcNAc side chain branching, inhibits cell attachment and spreading [228], and is associated with the oncogenic transformation of many types of animal cells. It is also conceivable that the cells with unstacked Golgi grow faster as the protein synthesis and cargo transport are enhanced, although the underlying mechanism is elusive.

A variety of cellular stresses, such as the disruption of post-ER protein modification or folding, membrane traffic overload, changes in Golgi pH and ion content, and viral assembly and budding at Golgi membranes, could results in Golgi fragmentation in the cells [134], which may be referred to as “Golgi stress”. For example, changing the Golgi pH interrupts the Golgi function and leads to aberrant glycosylation [233]. However, the morphological and functional definition of “Golgi stress” is unclear. Whether Golgi unstacking can be induced by “Golgi stress”, whether any signaling pathway is involved in “Golgi stress”, or whether it contributes to aberrant glycosylation in a multicellular environment remains to be determined.

Materials and Methods

All reagents were from Sigma Co., Roche or Calbiochem, unless otherwise stated. The following antibodies were used: monoclonal antibodies against β-actin (Sigma), α-tubulin (DSHB), α5 integrin (BIIG2, DSHB), β1 integrin (P5D2, DSHB), Human β1,4 Galactosyltransferase I (CB002, CellMab AB), cleaved caspase 3 (Cell Signalling, #9661), VSV-G extracellular domain (D. Sheff); polyclonal antibodies against human GRASP55 (Proteintech Group, Inc.) and GRASP65 (J. Seemann), α5 integrin C-terminus (Millipore, AB1928), β1 integrin C-terminus (Abcam, EP1041Y), IGF-IRβ (Santa Cruz, sc-713), GM130 (N73, J. Seemann), Bip (P. Arvan), cathepsin D (sc-6486, Santa Cruz).

Cell culture and transfections

HeLa and MDA-MB-231 cells were grown in DMEM (Invitrogen) containing 10% fetal bovine serum and L-glutamine at 37°C in a 5% CO_2 incubator. Knockdown transfections were performed with HeLa cells plated at 40% confluency following the manufacture's instruction. For cells in six-well plates, 3 µl of a 50 µM siRNA stock was added to 250 µl Opti-MEM. In a separate tube, 5 µl transfectamine^{TM} RNAiMAX (Invitrogen) were mixed with 250µl Opti-MEM and incubated for 5 min at room temperature (RT). The two mixtures were combined and incubated at RT for 20 min, and added to the cells in 2 ml DMEM containing 10% fetal bovine serum. siRNAs for human GRASP55 (AACTGTCGAGAAGTGATTATT) [23] and GRASP65 (CCTGAAGGCACTACTGAAAGCCAAT) [118] were purchased from Ambion and Invitrogen, respectively. Control non-specific siRNAs were purchased from Ambion.

Microscopy

Fluorescence images were captured with a Leica SP5 confocal laser-scanning microscope using a 100X oil lens or Zeiss Observer Z1 epifluorescence microscope using a 63X oil lens. Phase contrast images were taken with a Zeiss Observer Z1 microscope using a 40X lens. Bright field images of the MDA-MB-231 cells were taken with OLYMPUS 1X81 microscope, using a 4X lens and IMAGING ERTIGA 1300R camera. For images taken with the confocal microscope, each image was a maximum projection from a z-stack. Pictures were assembled in Adobe Photoshop.

VSV-G transport

A population of HeLa cell that stably express VSV-G-GFP (*ts*O45) in an inducible manner was established using the retroviral system as described previously [18] and enriched by FACS sorting. Cells were transfected with control, GRASP55, GRASP65, or both GRASP55 and GRASP65 siRNAs, and incubated at 37˚C. Eighty hours after transfection, 1 μg/ml doxycycline was added and cells were transferred to 40.5˚C. Fifteen hours later, 100 μM cycloheximide was added to inhibit protein synthesis. One hour after the addition of cycloheximide, the cells were shifted to 32˚C to release the VSV-G proteins from the ER. After 120 min incubation at 32˚C, the cells were harvested with PBS containing 20 mM EDTA, and fixed with 3.7% paraformaldehyde. Cells were blocked with PGA (PBS containing 0.2% gelatin and 0.04% azide) buffer, and surface VSV-G-GFP was labeled with the antibodies specifically against its extracellular domain [236] at 4˚C overnight. After washing with the PGA buffer, cells were incubated with Cy5 conjugated Goat-anti-mouse IgG antibody (Jackson ImmunoResearch Laboratories)

for 30 min at room temperature. The fluorescence intensity of GFP and Cy5 were analyzed on a FACScalibur flow cytometer (BD Biosciences). The amount of VSV-G on the cell surface after subtracting the background was normalized by the GFP intensity.

Lectin staining

For the immunofluorescence analysis, HeLa cells growing on cover slides were fixed with 3.7% paraformaldehyde. After blocking with 1% BSA (in PBS), surface glycosylated proteins were labeled with TRITC-conjugated lectins such as MAA or ECA (EY laboratories) in dark for 30min at 4˚C. After washing with 1% BSA, the cells were permeabilized with 0.3% Triton X-100 and processed for immunofluorescence wFor the flow cytometry analysis, HeLa cells were harvested with PBS/20 mM EDTA, blocked with cold BSA buffer, and labeled with FITC-conjugated lectins (EY laboratories) in the dark at 4˚C, for 30 min. After washing, the cells were fixed with 3.7% paraformaldehyde and analyzed on a FACScalibur flow cytometer (BD Biosciences).

Pulse/chase labeling and immunoprecipitation

HeLa cells growing on 60 mm dishes were incubated in methionine/cysteine-free DMEM medium (Invitrogen) for 1 h and labeled with 1 ml medium containing 250 μCi/ml TRANS ^{35}S-LABEL [^{35}S] (MP BIOMEDICALS) for 1 h. After washing with PBS, cells were either collected immediately on ice, or after incubating with 4 ml complete growth medium containing 2 mM L-cysteine and L-methionine for indicated time periods. 0.8 ml lysis buffer (PBS containing 1 mM $CaCl_2$, 0.5 mM $MgCl_2$, 1% TritonX-100, cocktail Protease inhibitors, 1 μM pepstatin A) was added to lyze the cells.

After centrifuge at 14,000 rpm for 15 min, the protein concentration of the supernatant was measured using the Bio-Rad protein assay (Bio-Rad Laboratories, Inc., CA). 60 ng β1-integrin antibody P5D2 and 50 ng α5 integrin antibody BIIG2 were added to 2 mg supernatant of the cell lysate, and incubated at 4˚C, overnight. The antibodies were precipitated with 30 µl protein G beads (Roche Diagnostics GmbH, Germany) at 4˚C for 2 hours. Beads were washed five times with the lysis buffer, and the immunoisolated materials were eluted by boiling for 5 min in nonreducing SDS sample buffer. Integrins were resolved by 6.5% nonreducing SDS-PAGE.

To determine the total protein synthesis, 40 µl of the cell lysate were precipitated with 10 µl 100% (w/v) Trichloroacetic acid (TCA) at 4˚C for 10 min. The protein pellets were washed with acetone, dissolved in 0.2 M NaOH, and neutralized with 0.2 M HCl. The radioactivity intensity was analyzed by scintillation counting (Fisher scintiverse ™ BD cocktail), and normalized with the total protein amount.

Attachment assay

The 12 well plates were coated with fibronectin from human plasma (Sigma, F0895) at 1 mg/ml in Tris-buffered saline (pH7.5) at 4 ˚C for 16 h, and blocked with 2% BSA. HeLa cells transfected with indicated siRNA were detached with PBS containing 20 mM EDTA and the cell numbers were counted with hemocytometer. Cells were pelleted and resuspended in serum-free DMEM. 300,000 cells were seeded per well on fibronectin coated 12 well plates (3 wells for each condition), and cultured with serum-free DMEM at 37˚C for 30 min. Cells were then rinsed 4 times with PBS, attached cells were

collected and counted. The attachment is represented as the percentage of attached cells out of the total number of cells.

Wound-healing assay

The wound-healing assay was performed using the protocol described by Jun-Lin Guan and colleagues [221]. MDA-MB-231 cells were transfected with indicated siRNAs. Fourth-eight hours after transfection, the cells were re-plated in 12 well plates at 80% confluency in complete growth medium. Twenty-four hours later, after the cells became confluent and formed monolayer, the medium was replaced with serum-free DMEM. Twenty-four hours later, the cell monolayer was scraped in a straight line to create a ‘‘scratch’’ with a p200 pipet tip. The cells were washed once with DMEM, and images were taken using inverted bright field microscope with a 4X lens and an IMAGING ERTIGA 1300R camera. The cells were then allowed to grow in complete growth medium for 20 h, and images of the same area were taken. Images were analyzed with the NIH Image J software.

Growth rate analysis

HeLa cells transfected with indicated siRNAs were trypsinized 24 hours after transfection. 10000 cells were added into each well of 24-well plates and incubated in complete growth medium. One day later, the cell numbers were measured every 24 h for 6 days by crystal violet staining as described previously [119]. Briefly, cells were washed with PBS, fixed in 3.7% paraformaldehyde for 30 min and stained with 0.5% crystal violet (in 30% methanol) for 15 min, followed by extensive wash with H_2O. The DNA-

bound dye was extracted using 1 ml 10% acetic acid for 5 min, and measured for optical density (OD) at 590nm. The cell numbers at different time were normalized to the cell number from the first measurement (Day 0).

Annexin V assay

HeLa cells grown on cover slides were incubated at room temperature in dark with annexin V-EGFP diluted at 1:100 in the binding buffer provided by the manufacturer (BioVision, K104-25). After wash with PBS, the cells were fixed, permeabilized and stained with Hoechst. Images were taken using the Zeiss inverted microscope Observer Z1 with 40X lens.

Endo H and PNGase F treatment

Both Endo H and PNGase F were purchased from New England BioLabs. 100 µg of HeLa cell lysate were denatured with 100 µl denaturing buffer at 100 ˚C for 10 min, 11 µl 10X reaction buffer was added to the lysate after cooling down at RT. 500 unit Endo H or PNGase F diluted in 90 µl 1X reaction buffer was added to the cell lysate and incubated at 37 ˚C for 1 h. Reactions were stopped with 50 µl 5X SDS sample buffer. 1% NP-40 was included in the PNGase F reaction.

Acknowledgements

We thank Dr. Hiroyasu Kamei, Cunming Duan, Olga Makarova, David Sheff, Dennis Larkin, A. Roberto Lara-Lemus, Peter Arvan, Xiao-wei Chen, Joachim Seemann and Graham Warren for antibodies and cDNA constructs. The monoclonal antibody BIIG2 and P5D2 developed by Caroline H. Damsky and Elizabeth A. Wayner, respectively, were obtained from the Developmental Studies Hybridoma Bank (DSHB). We also thank Dr. Ming Liu for technical help with pulse chase assay, members of the Wang Lab for suggestions and reagents. This work was supported by the Pardee Cancer Research Foundation, the National Institute of Health (GM087364), American Cancer Society (RGS-09-278-01-CSM), a University of Michigan Rackham Faculty Research Grant, the NIH-funded Michigan Alzheimer's Disease Research Center (P50 AG08761) and an anonymous donation to Y. Wang, and by a University of Michigan Rackham Predocotoral Fellowship to Y. Xiang. The authors declare no conflicts of interest.

Chapter IV. Active ADP-ribosylation factor-1 (ARF1) is required for mitotic Golgi fragmentation

Abstract

In mammalian cells the Golgi apparatus undergoes an extensive disassembly process at the onset of mitosis that is believed to facilitate equal partitioning of this organelle into the two daughter cells. However, the underlying mechanisms for this fragmentation process are so far unclear. Here we have investigated the role of the ADP-ribosylation factor ARF1 in this process to determine whether Golgi fragmentation in mitosis is mediated by vesicle budding. ARF1 is a small GTPase which is required for COPI vesicle formation from the Golgi membranes. Treatment of Golgi membranes with mitotic cytosol or with purified coatomer together with wild type ARF1 or its constitutive active form, but not the inactive mutant, converted the Golgi membranes into COPI vesicles. ARF1-depleted mitotic cytosol failed to fragment Golgi membranes. ARF1 is associated with Golgi vesicles generated *in vitro* and with vesicles in mitotic cells. In addition, microinjection of constitutive active ARF1 did not affect mitotic Golgi fragmentation or cell progression through mitosis. Our results show that ARF1 is active during mitosis and that this activity is required for mitotic Golgi fragmentation.

Introduction

The Golgi apparatus is a membrane-bound organelle that serves as a central conduit for protein and lipid modification, processing, trafficking and secretion in all eukaryotic cells. The central and unique feature of the Golgi is a stack of flattened cisternal membranes with dilated rims [8]. The stack carries out post-translational processing of newly synthesized proteins as they pass through this organelle after assembly in the endoplasmic reticulum (ER) [1]. Processing enzymes, which include those involved in modifying bound oligosaccharides, are arranged across the stack (in the *cis* to *trans* direction) in the order in which they function [201]. In animals, stacks are often interconnected to form a ribbon that is localized adjacent to the nucleus. Despite its complicated morphology and function, the Golgi apparatus is dynamic, capable of rapid disassembly and reassembly during mitosis [2] or upon drug treatment [80, 237-239]. Mitotic fragmentation of the Golgi apparatus was first observed in the early 1900s. One particularly good example is the study by Ludford in 1924, in which the Golgi was described as forming 'rodlets' that were scattered throughout the dividing cell and that, at a late stage in cell division, re-associated to form two separate Golgi complexes, one in each daughter cell [240]. Studies using electron microscopy showed fragmentation of the characteristic stack-like organization of the Golgi at the onset of mitosis, and Golgi fragments were subsequently distributed to each daughter cell [241, 242]. In the late 1990s, when green fluorescent proteins and live cell imaging techniques became available, it was shown that early in mitosis, during prophase, the Golgi undergoes extensive fragmentation along the cell cycle progression [79, 82, 88, 243]. During

cytokinesis, the dispersed Golgi fragments are converted into larger Golgi fragments that finally re-form the pericentriolar ribbon structure.

Several reasons have been put forward to explain the biological significance of mitotic Golgi fragmentation. The first concerns the mechanism of Golgi partitioning between the two daughter cells during the cell cycle. The distribution of Golgi membranes over a larger space of the cell is expected to aid in the even distribution of this organelle into the daughter cells [2]. The second hypothesis concerns the release of "mitotic" components stored on the Golgi during interphase, which are important in the promotion of cytokinesis [244, 245]. For example, Nir2, a Golgi-associated protein in interphase cells, has been shown to move to the cleavage furrow and is essential for cytokinesis [246]. Thus, in addition to directly providing membrane for cleavage furrow invagination [247], it is likely that the Golgi mediates the coordinated release of proteins required for cytokinesis and other cytoplasmic events as the cell progresses through mitosis.

The underlying mechanisms mediating Golgi disassembly during mitosis are so far unclear. One possibility is that disassembly is achieved through a similar mechanism as Brefeldin A (BFA) treatment, a fungal metabolite known to redistribute the Golgi membranes, at least partially, into the ER. BFA exerts its effects by inactivating the ADP-ribosylation factor-1 (ARF1) recruitment to Golgi membranes. ARF1 is a small GTPase that is membrane-associated in its active GTP-bound form and recruits coatomer onto the membrane to form COPI vesicles. Inactivation of ARF1 in turn prevents recruitment of coatomer (and hence the formation of COPI vesicles) and leads to the redistribution of Golgi membranes to the ER [80]. The central idea of this hypothesis is

that mitosis phenocopies BFA treatment in terms of Golgi breakdown by inactivation of ARF1. Using live cell imaging, it has been shown that transiently overexpressed ARF1-GFP disappears from the Golgi region in the early stages of mitosis and that the expression of the constitutively active ARF1 (Q71L) mutant blocks mitotic Golgi disassembly as well as cell progression through mitosis [243, 245, 248], suggesting that ARF1 needs to be inactivated in order to disassemble the Golgi. However, whether the endogenous ARF1 is inactivated during mitosis is so far unclear.

Another explanation for the mitotic Golgi disassembly is the continuous budding of COPI vesicles. Isolated Golgi membranes, when treated with mitotic cytosol, undergo extensive fragmentation that mimics mitotic Golgi fragmentation seen *in vivo*. The fragmentation is mediated, in large part, by the continued budding of COPI vesicles [249]. Budding requires ARF1, suggesting that ARF1 is active. Consistently, budding is also enhanced in the presence of GTPγS, which is known to activate ARF1. However, GTPγS also activates other GTPases (such as Rab proteins) and impairs cargo uptake in the early stage of COPI vesicle formation [250]. So far there is no direct evidence that ARF1 itself is involved in mitotic Golgi fragmentation. Here we have examined the role of ARF1 in mitotic Golgi fragmentation using a variety of techniques. Our results show that ARF1 is active during mitosis and that this activity is required for mitotic fragmentation of the Golgi.

Results

Golgi fragmentation requires ARF1 activity

To test whether mitotic Golgi fragmentation requires ARF1 activity, we used a well-characterized system for COPI-vesicle formation *in vitro*. The incubation of highly enriched rat liver Golgi membranes (RLG) with coatomer and myristoylated ARF1 leads to budding of COPI vesicles [65, 250, 251]. Three forms of myristoylated ARF1, the wild type (WT), the constitutively active ARF1(Q71L), or the inactivated mutant ARF1(T31N) [252], were expressed in bacteria and purified following the established methods [253]. We first examined whether treatment of Golgi membranes with these purified ARF1 proteins, in the presence of purified coatomer, could lead to Golgi fragmentation. As shown in Fig. 4.1, treatment of Golgi membranes with purified WT ARF1 and coatomer led to extensive fragmentation of Golgi membranes (Fig. 4.1A). Quantitation of the results showed that about 43% of membranes were vesiculated in the presence of WT ARF1, a significant increase compared to treatment with coatomer alone (Fig. 4.1I). A similar result was obtained with the constitutively active form ARF1(Q71L) (Fig. 4.1B), a mutant restricted to the GTP-bound form, with 41% of membranes in vesicles (Fig. 4.1I). In contrast, no fragmentation was observed when the Golgi membranes were treated with the inactive form ARF1(T31N) (Fig. 4.1C), a mutant which has a preferential affinity for GDP compared to the wild-type protein [252]. Only about 13% of membrane in vesicles was observed, similar to untreated membranes (12%) (Fig. 4.1I). Detailed examination of EM images at higher magnification indicated that most of the vesicles were coated in the presence of WT ARF1, or ARF1(Q71L) (data not shown). Incubation of purified Golgi membranes with purified coatomer did not

significantly fragment the membranes (Fig. 4.1E), with about 12% of membrane in vesicles (Fig. 4.1I), suggesting that ARF1 activity is required for the vesiculation. This effect is due to the ARF1 protein added, since analysis of purified Golgi membranes by Western blotting showed that essentially no endogenous ARF1 proteins were associated with the membrane under the experimental conditions (data not shown).

To mimic mitotic conditions, we added purified mitotic kinases cdc2 (in complex with cyclin B1) and polo-like kinase (plk). These kinases mimic mitotic cytosol to phosphorylate most of the Golgi proteins known to be mitotically phosphorylated, such as GRASP65 and GM130 [17, 123, 254], which are involved in mitotic Golgi disassembly. In the presence of mitotic kinases, fragmentation of the Golgi by wild type (WT, Fig. 4.1F) and active ARF1(Q71L) (Fig. 4.1G) was significantly enhanced. The number of vesicles increased about 2-fold compared to ARF1 and coatomer, resulting in 80% of the total membranes fragmented into COPI vesicles (Fig. 4.1I). In contrast, the inactive ARF1(T31N) did not fragment Golgi membranes even in the presence of mitotic kinases (Fig. 4.1I), suggesting that ARF1 is not inactivated under mitotic conditions, at least not in this cell-free assay.

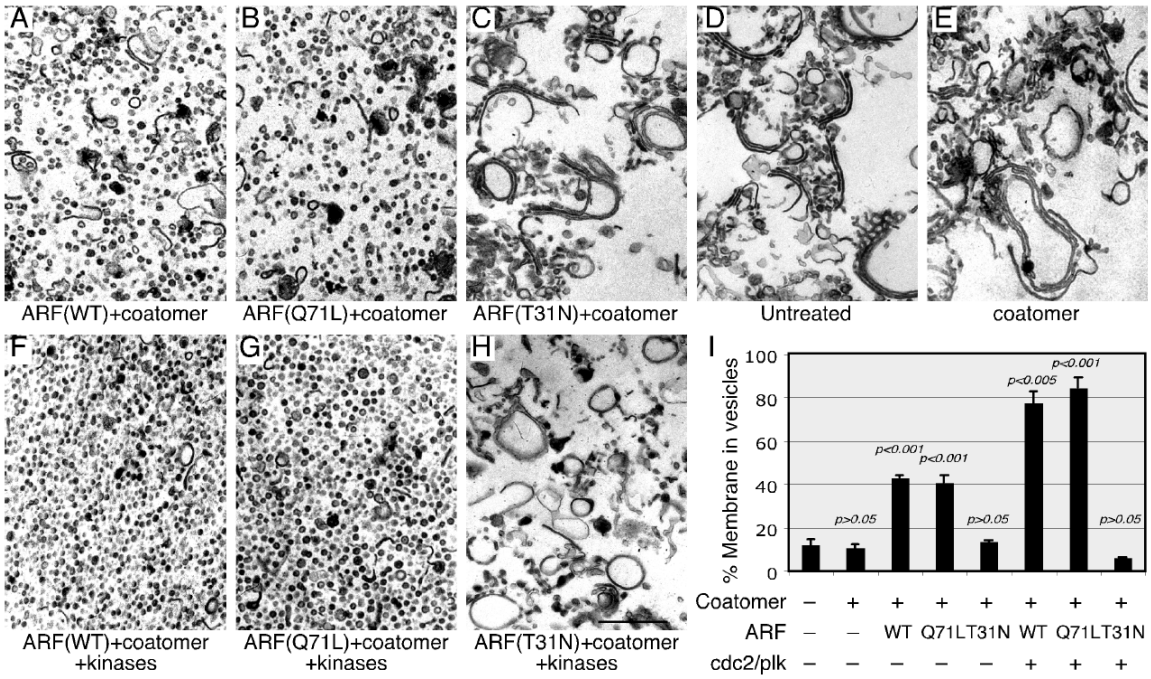

Figure 4.1. ***In vitro*** **Golgi fragmentation using purified coatomer and ARF1.** EM photographs showing fragmentation of purified Golgi membranes using purified ARF1, coatomer and kinases. Purified rat liver Golgi membranes were treated with wild type ARF1 and coatomer (A), constitutively active ARF1(Q71L) and coatomer (B), or with inactivated ARF1(T31N) and coatomer (C) at 37ºC for 20 min. Untreated (D) or coatomer alone (E) were used as controls. In some experiments, purified cdc2 and plk were included (F-H). Membranes were fixed and processed for EM. Bar, 0.5 μm. I. Quantitation of A-H, by the intersection method, to estimate the percentage of membrane in vesicles. Results represent the mean of three independent experiments ± SEM. To access the statistical significance, the result for treatment with coatomer alone was compared with that of no treatment; results for ARF1 WT, Q71L and T31N mutants in the absence of kinases were compared with that of treatment with coatomer alone; and results for WT, Q71L, and T31N mutants in the presence of kinases were compared with those without mitotic kinases, respectively. Note that the WT and the active Q71L mutant of ARF1 fragmented the Golgi but the inactive T31N mutant did not. Fragmentation was enhanced by the presence of purified cdc2 and polo-like kinases (kinases).

Active ARF1 associates with fragmented Golgi membranes

It has been shown that the active GTP-bound form of ARF1 associates with membranes, recruits coatomer and promotes vesicle budding. Upon GTP hydrolysis, ARF1 is inactivated and disassociates from the membrane [252, 255]. To test whether ARF1 is associated with the membranes after mitotic fragmentation of the Golgi membranes, we pelleted the membranes including the Golgi remnants and vesicles by high-speed centrifugation followed by analysis of ARF1 by Western blotting. As shown

in Fig. 4.2A, total membranes were pelleted efficiently, as indicated by GRASP65 and Gos28, two Golgi associated membrane proteins. Significant amounts of WT ARF1 and ARF1(Q71L) were found in the membrane pellets which contained COPI vesicles indicated by the β-COP subunit, while no signal was detected in the pellet with the inactive ARF1(T31N). Since recruitment of ARF1-GTP to the membrane is essential for COPI vesicle budding, this strongly suggests that ARF1 is active under mitotic conditions; without ARF1 activity, no vesicles were generated. Coatomer was also recruited onto the membrane by WT ARF1 or ARF1(Q71L), but not the inactive ARF1(T31N) (Fig. 4.2A, lanes 3 and 6 vs. 9), which is consistent with the ARF1 results. As β-COP was largely found in the pellet fraction with active ARF1 (Fig. 4.2), it indicates that most of the vesicles are coated, which further suggests that ARF1 is maintained in the GTP-bound form. The pattern of ARF1 association with membranes was not changed in the presence of mitotic kinases cdc2 and plk (Fig. 4.2B), with ARF1(WT) and ARF1(Q71L) largely associated with membranes and with no ARF1(T31N) in the membrane fraction. This result shows that ARF1 remains activate in the presence of these mitotic kinases.

The membrane binding property of ARF1 was then tested in the presence of BFA, a chemical compound that is known to inactivate ARF1 [256]. BFA abolished the membrane binding property of wild type ARF1 but not the Q71L mutant (Fig. 4.2C, lanes 6). This result confirms that only active ARF1 is associated with Golgi membranes under the experimental conditions.

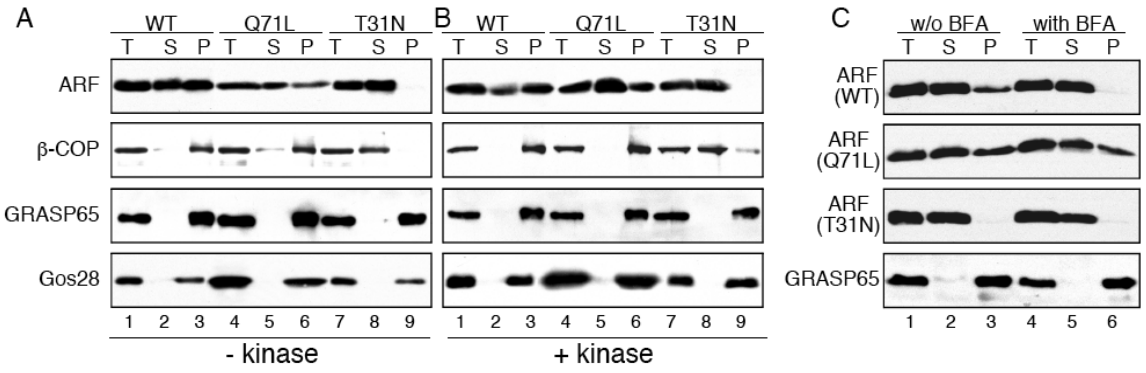

Figure 4.2. Association of activated ARF1 with membranes after the budding assay. Purified rat liver Golgi membranes were incubated with either wild type ARF1, constitutively active ARF1(Q71L), or with inactive ARF1(T31N) and coatomer, in the presence of (B) or absence of (A) purified mitotic kinases cdc2 and plk, at 37ºC for 20 min followed by isolation of the total membranes by centrifugation. Equal fractions (by volume) of the total (T, the reactions before centrifugation), the supernatant (S, the soluble fraction) and the pellet (P, the membranes) were analyzed by Western blotting for ARF1 and the membrane associated proteins GRASP65 and Gos28. Note that a large proportion of wild type and active ARF1(Q71L) proteins were found in the pellets (lanes 3 and 6), but not the inactive ARF1(T31N) mutant (lane 9). Note that addition of kinases did not reduce the amount of ARF1 bound to the membrane fractions. C. Only active ARF1 can bind to Golgi membrane. Purified ARF1 was incubated with Golgi membranes as in A except that Brefeldin A (BFA) was added in some reactions. Note that ARF1 WT and Q71L can bind to Golgi membranes in the absence of BFA (lane 3) and only Q71L can bind to membranes in the presence of BFA (lane 6).

To determine whether the ARF1 associated Golgi fragments are COPI vesicles, we separated the Golgi membranes treated with ARF1, coatomer and mitotic kinases on a 0.5-1.6 M sucrose gradient. After centrifugation to equilibrium, membrane bound proteins in each fraction were collected by high-speed centrifugation. Analysis by Western blotting revealed that the Golgi remnants were found in fractions 2 to 3, as indicated by GRASP65 (Fig. 4.3A), which is consistent with the density of Golgi membranes, equivalent to 0.8 M sucrose (Fig. 4.3B) [251]. The coated vesicle fraction peaked at fraction 8, as indicated by the β-COP subunit of the coatomer, which is consistent with the reported density of coated COPI vesicles, equivalent to 1.2 M sucrose (Fig. 4.3B) [65, 250]. With WT ARF1, the peak (fractions 7, 8 and 9) was broader than with the constitutively active ARF1 (fractions 8 and 9) (Fig. 4.3A), suggesting that uncoating of COPI vesicles occurs more frequently for WT ARF1 than that for

ARF1(Q71L) during the reaction and/or the centrifugation. Consistent with this result, the peak for β-COP was also broader with WT ARF compared with ARF1(Q71L) (Fig. 4.3A). The signal for WT ARF1 appeared stronger compared to ARF1(Q71L) because the antibody we used has a higher affinity to WT ARF1 and ARF1(T31N) compared to ARF1(Q71L) (Fig. 4.S1B). The inactive form of ARF1 was not found to be associated with membranes in any fraction; there was also no β-COP signal detected associated with membranes (Fig. 4.3A). Analysis of non-membrane-bound proteins in each fraction revealed that soluble ARF1 remained on the top of the gradient (Fig. 4.3A, sup), consistent with the result that ARF1(T31N) does not bind to the membrane and does not promote vesicle budding (Fig. 4.1). This result indicates that active ARF1 is associated with COPI vesicles under mitotic conditions. Besides ARF1 and coatomer, several membrane and secretory proteins were enriched in the vesicle containing fractions. These include the Golgi SNARE protein Bet1 (Fig. 4.3C) and syntaxin 6 (not shown), Golgi enzymes a-mannosidase I and II, Golgi structural protein Golgin-84 and Giantin, and the secretory protein rat serum albumin (Fig. 4.3C).

To further confirm that the membranes in β-COP concentrated fractions are COPI vesicles, we pooled fractions 1-3 and 7-9. Membranes in each pool were collected by centrifugation and analyzed by EM. As shown in Fig. 4.3D, fractions 1-3 contained the Golgi remnants, TGN membranes (indicated by the dense lipoproteins), and other vesicular-tubular structures. Fractions 7-9 contained essentially pure COPI vesicles (Fig. 4.3E), with a uniform size of about 70 nm in diameter. Coat proteins were visible on the vesicles at higher magnifications (Fig. 4.3F). Further measurements showed that the size of the vesicles generated by ARF1 and coatomer treatment (69.9 ±7.4 nm, n=50) was

identical to those generated by mitotic cytosol treatment (72.1 ± 6.0 nm, n=50). This size is consistent with the previous reports [257]. Taken together, these results show that active ARF1 is associated with COPI vesicles even when the Golgi membranes are mitotically fragmented.

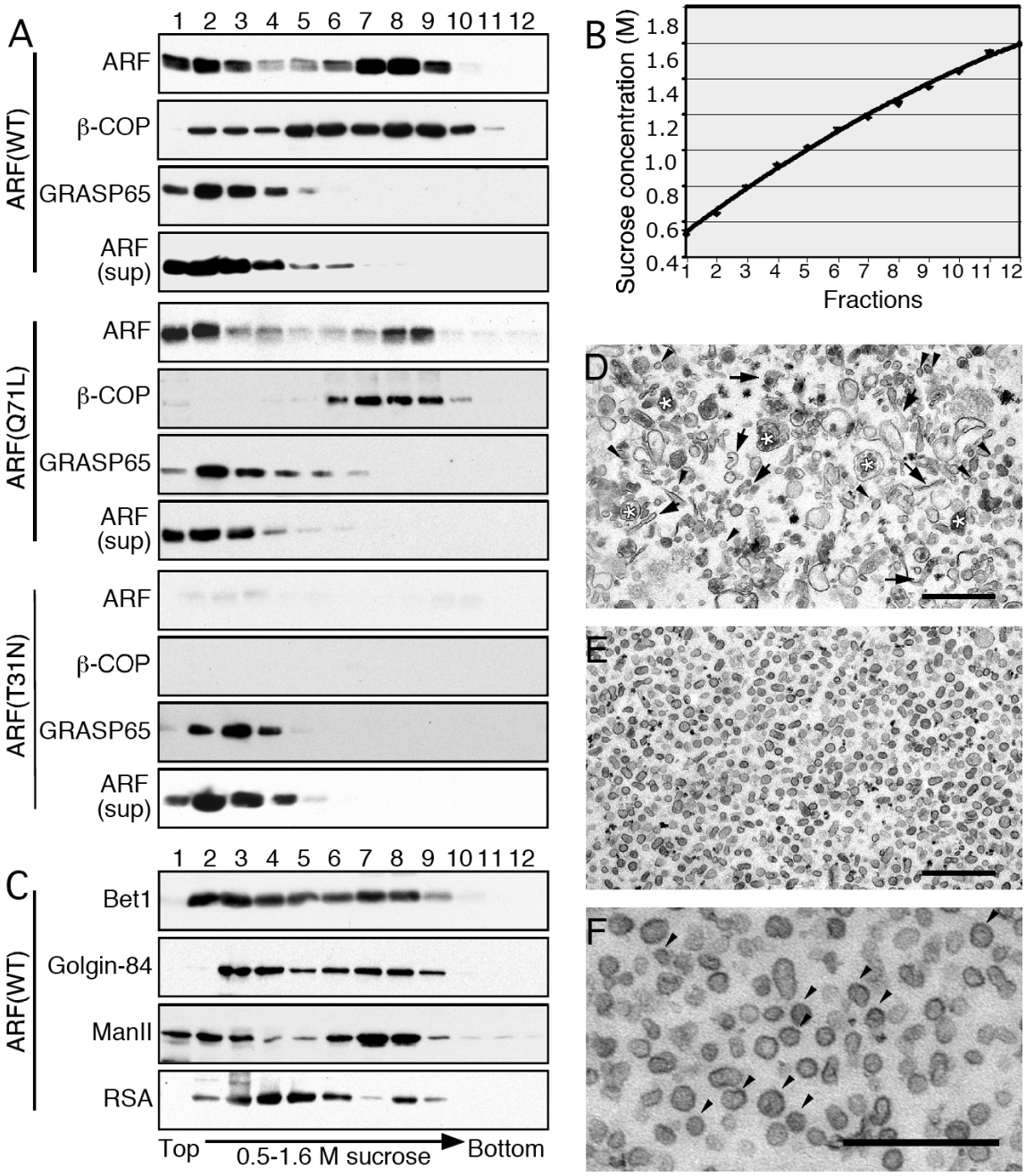

Figure 4.3. ARF1 binds to COPI vesicles. Purified rat liver Golgi membranes were treated with wild type ARF1 in the presence of purified coatomer and mitotic kinases at 37ºC for 20 min. Reactions were

fractionated by equilibrium centrifugation on a sucrose gradient (0.5-1.6 M). Membranes in each fraction were pelleted and equal fractions (by volume) were analyzed by Western blotting for ARF1, β-COP and GRASP65 and shown in (A). ARF1 (sup) refers to ARF1 in the supernatant after membrane pelleting. Sucrose concentrations were measured and shown in (B). Membrane and cargo proteins in samples from (A) using wild type ARF1 were further analyzed by Western blotting and shown in (C). ManII, a-mannosidase II; RSA, rat serum albumin. Membranes in fractions 1-3, which contained Golgi remnants, and in fractions 7-9, which contained COPI vesicles, were collected, and processed for EM. EM images are shown in (D) and (E), respectively. Golgi remnants are indicated by arrows and uncoated COPI vesicles by arrowheads (D). Lipoprotein enriched TGN elements are indicated by asterisks (D). A large magnification of vesicle enriched fraction is shown in (F) to illustrate the COPI coats, indicated by arrowheads. Bar, 0.5 μm.

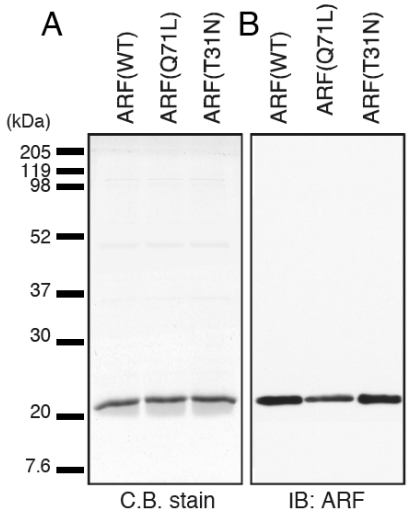

Figure 4.S1. Purification of myristoylated ARF1 WT and mutant proteins. Left panels show Coomassie blue stained gels with 1 μg purified myristoylated ARF1 proteins in each lane. The right panel shows a Western blot of ARF1 proteins using a monoclonal antibody.

ARF1-dependent Golgi fragmentation upon treatment with mitotic cytosol

To ensure that the results we obtained using purified mitotic kinases represent mitotic conditions, we examined fragmentation of Golgi membranes when treated with mitotic cytosol, or with interphase cytosol as a control. If mitotic Golgi fragmentation is due to COPI vesicle budding, which requires ARF1 activity, Golgi membranes should be fragmented upon treatment with mitotic cytosol treatment. Alternatively, no COPI vesicles should be generated if fragmentation of the Golgi during mitosis is due to inactivation of ARF1 [245]. As shown in Fig. 4.4, when Golgi membranes were treated with interphase cytosol, the stacks remained intact, with only a few vesicles, which is

similar to untreated Golgi membranes (Fig. 4.4D). However, when treated with mitotic cytosol, the Golgi membranes were fragmented to tubular and vesicular structures. Quantitation showed that about 50% of the membranes were found in vesicles (Fig. 4.4D) after treatment with mitotic cytosol, which is significantly higher than interphase cytosol treatment (22%). We then analyzed ARF1 association with vesicles by sucrose equilibrium centrifugation and Western blotting. The result showed that at least a fraction of ARF1 was associated with COPI vesicles which were enriched in fraction 8 (Fig. 4.4, E and F), as indicated by β-COP. This is consistent with the result described in Fig. 4.3A using purified proteins and shows that fragmentation of Golgi membranes upon mitotic cytosol treatment requires ARF1 activity. As noted in the figure legend, a higher molecular weight form of β-COP showed up when purified Golgi membranes were treated with cytosol (Fig. 4.4) or in living cells (Fig. 4.S3), especially under mitotic conditions. It is not clear whether this is due to phosphorylation of β-COP [258], or a different β-COP isoform [259], or ubiquitination, since the migration shift is about 8 kD. Our recent study indicated that a Golgi protein is ubiquitinated during mitosis, which is required for the subsequent Golgi reassembly [99]. The nature of this modification and its effect on COPI vesicle uncoating and/or fusion are worthwhile to explore.

To determine whether ARF1 activity is required for mitotic Golgi fragmentation, we depleted ARF1 from mitotic cytosol using a DEAE-Sepharose column following a procedure previously described [260]. The depletion efficiency for ARF1 was high (Fig. 4.4G, lanes 3 & 4 vs. 1 & 2). ARF1-depletion did not affect other proteins tested, such as β-COP and α-tubulin (Fig. 4.4G). ARF1-depleted mitotic cytosol failed to fragment the Golgi membranes, while replenishment of wild type ARF1 or the Q71L mutant, but not

the T31N mutant, restored the activity of the cytosol and led to fragmentation of the Golgi membranes to a similar extent as adding back the ARF1 containing fraction collected during the depletion procedures (Fig. 4.4H). This result showed that ARF1 activity in the mitotic cytosol is required for fragmentation of the Golgi membranes.

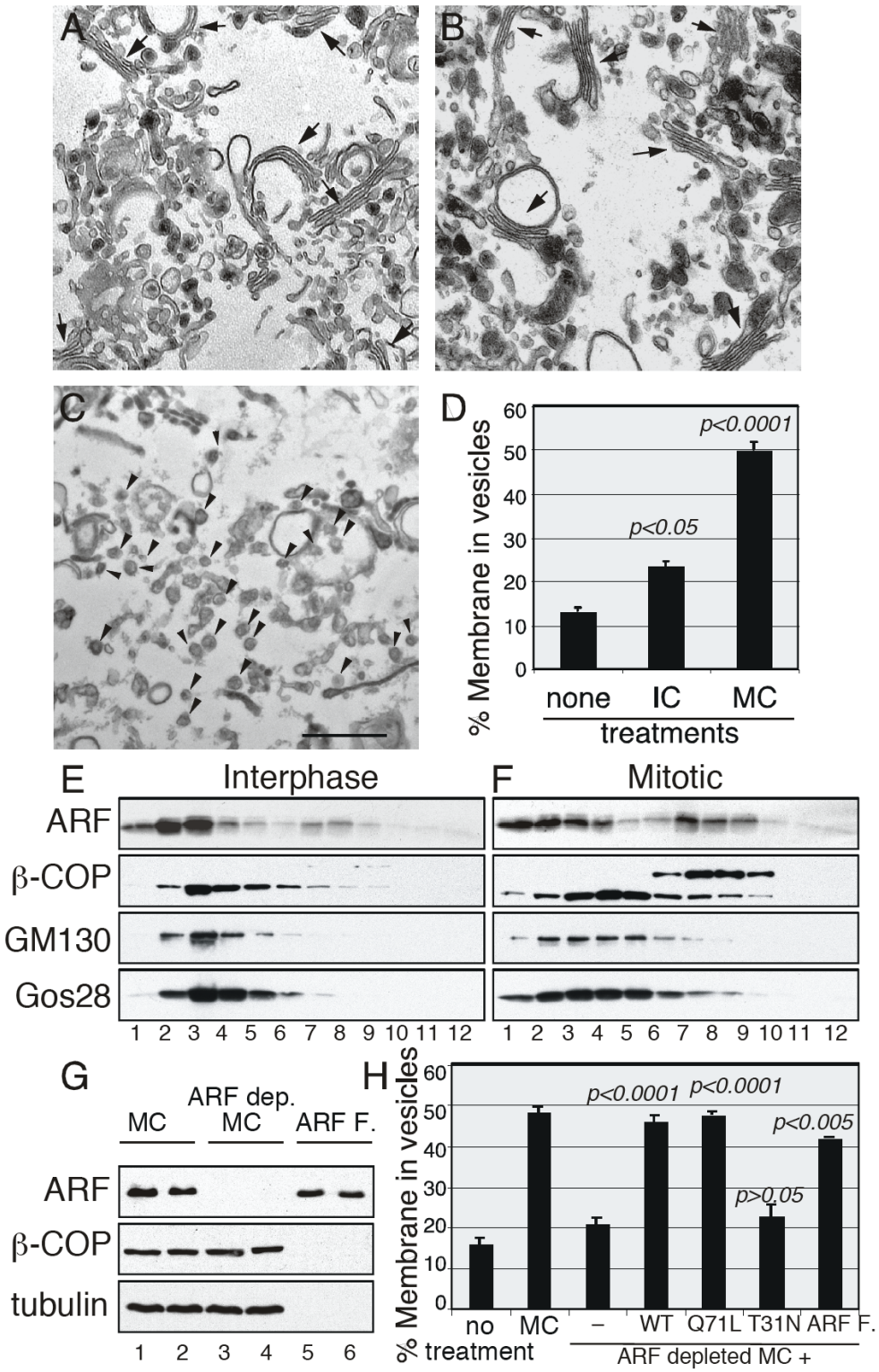

Figure 4.4. Fragmentation of Golgi membranes by mitotic cytosol treatment is ARF1-dependent. Purified Golgi membranes (A) were treated with interphase HeLa cell cytosol (IC) (B) or mitotic cytosol (MC) (C) at 37ºC for 20 min. Membranes were fixed and processed for EM. Golgi stacks (A and B) are indicated by arrows and COPI vesicles (C) by arrowheads. Bar, 0.5 µm. D. Quantitation of A-C, by the intersection method, to estimate the percentage of membrane in vesicles. Results represent the mean of

three independent experiments ± SEM. Note the increased number of vesicles after treatment with mitotic but not interphase cytosol. E and F. Analysis of protein components of B and C using sucrose equilibrium gradients. Membranes from B and C were loaded onto a 0.5-1.6 M (16-45%) sucrose gradient followed by ultracentrifugation to equilibrium and fractionated from the top to the bottom. Membranes were pelleted and equal proportions of membrane-bound proteins in each fraction were analyzed. A higher molecular weight form of β-COP appears after treatment with mitotic cytosol and peaks at COPI vesicle-containing fractions 7/8 (1.2-1.3 M sucrose). G. Non-treated mitotic cytosol (MC, lanes 1 & 2), ARF1-depleted cytosol (ARF dep. MC, lanes 3 & 4) and ARF1-enriched fraction (ARF F., lanes 5 & 6) collected during ARF1 depletion were analyzed by Western blotting for ARF1, β-COP and α-tubulin. H. Mitotic cytosol or ARF1-depleted mitotic cytosol were tested for Golgi fragmentation as in A and quantified as in D. In some reactions, purified ARF1 proteins or ARF1-enriched fraction (ARF F.) were added to ARF1-depleted cytosols, as indicated. Values represent means ±SEM (n=5). Statistical significance was analyzed against ARF1-depleted cytosol.

ARF1 remains active during mitosis in cells

Next, we tested whether ARF1 remains active or is inactivated in mitotic cells. Interphase or mitotic NRK cells (collected by nocodazole block and shake-off) were subjected to subcellular fractionation. Membranes from the post-nuclear (PNS) or post-chromosomal supernatants were pelleted by ultracentrifugation at 150,000 *g* for 60 min. Proteins in the membrane and the cytosol (supernatant) were analyzed by Western blotting. Under interphase conditions, about 22% of ARF1 was associated with membranes (Fig. 4.5A, B), indicating that this fraction of ARF1 is active in interphase cells. Under mitotic conditions, about 60% of ARF1 was found in the membrane fraction, which is significantly higher than under interphase conditions. To ensure that this result was not an unspecific pharmacological effect caused by nocodoazol treatment, we collected mitotic NRK cells by shake-off. NRK cells were first enriched in G1/S phase by aphidicolin block and released. Cells that entered mitosis were collected by shake-off and analyzed by a similar method described above. A significant amount of ARF1 was associated with the membranes in mitotic cells, which was larger than the amount in interphase cells (Fig. 4.S2). A similar result was obtained when a different cell line, HeLa

cells, was used (data not shown). Taken together, these results indicated that a significant amount of ARF1 is active in mitotic cells.

We then performed the subcellular fractionation experiment using mitotic cells treated with BFA, which is known to inactivate ARF1 [256]. Treatment of mitotic cells with BFA for 10 minutes was sufficient to remove essentially all ARF1 from the membrane fraction (Fig. 4.5C). Since the Golgi was already fragmented prior to BFA treatment, this result indicated that the membrane–associated active ARF1 in mitotic cells could be inactivated, but ARF1 inactivation is not a cause of mitotic Golgi fragmentation.

We then used sucrose gradients to analyze whether the membranes that ARF1 associated with are COPI vesicles. As shown in Fig. 4.S3, Golgi membranes were found on the top of the gradient, which peaked in fractions 3 or 4, as indicated by the Golgi matrix protein GM130, or the Golgi t-SNARE Gos28 (Fig. 4.S3). The Golgi v-SNARE Bet1, however, showed an additional peak in fraction 7 together with β-COP especially under mitotic conditions, suggesting that some of this protein was recruited into COPI vesicles. ARF1 was found in two peaks under both interphase and mitotic conditions: fractions 3-4, which contained Golgi membranes; and fractions 7-9, which contained COPI vesicles with the density of about 1.2 M sucrose (Fig. 4.S3) and indicated by β-COP. This is consistent with our result using purified components (Fig. 4.3 A and B) and further shows that ARF1 exists as the membrane–bound active form in mitotic cells and is required for mitotic Golgi fragmentation.

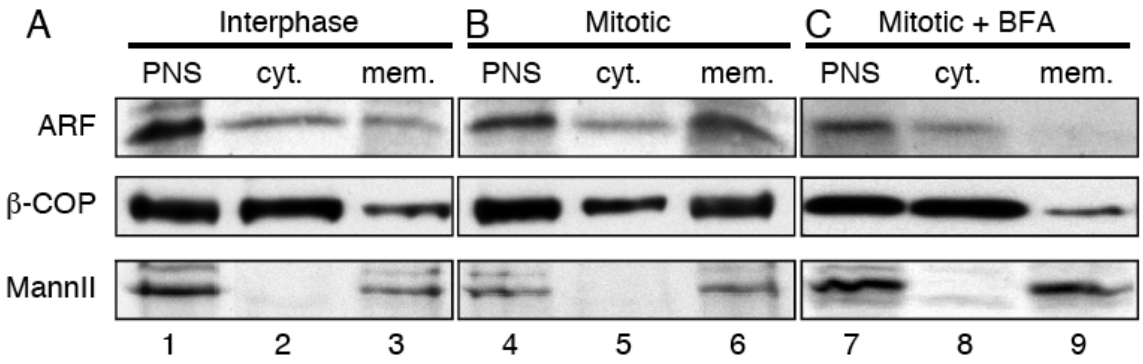

Figure 4.5. ARF1 is associated with membranes during mitosis. Non-treated interphase NRK cells or mitotic NRK cells synchronized by treatment with nocodazole were homogenized and postnuclear and post chromosomal supernatants centrifuged to separate membranes (P) and cytosol (S). Equal volume proportions of each sample were separated by SDS-PAGE followed by Western blotting for the indicated proteins. Quantitation of the bands showed that about 26% of ARF1 is associated with membranes under interphase conditions (Lane 3), and about 50% under mitotic conditions (Lane 6).

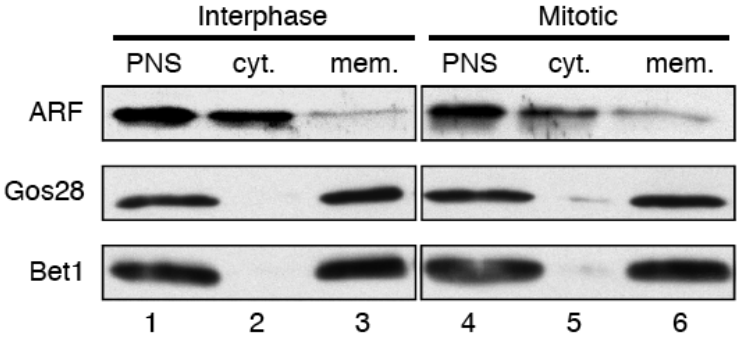

Figure 4.S2. ARF1 is associated with membranes in mitotic NRK cells collected by shake-off. NRK cells were blocked by aphidicolin and cultured in a fresh medium for 6-9 hours and mitotic cells were collected by shake-off. Interphase or mitotic NRK cells were homogenized and postnuclear and post chromosomal supernatants centrifuged to separate membranes (P) and cytosol (S). Equal volume proportions of each sample were separated by SDS-PAGE followed by Western blotting for the indicated proteins. Quantitation of the bands showed that about 15% of ARF1 is associated with membranes under interphase conditions (Lane 3), and about 30% under mitotic conditions (Lane 6).

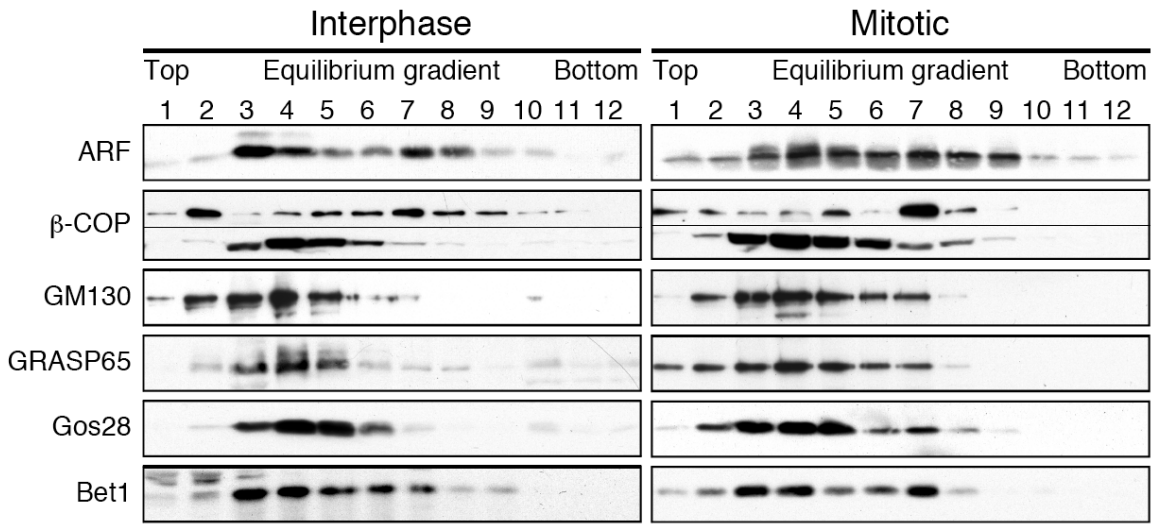

Figure 4.S3. ARF1 is associated with COPI vesicles during mitosis. Post-nuclear and post chromosomal supernatants from interphase and mitotic NRK cells were fractionated by equilibrium centrifugation using a 0.5-1.6 M sucrose gradient. Recovered membranes were analyzed by SDS-PAGE and Western blotting for the indicated proteins. Note that ARF1 is enriched in fractions 3 and 4, which contain Golgi remnants, and 7 and 8, which contain COPI vesicles.

Microinjection of the constitutive active ARF1 does not block mitotic Golgi fragmentation

Our data described above showed that ARF1 is active during mitosis and that this activity is required for mitotic Golgi fragmentation. To test the effect of ARF1(Q71L) on mitotic Golgi fragmentation in tissue culture cells, we microinjected purified ARF1(Q71L) into NRK cells enriched in G2 phase 60 min before the cells were about to enter mitosis. Cells were fixed as soon as they entered mitosis and stained for GM130. Microinjection of ARF1(Q71L) caused partial disassembly of the Golgi in interphase cells (Fig. 4.6A); however, this did not seem to affect cell progression into mitosis, as indicated by the condensed chromosomes in the metaphase plate and the round cell shape. In most prometaphase and metaphase cells we observed (22 cells out of 26 counted), the Golgi was fragmented (Fig. 4.6 B+C). Later in telophase, the Golgi reformed in both daughter cells (Fig. 4.6D). To demonstrate that the microinjected

ARF1(Q71L) was functional, injected interphase cells were treated for 5 min with BFA. In 190 injected cells out of 191 counted, the COPI coat proteins still decorated the Golgi (Fig. 4.6E, β-COP), indicating that ARF1(Q71L) could not be inactivated by BFA treatment, which is consistent with the result described in Fig. 4.2C. In the same experiment, β-COP was stripped off the Golgi membrane in non-injected neighboring cells (Fig. 4.6E). The results suggest that constitutively active ARF1 has no significant effect on the mitotic fragmentation of the Golgi apparatus or on the mitotic progression of the observed cells.

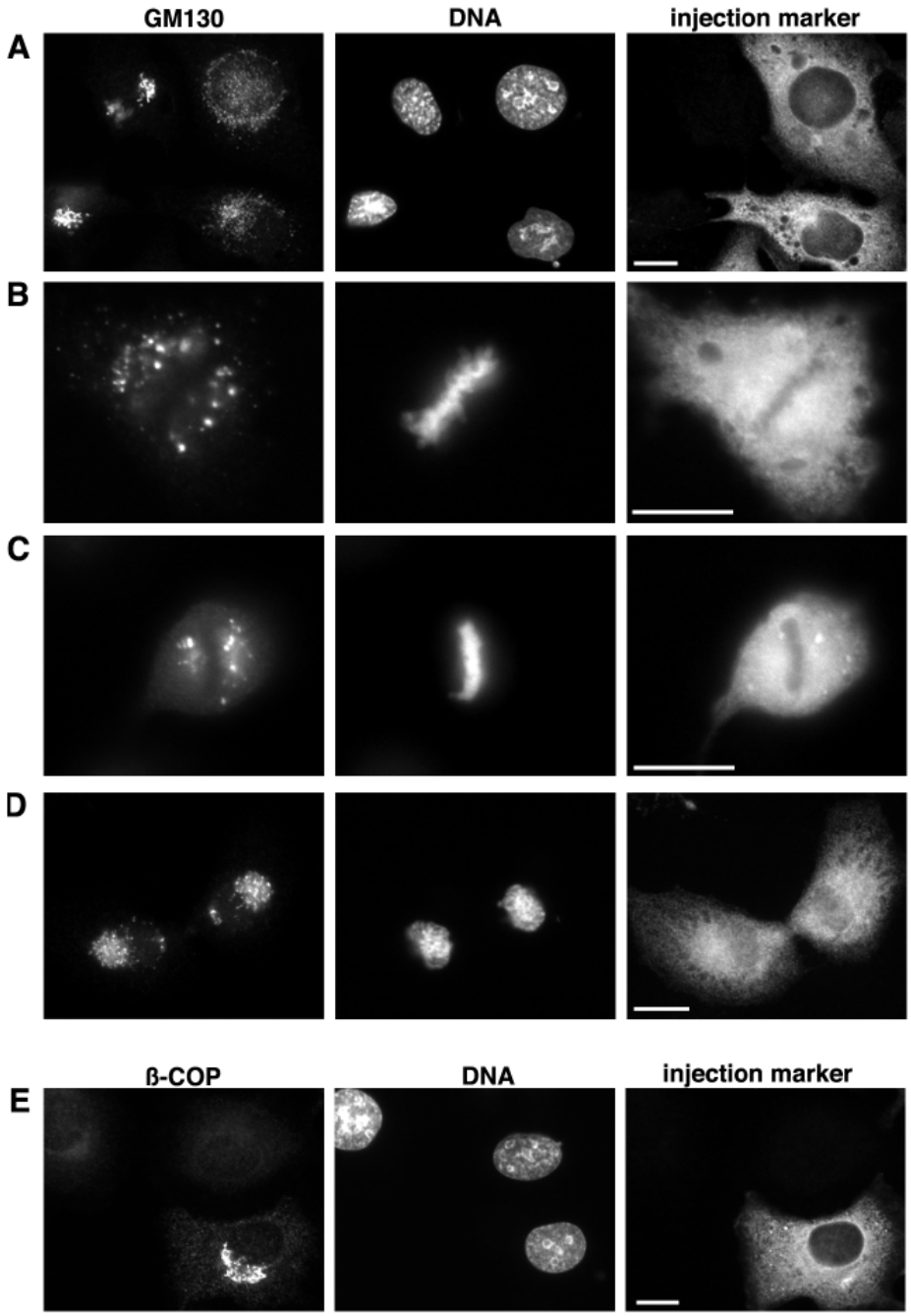

Figure 4.6. Microinjection of ARF1(Q71L) does not block Golgi fragmentation and progression through mitosis. NRK cells enriched in G2 were microinjected with purified ARF1(Q71L) protein (together with an injection marker) 60 min before entering mitosis. As the cells entered mitosis they were fixed and stained for the Golgi marker GM130 (left panels), DNA (middle panels) and the injection marker (right panels). A. Interphase. Injection of ARF1(Q71L) led to partial fragmentation of the Golgi. B - C. Prometaphase cells with condensed DNA showed that the Golgi was fragmented. D. Telophase/late mitosis. Chromosome separation was completed and the injected cell divided into two daughter cells containing a reformed Golgi apparatus. E. Control. Interphase NRK cells were injected with ARF1(Q71L). After 30 min incubation in growth medium, they were treated for 5 min with BFA. Note that β-COP is removed from the Golgi in non-injected cells but not in the injected cell, suggesting that the injected ARF1(Q71L) protein remained active in the presence of BFA. Bar = 15 μm.

Discussion

We have used several biochemical and cell biological approaches to determine the contribution of ARF1 to the disassembly process of the Golgi apparatus at the beginning of mitosis. Our results show that ARF1 remains active during mitosis and that this activity is required for mitotic Golgi fragmentation. A previous study has shown that vesicle budding is involved in mitotic fragmentation of Golgi membranes in a cell-free system [249]. However, this study used mitotic cytosol and the role of COPI vesicle formation was not confirmed. In the current study, we chose to use the well established *in vitro* COPI vesicle budding assay using purified ARF1 and coat proteins and confirmed the role of COPI vesicle budding in mitotic Golgi fragmentation. We used the mitotic kinases cdc2 and plk to mimic mitotic conditions. Previous studies have shown that these two mitotic kinases mimic mitotic cytosol by modifying most of the mitotically phosphorylated Golgi proteins so far identified, including GRASP65 [17, 123], GM130 [254], RIIalpha regulatory subunit of cAMP-dependent protein kinase [261] golgin-67 [145], and Nir2 [246]. These kinases were also shown to mimic mitotic conditions for mitotic Golgi fragmentation [17, 190, 262]. In the presence of mitotic kinases, the Golgi was fragmented (Fig. 4.1, A and B), and the amount of ARF1 bound to membranes remained high (Fig. 4.2), showing that ARF1 is not inactivated in the presence of mitotic kinases. This evidence was further strengthened using mitotic cytosol, which fragmented the Golgi membranes into vesicles much more efficiently than interphase cytosol. This activity was abolished when ARF1 was depleted from the cytosol and was restored when recombinant active ARF1 was replenished (Fig. 4.4). Therefore our *in vitro* experiments provided strong evidence that ARF1 activity is required for mitotic Golgi disassembly.

We then showed that this conclusion is also true in cells. Fractionation of interphase and mitotic NRK cells showed that a fraction of ARF1 is associated with COPI vesicles and Golgi membranes during mitosis (Fig. 4.5, 2S.2), suggesting that this population of ARF1 is active during mitosis. Compared with interphase cells, the membrane-bound portion is more prominent in mitotic cells (Figure 4.5, 2S.2), suggesting that ARF1 remains active during mitosis. Furthermore, using sucrose gradient centrifugation we confirmed that at least some of the ARF1-bound membranes are COPI vesicles (Fig. 4.S3). Therefore we conclude that mitotic Golgi fragmentation utilizes a different mechanism than the effect caused by BFA. Our study combined a variety of techniques to study the role in ARF1 in mitotic Golgi disassembly, both *in vitro* and *in vivo*, and provided strong evidence that mitotic Golgi fragmentation requires ARF1 activity and COPI vesicle budding. Further study on the machinery governing disassembly and reassembly of the Golgi apparatus is essential for understanding the mechanism of Golgi inheritance in mammalian cells.

Another study based on live cell imaging to localize ARF1 tagged with GFP in mitotic cells [243, 245] showed that the distribution of ARF1-GFP on Golgi membranes and in the cytosol changed as the cells entered mitosis, with the pool bound to the Golgi decreasing and the pool in the cytosol increasing [245]. However, it is not clear whether the diffused pattern of ARF1 during mitosis consists of soluble cytosolic ARF1, or if ARF1 is bound to Golgi derived vesicles, since the size of these vesicles is well below the spatial resolution of light microscopy [88, 243]. Another piece of evidence is the fact that overexpression of ARF1(Q71L) blocks mitotic Golgi fragmentation [245]. ARF1(Q71L) was overexpressed by transient transfection over a long time period. Since

ARF1(Q71L) directly affects membrane trafficking, it is unclear whether mitotic Golgi fragmentation is directly blocked by ARF1(Q71L) or by an unspecific effect caused by its chronic overexpression. In fact, when we microinjected purified ARF1(Q71L) protein into cells, mitotic Golgi fragmentation and cell cycle progression through mitosis appeared essentially unchanged (Fig. 4.6). Since in this experiment the presence of ARF1(Q71L) in the cell was reduced to 60 min, this result provided more direct evidence that ARF1 is not inactivated in the progress of mitotic Golgi fragmentation. In addition, using a biochemical approach combined with electron microscopy, our result showed for the first time that ARF1 is bound to vesicles when Golgi membranes are disassembled in the presence of wild type or active ARF1, but not the inactive ARF1 mutant. This result was further confirmed using mitotic cytosol and synchronized cells. Our results showed that at least a portion of the endogenous ARF1 is associated with the membranes even when the Golgi is fragmented and this association is abolished when cells were treated with BFA (Fig. 4.5). ARF1 itself has a very low intrinsic GTPase activity and GTP hydrolysis by ARF1 requires the GTPase activating proteins (ARF-GAP) [263, 264]. The distribution and activity of ARF-GAP proteins during mitosis have not yet been investigated. In addition, we observed a significant migration shift of β-COP on the gel, especially under mitotic conditions (Fig. 4.4, 2S.3), which might be due to the modification of this protein. Whether this modification inhibits vesicle uncoating and thus fusion during mitosis is an intriguing possibility. Nevertheless, our results strongly suggest that ARF1 is not inactivated during mitosis, and that active ARF1 is required for mitotic Golgi fragmentation.

Materials and Methods

Reagents

All reagents were from Sigma Co., Roche Diagnostics or Calbiochem, unless otherwise stated. The following antibodies were used: monoclonal antibodies against ARF1 (1D9, Abcam), GM130 and Gos28 (Transduction Laboratories), GRASP65 (F. Barr), β-COP (M3A5, T. Kreis), α-tubulin (K. Gull); polyclonal antibodies against ARF (D. Shields and D. Sheff), β-COP (EAGE, T. Kreis), GM130 (MLO7, M. Lowe), GRASP65 [17], α-Mannosidase II (K. Moremen), Golgin-84 (A. Satoh), rat serum albumin (G. Warren), TGN38 [265]. Secondary antibodies for immunofluorescence and for Western blotting were from Molecular Probes and Jackson Immunoresearch Laboratories, respectively. Brefeldin A (BFA) was obtained from Invitrogen and Epicentre Biotechnologies and applied to the tissue culture medium at 5 μg/ml final concentration. Nocodazole (Sigma) was prepared as 0.2 mg/ml stock in DMSO and used at 0.5 μg/ml in the medium. Hoechst 33342 was purchased from Invitrogen.

ARF1 mutagenesis, expression and purification

cDNA constructs for wild type (WT) and the constitutively active mutant (Q71L) ARF1 were obtained from J. Rothman [48, 252]. ARF1 inactive mutant (T31N) [252] was made by site-directed mutagenesis and confirmed by DNA sequencing. For preparation of myristoylated ARF1 proteins, BL21(DE3)Gold bacterial cells were co-transformed with a second plasmid encoding the yeast N-myristoyltransferase [266]. Briefly, ARF1 expression was induced in the presence of 50 μM myristic acid. Myristoylated ARF1 proteins were enriched by 35% saturation of ammonium sulfate

followed by purification on a DEAE-Sepharose column as described previously [253]. Fractions containing myristoylated ARF1 eluted between 50-150 mM NaCl were pooled, buffer exchanged and concentrated on an AmiconUltra-10 filter device (Millipore) in 50 mM Tris-HCl, pH8.0, 1 mM $MgCl_2$, 1 mM DTT, 2 μM GDP, to a concentration of 2-5 mg/ml and aliquots were stored at -80ºC. SDS-PAGE analysis showed that ARF1 is purified to over 90% homogeneity (Fig. 4.S1A). Western blot analysis using a monoclonal antibody against ARF1 confirmed this result. This antibody, however, has lower affinity to ARF1(Q71L) compared to wild-type or T31N mutant (Fig. 4.S1 B).

In vitro budding assay and analysis

Golgi membranes were purified from rat liver [213]. Interphase (IC) and mitotic (MC) cytosols were prepared from HeLa S3 cells [249]. Cdc2 kinase (cdc2/ cyclin B1) and plk kinase were expressed and purified as described and kinase activity was measured [17]. Coatomer complex was purified from rabbit cytosol [267]. Golgi budding assay was performed as previously described [65, 250]. Briefly, Golgi membranes (200 μg) were mixed with 10 mg IC or MC, or with purified coatomer (100 μg), recombinant myristoylated ARF1 (50 μg), 1 mM GTP and an ATP regenerating system (10 mM creatine phosphate, 1 mM ATP, 20 μg/ml creatine kinase, 20 ng/ml cytochalasin B), in assay buffer (50 mM Tris-HCl, pH7.4, 0.2 M sucrose, 50 mM KCl, 20 mM β-glycerophosphate, 15 mM EGTA, 10 mM $MgCl_2$, 2 mM ATP, 1 mM GTP, 1 mM glutathione, and protease inhibitors), in a final volume of 1000 μl. After incubation for 20 min at 37°C, 250 mM KCl in cold assay buffer was added to stop the reaction and to release the vesicles. In some experiments 50 μg/ml BFA (Invitrogen) was included. To

separate the membranes from the soluble proteins, samples were centrifuged in a TLA55 rotor at 55,000 rpm for 60 min. To analyze the membranes by equilibrium gradients, reactions were directly loaded onto a step gradient comprised of 1.0 ml 0.5 M, 1.5 ml 0.8 M, 2 ml 1.2 M, 2 ml 1.4 M and 2 ml 1.6 M sucrose in assay buffer containing 250 mM KCl. Membranes were centrifuged to equilibrium at 200,000 *g*, 4°C for 3 h in a near vertical rotor (NVT65, Beckman Instruments, 50000 rpm). COPI-coated vesicles typically peaked at 1.2-1.3 M sucrose, while uncoated Golgi remnants peaked at about 0.8 M sucrose. Fractions were diluted 3-fold with a buffer without sucrose and membranes in each fraction were pelleted by centrifugation in a Beckman TLA55 rotor at 55000 rpm for 60 minutes followed by Western blotting analysis. Membrane samples were also fixed and processed for EM. Vesicles were defined as round profiles of approximately 70 nm in diameter. The percentage of membranes in cisternae was determined by the intersection method [17]. The statistical significance of the quantitated results was accessed by Student's *t*-test.

ARF1 was depleted from mitotic cytosol on a DEAE-Sepharose column used for ARF1 purification following the method previously described [260]. Briefly, mitotic cytosol was loaded onto the column and three fractions were collected: ARF-depleted pool 1 that did not bind to the column; ARF-enriched pool 2 that bound to the column but was eluted with a buffer containing 65 mM KCl; and ARF-depleted pool 3 that contained proteins eluted with a buffer containing 500 mM KCl. Pools 1 and 3 were mixed and concentrated by on a centricon filter device to the original concentration as ARF1-depleted mitotic cytosol.

Cell Culture, synchronization and subcellular fractionation

NRK cells were routinely cultured in DMEM supplemented with 7.5% fetal calf serum, 2 mM L-glutamine, penicillin (100 U/ml), and streptomycin (100 µg/ml). To enrich NRK cells in M phase, subconfluent cells (~75% confluent) were washed by phosphate buffer (PBS) and incubated in growth medium supplemented with 0.5 µg/ml nocodazole for 15 hours (Sigma, St. Louis, MO). Mitotic cells were collected by shake-off [83, 268]. Typically, the mitotic index was about 80% when examined under a fluorescent microscope according to the condensation of the chromosomes stained with Hoechst 33258. To avoid unspecific pharmacological effects of nocodazole on mitotic cells, NRK cells were treated for 14 h with 2.5 µg/ml Aphidicolin (Calbiochem) to enrich cells in G1/S-phase. Six to nine hours after removal of the drug, mitotic cells were collected by shake-off. Confluent interphase (non-synchronized) cultures were cleaned by shake-off method to remove mitotic cells, washed with PBS and harvested using a cell scraper. Normally 8x 15 cm dishes of NRK cells were used for mitotic cell collection and 2 dishes for interphase collection. The mitotic index of interphase cells was lower than 1%. For Brefeldin A (BFA) treatment, mitotic cells were treated with 5 µg/ml BFA in growth medium at 37ºC for 10 min before the collection of the cells.

Spinner HeLa cells were cultured in RPMI1640 supplemented with 7.5% fetal calf serum, 2 mM L-glutamine, penicillin (100 U/ml), and streptomycin (100 µg/ml). Cells grown in suspension were synchronized by incubation in growth medium with 0.5 µg/ml Nocodazole for 20-22 hours until the mitotic index reached 95% or higher. Synchronized and non-synchronized HeLa cells were collected by centrifugation. 200 ml HeLa cells in suspension culture were used for mitotic or interphase cell collection.

NRK or spinner HeLa cells were washed with homogenization buffer (0.25 M sucrose, 1 mM EDTA, 1 mM Mg acetate, 10 mM HEPES-KOH, pH 7.2 and protease inhibitors) and resuspended in 800 µl homogenization buffer by pipetting (4x blue tip, 6x syringe). Cells were cracked with a ball-baring homogenizer as monitored under a microscope by Trypan-Blue exclusion to a breakage of 75-80%. The homogenate was centrifuged for 10 min at 1000 *g*, 4°C. The postnuclear supernatant (PNS) was removed and subjected to ultracentrifugation in a TLA55 rotor at 120000 *g* for 1 hour. The supernatant (cytosol) was removed and the membranes in the pellet were resuspended in homogenization buffer. Equal volume fractions of the PNS, cytosol and membrane fractions were analyzed by SDS-PAGE and Western blotting. Protein bands were quantitated using the NIH ImageJ software. The PNS was also fractionated on a sucrose gradient as described above and fractions were analyzed by Western blotting.

Microinjection and immunofluorescence analysis

Capillary microinjection was performed with a semiautomatic system consisting of a Transjector 5246 and a Micromanipulator 5171 (Eppendorf). NRK cells grown on glass coverslips were treated for 14 h with 2.5 µg/ml Aphidicolin (Calbiochem) to enrich cells in G1/S-phase. Eight hours after removal of the drug, the cells were injected with 1.2 mg/ml ARF1(Q71L) together with 2 mg/ml mouse IgG (Sigma) as an injection marker. The cells were incubated for 60-90 min at 37ºC and fixed and permeabilized for 10 min in methanol at -20ºC. For Brefeldin A treatments, the injected cells were incubated in growth medium for 30 min followed by a 5 min incubation in the presence of 5 µg/ml Brefeldin A. The cells were then labeled with polyclonal antibodies against GM130 or β-

COP followed by goat anti-rabbit secondary antibodies conjugated to Alexa Fluor 488 (Molecular Probes). The co-injected mouse IgG were stained with goat anti-mouse Alexa Fluor 594 antibodies (Molecular Probes). DNA was stained with Hoechst 33342 and the cells were mounted in Moviol 4-88 (Calbiochem). Fluorescence analysis was performed using a Plan-Apochromat 63x/1.4 DIC objective (Zeiss) and an Axiovert 200M microscope (Zeiss). Images were captured with an Orca-285 camera (Hamamatsu) and the software package Openlab 4.02 (Improvision).

Acknowledgements

We thank F. Barr, K. Gull, T. Kreis, M. Lowe, D. Sheff, D. Shields, G. Warren for antibodies, J. Rothman for ARF1 cDNAs, and J. Malsam for technical help with ARF1 and coatomer purification. We also thank K. Mar for help with EM processing and data analysis, H. Yuan and other members of the Wang Lab for suggestions, reagents, and critical reading of the manuscript. This work was initiated in Dr. G. Warren's laboratory and we are indebted to his continuous support and encouragement.

Chapter V. The ubiquitin ligase HACE1 is involved in regulating Golgi membrane dynamics during the cell cycle

Abstract

Partitioning of the Golgi membrane into each daughter cell after mammalian cell division occurs through a unique disassembly and reassembly process that is regulated by ubiquitination. However, the identity of the ubiquitin ligase and the ubiquitinated substrates on the Golgi membrane are unknown. Here, we show that the HECT-domain containing ubiquitin ligase HACE1 is targeted to the Golgi membrane through interactions with Rab proteins. HACE1 ubiquitin ligase activity is involved in mitotic Golgi disassembly and is required for subsequent post-mitotic Golgi membrane fusion. Depletion of this protein using siRNAs and expression of an inactive HACE1 mutant both affect Golgi membrane fusion. Further biochemical analysis indicated that syntaxin 5 is a substrate of HACE1 on the Golgi membrane. The identification of HACE1 as a Golgi-localized ubiquitin ligase, and syntaxin 5 as its substrate, provides evidence that ubiquitin plays a critical role in Golgi biogenesis during the cell cycle.

Introduction

Mitosis requires the duplication and even partitioning of all cellular components into two daughter cells. In mammalian cells, inheritance of the Golgi apparatus during each cell division occurs through a unique disassembly and reassembly process [2, 202]. The Golgi is fragmented at the onset of mitosis to disperse the stacks, which then undergo further vesiculation. This yields thousands of vesicles that are distributed throughout the cytoplasm [269]. Studies using a cell free assay that reconstitutes mitotic Golgi fragmentation [90, 214, 249, 270] showed that mitotic Golgi disassembly involves two processes: cisternal unstacking and membrane vesiculation. Unstacking is mediated by mitotic kinases that phosphorylate the Golgi stacking proteins GRASP65 and GRASP55 [17, 18, 119, 120]. In interphase cells, GRASP proteins form oligomers between adjacent cisternal membranes and hold the membranes in stacks. During mitosis, phosphorylation of GRASPs leads to de-oligomerization of the proteins and cisternal unstacking. Vesiculation of the unstacked cisternae occurs through continuous formation of COPI vesicles, which is mediated by the small GTPase ARF1 (ADP-ribosylation factor 1) and the coatomer complex [89]. Phosphorylation of Golgi tethering proteins, such as GM130, disrupts membrane fusion, and continuous COPI vesicle budding without membrane fusion results in vesiculation of the Golgi membranes during mitosis [254]. During telophase, Golgi vesicles are distributed equally between daughter cells, where they are assembled into stacks and ribbons. Post-mitotic Golgi reassembly is mediated by membrane fusion to form single cisternae and cisternal stacking. Post-mitotic Golgi membrane fusion is mediated by two AAA (ATPases Associated with various cellular Activities) ATPases, N-ethylmaleimide-sensitive factor (NSF) and p97 (also referred to

as valosin-containing protein, VCP, or Cdc48 in yeast), which work together with their adaptor proteins [93, 97, 271-274]. Golgi membrane restacking is mediated by dephosphorylation and subsequent re-oligomerization of Golgi stacking proteins [17, 18, 90, 99, 119, 120, 202].

Several converging lines of evidence have suggested that ubiquitination, a process often associated with protein degradation, plays an essential role in the regulation of post-mitotic Golgi membrane fusion. First, the p97/p47 complex binds to mono-ubiquitin through the UBA domain of the adaptor protein p47. Inhibition of the p47-ubiquitin interaction suppresses p97-mediated Golgi membrane fusion [98]. Second, mono-ubiquitination occurs during mitotic Golgi disassembly and is required for subsequent Golgi reassembly [98]. Third, VCIP135, a cofactor of the p97/p47 complex, is a deubiquitinating enzyme whose activity is required for post-mitotic Golgi reassembly [99]. Finally, proteasome activity is not involved in either Golgi disassembly or reassembly [99]. These data suggest that cycles of addition and removal of ubiquitin to and from substrates is necessary for Golgi reassembly. The role of ubiquitination in Golgi membrane fusion is likely not restricted to the p97/p47 complex, as it has been shown that another required ATPase, NSF, binds to GATE-16, a ubiquitin-like protein [96, 275]. These results suggest that ubiquitination may operate as a general mechanism to regulate Golgi membrane dynamics during the cell cycle.

Acquiring a deeper understanding of the underlying mechanism of ubiquitin in the regulation of Golgi membrane dynamics during cell division requires identification of the ubiquitin ligase and its substrates on the Golgi membranes. Here, we show that HACE1, a HECT domain (Homologous to the E6-AP Carboxyl Terminus)-containing ubiquitin

ligase, is involved in this process and that syntaxin 5, which is found on the Golgi membrane, is a HACE1 substrate. The identification of HACE1 as a Golgi-localized ubiquitin ligase, and syntaxin 5 as its substrate, provides further evidence that ubiquitin plays a critical role in Golgi biogenesis during the cell cycle.

Results

Rab proteins have been shown to be important for membrane organization [276]. In an effort to identify Rab-interacting proteins using an affinity chromatography-based proteomic approach [277], we identified HACE1, which binds specifically to the GTP-bound state of Rab4 (Fig. 5.1A). The HACE1 cDNA was cloned from a human cDNA library. It consisted of 909 amino acids and migrated at 100 kDa on an SDS-PAGE gel (Fig. 5.1A). HACE1 contains six ankyrin repeats and a HECT domain, a defining feature of one family of ubiquitin E3 ligases. Using a thioester bond formation assay containing ubiquitin, an E1 activating enzyme, the E2 conjugating enzyme UbcH7 and either recombinant wild-type (WT) HACE1 or the inactive C876A (CA) point mutant, we demonstrated that WT HACE1 is capable of catalyzing the formation of thioester bonds, but the C876A mutant is not (Fig. 5.1B). This result is consistent with previous reports that HACE1 functions as an active ubiquitin ligase [278, 279].

When examined by fluorescence microscopy, both Rab4 and HACE1 were concentrated in the perinuclear region, which appeared to be on the Golgi apparatus (Fig. 5.1C). In addition to the Golgi, Rab4, but not HACE1, was also found on endosomal membranes that were irregularly shaped and dispersed throughout the cytosol (Fig. 5.1C). Because HACE1 binds to Rab4, which is only partially localized to the Golgi, we examined whether HACE1 also interacts with other Rabs, including those localized on Golgi membranes, using a well-established Rab pull-down assay [277, 280]. Immobilized GST-tagged Rab1, Rab2, Rab5, Rab6 and Rab11 proteins were incubated with purified recombinant HACE1 in the presence of GDP or GTPγS. After washing, the bound proteins were eluted, and the presence of HACE1 was detected by Western blot. As

shown in Fig. 5.1D, HACE1 bound to Rab1 and Rab11 but not Rab2, 5 or 6 in a GTP-dependent manner. Because the interaction with Rab1 was relatively strong (Fig. 5.1D), we tested binding to the GDP- (Rab1 S25N) and GTP-restricted (Rab1 Q67L) mutants of Rab1. As shown in Fig. 5.1E, HACE1 bound to the wild-type and Q67L mutant forms of Rab1 but not the S25N mutant, confirming that HACE1 interacts with Golgi localized Rab1 in a GTP-dependent manner. We also tested whether endogenous HACE1 could bind to different Rabs. Immobilized GST-tagged Rab1, Rab5, Rab6 and Rab11 were incubated with HeLa cell lysates, and the bound proteins were analyzed. As shown in Fig. 5.1F, endogenous HACE1 bound to Rab1-GTP in a similar pattern as p115, a protein known to interact with Rab1. A strong interaction was also observed for Rab11, but no interactions were detected for Rab5 or Rab6 (Fig. 5.1F). These results demonstrate that HACE1 interacts with Rab1, Rab4 and Rab11 in a GTP-dependent manner.

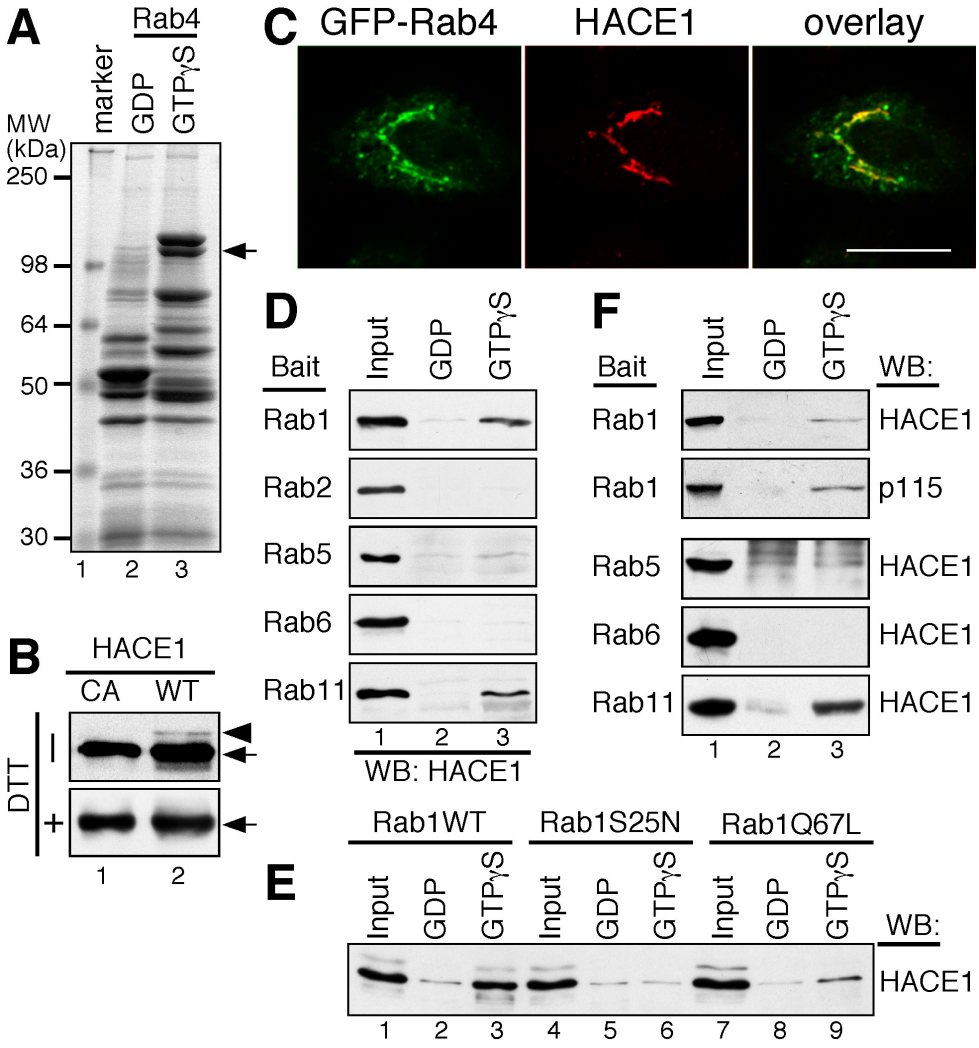

Figure 5.1. HACE1 binds to Golgi-associated Rab proteins. (A) HACE1 binds Rab4-GTP. Immobilized GST-tagged Rab4 was incubated with bovine brain cytosol in the presence of GDP or GTPγS. After washing, the bound proteins were eluted and analyzed by SDS-PAGE and coomassie blue staining. Specific bands in the GTPγS lane were excised and identified by mass spectrometry. The arrow indicates HACE1. **(B)** HACE1 exhibits ubiquitin ligase activity *in vitro*. The thioester bond formation assay was performed using the C876A (CA) point mutant and wild-type (WT) recombinant HACE1 protein, ubiquitin, E1 activating enzyme and the E2 conjugating enzyme UbcH7. Following incubation, the reactions were boiled in SDS buffer containing DTT, or mixed with SDS buffer that lacked DTT without boiling. HACE1 was detected by Western blot. The arrows indicate HACE1 and the arrowhead indicates Ub-HACE1. Note that the Ub-HACE1 band was observed in the absence of DTT with WT HACE1. **(C)** HACE1 co-localizes with Rab4 in the perinuclear region. Immunofluorescence images of A431 cells expressing GFP-Rab4 (in green) and stained for HACE1 (in red). Note that HACE1 co-localizes with Rab4 in the perinuclear region, while additional Rab4 signal is found in the cytoplasm. Scale bar: 20 μm. **(D)** Recombinant HACE1 binds Golgi Rabs. Immobilized GST-tagged Rab1, Rab2, Rab5, Rab6 and Rab11 proteins were incubated with purified recombinant HACE1 in the presence of GDP or GTPγS. After washing, HACE1 was detected by Western blot. Input, 5%. **(E)** HACE1 interacts with Rab1 in a nucleotide-dependent manner. Same as in D but with the wild-type Rab1 (Rab1WT, lanes 1-3) and its "GDP" (Rab1S25N, lanes 4-6) and "GTP" (Rab1Q67L) locked forms. Samples were analyzed for HACE1 and Rab1. Note that HACE1 bound to the WT and GTP form of Rab1 but not Rab1 S25N. Input, 5%. **(F)** Endogenous HACE1 binds Golgi-associated Rabs. Same as in D, but HeLa cell lysates were used instead of purified HACE1 protein. Input, 10%.

HACE1 lacks a transmembrane domain and has been shown to be associated, at least in part, with the endoplasmic reticulum (ER) [278]. Considering its interactions with Rab1, Rab4 and Rab11, which are at least partially localized to Golgi membranes [38, 280-283], we determined whether HACE1 localizes to the Golgi during interphase in normal rat kidney (NRK) cells. A fraction of HACE1 co-localized with GRASP65, a Golgi marker, and the rest of the protein appeared to be cytosolic (Fig. 5.2A). Similar results were observed with other cell lines, such as A431 (Fig. 5.1C) and HeLa cells (Fig. 5.3). Both the Golgi and cytosolic signals were diminished by the addition of recombinant HACE1 protein to displace the antibodies (Fig. 5.2B, anti-HACE1+peptide), suggesting that the antibody had high specificity.

Nocodazole treatment leads to fragmentation of the Golgi ribbon. After nocodazole treatment, HACE1 fragmented with the Golgi protein GM130 and was associated with remnants of the Golgi (Fig. 5.2C). Brefeldin A (BFA) treatment leads to Golgi membrane fusion with the ER. In the presence of BFA, Golgi remnants, which are marked by GRASP65, were dispersed throughout the cell along with HACE1 (Fig. 5.2D). After BFA was washed out, HACE1 accumulated in perinuclear regions where the Golgi membranes were concentrated (Fig. 5.2E). Finally, in mitotic cells with fragmented Golgi membranes, HACE1 associated with mitotic Golgi clusters, which was determined by the presence of GM130 (Fig. 5.2F).

Further microscopic analysis indicated that HACE1 co-localized with the *cis*-Golgi markers GRASP65 and GM130 (Fig. 5.2) and with GalNac-T2-GFP (N-acetylgalactosaminyltransferase 2), a Golgi enzyme localized throughout the Golgi stack (Fig. 5.S1B) [284]. HACE1 showed a less strong co-localization with the *medial* and

trans Golgi markers α-mannosidase II [12] (Fig. 5.S1C) and syntaxin 6 [285] (Fig. 5.S1D). In addition, it showed partial co-localization with the ER-Golgi intermediate compartment marker ERGIC53 [286] in the perinuclear region where Golgi membranes were concentrated (Fig. 5.S1A). Co-localization of HACE1 with *cis*-Golgi markers, compared to other Golgi compartment markers, was more evident when the Golgi apparatus was fragmented by nocodazole treatment (Fig. 5.2C, Fig. 5.S1).

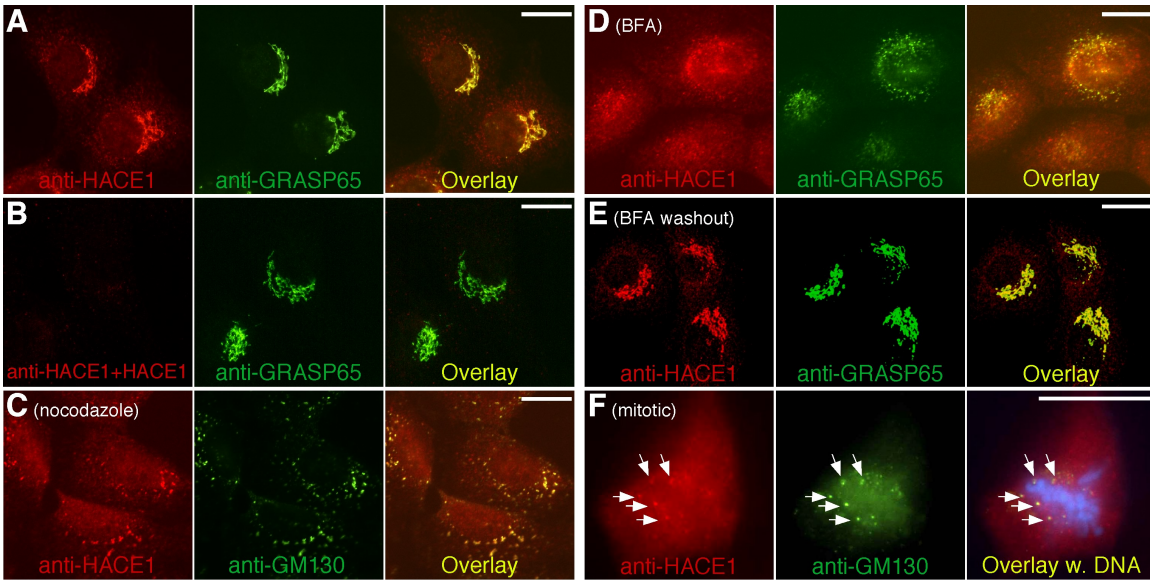

Figure 5.2. HACE1 is concentrated on the Golgi apparatus. (A) HACE1 is concentrated on the Golgi in interphase cells. NRK cells were immunostained with an affinity-purified polyclonal antibody to HACE1 (left panel, in red) and a monoclonal antibody to GRASP65 (middle panel, in green). **(B)** The HACE1 antibodies are specific. Same as in A, except the HACE1 antibodies were pre-incubated with purified HACE1 recombinant protein to quench the antibodies. Note that the HACE1 fluorescence was displaced by the recombinant HACE1. **(C)** HACE1 is associated with Golgi fragments after nocodazole treatment. NRK cells were treated with 0.5 µg/ml nocodazole for 2 hours and stained for HACE1 and GM130. **(D)** Brefeldin A (BFA) treatment leads to the dispersal of HACE1 in the cell. NRK cells were treated with 5 µg/ml BFA for 2 hours and analyzed as in A. **(E)** BFA washout. After the removal of BFA, cells were further incubated in growth media for 2 hours and stained for HACE1 and GRASP65. **(F)** HACE1 is partially associated with the Golgi fragments in prometaphase cells. Prometaphase NRK cells stained for HACE1 (red), GM130 (green), and DNA (blue). Note that HACE1 is localized on the mitotic Golgi fragments (indicated by arrows). Scale bars in all panels: 10 µm.

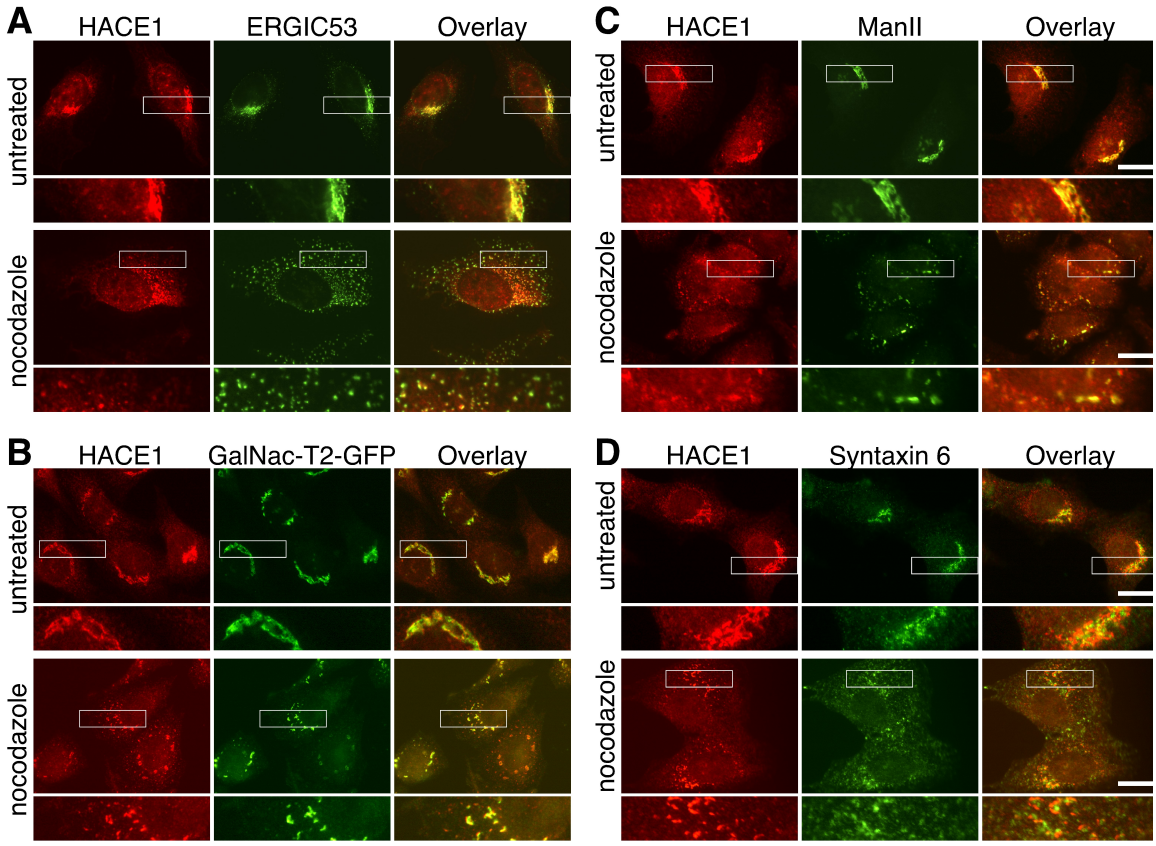

Figure 5.S1. HACE1 co-localizes with *cis*-Golgi markers. (A) Co-localization of HACE1 with ERGIC53, an endoplasmic reticulum-Golgi intermediate compartment marker (ERGIC). Untreated (upper panels) and nocodazole-treated (lower panels) NRK cells were immunostained with an affinity-purified HACE1 polyclonal antibody (left panels, in red) and a monoclonal ERGIC53 antibody (middle panel, in green). The overlay is shown on the right. Lower panels are enlarged images of the boxed regions. **(B)** Co-localization of HACE1 with GFP-tagged N-acetylgalactosaminyltransferase 2 (GalNAc-T2-EGFP). Same as in A but with the EGFP signal from GalNac-T2-EGFP. **(C)** Co-localization of HACE1 with mannosidase II (ManII), an enzyme localized in the *medial*-Golgi. **(D)** Co-localization of HACE1 with syntaxin 6, a *trans*-Golgi-localized SNARE protein. Scale bars in all panels: 10 µm.

Biochemical analysis also confirmed the association of HACE1 with Golgi membranes. When subcellular membrane organelles were separated using equilibrium sucrose gradients, the distribution of HACE1 was similar to the Golgi markers GM130, GRASP65, syntaxin 5 and Gos28 but was different from the ER markers Sec61 and protein disulfide isomerase (PDI) (Fig. 5.S2). Taken together, these results show that HACE1 is associated with Golgi membranes.

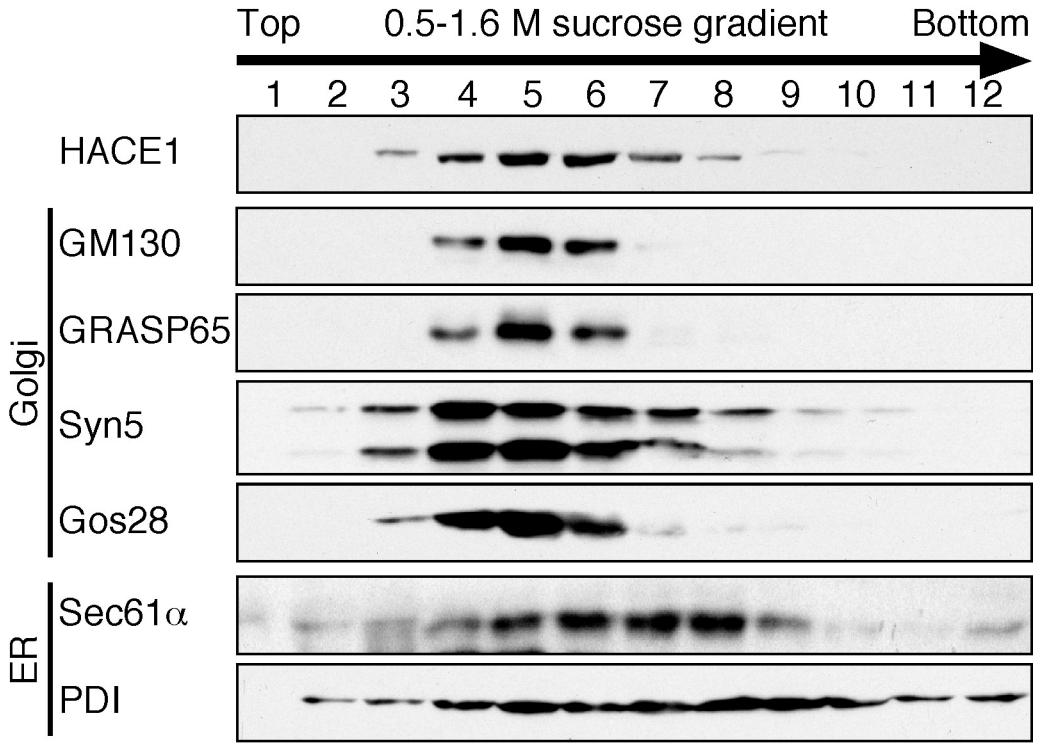

Figure 5.S2. HACE1 is a ubiquitin ligase bound to Golgi membranes. HACE1 co-localizes with the Golgi in sucrose gradients. Post-nuclear supernatant (PNS) from interphase NRK cells was fractionated by equilibrium centrifugation on a sucrose gradient (0.5-1.6 M). Membranes from each fraction were pelleted and equal volumes were analyzed by Western blot for the indicated proteins. Golgi membranes were enriched in fraction 5, while ER membranes are more widely distributed and concentrated in heavier fractions.

If Rabs target HACE1 to the Golgi, inhibition of Rab activity may affect HACE1 Golgi localization. We therefore used wild-type or mutant Rabs to test this hypothesis. Expression of wild-type Rabs did not affect HACE1 Golgi localization or Golgi structure (Fig. 5.S1, Fig. 5.3). In addition, Rab1, Rab4 and Rab11, but not Rab5, were partially concentrated on Golgi membranes (Fig. 5.1C, Fig. 5.3). Because HACE1 showed strong co-localization and interaction with Rab1, we analyzed HACE1 localization after the expression of Rab1 mutants. Expression of the active Rab1 Q67L mutant had no effect on HACE1 localization or Golgi morphology. In contrast, expression of the S25N mutant at a relatively low level (Fig. 5.3K, lane 2 vs. other lanes) disrupted the HACE1 Golgi

localization (Fig. 5.3D). Furthermore, expression of the Rab1 S25N mutant also caused Golgi fragmentation, which is consistent with previous reports [287] and suggests the possibility that HACE1 may be a Rab1 effector required for Golgi apparatus integrity. Taken together, our data suggest that HACE1 interacts with Rabs, and this interaction may be important for HACE1 Golgi localization and function.

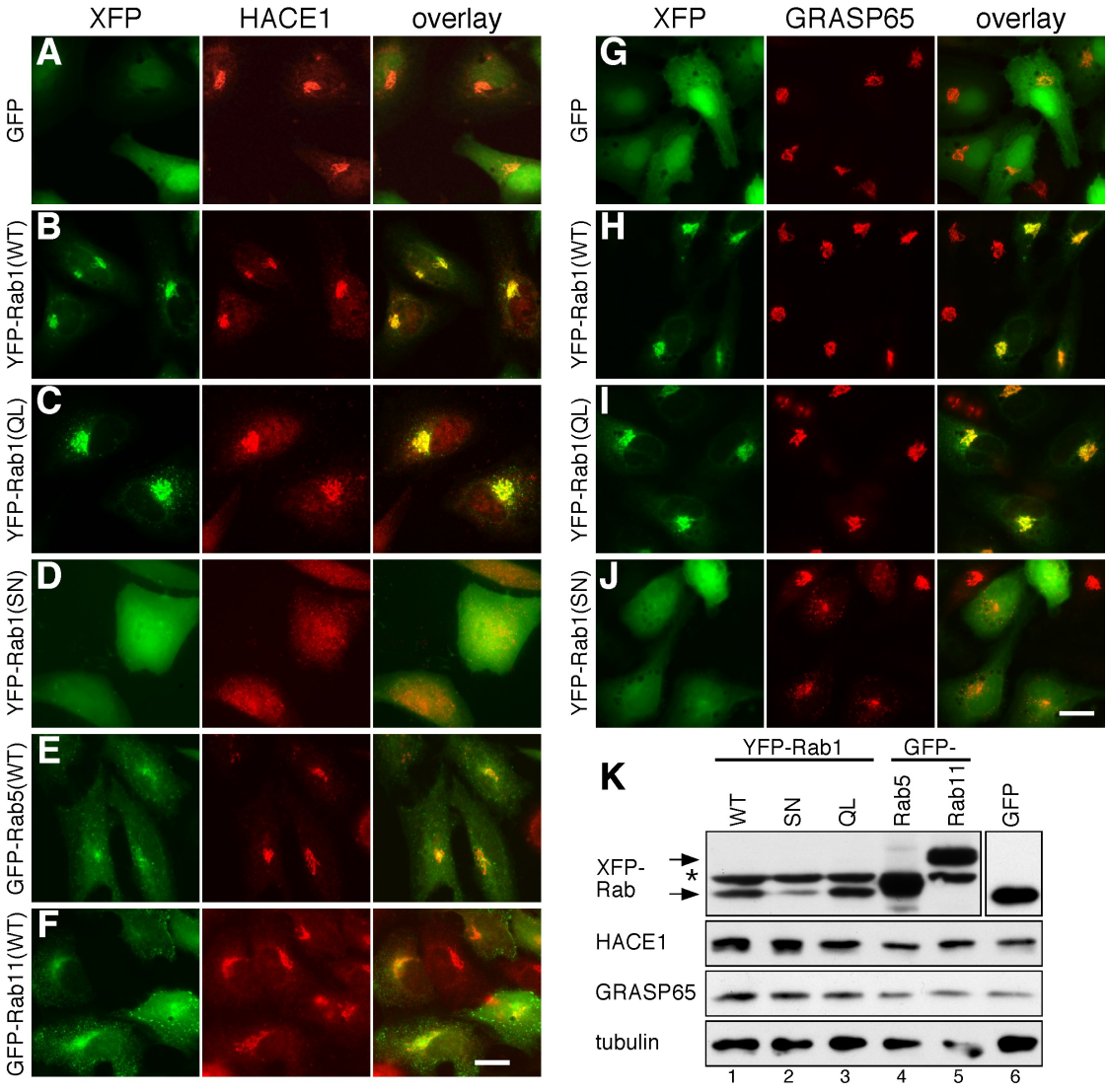

Figure 5.3. Expression of an inactive Rab1 mutant leads to HACE1 dissociation from the Golgi membranes and Golgi fragmentation. (A-J) HeLa cells expressing the indicated Rab constructs (YFP-Rab1 and mutants, GFP-Rab5 and GFP-Rab11) were immunostained for HACE1 (A-F) or GRASP65 (G-J). Note that expression of the Rab1 (SN) mutant, but not any other Rab constructs, leads to HACE1 dispersal from Golgi membranes (D) and Golgi fragmentation (J). Scale bars in all panels: 20 µm. **(K)** Western blots of cells described in A-F. Cells were lysed in SDS buffer followed by Western blots to detect indicated proteins. The asterisk indicates a non-specific band for the GFP-antibody.

To test the role of HACE1 in the formation of Golgi structure, we expressed FLAG-tagged wild-type (WT) and mutant HACE1 in HeLa cells and examined Golgi morphology. The use of a smaller FLAG tag instead of GFP increased the possibility that the exogenous protein is functional in the cells. Expression of the WT HACE1 did not affect Golgi structure. However, expression of the inactive C876A (CA) mutant or the C-terminal deletion (aa 1-553 lacking the HECT domain, designated HACE1 ΔC) led to fragmentation of the Golgi apparatus at lower protein expression levels (Fig. 5.4A, 4B). When the CA and the ΔC mutants were expressed, 31.7 ± 0.8% and 48.1 ± 2.1% of the cells had fragmented Golgi, which was significantly higher than control cells transfected with the GFP vector (12.1 ± 0.3%) or cells transfected with WT HACE1 (14.6 ± 0.9%). These mutant HACE1 proteins lack ubiquitin ligase activity, suggesting that HACE1 ubiquitin ligase activity is involved in maintaining the integrity of the Golgi.

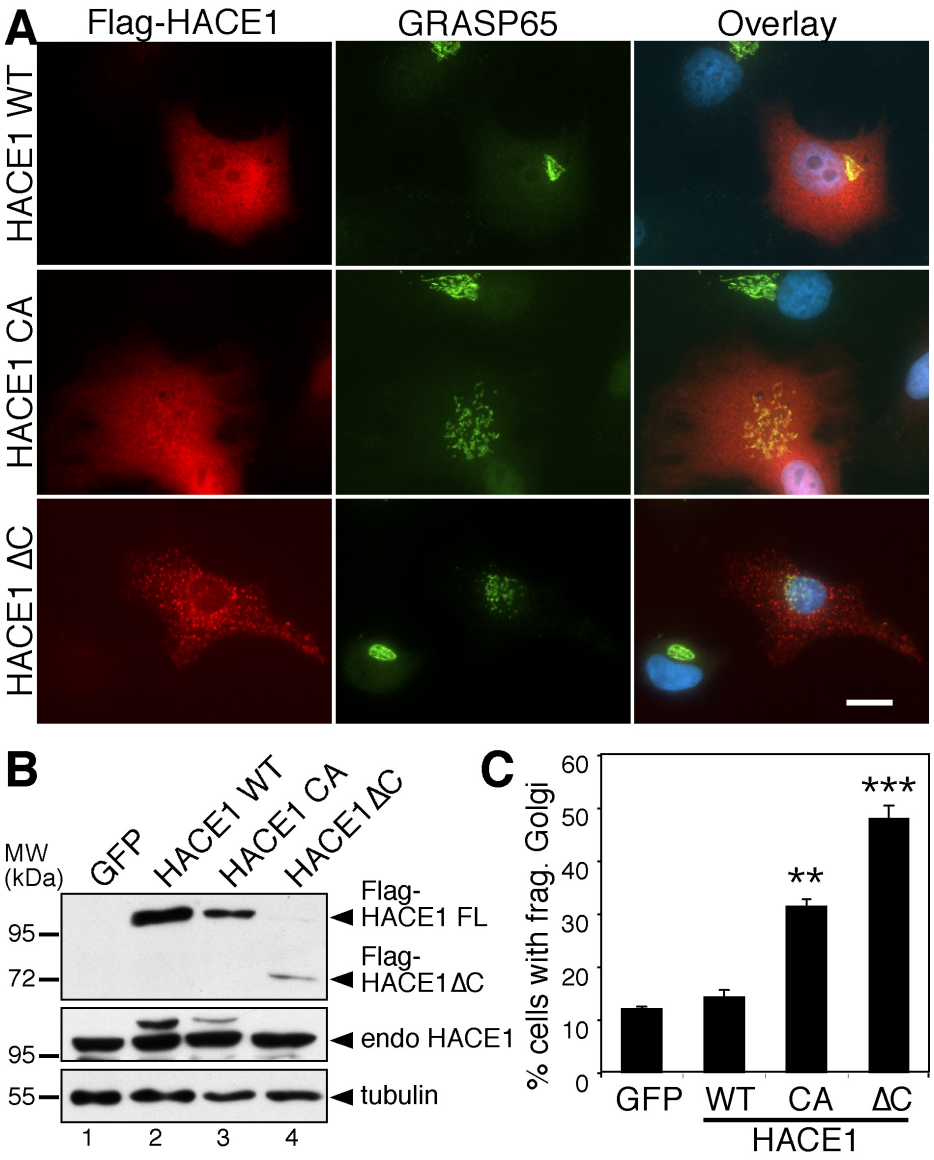

Figure 5.4. Expression of HACE1 mutants leads to Golgi fragmentation. (A) HeLa cells expressing Flag-tagged wild-type HACE1 protein, the inactive C876A (CA) mutant and the C-terminal deletion mutant (HACE1 ΔC). Note that expression of the CA and ΔC mutants leads to Golgi fragmentation. Scale bar: 20 µm. **(B)** Western blots illustrating that the correct proteins were expressed. Endo HACE1 refers to endogenous HACE1. **(C)** Quantification of Golgi fragmentation in 300 Flag-tagged HACE1-expressing cells for each set of experiments. Shown are representative results (mean ± SEM) from three independent experiments. Statistical significance was assessed by comparison to the GFP cell line. **, *p<0.005*; ***, *p<0.001*.

Previous experiments have suggested that ubiquitin plays a role in p97/p47-mediated post-mitotic Golgi membrane fusion [98, 99], and it is possible that HACE1 may also be involved in the same ubiquitination-deubiquitination pathway. Therefore, we used the

standard Golgi disassembly and reassembly assay [270] to test the role of HACE1 in regulation of Golgi membrane dynamics. We first treated purified Golgi membranes with mitotic cytosol, which induced membrane fragmentation. These mitotic Golgi fragments were reisolated and further treated with either interphase cytosol (none) or interphase cytosol containing control rabbit IgG, affinity purified anti-HACE1 antibodies, or purified wild-type HACE1 or C876A mutant proteins. After incubation, membranes were fixed and examined by electron microscopy (EM). The results were quantified to estimate the percentage of membranes in cisternae [99, 280]. In this experiment, mitotic Golgi fragments that did not reassemble were used as a negative control and were normalized to 0% reassembly. Golgi fragments that reassembled after treatment with interphase cytosol without additional components were normalized to 100%. As shown in Fig. 5.S3, membrane reassembly activity was not affected by the presence of HACE1 antibodies or the presence of either wild-type or inactive mutant proteins, suggesting that HACE1 may not be required for post-mitotic Golgi membrane assembly.

Our previous results have demonstrated that ubiquitination occurs during Golgi disassembly and is required for subsequent reassembly [99]; therefore, it is possible that HACE1 functions in disassembly, which may impact subsequent Golgi reassembly. To test this idea, we first treated purified Golgi membranes with mitotic HeLa cell cytosol in the presence of either recombinant HACE1 fusion protein or affinity purified HACE1 antibodies. The resulting membrane fragments were isolated and either fixed or incubated with interphase cytosol and analyzed by EM to determine cisternal growth. The addition of the above reagents had no significant effect on disassembly (Fig. 5.S3). Although the addition of control IgG to disassembled Golgi had no effect on the subsequent

reassembly, the addition of HACE1 antibody or the purified inactive HACE1 C876A mutant protein inhibited Golgi membrane reassembly. In contrast, the addition of wild-type HACE1 protein enhanced the subsequent Golgi membrane reassembly (Fig. 5.5A). These results suggest that the HACE1 ubiquitin ligase activity in mitotic Golgi membrane disassembly is required for subsequent post-mitotic Golgi membrane reassembly.

To ensure that the observed effects resulted from the addition of HACE1, we titrated different amounts of HACE1 recombinant protein into the disassembly reaction and used the membranes for subsequent reassembly. Higher concentrations of the WT HACE1 protein increased the stimulatory effects, whereas increasing the amount of HACE1 C876 increased the inhibitory effects (Fig. 5.5B). These results show that HACE1 ligase activity levels are correlated with the efficiency of post-mitotic Golgi membrane assembly in a dose-dependent manner, further confirming that HACE1 plays an important role in regulating Golgi membrane dynamics during the cell cycle.

We then used the defined Golgi disassembly and reassembly assay [270] to determine whether HACE1 functions through p97/p47-mediated membrane fusion. Similar to the experiments described above, HACE1 antibodies and purified proteins were added to the disassembly reactions, and the generated mitotic Golgi membranes were subsequently incubated with purified p97/p47 proteins. As shown in Fig. 5.5C, the addition of anti-HACE1 antibodies or the purified HACE1 C876A mutant protein inhibited Golgi membrane reassembly, in contrast with the stimulatory effect of the WT protein. Because the experimental conditions were optimized for Golgi membrane fusion, the increased reassembly efficiency caused by the addition of wild-type HACE1 strengthened the conclusion that HACE1 is involved in the regulation of Golgi membrane

dynamics. Taken together, these results strongly suggest that HACE1 ubiquitin ligase activity during mitotic Golgi disassembly is required for p97/p47-mediated post-mitotic Golgi membrane reassembly *in vitro*.

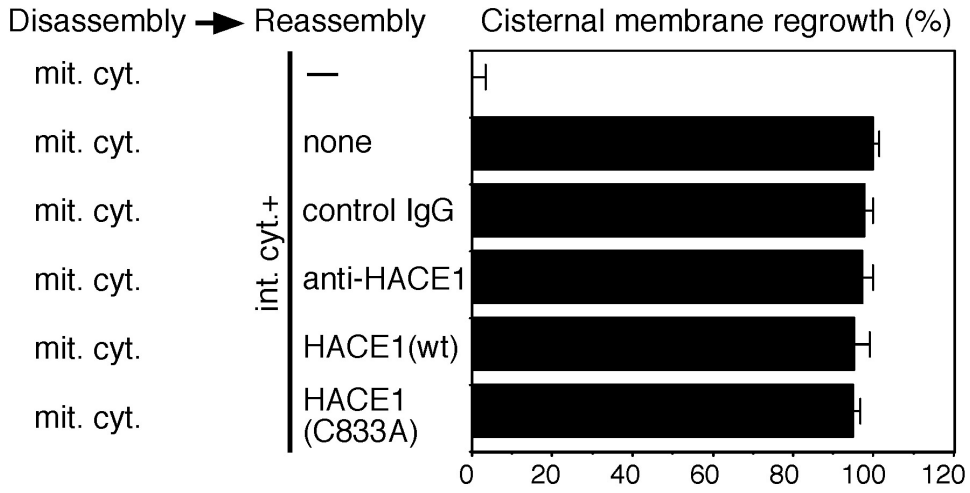

Figure 5.S3. HACE1 is not directly involved in post-mitotic Golgi membrane assembly. Purified rat Golgi stacks were first treated with mitotic cytosol (mit. cyt.) for 20 min at 37ºC. The fragmented Golgi membranes were reisolated and then treated for 60 min at 37ºC with either interphase cytosol (none) or interphase cytosol containing control rabbit IgG, affinity purified anti-HACE1 antibodies or purified proteins of wild-type HACE1 or the C876A mutant, as indicated. Membranes were fixed and processed for EM, and the results were quantified using the intersection method to estimate the percentage of cisternal membranes. Mitotic Golgi fragments that did not reassemble (–, 23.6 ± 1.1% membranes in cisternae) were used as a negative control and were normalized to 0% reassembly. Reassembly in interphase cytosol without any additional components (none, 57.1 ± 0.5% membranes in cisternae) was normalized to 100%. The results represent the mean of three independent experiments ± SEM. Note that the membrane reassembly activity was not affected by the presence of HACE1 antibodies, or the presence of wild-type or inactive mutant proteins.

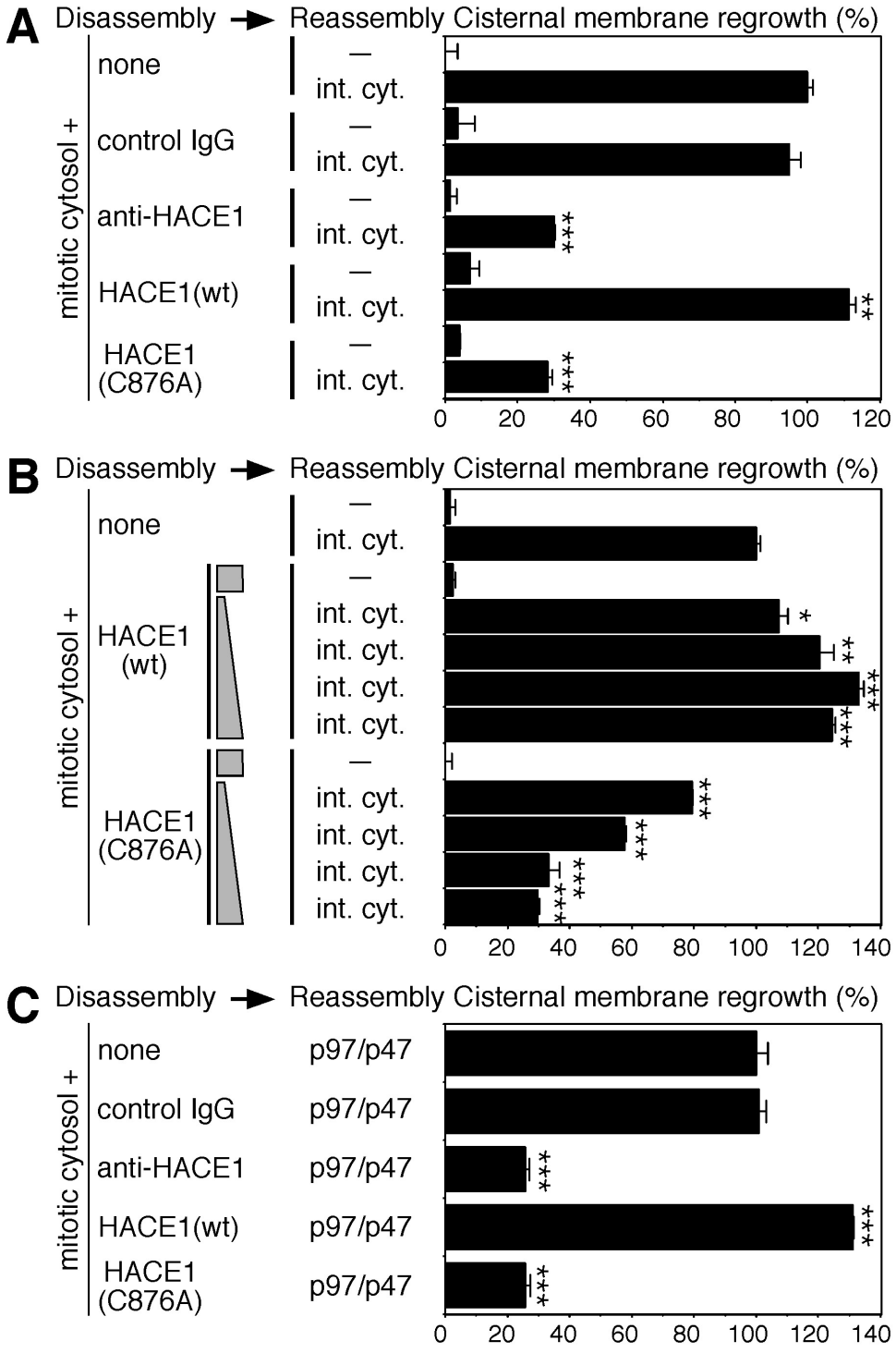

Figure 5.5. HACE1 ubiquitin ligase activity in mitotic Golgi disassembly is required for p97/p47-mediated post-mitotic Golgi membrane reassembly *in vitro*. (A) HACE1 ubiquitin ligase activity in mitotic Golgi membrane disassembly is required for subsequent post-mitotic Golgi membrane reassembly. Golgi membranes were fragmented by incubation with mitotic HeLa cell cytosol in the presence of the indicated reagents. The resulting membrane fragments were reisolated and either fixed (–) or incubated with interphase cytosol (int. cyt.). Membranes were processed for EM, and cisternal growth was determined. The results are presented as the mean percentages (mean ± SEM), where 0% represents mitotic

Golgi fragments treated with mitotic cytosol and then fixed (23.6 ± 1.1% of the membranes were in cisternae), and 100% represents membranes reassembled in the interphase cytosol (57.1 ± 0.5% of the membranes were in cisternae). Note that no effect was observed on reassembly. Subsequent reassembly was inhibited by anti-HACE1 antibodies or purified inactive HACE1 C876A mutant protein and enhanced by HACE1 wild-type protein when added into the disassembly reaction. Statistical significance was assessed by comparison to the standard disassembly and reassembly reactions in mitotic or interphase cytosol without the addition of antibodies or recombinant HACE1 protein. **(B)** HACE1 ligase activity levels correlate with the efficiency of post-mitotic Golgi membrane assembly in a dose-dependent manner. Same as in A except with a serial increasing amount (0.1 – 1 μM) of purified wild-type HACE1 or C876A mutant included in the reassembly reactions. The results are presented as the mean percentages (mean ± SEM), where 0% represents mitotic Golgi fragments treated with mitotic cytosol and then fixed (24.1 ± 0.6% membranes in cisternae), and 100% represents membranes reassembled in interphase cytosol (58.5 ± 0.5% membranes in cisternae). Note that the stimulatory effects correlate with the amount of WT protein added, whereas the inhibitory effects correlate with the amount of mutant protein added. Statistical significance was assessed by comparison to the standard disassembly and reassembly reactions in mitotic or interphase cytosol without any additional proteins added. **(C)** HACE1 affects p97/p47-mediated membrane fusion. Same as in A, except that HACE1 antibodies and purified proteins were added to the disassembly reactions, and the resulting mitotic Golgi membranes were subsequently incubated with the purified p97/p47 proteins. Membranes were processed for EM, and cisternal growth was determined, where 0% represents mitotic Golgi fragments treated with mitotic cytosol and then fixed (26.5 ± 0.1% membranes in cisternae), and 100% represents membranes reassembled with p97/47 (53.6 ± 1.1% membranes in cisternae). Note that the addition of anti-HACE1 antibodies or purified HACE1 mutant protein C876A both inhibited Golgi membrane reassembly, in contrast with the stimulatory effect seen by the addition of WT protein. Statistical significance was assessed by comparison to the p97/p47-mediated reassembly with no additional proteins added. *, $p<0.05$; **, $p<0.005$; ***, $p<0.001$.

To determine whether HACE1 is needed for Golgi integrity *in vivo*, we decreased HACE1 protein levels using small interfering RNAs (siRNA). We generated and tested four pairs of RNA oligos, and the most efficient pair was selected. *HACE1* mRNA levels determined by real-time PCR (RT-PCR) were reduced by 66.8 ± 4.8% and 74.1 ± 4.3% 2 days and 4 days after transfection, respectively (Fig. 5.6C). At the protein level, there was a 62.0 ± 4.8% reduction 4 days after transfection determined by Western blots (Fig. 5.6D). These results indicate that HACE1 is a relatively stable protein. Indeed, when cells were treated with the protein synthesis inhibitor cycloheximide (CHX) for 24 hours, HACE1 protein levels were not significantly affected; in contrast, the same treatment caused a noticeable reduction in GRASP65 (Fig. 5.S4A). To confirm the specificity of our siRNA oligos, HeLa cells were transiently transfected with a myc-HACE1 cDNA and HACE1 or control siRNA oligos. Myc-HACE1 was expressed well when co-transfected

with the control siRNA but not with the HACE1 siRNA (Fig. 5.S4B). These results confirmed that the siRNA used to deplete the HACE1 mRNA and protein is specific and, to some degree, effective.

We then analyzed the Golgi morphology in HACE1-depleted cells. Depletion of HACE1 led to Golgi fragmentation using GM130 (Fig. 5.6A), GRASP65 or syntaxin 5 (data not shown) as Golgi markers; 83.0 ± 0.9% of the HACE1-depleted cells exhibited Golgi fragmentation, a significant increase compared to control siRNA transfected cells (4.8 ± 0.2%, Fig. 5.6E). To examine the Golgi structure more closely, we performed an EM analysis. Control siRNA transfected cells showed well-organized stacks, which often aligned in the cell to form a ribbon. In contrast, HACE1-depleted cells had fragmented Golgi. The Golgi membranes were disorganized and the cisternae were relatively short, while a large part of the membranes were vesiculated (indicated by asterisks), and small stacks or single cisterna were dispersed throughout the cells (Fig. 5.6, G vs. F). The average cisternal length was reduced from 1.01 ± 0.04 μm in control siRNA transfected cells to 0.53 ± 0.04 μm in HACE1-depleted cells (Fig. 5.6H). These results suggest that HACE1 depletion reduces membrane fusion activity, which is consistent with the observation that inhibition of HACE1 activity reduces p97/p47-mediated post-mitotic Golgi membrane fusion (Fig. 5.5).

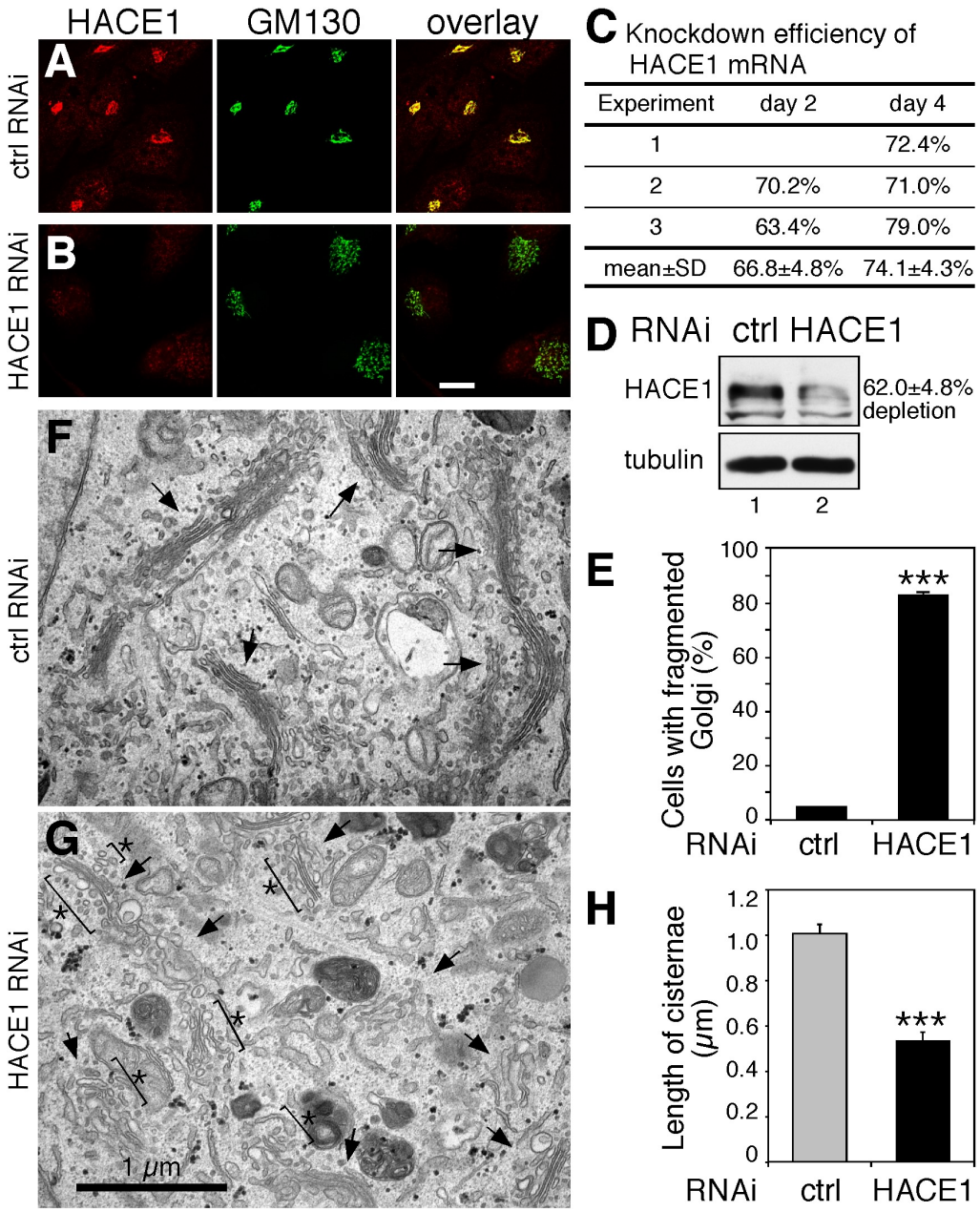

Figure 5.6. Depletion of HACE1 leads to Golgi fragmentation. (A-B) Confocal fluorescence images of HACE1 knockdown cells. HeLa cells transfected with the indicated siRNA oligos were fixed and stained for HACE1 and GM130. Scale bars in all panels: 20 μm. **(C)** Knockdown efficiency of HACE1 mRNA on days 2 and 4 quantified by RT-PCR. The results presented are the percent reduction in the HACE1 mRNA in HACE1 knockdown cells compared to cells treated in parallel with a control siRNA. **(D)** Immunoblots of HeLa cells described in A-B. The knockdown efficiency of HACE1 was 62.0% ± 4.8% from three independent experiments. **(E)** Quantitation of the fluorescence images in A-B from three independent experiments. Shown is the percentage of cells with fragmented Golgi, and 300 cells were counted for each experiment. The results expressed are the means ± SEM. **(F-G)** Representative EM micrographs of the cells described in A-B. The arrowheads indicate Golgi stacks, and asterisks indicate fragmented cisternal membranes. Note that the Golgi ribbon in HACE1-depleted cells are disorganized, and the cisternae are shorter compared to control siRNA-treated cells. **(H)** Quantitation of the EM images in F-G from three independent experiments. Note that cisternal length is reduced by HACE1 depletion. Statistical significance was assessed by comparison to the control siRNA-treated cells. ***, $p < 0.001$.

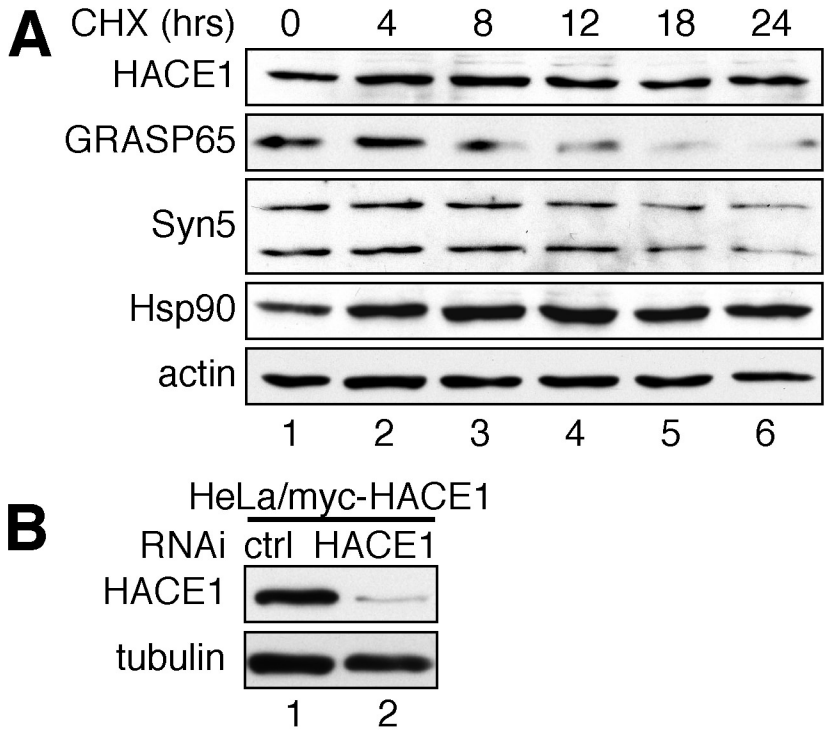

Figure 5.S4. HACE1 protein has a long half-life in the cell. (A) HACE1 protein levels do not significantly decrease 24 h after cycloheximide (CHX) treatment. NRK cells were incubated in growth media with 20 μg/ml CHX (a protein synthesis inhibitor) for the indicated time periods (0-24 hours). Cells were lysed in SDS buffer and analyzed for the indicated proteins by Western blot. Note that HACE1 levels remained relatively unchanged 24 h after treatment, while GRASP65 levels reduced. **(B)** Exogenous HACE1 is readily depleted by siRNA treatment. HeLa cells were treated with HACE1 or control siRNA oligos for 3 days followed by transient transfection with a myc-HACE1 cDNA. Cells were lysed, and HACE1 and tubulin were detected by Western blot. Note that myc-HACE1 expression was reduced in the presence of HACE1 siRNA (lane 2).

It has been previously observed that the SK-NEP-1 cell line expresses relatively low levels of HACE1 protein [278]; therefore, we examined the Golgi morphology in these cells. Indeed, HACE1 protein levels in this cell line were 30.9 ± 3.1% compared to HeLa cells determined by Western blots (Fig. 5.S5C). The expression levels of HACE1 were similar in several cell lines, such as HeLa, A431 and NRK cells (data not shown). When analyzed by fluorescence microscopy, a large number of SK-NEP-1 cells showed fragmentation of the Golgi apparatus. Compared to HeLa cells (Fig. 5.S5B) and several other cell lines in which the Golgi membranes were well organized into a pericentriolar

ribbon-like structure, the Golgi membranes in SK-NEP-1 cells were disconnected, not localized to the perinuclear region and dispersed throughout the cell (Fig. 5.S5A). Fragmented Golgi structures were observed in 34.9 ± 2.2% of the SK-NEP-1 cells compared to 5.6 ± 1.0% in HeLa cells (Fig. 5.S5D). These Golgi were not completely fragmented and appeared as if the major part of the Golgi was irregularly shaped with disconnected elements, suggesting that these cells had a possible membrane fusion defect.

The SK-NEP-1 cells were then analyzed by EM in parallel with HeLa cells. HeLa cells contained well-organized stacks that often aligned into a ribbon-like structure (Fig. 5.S5E). SK-NEP-1 Golgi structure was less organized. The cisternae were often not aligned into stacks, and the stacks were less well organized in the ribbon. More importantly, cisternae were shorter compared to those in HeLa cells. Cisternal length was similar in several cell lines tested, including NRK cells and CHO cells (data not shown). The average length of the SK-NEP-1 cisternae was 0.63 ± 0.02 μm, a significant reduction compared to the average length (1.12 ± 0.05 μm) found in HeLa cells (Fig. 5.S5G). These results agree with the HACE1 knockdown experiment, suggesting that HACE1 regulates Golgi membrane fusion.

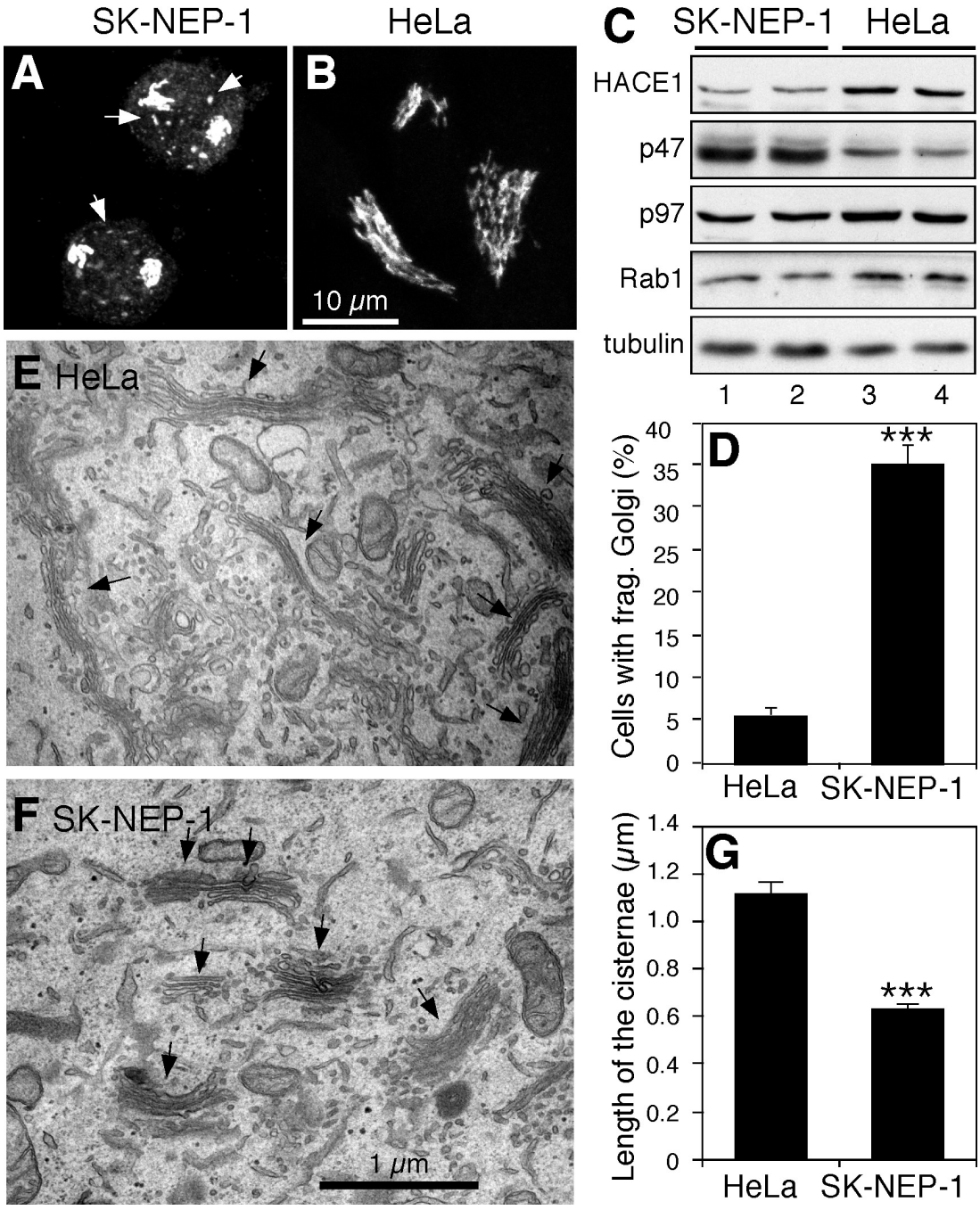

Figure 5.S5. The Golgi apparatus is fragmented in SK-NEP-1 cells, which have reduced HACE1 expression. (A-B) Representative fluorescence images of SK-NEP-1 cells showing that the Golgi apparatus is fragmented compared to HeLa cells. The arrows indicate isolated Golgi fragments. **(C)** HACE1 expression is reduced in SK-NEP-1 cells. Western blot detecting HACE1, tubulin, p97 and p47 in HeLa cells and SK-NEP-1 cell lysates. **(D)** Quantitation of the number of HeLa and SK-NEP-1 cells containing fragmented Golgi. An average of 34.9 ± 2.2% (mean ± SEM) SK-NEP-1 cells had fragmented Golgi, which was significantly higher than HeLa cells (5.6 ± 1.0%). **(E-F)** EM images of HeLa and SK-NEP-1 cells. Note that SK-NEP-1 cells have isolated stacks with relatively short cisternae. **(G)** Quantitation of E-F. Note that the average length of the cisternae in HeLa cells was 1.12 ± 0.05 μm (mean ± SEM), while the cisternal length in SK-NEP-1 cells was 0.63 ± 0.02 μm.

Finally, we used HACE1 and a biochemical approach to identify ubiquitinated Golgi membrane substrates. Purified Golgi membranes were mixed with purified His-tagged ubiquitin, wild-type or inactive HACE1 mutant recombinant proteins and the minimal amount of mitotic cytosol to provide ubiquitin E1 and E2 enzymes and perhaps additional factors. Following incubation, the membranes were reisolated by centrifugation through a 0.5 M sucrose cushion and solubilized in 0.5% Triton X-100 in the presence of 8 M urea to denature and inactivate all ubiquitin-related enzymes. Proteins attached to His-tagged ubiquitin moieties were isolated using nickel beads and analyzed by Western blot for ubiquitin. A major band of ~28 kDa was recognized by ubiquitin antibodies (Fig. 5.7B). In addition, several higher molecular weight bands were also labeled, including two bands of ~37 kDa and 50 kDa that correspond well with syntaxin 5. It has previously been shown that syntaxin 5 has two isoforms in mammalian cells, a 35-kDa short form and a 42-kDa long form [288]. Syntaxin 5 is a Golgi SNARE protein that is essential for p97/p47-mediated post-mitotic Golgi reassembly [97]; depletion of syntaxin 5 causes Golgi fragmentation without inhibiting vesicle transport [289], indicating that syntaxin 5 is a potential target of HACE1 on the Golgi membrane. Indeed, when the same blots were reprobed with syntaxin 5 antibodies, both bands were recognized (Fig. 5.7B). Notably, ubiquitinated proteins were not observed when Golgi membranes were not added (lane 1). In addition, ubiquitination decreased when the mutant HACE1 (ΔC) was added but increased significantly in the presence of the wild-type HACE1 (lanes 3 and 4 vs. 2), which are consistent with the Golgi disassembly and reassembly assay (Fig. 5.5). Additional Western blot analysis excluded a number of Golgi membrane proteins including GRASP65, Gos28, ARF1 as well as Rab1 and Rab6. These results strongly

suggest that syntaxin 5 is a specific substrate for HACE1 on the Golgi membranes. Taken together, the identification of HACE1 as a Golgi-localized ubiquitin ligase and syntaxin 5 as a ubiquitinated protein on the Golgi membrane provides evidence that ubiquitin plays a critical role in Golgi biogenesis during the cell cycle.

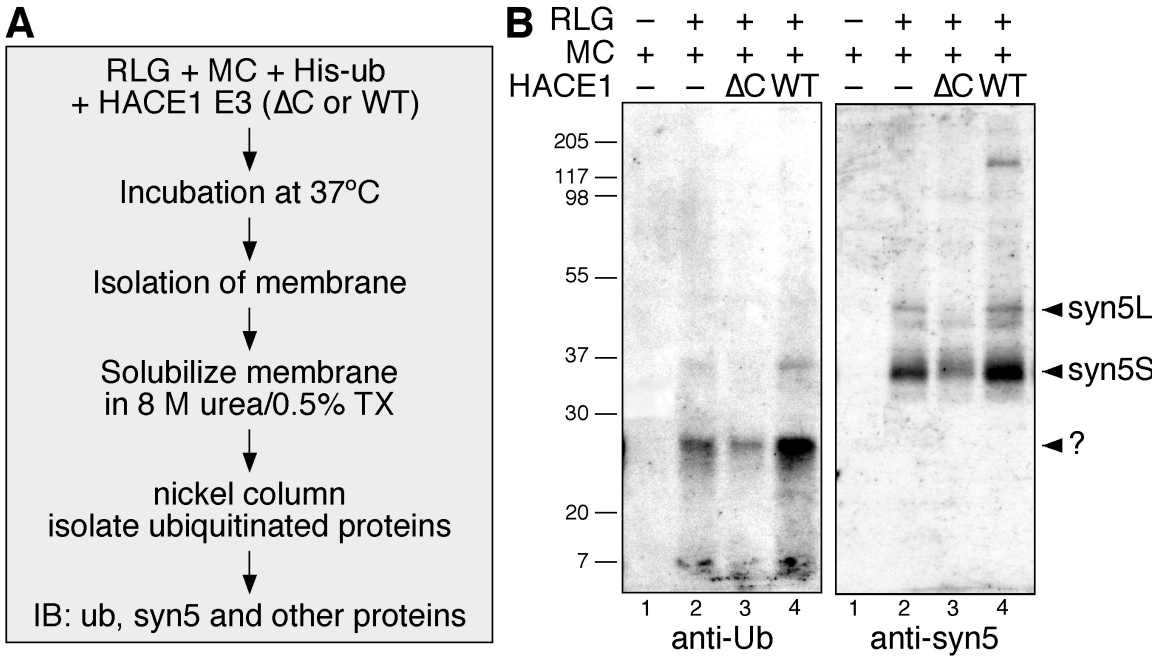

Figure 5.7. Syntaxin 5 is a target of the ubiquitin ligase HACE1 on the Golgi membrane. (A) Schematic flow of the experimental design. **(B)** Western blot of ubiquitinated proteins isolated using nickel columns with anti-ubiquitin (left panel) and anti-syntaxin 5 (right) antibodies. Note that both syntaxin 5 short (syn5S) and long (syn5L) forms are ubiquitinated in addition to an unknown protein (?). Signals were observed only when the Golgi membranes were added. A decrease in signal was observed in the presence of HACE1 ΔC, but the signal increased significantly in the presence of HACE1 wild-type (WT) protein (lanes 3 and 4 vs. 2). Shown are representative results from 4 independent experiments.

Discussion

We have identified the ubiquitin ligase HACE1 that interacts with Golgi-localized Rabs and is targeted to the Golgi membrane. Its activity during Golgi disassembly is required for subsequent post-mitotic Golgi reassembly mediated by the p97/p47 complex. Depletion of HACE1, or expression of inactive HACE1 mutants, affected the length of cisternae found in the stacks and the overall Golgi structure. These findings provided evidence that ubiquitination and deubiquitination play a role in regulating Golgi membrane dynamics during the cell cycle.

HACE1 was previously identified as a critical tumor suppressor involved in multiple cancers, such as sporadic Wilms' tumor [278, 279, 290]. The mechanism by which HACE1 depletion leads to cancer formation, however, remains elusive. Our results suggest that the role of HACE1 in cell proliferation might be related to its role in regulating Golgi biogenesis during the cell cycle. The Golgi is the central machinery for protein modification, processing, trafficking and secretion. Defects in the Golgi structure and function may directly affect cell growth and proliferation. Golgi defects may also impair glycosylation of cell surface proteins, such as cell adhesion molecules, which may lead to metastasis. Indeed, abnormal Golgi division has been observed in cancer cells [291], and defects in protein processing and secretion have been related to cancer cell metastasis [292-294]. Our study also suggests that HACE1 is an effector of Rab GTPases. The tight interaction between HACE1 and Golgi-localized Rabs suggests that the subcellular localization and function of HACE1 are regulated by Golgi-localized Rab proteins. This result is consistent with the requirement of a functional Rab1 for Golgi structure and function [287].

The mechanism by which ubiquitination and deubiquitination regulate Golgi dynamics remains elusive. It is known that the activity of the VCIP135 deubiquitinating enzyme is required for post-mitotic Golgi membrane fusion [99]. Therefore, it is likely that at least one Golgi membrane protein is ubiquitinated by HACE1 at the onset of mitosis when the Golgi undergoes mitotic fragmentation. Mono-ubiquitination does not result in the degradation of the substrate; instead, it recruits the p97/p47 complex to the Golgi membrane through interaction between the p47 UBA domain and mono-ubiquitin [98, 99]. Subsequently, the p97/p47 complex recruits VCIP135 to the membrane. When the monoubiquitin is removed from the substrate(s) by VCIP135, the membranes are subjected to p97/p47-mediated fusion. Consistently, our results indicate that syntaxin 5, a member of the membrane fusion machinery, is a target of this pathway. Taken together, our results suggest a mechanism by which ubiquitination functions as a signal that regulates Golgi reassembly after cell division. A key question that remains to be answered is whether the lack of Golgi membrane fusion during mitosis is due to the ubiquitination of syntaxin 5 and other Golgi membrane proteins. Further experiments are necessary to identify the ubiquitination sites in syntaxin 5 and other ubiquitinated proteins found on the Golgi membrane.

Materials and Methods

Reagents

All reagents were purchased from Sigma Co., Roche or Calbiochem, unless otherwise stated. The following antibodies were used: monoclonal antibodies against ARF1[89], ERGIC53 (P. Arvan), Gos28 and GM130 (Transduction Laboratories), syntaxin 6 (BD Biosciences) and α-tubulin (Developmental Studies Hybridoma Bank University of Iowa); polyclonal antibodies against PDI (P. Arvan), GFP[18], GM130[119], rat GRASP55[18], GRASP65[17] and human GRASP65 (J. Seemann), α-mannosidase II (G. Warren), p47 and p97[99], Rab1A, , Rab6 and Rab11[295], sec61α (Upstate), syntaxin 5 (A. Price), and ubiquitin (Sigma-Aldrich). The HACE1 antibodies were generated in rabbits using recombinant GST-HACE1 (aa 1-548) as the immunogen and subsequently affinity purified. The GalNAc-T2-GFP cDNA was a gift from G. Warren.

Affinity Purification of Rab4 effectors

To purify Rab4 effectors, GST-Rab4 was expressed in 20 L of DH5α cells and bound to 2 ml of glutathione beads (GE Healthcare). The sample was equally divided into two tubes and incubated with nucleotide-exchange buffer (NE buffer; 20 mM Hepes-KOH, pH 7.5, 100 mM NaCl, 10 mM EDTA, 5 mM $MgCl_2$ and 1 mM DTT), containing 1 mM GTPγS in one tube and 1 mM GDP in the other, for 20 min at room temperature with rotation. This step was repeated three times. GST-Rab4 bound to beads was then stabilized with nucleotide-stabilization buffer (NS buffer; 20 mM Hepes-KOH, pH 7.5, 100 mM NaCl, 5 mM $MgCl_2$ and 1 mM DTT) in the presence of 1 mM GTPγS or GDP

for 20 min at room temperature with rotation. Beads were then incubated with 50 ml of bovine brain cytosol (20 mg/ml)[277] for 2 h at 4°C. After incubation, the beads were washed with 10 column volumes of NS buffer with 10 μM GTPγS or GDP; 10 volumes of NS buffer containing 250 mM NaCl and 10 μM GTPγS or GDP and 1 volume of 20 mM Hepes-KOH, pH 7.5, 250 mM NaCl and 1 mM DTT. To elute the bound proteins, the beads were incubated with 1.5 column volumes of elution buffer (20 mM Hepes-KOH, pH 7.5, 1.5 M NaCl, 20 mM EDTA, 1 mM DTT and 5 mM GDP) for 20 min at room temperature with rotation. Eluted proteins were analyzed by SDS-PAGE and coomassie blue staining. The bands in the GTPγS lane were excised and analyzed by mass spectrometry.

HACE1 cloning

The ILTSLAEVA peptide identified by mass spectrometry was found in a HACE1 EST clone (NCBI accession no. AI130909). This EST clone was sequenced, and the translated sequence contained the three other peptides identified by mass spectrometry: VLEHLSQQE, QNEDLR and DTAQILLLR. The full-length HACE1 cDNA clone was isolated by screening the SUPERSCRIPT HeLa cDNA library (Life Technologies) using a primer derived from the 5' end of this EST sequence. The *HACE1* coding sequence was amplified by PCR using primers that contained EcoRI and NotI sites at the 5'- or 3'-ends and inserted into pCDNA3 MycN1 (Invitrogen) for mammalian expression or pGEX-6p-1 (GE Healthcare) for expression in *E. coli*. The C876A mutation was introduced using the QuikChange mutagenesis kit (Stratagene). The HACE1 ΔC construct was generated

by inserting an EcoRI/EcoRV fragment into pCDNA3.1 or pGEX-6p-1 for antigen preparation. All of the constructs were confirmed by DNA sequencing.

Preparation of HACE1 fusion proteins and pull-down assay for HACE1-Rab interactions.

Proteins were expressed in BL21 (DE3) Gold bacteria and purified on glutathione Sepharose beads (GE Healthcare). For the HACE1-Rab interaction assay, the HACE1 protein on glutathione Sepharose beads was cleaved from the tag by PreScission protease, and the supernatant was further incubated with glutathione beads to remove GST-tagged proteins. Untagged HACE1 protein in the supernatant was used to assay binding to Rab proteins.

The GST-Rab1, GST-Rab1a Q67L, GST-Rab1a S25N and GST-Rab2 cDNA constructs were kindly provided by Dr. Graham Warren. The GST-Rab5, GST-Rab6 and GST-Rab11 plasmids were a gift from Dr. Suzanne Pfeffer. The interactions between HACE1 and Rab were determined by a pull-down assay following a previously established procedure[280]. For each reaction, GST-tagged Rabs were expressed in BL21 (DE3) bacteria with 125 ml of LB media. The GST-Rabs were immobilized on 25 μl of glutathione beads (bed volume) in a 1.5 ml Eppendorf tube. The beads were washed with 1 ml of NE buffer containing 10 μM GDP or GTPγS and incubated two times with NE buffer containing 1 mM GDP or GTPγS at RT for 30 min. The beads were then washed with 1 ml of NS buffer containing 10 μM GDP or GTPγS and incubated with NS buffer containing 1 mM GDP or GTPγS at room temperature for 30 min.

Five micrograms of HACE1 protein (without a tag) prepared above was incubated with the GDP or GTPγS charged beads in 150 µl of cytosol buffer (20 mM Hepes-KOH pH 7.4, 250 mM NaCl, 5 mM $MgCl_2$, 1 mM DTT, 1% Triton X-100 and protease inhibitors) containing 1 mM GDP or GTPγS at 4ºC for 2 h. The beads were washed three times with cytosol buffer containing 10 µM GDP or GTPγS at 4ºC for 10 min. To elute the bound proteins, the beads were incubated with 12.5 µl of elution buffer (20 mM Hepes-KOH, pH 7.4, 1.5 M NaCl, 20 mM EDTA, 1 mM DTT, 1% Triton X-100 and protease inhibitor cocktail) for 10 min at room temperature. Elution was repeated three times, and the elutions were pooled. Equal volumes were analyzed by Western blot.

To test the interaction between endogenous HACE1 and Rabs, cell lysates were prepared as previously described[89]. Briefly, cells were grown in 10 X 15 cm dishes to 80% confluency, washed with PBS three times, and harvested with 3 ml of homogenization buffer (20 mM Hepes-KOH, pH 7.4, 100 mM NaCl, 5 mM $MgCl_2$, 1 mM DTT and protease inhibitor cocktail). Cells were cracked with a ball bearing homogenizer to reach 75-80% breakage determined by Trypan blue exclusion. The homogenate was centrifuged for 10 min at 1000 g and 4˚C. The post-nuclear supernatant (PNS) was supplemented with 1% Triton X-100 and rotated at 4˚C for 30 min. Solubilized proteins were exchanged into cytosol buffer (20 mM Hepes-KOH pH 7.4, 100 mM NaCl, 5 mM $MgCl_2$, 1 mM DTT, 1% Triton X-100 and protease inhibitors) using the BIO-RAD Econo-Pac® 10DG column following the manufacturer's instructions. Five milligrams of cell lysate was incubated with GDP or GTPγS charged beads in 800 µl of cytosol buffer containing 1 mM GDP or GTPγS at 4ºC overnight. The beads were washed three times with cytosol buffer containing 10 µM GDP or GTPγS at

4ºC for 10 min and once with cytosol buffer containing 250 mM NaCl and eluted with 80 µl of elution buffer for 20 min at RT and subjected to Western blot analysis.

Thioester bond formation assay

To test whether HACE1 is an active ubiquitin ligase, 60 nM recombinant human ubiquitin activating enzyme E1 (Biomol International), 200 nM recombinant human UbcH7 (Biomol International)[278], 19 µM biotinylated ubiquitin and 600 nM recombinant GST-tagged WT or mutant HACE1 were mixed in 40 µl reactions in reaction buffer that contained 20 mM Tris-HCl, pH 7.4, 50 mM KCl, 5 mM $MgCl_2$, 2 mM ATP, 0.2 M sucrose and protease inhibitors (Roche). Reactions were incubated at 30°C for 60 min and mixed with SDS-PAGE sample buffer with or without DTT followed by detection of HACE1 by Western blot.

Cell culture, nocodazole and Brefeldin A (BFA) treatments, siRNA, and protein expression

HeLa and NRK cells were routinely cultured in DMEM supplemented with 7.5% fetal calf serum, 2 mM L-glutamine, penicillin (100 U/ml), and streptomycin (100 µg/ml). SK-NEP-1 cells were cultured in McCoy's medium with 15% FCS. For nocodazole treatment, cells were treated with 0.5 µg/ml nocodazole for 2 hours and immunostained for HACE1 and Golgi markers, such as GM130. For BFA treatment and washout, cells were treated with 5 µg/ml BFA for 2 hours, washed twice with PBS and further incubated in growth media for 2 hours. siRNA oligos were designed using the Invitrogen BLOCK-iT™ RNAi Designer software according to the human HACE1 sequence (sense: UAU

AGC GCU GAU GUC AAC A(TT), antisense: UGU UGA CAU CAG CGC UAU A(TT)). In a previous report[279], three pairs of RNA oligos from Invitrogen were used to deplete HACE1. These oligos were less effective at knocking down HACE1 than our newly designed oligos. HeLa and HEK 293T cells were transfected using Lipofectamine RNAiMAX (Invitrogen) following the manufacturer's instructions. Control transfections were performed simultaneously using non-specific siRNA oligos purchased from Ambion. Assays were performed 96 h after transfection unless otherwise stated. Depletion efficiency of endogenous HACE1 was quantified from the Western blot results using the NIH ImageJ software and normalized to tubulin levels. For transient expression, HeLa cells were transfected with the indicated HACE1 constructs using Lipofectamine 2000 (Invitrogen).

RT-PCR

mRNA was purified from a 6-cm dish of HeLa cells using RNeasy columns (QIAGEN Inc.). First-strand cDNA was synthesized using Superscript III RT (Invitrogen) and utilized for semi-quantitative real-time PCR using IQ SYBR Green Supermix (Bio-Rad). A Bio-Rad IQ iCycler was used to measure the expression levels of transcripts. The HACE1 mRNA level was normalized to glyceraldehyde 3-phosphate dehydrogenase (GAPDH). Intron-spanning primers are designed using the "Primer 3" software. The following primer sequences were used for HACE1: forward primer: GCTCTTGCAGGGAGACAGGA, reverse primer: AGTCATTCCCGGAGGCATCT. The GAPDH primers were provided by Dr. Haoxing Xu[296].

Subcellular fractionation and equilibrium gradients

NRK cells at 80% confluency were washed with homogenization buffer (0.25 M sucrose, 1 mM EDTA, 1 mM Mg acetate, 10 mM Hepes-KOH, pH 7.2 and protease inhibitors) and resuspended in 800 µl of homogenization buffer. Cells were cracked with a ball-baring homogenizer to a breakage of 75-80%. The homogenate was centrifuged for 10 min at 1000 *g*, 4°C. The postnuclear supernatant (PNS) was removed and subjected to ultracentrifugation in a TLA55 rotor at 120,000 *g* for 60 min. The supernatant (cytosol) was removed, and the membranes in the pellet were resuspended in homogenization buffer. Equal volumes of the PNS, cytosol and membrane fractions were analyzed by SDS-PAGE and Western blot. The PNS was also fractionated on a sucrose gradient as previously described[89, 90, 270].

Microscopy, quantitation and statistical analyses

Immunofluorescence microscopy and the collection of mitotic cells were previously reported[89]. Pictures were taken with a Leica SP5 laser-scanning confocal microscope using a 100X oil lens or a Zeiss Observer Z1 epifluorescence microscope with a 63X oil lens. In interphase cells, fragmented Golgi were defined as scattered dots that were not connected in the perinuclear region. Although some Golgi membranes were concentrated near the nucleus in SK-NEP-1 cells, multiple mini-Golgi (isolated dots detected by fluorescence microscopy) were observed to be dissociated from the major Golgi apparatus. These cells were categorized as containing fragmented Golgi. To quantify the percentage of cells with fragmented Golgi, more than 300 cells transfected with control or HACE1 siRNAs were counted, and the results are presented as mean ± SEM (n=3).

For EM analysis, Golgi stacks and clusters were identified using morphological criteria and quantified using standard stereological techniques[120, 270]. Interphase cells were defined as profiles that contained an intact nuclear envelope. Only stacked structures containing three or more obvious cisternae were measured for cisternal length. Golgi stack images were captured at 11000x magnification to obtain a better view of the stacks. The longest cisterna was measured as the cisternal length of a Golgi stack using the ruler tool in the Photoshop CS3 software or the line tools in ImageJ, both of which gave essentially identical results. At least 20 cells were quantified in each experiment, and the results represent at least three independent experiments. Statistical significance was assessed by Student's *t*-test.

Golgi disassembly and reassembly assay and quantitation

Golgi membranes were purified from rat liver as previously described[297]. Interphase (IC) and mitotic (MC) cytosols were prepared from HeLa S3 cells[214]. The cytosol fractions were exchanged into related buffers using Bio-Spin 6 columns and cleared by centrifugation before they were used to treat Golgi membranes. His-tagged p47 was expressed in bacteria and purified using nickel beads[98]. p97 was prepared using a bacterial expression system or purified from rat liver cytosol by gel filtration[98, 272]. The Golgi disassembly assay was performed as described previously[90]. Briefly, purified Golgi membranes (20 μg) were mixed with 2 mg of mitotic cytosol, 1 mM GTP and an ATP-regenerating system (10 mM creatine phosphate, 1 mM ATP, 20 μg/ml creatine kinase and 20 ng/ml cytochalasin B) in MEB buffer (50 mM Tris-HCl, pH 7.4, 0.2 M sucrose, 50 mM KCl, 20 mM β-glycerophosphate, 15 mM EGTA, 10 mM $MgCl_2$,

2 mM ATP, 1 mM GTP, 1 mM glutathione and protease inhibitors) in a final volume of 200 µl. In some reactions, 1 µM or an increasing amount (0.1-1 µM) of wild-type or mutant HACE1 recombinant proteins or 10 ng/µl anti-HACE1 antibodies were added into the disassembly assay as indicated. After incubation for 60 min at 37°C, mitotic Golgi fragments (MGF) were isolated and soluble proteins were removed by centrifugation (55,000 rpm for 30 min in a TLA55 rotor) through a 0.4 M sucrose cushion in KHM buffer (20 mM Hepes-KOH, pH 7.0, 0.2 M sucrose, 60 mM KCl, 5 mM $Mg(OAc)_2$, 2 mM ATP, 1 mM GTP, 1 mM glutathione and protease inhibitors) onto a 6-µl 2 M sucrose cushion. The membranes were resuspended in KHM buffer and were either fixed and processed for EM[17, 89, 90] or used in reassembly reactions. For Golgi reassembly, 20 µg of Golgi fragments were resuspended in KHM buffer, mixed with either 400 µg IC or 100 ng/µl p97 and 25 ng/µl p47 in KHM buffer in the presence of an ATP regeneration system in a final volume of 30 µl and incubated at 37°C for 60 min. The membranes were pelleted by centrifugation, processed for EM.

For EM analysis, the percentage of membranes in cisternae or in vesicles was determined by the intersection method [17, 249]. Cisternae were defined as long membrane profiles with a length greater than four times their width, and the latter did not exceed 60 nm. Normal cisternae ranged from 20-30 nm in width and were longer than 200 nm. Stacks were defined as two or more cisternae that were separated by no more than 15 nm and overlapped in parallel by more than 50% of their length.

Golgi ubiquitination assay and identification of syntaxin 5 as a ubiquitinated protein

Purified Golgi membranes (100 μg) were mixed with 600 μg mitotic cytosol, 2 μM wild-type or mutant HACE1 recombinant proteins, 50 μM His-ubiquitin and 0.5 μM Epoxomicin in a 1-ml reaction in MEB buffer containing an ATP-regenerating system. Reactions were incubated at 30ºC for 60 min and supplemented with 20 mM N-ethylmaleimide (NEM). The membranes were isolated by centrifugation through a 0.4 M cushion and dissolved in 1 ml of lysis buffer (100 mM Tris-HCl, pH 8.0, 8 M urea, 0.5% Triton X-100 w/v and 150 mM NaCl), and the samples were centrifuged in a microcentrifuge at maximum speed for 30 min at 4ºC. The supernatant was incubated with 30 μl bed volume of Ni-NTA beads for 3 hours at 4ºC, and the bound proteins were analyzed by Western blot for the indicated proteins.

Acknowledgements

We thank Suzanne Pfeffer and Graham Warren for the Rab constructs, David Sheff for the Rab antibodies, Peter Arvan and Jaemin Lee for the ERGIC and PDI antibodies, Poul Sorensen for the SK-NEP-1 cells, Youjian Chi and Hui Jiang for technical support, and other members of the Wang Lab for suggestions and reagents. We thank Hemmo Meyer for providing us with the purified p97 and p47 proteins, Xiping Chen and Haoxing Xu for help with RT-PCR, and Graham Warren for ideas and support pertaining to this project. This work was supported by the National Institutes of Health (GM087364) and the American Cancer Society (RGS-09-278-01-CSM) to Y. Wang. Author contributions: Y. W. and M. Z. designed the research; Y. W., D. T., Y. X., G. Z. and S. D. Z. performed the experiments; Y. W., D. T., Y. X., G. Z., and S. D. Z. analyzed the data; and Y. W. wrote the paper. The authors declare no conflicts of interests.

Chapter VI. Conclusion

The Golgi apparatus is the central conduit in the secretory pathway. It receives and modifies newly synthesized proteins from the ER, and sorts them to the plasma membrane or the endosomal/lysosomal system via different transport carriers [2]. In almost all eukaryotic cells, the basic structural unit of the Golgi apparatus is a stack of flattened cisternae that are arranged in parallel [8]. In mammalian cells, individual Golgi stacks are connected laterally by tubular continuities to form a ribbon-like structure that localizes adjacent to the centrosome in interphase cells [2]. How the Golgi apparatus forms this unique morphology, and how it regulates the physiological functions of this organelle are central questions of cell biology. In addition, Golgi is a highly dynamic organelle that undergoes rapid disassembly and reassembly during the cell cycle, which is a highly regulated process and plays essential role for the inheritance of this organelle in mammalian cells [2]. However, the underlying mechanism of Golgi biogenesis during mitosis is unclear. My research has focused on the following four questions: 1) How does the Golgi form polarized stacks? 2) Why does the Golgi form stacks? 3) Is mitotic Golgi disassembly mediated by redistribution of this organelle into the ER, or continuous COPI vesicle formation? 4) How is ubiquitination involved in the regulation of Golgi biogenesis during the cell cycle?

The molecular mechanism of Golgi stack formation

In chapter II, I studied the molecular mechanism of Golgi stack formation. Two homologous proteins GRASP65 (Golgi Reassembly Stacking Protein of 65 kDa) and GRASP55 have been initially identified as Golgi stacking factors through the use of an *in vitro* assay that reconstitutes the cell-cycle regulated Golgi disassembly and reassembly process [15, 16]. GRASP65 and GRASP55 are both peripheral membrane proteins and localize to the *cis*- and *medial*-to-*trans*-Golgi, respectively, via the N-terminal myristoylation [15, 16]. Adding either GRASP65 or GRASP55 antibody inhibited restacking of newly formed Golgi cisternae in this assay [15, 16]. Consistently, microinjection of anti-GRASP65 antibodies into mitotic cells inhibited subsequent Golgi stack formation in the daughter cells [17]. However, whether these proteins are involved in the cisternal stacking *in vivo* is under debate. The initial RNA interference experiment supported the role of GRASP65 in the stack formation [118], whereas another group reported that GRASP65-depletion caused Golgi unlinking instead of unstacking [22]. Similar arguments applied to GRASP55 [23]. To address these discrepancies, I optimized the experimental conditions to knockdown GRASP65 and GRASP55 with siRNA, and used systematic electron microscopic analysis to assess the roles of GRASP65 and GRASP55 in the formation of Golgi stacks. I found that the average number of cisternae per stack dropped from 5.7±0.2 in cells transfected with control siRNA to 3.7±0.1 in GRASP55-depleted cells, or 3.8±0.1 in GRASP65-depleted cells, which could be rescued by exogenous expression of siRNA resistant GRASP55 or GRASP65. In addition, depletion of both GRASP55 and GRASP65 using siRNA led to a complete disassembly of the Golgi stacks in 80% of the cells. Expression of either exogenous GRASP55 or

GRASP65 could partially but not completely rescue the effect. These results demonstrated that GRASP55 and GRASP65 play complementary and essential roles in Golgi cisternal stacking [18].

I have also studied the mechanism of GRASP55 mediated cisternal stacking. Previous studies revealed that GRASP65 forms mitotic regulated *trans*-oligomers via the N-terminal GRASP domain to link adjacent Golgi cisternae together [17, 120]. GRASP55 exhibits a high level of sequence identity to GRASP65. The N-terminal GRASP domain is 80% similar and 66% identical to that of GRASP65 in rat [16]; and the C-terminal Serine/Proline-Rich (SPR) domain, although less conserved, contains a number of potential phosphorylation sites. Using biochemical methods, I demonstrated that similar to GRASP65, GRASP55 forms homodimers, which further interact with each other to form higher oligomers and link adjacent cisternae together. Both dimerization and oligomerization are mediated via the N-terminal GRASP domain. The dimerization of GRASP55 is stable during the cell cycle, whereas the oligomerization of GRASP55 is regulated by its phosphorylation status, phosphorylation of GRASP55 disrupts its oligomerization and leads to unstacking of Golgi cisternae. Unlike GRASP65 that is phosphorylated by mitotic kinases Cdk1/cdc2 and plk, GRASP55 is phosphorylated by mitogen-activated protein kinase ERK2. The phosphorylation sites of GRASP55 are mapped in the SRP domain, and the non-phosphorylatable mutants (i.e., the GRASP domain and the T222A/T225A/S245A mutant) form oligomers that are resistant to the regulation of phosphorylation. When expressed in cells, these non-phosphorylatable mutants of GRASP55 enhanced Golgi stacking in interphase cells and inhibited Golgi unstacking and disassembly in mitotic cells [18]. Similar observations have been made in

cells expressing the non-phosphorylatable mutants of GRASP65 [119]. These results confirmed the role of GRASP55 and GRASP65 in the stack formation *in vivo*, and demonstrated that GRASP55 and GRASP65 employ a common mechanism, that is, by forming *trans*-oligomers via the GRASP domain, to stack the Golgi cisternae, although they may subject to different regulations (Fig. 6.1).

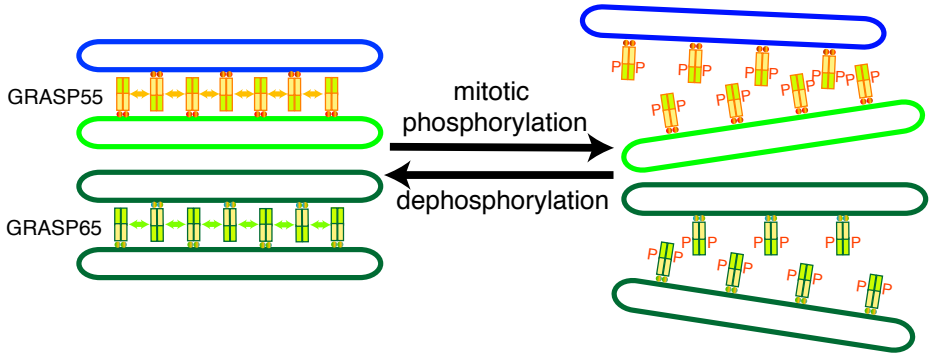

Figure 6.1. GRASP65 and GRASP55 form mitotic regulated oligomers to link adjacent Golgi cisternae together. GRASP65 and GRASP55 localize to the *cis*- and *medial-trans*-Golgi via myristoylation, respectively. The dimers of GRASP65 or GRASP55 from adjacent cisternae interact to form *trans*-oligomers to stack the Golgi cisternae together during interphase. Both GRASP65 and GRASP55 are phosphorylated during mitosis, which disrupts the oligomerization and causes Golgi unstacking. The two proteins are dephosphorylated after mitosis, and Golgi stacks rebuild subsequently.

An unsolved question is whether depletion of GRASP65 causes the unstacking of the *cis*-Golgi cisternae, whereas depletion of GRASP55 causes the unstacking of the *medial*-to-*trans* part of the Golgi. This question can not be addressed using transmission EM, but may be answered by immuno-EM or immunoperoxidase-EM. For example, cells stably expressing the CGN/*cis*-Golgi marker ERGIC-horseradishperoxidase, *cis*-to-*medial* Golgi marker Mannosidase II-horseradishperoxidase, or the *trans*-Golgi enzyme sialyltransferase-horseradishperoxidase could be treated with control or GRASP siRNA, and different Golgi compartments could be identified under EM by the HRP signal.

The physiological relevance of Golgi stack formation

Although stack formation is a conserved feature in most eukaryotic cells, its physiological role remains elusive. It has been speculated that cisternal stacking improves the efficiency of vesicular transport because the close spatial arrangement of cisternae in a Golgi stack minimizes the distance of vesicular transport [140]. In addition, tethering complexes hold the vesicles to the target cisternae and thereby enhance membrane fusion [216]. To investigate the physiological role of cisternal stacking, I inhibited Golgi stacking by depleting the Golgi stacking factors GRASP65 and GRASP55, and assessed protein trafficking, sorting, modification in those cells. As shown in chapter III, the trafficking of VSV-G and α5/β1 integrins are enhanced when the Golgi is unstacked, which is consistent with a previous study showing that microinjection of GRASP65 antibodies inhibited Golgi stack formation, and resulted in an increased trafficking of an artificial marker CD8 [208]. A plausible explanation for this observation is that when the Golgi cisternae are fully stacked, vesicles can only form and fuse at the rims, whereas when the cisternae are unstacked, more membrane area becomes accessible to COPI machinery, thereby increasing the rate of vesicle budding/fusion, as well as cargo transport through the Golgi (Fig. 6.2) [208]. This speculation is supported by the *in vitro* budding assay showing that unstacking of Golgi membranes increases the rate of COPI vesicle formation [208].

Why do cells form Golgi stacks to reduce the rate of trafficking? Since the Golgi is the main station of glycosylation, cargos are modified sequentially as they travel through the Golgi stacks [201, 231], I determined whether unstacking of the Golgi affected protein glycosylation. By using fluorescence-conjugated lectins, I demonstrated that

GRASP-depletion led to an incomplete glycosylation, suggesting that cisternal stacking ensures accurate post-translational modifications (i.e., glycosylation) of cargo proteins [187]. In addition, the lysosomal hydrolase cathepsin D precursor was missorted to the extracellular space instead of the endosomal/lysosomal system when the Golgi was unstacked. Furthermore, there is a reduction of cell adhesion and migration in the cells with unstacked Golgi, in agreement with the reduction of cell adhesion molecules α5/β1 integrins and aberrant glycosylation pattern on the cell surface. I also showed that the cell proliferation and protein synthesis are enhanced in those cells with unstacked Golgi, which may be attributed to the increased protein trafficking.

Those data suggested that the Golgi cisternal stacking functions as a "flux regulator" to control the flow of cargo through this organelle [208], and thus provides a mechanism of quality control for protein sorting and modification. The quality of the biosynthetic process in the ER is controlled by chaperones and folding enzymes, and improperly modified or folded cargos are retained or degradated. Unlike the ER, the Golgi apparatus does not have a known robust system to control the accuracy of the post-translational modifications that occur there [185]. Membrane and secretory glycoproteins with defective glycans can still be exported without retention or degradation [232]. In addition, since the Golgi resident enzymes are mostly transmembrane proteins, the lumen of the Golgi apparatus is filled with cargo proteins at a much higher concentration than that in the ER [185]. Therefore, a controlled slow cargo flow through the Golgi apparatus could provide enough time for the cargos to be correctly modified. In higher multicellular organisms, particularly mammals, accurate glycosylation of cell surface proteins such as receptors and cell adhesion molecules is essential for their cellular functions [226]. In

contrast, the budding yeast *S. cerevisiae*, in which Golgi membranes do not form stacks under normal growth conditions, has much simpler N-glycosylation in the Golgi compared with that in mammalian cells [234]. Therefore, Golgi cisternal stacking may be a gained feature during evolution to improve the accuracy of protein modifications.

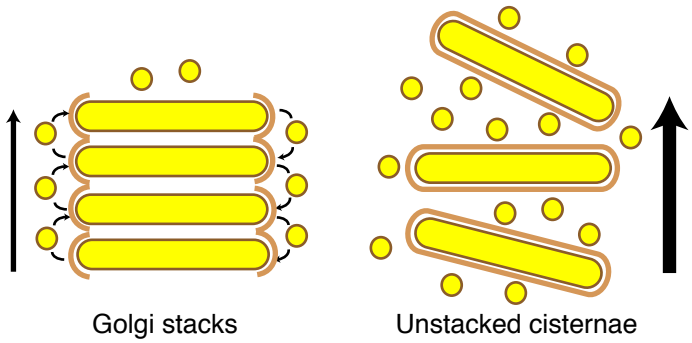

Figure 6.2. Golgi cisternal stacking regulates cargo flow through the Golgi. COPI machinery can only get assess to the rims of cisternae in a stacked Golgi, whereas COPI vesicles can bud from the whole surface area of unstacked cisternae. Therefore, the vesicle budding and cargo transport rates are enhanced when the Golgi is unstacked [208].

To further determine whether Golgi unstacking accelerates protein trafficking, we could examine the rate of protein secretion in GRASP siRNA treated cells using pulse-chase experiment. Different protein markers could be used, for example, heavily glycosylated proteins *vs*. mildly glycosylated proteins. Alternatively, the transport of cell surface proteins, such as CD44, could also be monitored in GRASP siRNA treated cells.

The glycosylation patterns of cell surface proteins could be further determined by mass spectrometry. Cell surface proteins could be labeled with biotin and isolated with avidin-conjugated beads. These proteins could be analyzed with mass spectrometry to identify glycan structures conjugated on them. Compared with the lectin staining method, this method can reveal the details of glycosylation alteration, and identify glycoproteins whose glycosylation patterns have been changed.

We have showed that the protein levels of α5/β1 integrins were reduced when the Golgi was unstacked, we could further examine protein levels of other integrins. In addition, we can examine whether the glycosylation patterns of integrins are changed by immunoprecipitating integrins followed by lectin blot.

It can also be interesting to determine the correlation between the increase of cell proliferation, total protein synthesis and Golgi unstacking. We could first examine whether a given signaling pathway is activated when the Golgi is unstacked. As mentioned before, the disassembly of Golgi membranes during mitosis may relieve some inhibitory effect on mitotic progression by releasing Golgi localized proteins that play special roles during mitosis [7], it is possible that Golgi unstacking may trigger certain signaling pathway.

The molecular mechanism of mitotic Golgi disassembly

In mammalian cells the Golgi apparatus undergoes an extensive disassembly process during mitosis followed by post-mitotic reassembly, which facilitates equal inheritance of this organelle in the two daughter cells [2].

Two models have been proposed to explain the underlying mechanism of Golgi disassembly during mitosis [78]. One proposes that the disassembly is achieved through a similar mechanism as Brefeldin A (BFA) treatment, a fungal metabolite that inactivates the guanine nucleotide exchange factor (GEF) for the ADP-ribosylation factor-1 (ARF1), and thereby redistributes the Golgi membranes, at least partially, into the ER [50]. ARF1 is a small GTPase that associates with Golgi membranes in its active GTP-bound form and recruits coatomer onto the membrane to form COPI vesicles [47]. Inactivation of ARF1 in turn prevents the recruitment of coatomer and the formation of COPI vesicles, which subsequently leads to the redistribution of Golgi membranes to the ER [80]. Another explanation is the direct fragmentation model, which proposes that the mitotic Golgi fragmentation is mediated through the continuous budding of COPI vesicles [78], which is dependent on ARF1 activity. The key issue among the arguments is the role of ARF1 in the mitotic Golgi disassembly. Therefore, I investigated whether ARF1 is required for mitotic Golgi fragmentation. In Chapter IV, I showed that mitotic cytosol treatment to purified Golgi membranes leads to Golgi fragmentation, while ARF1-depleted mitotic cytosol fails to fragment Golgi membranes, suggesting that ARF1 is required for mitotic Golgi fragmentation. ARF1 associates with membranes, in particular, Golgi vesicles generated *in vitro* or vesicles in mitotic cells, as shown by subcellular fractionation and sucrose gradient, indicating that ARF1 is in its active, membrane-

associated form during mitosis. Golgi membranes are converted to vesicles by purified coatomer together with wild type ARF1 or its constitutive active form, but not the inactive mutant, confirming that ARF1 activity is required for Golgi vesiculation [89]. A previous study showed that ARF1 activity blocks mitotic Golgi fragmentation by overexpressing the constitutive active mutant(Q71L) [245]. To avoid unspecific effects caused by the chronic expression of ARF1 mutant, we microinjected purified ARF1(Q71L) protein into cells, and observed no change of mitotic Golgi fragmentation and cell cycle progression through mitosis. These results demonstrated that ARF1 is active during mitosis and this activity is required for mitotic Golgi fragmentation. Our results support the direct Golgi fragmentation model that mitotic Golgi disassembly is mediated by continuous COPI vesicle budding [89].

Identification of the Ubiquitin ligase HACE1 that regulates the Golgi biogenesis in cell cycle

The disassembly and reassembly of the Golgi during cell division is a highly regulated process. The Golgi stacking proteins GRASP65 and GRASP55 are phosphorylated at the onset of mitosis by Cdk1/plk and ERK2, respectively, which leads to the unstacking of cisternae [17, 18]. These isolated cisternae further break down to vesicles and tubules via COPI-mediated vesiculation [77]. Postmitotic Golgi reassembly could also be divided into two processes: cisternal regrowth and restacking. Cisternal regrowth is mediated by two AAA ATPases, p97 and NSF [90]. Restacking of the Golgi cisternae is regulated by the dephosphorylation of GRASP65 and GRASP55 [90]. An unknown question is, how does the cell recognize mitotic Golgi fragments and reassemble them into Golgi cisternae? A plausible explanation is that the cell marks these membranes, and ubiquitin is a potential marker (Fig. 1.9).

Previous studies indicate the mitotic disassembly and reassembly of the Golgi is regulated by ubiquitination [98, 99]. Ubiquitination that occurs in mitosis is required for post-mitotic reformation of Golgi cisternae, block of ubiquitination inhibits subsequent Golgi reassembly [98]. The AAA ATPase p97 binds to ubiquitin via the UBA domain of its cofactor, p47 [98]. VCIP135, another cofactor of p97 that is required for the reassembly process, is a deubiquitinating enzyme [99, 298]. However, the identity of the ubiquitin ligase and the ubiquitinated substrates on the Golgi membranes are unknown. In chapter V, we identified a Golgi localized HECT-domain containing protein HACE1 as the potential ubiquitin ligase in Golgi biogenesis during the cell cycle. HACE1 is targeted to the Golgi membrane through interaction with Rab proteins. HACE1 ubiquitin

ligase activity is involved in mitotic Golgi disassembly and is required for subsequent post-mitotic Golgi membrane fusion. Depletion of this protein using siRNAs or expression of an inactive HACE1 mutant affects Golgi membrane fusion. Consistently, SK-NEP-1 cells with reduced level of HACE1 contain fragmented Golgi with shorter cisternae. Further biochemical analysis indicated that the t-SNARE syntaxin 5 is a substrate of HACE1 on the Golgi membranes. The identification of HACE1 as a Golgi-localized ubiquitin ligase, and syntaxin 5 as its substrate, supports the hypothesis that ubiquitin plays a critical role in Golgi biogenesis during the cell cycle. Future work is needed to confirm syntaxin 5 is ubiquitinated by HACE1 *in vivo*, and the significance of ubiquitination of the substrate(s) in Golgi biogenesis *in vivo.*

To confirm that syntaxin 5 is ubiquitinated during mitosis *in vivo*, we could immunoprecipitate ubiquitinated proteins from cell lysates collected from synchronized interphase or mitotic cells, and determine if syntaxin 5 is one of the ubiquitin substrates during mitosis. To further confirm that syntaxin 5 is ubiquitinated by HACE1 during mitosis, HACE1-depleted cells could be employed.

To further investigate the role of HACE1-mediated ubiquitination in the Golgi disassembly and reassembly process, we could examine the Golgi fragmentation and reconstruction with live cell imaging in cells transfected with control or HACE1 siRNA. In addition, Golgi reassembly could be assessed in cells microinjected with control IgG or HACE1 antibody (or wild type HACE1 *vs*. inactive HACE1) during mitosis.

References

1. Farquhar, M.G., and Palade, G.E. (1998). The Golgi apparatus: 100 years of progress and controversy. Trends Cell Biol *8*, 2-10.
2. Shorter, J., and Warren, G. (2002). Golgi architecture and inheritance. Annu Rev Cell Dev Biol *18*, 379-420.
3. Mironov, A.A., and Pavelka, M. (2008). The Golgi apparatus : state of the art 110 years after Camillo Golgi's discovery, (Wien ; New York: Springer).
4. De Matteis, M.A., and Luini, A. (2008). Exiting the Golgi complex. Nat Rev Mol Cell Biol *9*, 273-284.
5. Mironov, A.A., Beznoussenko, G.V., Polishchuk, R.S., and Trucco, A. (2005). Intra-Golgi transport: a way to a new paradigm? Biochim Biophys Acta *1744*, 340-350.
6. Machamer, C.E. (2003). Golgi disassembly in apoptosis: cause or effect? Trends Cell Biol *13*, 279-281.
7. Sutterlin, C., and Colanzi, A. (2010). The Golgi and the centrosome: building a functional partnership. J Cell Biol *188*, 621-628.
8. Ladinsky, M.S., Mastronarde, D.N., McIntosh, J.R., Howell, K.E., and Staehelin, L.A. (1999). Golgi structure in three dimensions: functional insights from the normal rat kidney cell. J Cell Biol *144*, 1135-1149.
9. Rambourg, A., Clermont, Y., Ovtracht, L., and Kepes, F. (1995). Three-dimensional structure of tubular networks, presumably Golgi in nature, in various yeast strains: a comparative study. Anat Rec *243*, 283-293.
10. Trucco, A., Polishchuk, R.S., Martella, O., Di Pentima, A., Fusella, A., Di Giandomenico, D., San Pietro, E., Beznoussenko, G.V., Polishchuk, E.V., Baldassarre, M., et al. (2004). Secretory traffic triggers the formation of tubular continuities across Golgi sub-compartments. Nat Cell Biol *6*, 1071-1081.
11. Gillin, F.D., Reiner, D.S., and McCaffery, J.M. (1996). Cell biology of the primitive eukaryote Giardia lamblia. Annu Rev Microbiol *50*, 679-705.
12. Rabouille, C., Hui, N., Hunte, F., Kieckbusch, R., Berger, E.G., Warren, G., and Nilsson, T. (1995). Mapping the distribution of Golgi enzymes involved in the construction of complex oligosaccharides. J Cell Sci *108*, 1617-1627.
13. Orci, L., Montesano, R., Meda, P., Malaisse-Lagae, F., Brown, D., Perrelet, A., and Vassalli, P. (1981). Heterogeneous distribution of filipin--cholesterol complexes across the cisternae of the Golgi apparatus. Proc Natl Acad Sci U S A *78*, 293-297.
14. Cluett, E.B., Kuismanen, E., and Machamer, C.E. (1997). Heterogeneous distribution of the unusual phospholipid semilysobisphosphatidic acid through the Golgi complex. Mol Biol Cell *8*, 2233-2240.

15. Barr, F.A., Puype, M., Vandekerckhove, J., and Warren, G. (1997). GRASP65, a protein involved in the stacking of Golgi cisternae. Cell *91*, 253-262.
16. Shorter, J., Watson, R., Giannakou, M.E., Clarke, M., Warren, G., and Barr, F.A. (1999). GRASP55, a second mammalian GRASP protein involved in the stacking of Golgi cisternae in a cell-free system. Embo J *18*, 4949-4960.
17. Wang, Y., Seemann, J., Pypaert, M., Shorter, J., and Warren, G. (2003). A direct role for GRASP65 as a mitotically regulated Golgi stacking factor. Embo J *22*, 3279-3290.
18. Xiang, Y., and Wang, Y. (2010). GRASP55 and GRASP65 play complementary and essential roles in Golgi cisternal stacking. J Cell Biol *188*, 237-251.
19. Hashimoto, H., Abe, M., Hirata, A., Noda, Y., Adachi, H., and Yoda, K. (2002). Progression of the stacked Golgi compartments in the yeast Saccharomyces cerevisiae by overproduction of GDP-mannose transporter. Yeast *19*, 1413-1424.
20. Hawes, C. (2005). Cell biology of the plant Golgi apparatus. New Phytol *165*, 29-44.
21. Kodani, A., and Sutterlin, C. (2008). The Golgi protein GM130 regulates centrosome morphology and function. Mol Biol Cell *19*, 745-753.
22. Puthenveedu, M.A., Bachert, C., Puri, S., Lanni, F., and Linstedt, A.D. (2006). GM130 and GRASP65-dependent lateral cisternal fusion allows uniform Golgi-enzyme distribution. Nat Cell Biol *8*, 238-248.
23. Feinstein, T.N., and Linstedt, A.D. (2008). GRASP55 Regulates Golgi Ribbon Formation. Mol Biol Cell *19*, 2696-2707.
24. Diao, A., Rahman, D., Pappin, D.J., Lucocq, J., and Lowe, M. (2003). The coiled-coil membrane protein golgin-84 is a novel rab effector required for Golgi ribbon formation. J Cell Biol *160*, 201-212.
25. Yadav, S., Puri, S., and Linstedt, A.D. (2009). A primary role for Golgi positioning in directed secretion, cell polarity, and wound healing. Mol Biol Cell *20*, 1728-1736.
26. Sohda, M., Misumi, Y., Yoshimura, S., Nakamura, N., Fusano, T., Sakisaka, S., Ogata, S., Fujimoto, J., Kiyokawa, N., and Ikehara, Y. (2005). Depletion of vesicle-tethering factor p115 causes mini-stacked Golgi fragments with delayed protein transport. Biochem Biophys Res Commun *338*, 1268-1274.
27. Bisel, B., Wang, Y., Wei, J.H., Xiang, Y., Tang, D., Miron-Mendoza, M., Yoshimura, S., Nakamura, N., and Seemann, J. (2008). ERK regulates Golgi and centrosome orientation towards the leading edge through GRASP65. J Cell Biol *182*, 837-843.
28. Colanzi, A., Carcedo, C.H., Persico, A., Cericola, C., Turacchio, G., Bonazzi, M., Luini, A., and Corda, D. (2007). The Golgi mitotic checkpoint is controlled by BARS-dependent fission of the Golgi ribbon into separate stacks in G2. Embo J *26*, 2465-2476.
29. Duran, J.M., Kinseth, M., Bossard, C., Rose, D.W., Polishchuk, R., Wu, C.C., Yates, J., Zimmerman, T., and Malhotra, V. (2008). The Role of GRASP55 in Golgi Fragmentation and Entry of Cells into Mitosis. Mol Biol Cell *19*, 2579-2587.

30. Heuer, D., Rejman Lipinski, A., Machuy, N., Karlas, A., Wehrens, A., Siedler, F., Brinkmann, V., and Meyer, T.F. (2009). Chlamydia causes fragmentation of the Golgi compartment to ensure reproduction. Nature *457*, 731-735.
31. Zhang, T., and Hong, W. (2001). Ykt6 forms a SNARE complex with syntaxin 5, GS28, and Bet1 and participates in a late stage in endoplasmic reticulum-Golgi transport. J Biol Chem *276*, 27480-27487.
32. Losev, E., Reinke, C.A., Jellen, J., Strongin, D.E., Bevis, B.J., and Glick, B.S. (2006). Golgi maturation visualized in living yeast. Nature *441*, 1002-1006.
33. daSilva, L.L., Snapp, E.L., Denecke, J., Lippincott-Schwartz, J., Hawes, C., and Brandizzi, F. (2004). Endoplasmic reticulum export sites and Golgi bodies behave as single mobile secretory units in plant cells. Plant Cell *16*, 1753-1771.
34. Lee, M.C., Miller, E.A., Goldberg, J., Orci, L., and Schekman, R. (2004). Bi-directional protein transport between the ER and Golgi. Annu Rev Cell Dev Biol *20*, 87-123.
35. Rossanese, O.W., Soderholm, J., Bevis, B.J., Sears, I.B., O'Connor, J., Williamson, E.K., and Glick, B.S. (1999). Golgi structure correlates with transitional endoplasmic reticulum organization in Pichia pastoris and Saccharomyces cerevisiae. J Cell Biol *145*, 69-81.
36. Stephens, D.J., and Pepperkok, R. (2001). Illuminating the secretory pathway: when do we need vesicles? J Cell Sci *114*, 1053-1059.
37. Alvarez, C., Fujita, H., Hubbard, A., and Sztul, E. (1999). ER to golgi transport. Requirement for p115 at a pre-golgi vtc stage [In Process Citation]. J Cell Biol *147*, 1205-1222.
38. Allan, B.B., Moyer, B.D., and Balch, W.E. (2000). Rab1 recruitment of p115 into a cis-SNARE complex: programming budding COPII vesicles for fusion. Science *289*, 444-448.
39. Seemann, J., Jokitalo, E.J., and Warren, G. (2000). The role of the tethering proteins p115 and GM130 in transport through the Golgi apparatus in vivo. Mol Biol Cell *11*, 635-645.
40. Munro, S., and Pelham, H.R. (1987). A C-terminal signal prevents secretion of luminal ER proteins. Cell *48*, 899-907.
41. Dominguez, M., Dejgaard, K., Fullekrug, J., Dahan, S., Fazel, A., Paccaud, J.P., Thomas, D.Y., Bergeron, J.J., and Nilsson, T. (1998). gp25L/emp24/p24 protein family members of the cis-Golgi network bind both COP I and II coatomer. J Cell Biol *140*, 751-765.
42. Lodish, H.F. (2008). Molecular cell biology, 6th Edition, (New York: W.H. Freeman).
43. Barlowe, C., and Schekman, R. (1993). SEC12 encodes a guanine-nucleotide-exchange factor essential for transport vesicle budding from the ER. Nature *365*, 347-349.
44. Huang, M., Weissman, J.T., Beraud-Dufour, S., Luan, P., Wang, C., Chen, W., Aridor, M., Wilson, I.A., and Balch, W.E. (2001). Crystal structure of Sar1-GDP at 1.7 A resolution and the role of the NH2 terminus in ER export. J Cell Biol *155*, 937-948.

45. Futai, E., Hamamoto, S., Orci, L., and Schekman, R. (2004). GTP/GDP exchange by Sec12p enables COPII vesicle bud formation on synthetic liposomes. Embo J *23*, 4146-4155.
46. Hsu, V.W., and Yang, J.S. (2009). Mechanisms of COPI vesicle formation. FEBS Lett *583*, 3758-3763.
47. Franco, M., Chardin, P., Chabre, M., and Paris, S. (1996). Myristoylation-facilitated binding of the G protein ARF1GDP to membrane phospholipids is required for its activation by a soluble nucleotide exchange factor. J Biol Chem *271*, 1573-1578.
48. Serafini, T., Orci, L., Amherdt, M., Brunner, M., Kahn, R.A., and Rothman, J.E. (1991). ADP-ribosylation factor is a subunit of the coat of Golgi-derived COP-coated vesicles: a novel role for a GTP-binding protein. Cell *67*, 239-253.
49. Vasudevan, C., Han, W., Tan, Y., Nie, Y., Li, D., Shome, K., Watkins, S.C., Levitan, E.S., and Romero, G. (1998). The distribution and translocation of the G protein ADP-ribosylation factor 1 in live cells is determined by its GTPase activity. J Cell Sci *111 (Pt 9)*, 1277-1285.
50. Sciaky, N., Presley, J., Smith, C., Zaal, K.J., Cole, N., Moreira, J.E., Terasaki, M., Siggia, E., and Lippincott-Schwartz, J. (1997). Golgi tubule traffic and the effects of brefeldin A visualized in living cells. J Cell Biol *139*, 1137-1155.
51. Glick, B.S., and Nakano, A. (2009). Membrane traffic within the Golgi apparatus. Annu Rev Cell Dev Biol *25*, 113-132.
52. Patterson, G.H., Hirschberg, K., Polishchuk, R.S., Gerlich, D., Phair, R.D., and Lippincott-Schwartz, J. (2008). Transport through the Golgi apparatus by rapid partitioning within a two-phase membrane system. Cell *133*, 1055-1067.
53. Pfeffer, S.R. (2010). How the Golgi works: a cisternal progenitor model. Proc Natl Acad Sci U S A *107*, 19614-19618.
54. Becker, B., and Melkonian, M. (1996). The secretory pathway of protists: spatial and functional organization and evolution. Microbiol Rev *60*, 697-721.
55. Bonfanti, L., Mironov, A.A., Jr., Martinez-Menarguez, J.A., Martella, O., Fusella, A., Baldassarre, M., Buccione, R., Geuze, H.J., Mironov, A.A., and Luini, A. (1998). Procollagen traverses the Golgi stack without leaving the lumen of cisternae: evidence for cisternal maturation. Cell *95*, 993-1003.
56. Mollenhauer, H.H., and Morre, D.J. (1991). Perspectives on Golgi apparatus form and function. J Electron Microsc Tech *17*, 2-14.
57. Mironov, A.A., Beznoussenko, G.V., Nicoziani, P., Martella, O., Trucco, A., Kweon, H.S., Di Giandomenico, D., Polishchuk, R.S., Fusella, A., Lupetti, P., et al. (2001). Small cargo proteins and large aggregates can traverse the Golgi by a common mechanism without leaving the lumen of cisternae. J Cell Biol *155*, 1225-1238.
58. Matsuura-Tokita, K., Takeuchi, M., Ichihara, A., Mikuriya, K., and Nakano, A. (2006). Live imaging of yeast Golgi cisternal maturation. Nature *441*, 1007-1010.
59. Gilchrist, A., Au, C.E., Hiding, J., Bell, A.W., Fernandez-Rodriguez, J., Lesimple, S., Nagaya, H., Roy, L., Gosline, S.J., Hallett, M., et al. (2006). Quantitative proteomics analysis of the secretory pathway. Cell *127*, 1265-1281.

60. Love, H.D., Lin, C.C., Short, C.S., and Ostermann, J. (1998). Isolation of functional Golgi-derived vesicles with a possible role in retrograde transport. J Cell Biol *140*, 541-551.
61. Cosson, P., Amherdt, M., Rothman, J.E., and Orci, L. (2002). A resident Golgi protein is excluded from peri-Golgi vesicles in NRK cells. Proc Natl Acad Sci U S A *99*, 12831-12834.
62. Kweon, H.S., Beznoussenko, G.V., Micaroni, M., Polishchuk, R.S., Trucco, A., Martella, O., Di Giandomenico, D., Marra, P., Fusella, A., Di Pentima, A., et al. (2004). Golgi enzymes are enriched in perforated zones of golgi cisternae but are depleted in COPI vesicles. Mol Biol Cell *15*, 4710-4724.
63. Orci, L., Amherdt, M., Ravazzola, M., Perrelet, A., and Rothman, J.E. (2000). Exclusion of golgi residents from transport vesicles budding from Golgi cisternae in intact cells. J Cell Biol *150*, 1263-1270.
64. Orci, L., Stamnes, M., Ravazzola, M., Amherdt, M., Perrelet, A., Sollner, T.H., and Rothman, J.E. (1997). Bidirectional transport by distinct populations of COPI-coated vesicles. Cell *90*, 335-349.
65. Malsam, J., Satoh, A., Pelletier, L., and Warren, G. (2005). Golgin tethers define subpopulations of COPI vesicles. Science *307*, 1095-1098.
66. Marsh, B.J., Volkmann, N., McIntosh, J.R., and Howell, K.E. (2004). Direct continuities between cisternae at different levels of the Golgi complex in glucose-stimulated mouse islet beta cells. Proc Natl Acad Sci U S A *101*, 5565-5570.
67. Ortiz, D., Medkova, M., Walch-Solimena, C., and Novick, P. (2002). Ypt32 recruits the Sec4p guanine nucleotide exchange factor, Sec2p, to secretory vesicles; evidence for a Rab cascade in yeast. J Cell Biol *157*, 1005-1015.
68. Rivera-Molina, F.E., and Novick, P.J. (2009). A Rab GAP cascade defines the boundary between two Rab GTPases on the secretory pathway. Proc Natl Acad Sci U S A *106*, 14408-14413.
69. Bonifacino, J.S., and Rojas, R. (2006). Retrograde transport from endosomes to the trans-Golgi network. Nat Rev Mol Cell Biol *7*, 568-579.
70. Foresti, O., and Denecke, J. (2008). Intermediate organelles of the plant secretory pathway: identity and function. Traffic *9*, 1599-1612.
71. Wang, C.W., Hamamoto, S., Orci, L., and Schekman, R. (2006). Exomer: A coat complex for transport of select membrane proteins from the trans-Golgi network to the plasma membrane in yeast. J Cell Biol *174*, 973-983.
72. Bentley, M., Liang, Y., Mullen, K., Xu, D., Sztul, E., and Hay, J.C. (2006). SNARE status regulates tether recruitment and function in homotypic COPII vesicle fusion. J Biol Chem *281*, 38825-38833.
73. Staehelin, L.A., and Kang, B.H. (2008). Nanoscale architecture of endoplasmic reticulum export sites and of Golgi membranes as determined by electron tomography. Plant Physiol *147*, 1454-1468.
74. Bevis, B.J., Hammond, A.T., Reinke, C.A., and Glick, B.S. (2002). De novo formation of transitional ER sites and Golgi structures in Pichia pastoris. Nat Cell Biol *4*, 750-756.
75. He, C.Y. (2007). Golgi biogenesis in simple eukaryotes. Cell Microbiol *9*, 566-572.

76. Reinke, C.A., Kozik, P., and Glick, B.S. (2004). Golgi inheritance in small buds of Saccharomyces cerevisiae is linked to endoplasmic reticulum inheritance. Proc Natl Acad Sci U S A *101*, 18018-18023.
77. Wei, J.H., and Seemann, J. (2009). Mitotic division of the mammalian Golgi apparatus. Semin Cell Dev Biol *20*, 810-816.
78. Barr, F.A. (2004). Golgi inheritance: shaken but not stirred. J Cell Biol *164*, 955-958.
79. Shima, D.T., Haldar, K., Pepperkok, R., Watson, R., and Warren, G. (1997). Partitioning of the Golgi apparatus during mitosis in living HeLa cells. J Cell Biol *137*, 1211-1228.
80. Lippincott-Schwartz, J., Yuan, L.C., Bonifacino, J.S., and Klausner, R.D. (1989). Rapid redistribution of Golgi proteins into the ER in cells treated with brefeldin A: evidence for membrane cycling from Golgi to ER. Cell *56*, 801-813.
81. Storrie, B., White, J., Rottger, S., Stelzer, E.H., Suganuma, T., and Nilsson, T. (1998). Recycling of golgi-resident glycosyltransferases through the ER reveals a novel pathway and provides an explanation for nocodazole-induced Golgi scattering. J Cell Biol *143*, 1505-1521.
82. Zaal, K.J., Smith, C.L., Polishchuk, R.S., Altan, N., Cole, N.B., Ellenberg, J., Hirschberg, K., Presley, J.F., Roberts, T.H., Siggia, E., et al. (1999). Golgi membranes are absorbed into and reemerge from the ER during mitosis. Cell *99*, 589-601.
83. Jesch, S.A., and Linstedt, A.D. (1998). The Golgi and endoplasmic reticulum remain independent during mitosis in HeLa cells. Mol Biol Cell *9*, 623-635.
84. Jesch, S.A., Mehta, A.J., Velliste, M., Murphy, R.F., and Linstedt, A.D. (2001). Mitotic Golgi is in a dynamic equilibrium between clustered and free vesicles independent of the ER. Traffic *2*, 873-884.
85. Jokitalo, E., Cabrera-Poch, N., Warren, G., and Shima, D.T. (2001). Golgi clusters and vesicles mediate mitotic inheritance independently of the endoplasmic reticulum. J Cell Biol *154*, 317-330.
86. Pelletier, L., Jokitalo, E., and Warren, G. (2000). The effect of Golgi depletion on exocytic transport. Nat Cell Biol *2*, 840-846.
87. Pecot, M.Y., and Malhotra, V. (2004). Golgi membranes remain segregated from the endoplasmic reticulum during mitosis in mammalian cells. Cell *116*, 99-107.
88. Axelsson, M.A., and Warren, G. (2004). Rapid, ER-independent diffusion of the mitotic Golgi haze. Mol Biol Cell *15*, 1843-1852.
89. Xiang, Y., Seemann, J., Bisel, B., Punthambaker, S., and Wang, Y. (2007). Active ADP-ribosylation factor-1 (ARF1) is required for mitotic Golgi fragmentation. J Biol Chem *282*, 21829-21837.
90. Tang, D., Mar, K., Warren, G., and Wang, Y. (2008). Molecular mechanism of mitotic Golgi disassembly and reassembly revealed by a defined reconstitution assay. J Biol Chem *283*, 6085-6094.
91. Hidalgo Carcedo, C., Bonazzi, M., Spano, S., Turacchio, G., Colanzi, A., Luini, A., and Corda, D. (2004). Mitotic Golgi partitioning is driven by the membrane-fissioning protein CtBP3/BARS. Science *305*, 93-96.

92. Colanzi, A., Deerinck, T.J., Ellisman, M.H., and Malhotra, V. (2000). A specific activation of the mitogen-activated protein kinase kinase 1 (MEK1) is required for Golgi fragmentation during mitosis. J Cell Biol *149*, 331-339.
93. Rabouille, C., Levine, T.P., Peters, J.M., and Warren, G. (1995). An NSF-like ATPase, p97, and NSF mediate cisternal regrowth from mitotic Golgi fragments. Cell *82*, 905-914.
94. Rothman, J.E., and Warren, G. (1994). Implications of the SNARE hypothesis for intracellular membrane topology and dynamics. Curr Biol *4*, 220-233.
95. Muller, J.M., Rabouille, C., Newman, R., Shorter, J., Freemont, P., Schiavo, G., Warren, G., and Shima, D.T. (1999). An NSF function distinct from ATPase-dependent SNARE disassembly is essential for Golgi membrane fusion. Nat Cell Biolog *1*, 335-340.
96. Muller, J.M., Shorter, J., Newman, R., Deinhardt, K., Sagiv, Y., Elazar, Z., Warren, G., and Shima, D.T. (2002). Sequential SNARE disassembly and GATE-16-GOS-28 complex assembly mediated by distinct NSF activities drives Golgi membrane fusion. J Cell Biol *157*, 1161-1173.
97. Rabouille, C., Kondo, H., Newman, R., Hui, N., Freemont, P., and Warren, G. (1998). Syntaxin 5 is a common component of the NSF- and p97-mediated reassembly pathways of Golgi cisternae from mitotic Golgi fragments in vitro. Cell *92*, 603-610.
98. Meyer, H.H., Wang, Y., and Warren, G. (2002). Direct binding of ubiquitin conjugates by the mammalian p97 adaptor complexes, p47 and Ufd1-Npl4. Embo J *21*, 5645-5652.
99. Wang, Y., Satoh, A., Warren, G., and Meyer, H.H. (2004). VCIP135 acts as a deubiquitinating enzyme during p97-p47-mediated reassembly of mitotic Golgi fragments. J Cell Biol *164*, 973-978.
100. Sonnichsen, B., Lowe, M., Levine, T., Jamsa, E., Dirac-Svejstrup, B., and Warren, G. (1998). A role for giantin in docking COPI vesicles to Golgi membranes. J Cell Biol *140*, 1013-1021.
101. Rambourg, A., and Clermont, Y. (1990). Three-dimensional electron microscopy: structure of the Golgi apparatus. Eur J Cell Biol *51*, 189-200.
102. Cluett, E.B., and Brown, W.J. (1992). Adhesion of Golgi cisternae by proteinaceous interactions: intercisternal bridges as putative adhesive structures. J Cell Sci *103 (Pt 3)*, 773-784.
103. Slusarewicz, P., Nilsson, T., Hui, N., Watson, R., and Warren, G. (1994). Isolation of a matrix that binds medial Golgi enzymes. J Cell Biol *124*, 405-413.
104. Ramirez, I.B., and Lowe, M. (2009). Golgins and GRASPs: holding the Golgi together. Semin Cell Dev Biol *20*, 770-779.
105. Short, B., Haas, A., and Barr, F.A. (2005). Golgins and GTPases, giving identity and structure to the Golgi apparatus. Biochim Biophys Acta *1744*, 383-395.
106. Nakamura, N., Rabouille, C., Watson, R., Nilsson, T., Hui, N., Slusarewicz, P., Kreis, T.E., and Warren, G. (1995). Characterization of a cis-Golgi matrix protein, GM130. J Cell Biol *131*, 1715-1726.
107. Bascom, R.A., Srinivasan, S., and Nussbaum, R.L. (1999). Identification and characterization of golgin-84, a novel Golgi integral membrane protein with a cytoplasmic coiled-coil domain. J Biol Chem *274*, 2953-2962.

108. Infante, C., Ramos-Morales, F., Fedriani, C., Bornens, M., and Rios, R.M. (1999). GMAP-210, A cis-Golgi network-associated protein, is a minus end microtubule-binding protein. J Cell Biol *145*, 83-98.
109. Lu, L., and Hong, W. (2003). Interaction of Arl1-GTP with GRIP domains recruits autoantigens Golgin-97 and Golgin-245/p230 onto the Golgi. Mol Biol Cell *14*, 3767-3781.
110. Barr, F.A., Nakamura, N., and Warren, G. (1998). Mapping the interaction between GRASP65 and GM130, components of a protein complex involved in the stacking of Golgi cisternae. Embo J *17*, 3258-3268.
111. Shorter, J., Beard, M.B., Seemann, J., Dirac-Svejstrup, A.B., and Warren, G. (2002). Sequential tethering of Golgins and catalysis of SNAREpin assembly by the vesicle-tethering protein p115. J Cell Biol *157*, 45-62.
112. Kodani, A., Kristensen, I., Huang, L., and Sutterlin, C. (2009). GM130-dependent control of Cdc42 activity at the Golgi regulates centrosome organization. Mol Biol Cell *20*, 1192-1200.
113. Miller, P.M., Folkmann, A.W., Maia, A.R., Efimova, N., Efimov, A., and Kaverina, I. (2009). Golgi-derived CLASP-dependent microtubules control Golgi organization and polarized trafficking in motile cells. Nat Cell Biol *11*, 1069-1080.
114. Behnia, R., Barr, F.A., Flanagan, J.J., Barlowe, C., and Munro, S. (2007). The yeast orthologue of GRASP65 forms a complex with a coiled-coil protein that contributes to ER to Golgi traffic. J Cell Biol *176*, 255-261.
115. Kondylis, V., Spoorendonk, K.M., and Rabouille, C. (2005). dGRASP localization and function in the early exocytic pathway in Drosophila S2 cells. Mol Biol Cell *16*, 4061-4072.
116. Kinseth, M.A., Anjard, C., Fuller, D., Guizzunti, G., Loomis, W.F., and Malhotra, V. (2007). The Golgi-associated protein GRASP is required for unconventional protein secretion during development. Cell *130*, 524-534.
117. Marra, P., Maffucci, T., Daniele, T., Tullio, G.D., Ikehara, Y., Chan, E.K., Luini, A., Beznoussenko, G., Mironov, A., and De Matteis, M.A. (2001). The GM130 and GRASP65 Golgi proteins cycle through and define a subdomain of the intermediate compartment. Nat Cell Biol *3*, 1101-1113.
118. Sutterlin, C., Polishchuk, R., Pecot, M., and Malhotra, V. (2005). The Golgi-associated protein GRASP65 regulates spindle dynamics and is essential for cell division. Mol Biol Cell *16*, 3211-3222.
119. Tang, D., Yuan, H., and Wang, Y. (2010). The Role of GRASP65 in Golgi Cisternal Stacking and Cell Cycle Progression. Traffic *11*, 827-842.
120. Wang, Y., Satoh, A., and Warren, G. (2005). Mapping the functional domains of the Golgi stacking factor GRASP65. J Biol Chem *280*, 4921-4928.
121. Hung, A.Y., and Sheng, M. (2002). PDZ domains: structural modules for protein complex assembly. J Biol Chem *277*, 5699-5702.
122. Sengupta, D., Truschel, S., Bachert, C., and Linstedt, A.D. (2009). Organelle tethering by a homotypic PDZ interaction underlies formation of the Golgi membrane network. J Cell Biol *186*, 41-55.

123. Lin, C.Y., Madsen, M.L., Yarm, F.R., Jang, Y.J., Liu, X., and Erikson, R.L. (2000). Peripheral Golgi protein GRASP65 is a target of mitotic polo-like kinase (Plk) and Cdc2. Proc Natl Acad Sci U S A *97*, 12589-12594.
124. Preisinger, C., Korner, R., Wind, M., Lehmann, W.D., Kopajtich, R., and Barr, F.A. (2005). Plk1 docking to GRASP65 phosphorylated by Cdk1 suggests a mechanism for Golgi checkpoint signalling. Embo J *24*, 753-765.
125. Jesch, S.A., Lewis, T.S., Ahn, N.G., and Linstedt, A.D. (2001). Mitotic phosphorylation of Golgi reassembly stacking protein 55 by mitogen-activated protein kinase ERK2. Mol Biol Cell *12*, 1811-1817.
126. Short, B., Preisinger, C., Korner, R., Kopajtich, R., Byron, O., and Barr, F.A. (2001). A GRASP55-rab2 effector complex linking Golgi structure to membrane traffic. J Cell Biol *155*, 877-883.
127. Manjithaya, R., Anjard, C., Loomis, W.F., and Subramani, S. (2010). Unconventional secretion of Pichia pastoris Acb1 is dependent on GRASP protein, peroxisomal functions, and autophagosome formation. J Cell Biol *188*, 537-546.
128. Barr, F.A., Preisinger, C., Kopajtich, R., and Korner, R. (2001). Golgi matrix proteins interact with p24 cargo receptors and aid their efficient retention in the Golgi apparatus. J Cell Biol *155*, 885-891.
129. D'Angelo, G., Prencipe, L., Iodice, L., Beznoussenko, G., Savarese, M., Marra, P., Di Tullio, G., Martire, G., De Matteis, M.A., and Bonatti, S. (2009). GRASP65 and GRASP55 sequentially promote the transport of C-terminal valine bearing cargoes to and through the golgi complex. J Biol Chem *284*, 34849-34860.
130. Kuo, A., Zhong, C., Lane, W.S., and Derynck, R. (2000). Transmembrane transforming growth factor-alpha tethers to the PDZ domain-containing, Golgi membrane-associated protein p59/GRASP55. Embo J *19*, 6427-6439.
131. Lane, J.D., Lucocq, J., Pryde, J., Barr, F.A., Woodman, P.G., Allan, V.J., and Lowe, M. (2002). Caspase-mediated cleavage of the stacking protein GRASP65 is required for Golgi fragmentation during apoptosis. J Cell Biol *156*, 495-509.
132. Schotman, H., Karhinen, L., and Rabouille, C. (2008). dGRASP-mediated noncanonical integrin secretion is required for Drosophila epithelial remodeling. Dev Cell *14*, 171-182.
133. Barr, F.A., Preisinger, C., Kopajtich, R., and Korner, R. (2001). Golgi matrix proteins interact with p24 cargo receptors and aid their efficient retention in the Golgi apparatus. J Cell Biol *155*, 885-891.
134. Hicks, S.W., and Machamer, C.E. (2005). Golgi structure in stress sensing and apoptosis. Biochim Biophys Acta *1744*, 406-414.
135. Moyer, B.D., Allan, B.B., and Balch, W.E. (2001). Rab1 Interaction with a GM130 Effector Complex Regulates COPII Vesicle cis-Golgi Tethering. Traffic *2*, 268-276.
136. Alvarez, C., Garcia-Mata, R., Hauri, H.P., and Sztul, E. (2001). The p115-interactive Proteins GM130 and Giantin Participate in Endoplasmic Reticulum-Golgi Traffic. J Biol Chem *276*, 2693-2700.
137. Rivero, S., Cardenas, J., Bornens, M., and Rios, R.M. (2009). Microtubule nucleation at the cis-side of the Golgi apparatus requires AKAP450 and GM130. EMBO J *28*, 1016-1028.

138. Walker, A., Ward, C., Sheldrake, T.A., Dransfield, I., Rossi, A.G., Pryde, J.G., and Haslett, C. (2004). Golgi fragmentation during Fas-mediated apoptosis is associated with the rapid loss of GM130. Biochem Biophys Res Commun *316*, 6-11.
139. Preisinger, C., Short, B., De Corte, V., Bruyneel, E., Haas, A., Kopajtich, R., Gettemans, J., and Barr, F.A. (2004). YSK1 is activated by the Golgi matrix protein GM130 and plays a role in cell migration through its substrate 14-3-3{zeta}. J Cell Biol *164*, 1009-1020.
140. Shorter, J., and Warren, G. (1999). A role for the vesicle tethering protein, p115, in the post-mitotic stacking of reassembling golgi cisternae in a cell-free system. J Cell Biol *146*, 57-70.
141. Nakamura, N., Lowe, M., Levine, T.P., Rabouille, C., and Warren, G. (1997). The vesicle docking protein p115 binds GM130, a cis-Golgi matrix protein, in a mitotically regulated manner. Cell *89*, 445-455.
142. Sapperstein, S.K., Walter, D.M., Grosvenor, A.R., Heuser, J.E., and Waters, M.G. (1995). p115 is a general vesicular transport factor related to the yeast endoplasmic reticulum to Golgi transport factor Uso1p. Proc Natl Acad Sci U S A *92*, 522-526.
143. Chiu, R., Novikov, L., Mukherjee, S., and Shields, D. (2002). A caspase cleavage fragment of p115 induces fragmentation of the Golgi apparatus and apoptosis. J Cell Biol *159*, 637-648.
144. Mukherjee, S., and Shields, D. (2009). Nuclear import is required for the pro-apoptotic function of the Golgi protein p115. J Biol Chem *284*, 1709-1717.
145. Jakymiw, A., Raharjo, E., Rattner, J.B., Eystathioy, T., Chan, E.K., and Fujita, D.J. (2000). Identification and characterization of a novel Golgi protein, golgin-67. J Biol Chem *275*, 4137-4144.
146. Eystathioy, T., Jakymiw, A., Fujita, D.J., Fritzler, M.J., and Chan, E.K. (2000). Human autoantibodies to a novel Golgi protein golgin-67: high similarity with golgin-95/gm 130 autoantigen. J Autoimmun *14*, 179-187.
147. Sohda, M., Misumi, Y., Yamamoto, A., Nakamura, N., Ogata, S., Sakisaka, S., Hirose, S., Ikehara, Y., and Oda, K. (2010). Interaction of Golgin-84 with the COG complex mediates the intra-Golgi retrograde transport. Traffic *11*, 1552-1566.
148. Rejman Lipinski, A., Heymann, J., Meissner, C., Karlas, A., Brinkmann, V., Meyer, T.F., and Heuer, D. (2009). Rab6 and Rab11 regulate Chlamydia trachomatis development and golgin-84-dependent Golgi fragmentation. PLoS Pathog *5*, e1000615.
149. Lock, J.G., Hammond, L.A., Houghton, F., Gleeson, P.A., and Stow, J.L. (2005). E-cadherin transport from the trans-Golgi network in tubulovesicular carriers is selectively regulated by golgin-97. Traffic *6*, 1142-1156.
150. Lu, L., Tai, G., and Hong, W. (2004). Autoantigen Golgin-97, an effector of Arl1 GTPase, participates in traffic from the endosome to the trans-golgi network. Mol Biol Cell *15*, 4426-4443.
151. Tai, G., Lu, L., Johannes, L., and Hong, W. (2005). Functional analysis of Arl1 and golgin-97 in endosome-to-TGN transport using recombinant Shiga toxin B fragment. Methods Enzymol *404*, 442-453.

152. Jing, J., Junutula, J.R., Wu, C., Burden, J., Matern, H., Peden, A.A., and Prekeris, R. (2010). FIP1/RCP binding to Golgin-97 regulates retrograde transport from recycling endosomes to the trans-Golgi network. Mol Biol Cell *21*, 3041-3053.
153. Alzhanova, D., and Hruby, D.E. (2007). A host cell membrane protein, golgin-97, is essential for poxvirus morphogenesis. Virology *362*, 421-427.
154. Bundis, F., Neagoe, I., Schwappach, B., and Steinmeyer, K. (2006). Involvement of Golgin-160 in cell surface transport of renal ROMK channel: co-expression of Golgin-160 increases ROMK currents. Cell Physiol Biochem *17*, 1-12.
155. Mancini, M., Machamer, C.E., Roy, S., Nicholson, D.W., Thornberry, N.A., Casciola-Rosen, L.A., and Rosen, A. (2000). Caspase-2 is localized at the Golgi complex and cleaves golgin-160 during apoptosis. J Cell Biol *149*, 603-612.
156. Maag, R.S., Mancini, M., Rosen, A., and Machamer, C.E. (2005). Caspase-resistant Golgin-160 disrupts apoptosis induced by secretory pathway stress and ligation of death receptors. Mol Biol Cell *16*, 3019-3027.
157. Sbodio, J.I., Hicks, S.W., Simon, D., and Machamer, C.E. (2006). GCP60 preferentially interacts with a caspase-generated golgin-160 fragment. J Biol Chem *281*, 27924-27931.
158. Allinson, T.M., Parkin, E.T., Turner, A.J., and Hooper, N.M. (2003). ADAMs family members as amyloid precursor protein alpha-secretases. J Neurosci Res *74*, 342-352.
159. Linstedt, A.D., Jesch, S.A., Mehta, A., Lee, T.H., Garcia-Mata, R., Nelson, D.S., and Sztul, E. (2000). Binding relationships of membrane tethering components. The giantin N terminus and the GM130 N terminus compete for binding to the p115 C terminus. J Biol Chem *275*, 10196-10201.
160. Lowe, M., Lane, J.D., Woodman, P.G., and Allan, V.J. (2004). Caspase-mediated cleavage of syntaxin 5 and giantin accompanies inhibition of secretory traffic during apoptosis. J Cell Sci *117*, 1139-1150.
161. Misumi, Y., Sohda, M., Tashiro, A., Sato, H., and Ikehara, Y. (2001). An essential cytoplasmic domain for the Golgi localization of coiled- coil proteins with a COOH-terminal membrane anchor. J Biol Chem *276*, 6867-6873.
162. Derby, M.C., and Gleeson, P.A. (2007). New insights into membrane trafficking and protein sorting. Int Rev Cytol *261*, 47-116.
163. Hoogenraad, C.C., Akhmanova, A., Howell, S.A., Dortland, B.R., De Zeeuw, C.I., Willemsen, R., Visser, P., Grosveld, F., and Galjart, N. (2001). Mammalian Golgi-associated Bicaudal-D2 functions in the dynein-dynactin pathway by interacting with these complexes. EMBO J *20*, 4041-4054.
164. Matanis, T., Akhmanova, A., Wulf, P., Del Nery, E., Weide, T., Stepanova, T., Galjart, N., Grosveld, F., Goud, B., De Zeeuw, C.I., et al. (2002). Bicaudal-D regulates COPI-independent Golgi-ER transport by recruiting the dynein-dynactin motor complex. Nat Cell Biol *4*, 986-992.
165. Luke, M.R., Kjer-Nielsen, L., Brown, D.L., Stow, J.L., and Gleeson, P.A. (2003). GRIP domain-mediated targeting of two new coiled-coil proteins, GCC88 and GCC185, to subcompartments of the trans-Golgi network. J Biol Chem *278*, 4216-4226.

166. Hayes, G.L., Brown, F.C., Haas, A.K., Nottingham, R.M., Barr, F.A., and Pfeffer, S.R. (2009). Multiple Rab GTPase binding sites in GCC185 suggest a model for vesicle tethering at the trans-Golgi. Mol Biol Cell *20*, 209-217.
167. Derby, M.C., Lieu, Z.Z., Brown, D., Stow, J.L., Goud, B., and Gleeson, P.A. (2007). The trans-Golgi network golgin, GCC185, is required for endosome-to-Golgi transport and maintenance of Golgi structure. Traffic *8*, 758-773.
168. Reddy, J.V., Burguete, A.S., Sridevi, K., Ganley, I.G., Nottingham, R.M., and Pfeffer, S.R. (2006). A functional role for the GCC185 golgin in mannose 6-phosphate receptor recycling. Mol Biol Cell *17*, 4353-4363.
169. Efimov, A., Kharitonov, A., Efimova, N., Loncarek, J., Miller, P.M., Andreyeva, N., Gleeson, P., Galjart, N., Maia, A.R., McLeod, I.X., et al. (2007). Asymmetric CLASP-dependent nucleation of noncentrosomal microtubules at the trans-Golgi network. Dev Cell *12*, 917-930.
170. Ohta, E., Misumi, Y., Sohda, M., Fujiwara, T., Yano, A., and Ikehara, Y. (2003). Identification and characterization of GCP16, a novel acylated Golgi protein that interacts with GCP170. J Biol Chem *278*, 51957-51967.
171. Sohda, M., Misumi, Y., Yamamoto, A., Yano, A., Nakamura, N., and Ikehara, Y. (2001). Identification and characterization of a novel Golgi protein, GCP60, that interacts with the integral membrane protein giantin. J Biol Chem *276*, 45298-45306.
172. Zhou, Y., Atkins, J.B., Rompani, S.B., Bancescu, D.L., Petersen, P.H., Tang, H., Zou, K., Stewart, S.B., and Zhong, W. (2007). The mammalian Golgi regulates numb signaling in asymmetric cell division by releasing ACBD3 during mitosis. Cell *129*, 163-178.
173. Toki, C., Fujiwara, T., Sohda, M., Hong, H.S., Misumi, Y., and Ikehara, Y. (1997). Identification and characterization of rat 364-kDa Golgi-associated protein recognized by autoantibodies from a patient with rheumatoid arthritis. Cell Struct Funct *22*, 565-577.
174. Takahashi, M., Shibata, H., Shimakawa, M., Miyamoto, M., Mukai, H., and Ono, Y. (1999). Characterization of a novel giant scaffolding protein, CG-NAP, that anchors multiple signaling enzymes to centrosome and the golgi apparatus. J Biol Chem *274*, 17267-17274.
175. Drin, G., Morello, V., Casella, J.F., Gounon, P., and Antonny, B. (2008). Asymmetric tethering of flat and curved lipid membranes by a golgin. Science *320*, 670-673.
176. Gillingham, A.K., Tong, A.H., Boone, C., and Munro, S. (2004). The GTPase Arf1p and the ER to Golgi cargo receptor Erv14p cooperate to recruit the golgin Rud3p to the cis-Golgi. J Cell Biol *167*, 281-292.
177. Rios, R.M., Sanchis, A., Tassin, A.M., Fedriani, C., and Bornens, M. (2004). GMAP-210 recruits gamma-tubulin complexes to cis-Golgi membranes and is required for Golgi ribbon formation. Cell *118*, 323-335.
178. Follit, J.A., San Agustin, J.T., Xu, F., Jonassen, J.A., Samtani, R., Lo, C.W., and Pazour, G.J. (2008). The Golgin GMAP210/TRIP11 anchors IFT20 to the Golgi complex. PLoS Genet *4*, e1000315.

179. Chen, Y., Chen, P.L., Chen, C.F., Sharp, Z.D., and Lee, W.H. (1999). Thyroid hormone, T3-dependent phosphorylation and translocation of Trip230 from the Golgi complex to the nucleus. Proc Natl Acad Sci U S A *96*, 4443-4448.
180. Cruz-Garcia, D., Vazquez-Martinez, R., Peinado, J.R., Anouar, Y., Tonon, M.C., Vaudry, H., Castano, J.P., and Malagon, M.M. (2007). Identification and characterization of two novel (neuro)endocrine long coiled-coil proteins. FEBS Lett *581*, 3149-3156.
181. Van Valkenburgh, H., Shern, J.F., Sharer, J.D., Zhu, X., and Kahn, R.A. (2001). ADP-ribosylation factors (ARFs) and ARF-like 1 (ARL1) have both specific and shared effectors: characterizing ARL1-binding proteins. J Biol Chem *276*, 22826-22837.
182. Hennies, H.C., Kornak, U., Zhang, H., Egerer, J., Zhang, X., Seifert, W., Kuhnisch, J., Budde, B., Natebus, M., Brancati, F., et al. (2008). Gerodermia osteodysplastica is caused by mutations in SCYL1BP1, a Rab-6 interacting golgin. Nat Genet *40*, 1410-1412.
183. Al-Dosari, M., and Alkuraya, F.S. (2009). A novel missense mutation in SCYL1BP1 produces geroderma osteodysplastica phenotype indistinguishable from that caused by nullimorphic mutations. Am J Med Genet A *149A*, 2093-2098.
184. Yamane, J., Kubo, A., Nakayama, K., Yuba-Kubo, A., Katsuno, T., and Tsukita, S. (2007). Functional involvement of TMF/ARA160 in Rab6-dependent retrograde membrane traffic. Exp Cell Res *313*, 3472-3485.
185. Helenius, A., and Aebi, M. (2001). Intracellular functions of N-linked glycans. Science *291*, 2364-2369.
186. Ohtsubo, K., and Marth, J.D. (2006). Glycosylation in cellular mechanisms of health and disease. Cell *126*, 855-867.
187. Varki, A. (1998). Factors controlling the glycosylation potential of the Golgi apparatus. Trends Cell Biol *8*, 34-40.
188. Rudd, P.M., Elliott, T., Cresswell, P., Wilson, I.A., and Dwek, R.A. (2001). Glycosylation and the immune system. Science *291*, 2370-2376.
189. Lopez-Sanchez, I., Sanz-Garcia, M., and Lazo, P.A. (2009). Plk3 interacts with and specifically phosphorylates VRK1 in Ser342, a downstream target in a pathway that induces Golgi fragmentation. Mol Cell Biol *29*, 1189-1201.
190. Kano, F., Takenaka, K., Yamamoto, A., Nagayama, K., Nishida, E., and Murata, M. (2000). MEK and Cdc2 kinase are sequentially required for Golgi disassembly in MDCK cells by the mitotic Xenopus extracts. J Cell Biol *149*, 357-368.
191. Sutterlin, C., Hsu, P., Mallabiabarrena, A., and Malhotra, V. (2002). Fragmentation and dispersal of the pericentriolar Golgi complex is required for entry into mitosis in mammalian cells. Cell *109*, 359-369.
192. Chang, P., Coughlin, M., and Mitchison, T.J. (2005). Tankyrase-1 polymerization of poly(ADP-ribose) is required for spindle structure and function. Nat Cell Biol *7*, 1133-1139.
193. Lin, X., Liu, C.C., Gao, Q., Zhang, X., Wu, G., and Lee, W.H. (2007). RINT-1 serves as a tumor suppressor and maintains Golgi dynamics and centrosome integrity for cell survival. Mol Cell Biol *27*, 4905-4916.

194. Liu, Y., Boukhelifa, M., Tribble, E., Morin-Kensicki, E., Uetrecht, A., Bear, J.E., and Bankaitis, V.A. (2008). The Sac1 phosphoinositide phosphatase regulates Golgi membrane morphology and mitotic spindle organization in mammals. Mol Biol Cell *19*, 3080-3096.
195. Royle, S.J., Bright, N.A., and Lagnado, L. (2005). Clathrin is required for the function of the mitotic spindle. Nature *434*, 1152-1157.
196. Miserey-Lenkei, S., Couedel-Courteille, A., Del Nery, E., Bardin, S., Piel, M., Racine, V., Sibarita, J.B., Perez, F., Bornens, M., and Goud, B. (2006). A role for the Rab6A' GTPase in the inactivation of the Mad2-spindle checkpoint. Embo J *25*, 278-289.
197. Lane, J.D., Vergnolle, M.A., Woodman, P.G., and Allan, V.J. (2001). Apoptotic cleavage of cytoplasmic dynein intermediate chain and p150(Glued) stops dynein-dependent membrane motility. J Cell Biol *153*, 1415-1426.
198. Hicks, S.W., and Machamer, C.E. (2002). The NH2-terminal Domain of Golgin-160 Contains Both Golgi and Nuclear Targeting Information. J Biol Chem *277*, 35833-35839.
199. Linstedt, A.D. (2004). Positioning the Golgi apparatus. Cell *118*, 271-272.
200. Matsuki, T., Matthews, R.T., Cooper, J.A., van der Brug, M.P., Cookson, M.R., Hardy, J.A., Olson, E.C., and Howell, B.W. (2010). Reelin and stk25 have opposing roles in neuronal polarization and dendritic Golgi deployment. Cell *143*, 826-836.
201. Kornfeld, R., and Kornfeld, S. (1985). Assembly of asparagine-linked oligosaccharides. Ann. Rev. Biochem. *54*, 631-664.
202. Wang, Y. (2008). Golgi apparatus inheritance. In *The Golgi apparatus. State of the art 110 years after Camillo Golgi's discovery*, Volume Chapter 4.3, A. Mironov, M. Pavelka and A. Luini, eds. (Wien-New York: Springer-Verlag Gmbh.), pp. 580-607.
203. Pfeffer, S.R. (2001). Constructing a Golgi complex. J Cell Biol *155*, 873-875.
204. Heusser, K., Yuan, H., Neagoe, I., Tarasov, A.I., Ashcroft, F.M., and Schwappach, B. (2006). Scavenging of 14-3-3 proteins reveals their involvement in the cell-surface transport of ATP-sensitive K+ channels. J Cell Sci *119*, 4353-4363.
205. Cha, H., and Shapiro, P. (2001). Tyrosine-phosphorylated extracellular signal--regulated kinase associates with the Golgi complex during G2/M phase of the cell cycle: evidence for regulation of Golgi structure. J Cell Biol *153*, 1355-1367.
206. Yoshimura, S., Yoshioka, K., Barr, F.A., Lowe, M., Nakayama, K., Ohkuma, S., and Nakamura, N. (2005). Convergence of cell cycle regulation and growth factor signals on GRASP65. J Biol Chem *280*, 23048-23056.
207. Mitrovic, S., Ben-Tekaya, H., Koegler, E., Gruenberg, J., and Hauri, H.P. (2008). The cargo receptors Surf4, endoplasmic reticulum-Golgi intermediate compartment (ERGIC)-53, and p25 are required to maintain the architecture of ERGIC and Golgi. Mol Biol Cell *19*, 1976-1990.
208. Wang, Y., Wei, J.H., Bisel, B., Tang, D., and Seemann, J. (2008). Golgi Cisternal Unstacking Stimulates COPI Vesicle Budding and Protein Transport. PLoS ONE *3*, e1647.

209. Struck, N.S., Herrmann, S., Langer, C., Krueger, A., Foth, B.J., Engelberg, K., Cabrera, A.L., Haase, S., Treeck, M., Marti, M., et al. (2008). Plasmodium falciparum possesses two GRASP proteins that are differentially targeted to the Golgi complex via a higher- and lower-eukaryote-like mechanism. J Cell Sci *121*, 2123-2129.
210. Matheson, L.A., Hanton, S.L., Rossi, M., Latijnhouwers, M., Stefano, G., Renna, L., and Brandizzi, F. (2007). Multiple Roles of ARF1 in Plant Cells Include Spatially-Regulated Recruitment of Coatomer and Elements of the Golgi Matrix. Plant Physiol.
211. Latijnhouwers, M., Hawes, C., and Carvalho, C. (2005). Holding it all together? Candidate proteins for the plant Golgi matrix. Curr Opin Plant Biol *8*, 632-639.
212. Rambourg, A., Clermont, Y., and Kepes, F. (1993). Modulation of the Golgi apparatus in Saccharomyces cerevisiae sec7 mutants as seen by three-dimensional electron microscopy. Anat Rec *237*, 441-452.
213. Wang, Y., Taguchi, T., and Warren, G. (2006). Purification of Rat Liver Golgi Stacks. In Cell Biology: A Laboratory Handbook, 3rd Edition, J. Celis, ed. (San Diego: Elsevier Science (USA)), pp. 33-39.
214. Rabouille, C., Misteli, T., Watson, R., and Warren, G. (1995). Reassembly of Golgi stacks from mitotic Golgi fragments in a cell-free system. J Cell Biol *129*, 605-618.
215. Wittig, I., Braun, H.P., and Schagger, H. (2006). Blue native PAGE. Nat Protoc *1*, 418-428.
216. Lupashin, V., and Sztul, E. (2005). Golgi tethering factors. Biochim Biophys Acta *1744*, 325-339.
217. Gieselmann, V., Hasilik, A., and von Figura, K. (1985). Processing of human cathepsin D in lysosomes in vitro. J Biol Chem *260*, 3215-3220.
218. Zaidi, N., Maurer, A., Nieke, S., and Kalbacher, H. (2008). Cathepsin D: a cellular roadmap. Biochem Biophys Res Commun *376*, 5-9.
219. von Blume, J., Duran, J.M., Forlanelli, E., Alleaume, A.M., Egorov, M., Polishchuk, R., Molina, H., and Malhotra, V. (2009). Actin remodeling by ADF/cofilin is required for cargo sorting at the trans-Golgi network. J Cell Biol *187*, 1055-1069.
220. Wearne, K.A., Winter, H.C., and Goldstein, I.J. (2008). Temporal changes in the carbohydrates expressed on BG01 human embryonic stem cells during differentiation as embryoid bodies. Glycoconj J *25*, 121-136.
221. Liang, C.C., Park, A.Y., and Guan, J.L. (2007). In vitro scratch assay: a convenient and inexpensive method for analysis of cell migration in vitro. Nat Protoc *2*, 329-333.
222. Martin, S.J., Reutelingsperger, C.P., McGahon, A.J., Rader, J.A., van Schie, R.C., LaFace, D.M., and Green, D.R. (1995). Early redistribution of plasma membrane phosphatidylserine is a general feature of apoptosis regardless of the initiating stimulus: inhibition by overexpression of Bcl-2 and Abl. J Exp Med *182*, 1545-1556.
223. Verhoven, B., Schlegel, R.A., and Williamson, P. (1995). Mechanisms of phosphatidylserine exposure, a phagocyte recognition signal, on apoptotic T lymphocytes. J Exp Med *182*, 1597-1601.

224. Nicholson, D.W., and Thornberry, N.A. (1997). Caspases: killer proteases. Trends Biochem Sci *22*, 299-306.
225. Munro, S., and Pelham, H.R. (1986). An Hsp70-like protein in the ER: identity with the 78 kd glucose-regulated protein and immunoglobulin heavy chain binding protein. Cell *46*, 291-300.
226. Gu, J., and Taniguchi, N. (2004). Regulation of integrin functions by N-glycans. Glycoconj J *21*, 9-15.
227. Isaji, T., Sato, Y., Zhao, Y., Miyoshi, E., Wada, Y., Taniguchi, N., and Gu, J. (2006). N-glycosylation of the beta-propeller domain of the integrin alpha5 subunit is essential for alpha5beta1 heterodimerization, expression on the cell surface, and its biological function. J Biol Chem *281*, 33258-33267.
228. Guo, H.B., Lee, I., Kamar, M., Akiyama, S.K., and Pierce, M. (2002). Aberrant N-glycosylation of beta1 integrin causes reduced alpha5beta1 integrin clustering and stimulates cell migration. Cancer Res *62*, 6837-6845.
229. Zheng, M., Fang, H., and Hakomori, S. (1994). Functional role of N-glycosylation in alpha 5 beta 1 integrin receptor. De-N-glycosylation induces dissociation or altered association of alpha 5 and beta 1 subunits and concomitant loss of fibronectin binding activity. J Biol Chem *269*, 12325-12331.
230. Mowbrey, K., and Dacks, J.B. (2009). Evolution and diversity of the Golgi body. FEBS Lett *583*, 3738-3745.
231. Roth, J. (2002). Protein N-glycosylation along the secretory pathway: relationship to organelle topography and function, protein quality control, and cell interactions. Chem Rev *102*, 285-303.
232. Elbein, A.D. (1991). Glycosidase inhibitors: inhibitors of N-linked oligosaccharide processing. Faseb J *5*, 3055-3063.
233. Kellokumpu, S., Sormunen, R., and Kellokumpu, I. (2002). Abnormal glycosylation and altered Golgi structure in colorectal cancer: dependence on intra-Golgi pH. FEBS Lett *516*, 217-224.
234. Preuss, D., Mulholland, J., Franzusoff, A., Segev, N., and Botstein, D. (1992). Characterization of the Saccharomyces Golgi complex through the cell cycle by immunoelectron microscopy. Mol. Biol. Cell *3*, 789-803.
235. Capony, F., Rougeot, C., Montcourrier, P., Cavailles, V., Salazar, G., and Rochefort, H. (1989). Increased secretion, altered processing, and glycosylation of pro-cathepsin D in human mammary cancer cells. Cancer Res *49*, 3904-3909.
236. Henry, L., and Sheff, D.R. (2008). Rab8 regulates basolateral secretory, but not recycling, traffic at the recycling endosome. Mol Biol Cell *19*, 2059-2068.
237. Misumi, Y., Misumi, Y., Miki, K., Takatsuki, A., Tamura, G., and Ikehara, Y. (1986). Novel blockade by brefeldin A of intracellular transport of secretory proteins in cultured rat hepatocytes. J Biol Chem *261*, 11398-11403.
238. Ho, W.C., Allan, V.J., van Meer, G., Berger, E.G., and Kreis, T.E. (1989). Reclustering of scattered Golgi elements occurs along microtubules. Eur J Cell Biol *48*, 250-263.
239. Takizawa, P.A., Yucel, J.K., Veit, B., Faulkner, D.J., Deerinck, T., Soto, G., Ellisman, M., and Malhotra, V. (1993). Complete vesiculation of Golgi membranes and inhibition of protein transport by a novel sea sponge metabolite, ilimaquinone. Cell *73*, 1079-1090.

240. Ludford, R.J. (1924). The Distribution of the Cytoplasmic Organs in Transplantable Tumour Cells, with Special Reference to Dictyokinesis. Proc. Royal Soc. London *97*, 50-60.
241. Maul, G.G., and Brinkley, B.R. (1970). The Golgi apparatus during mitosis in human melanoma cells in vitro. Cancer Res *30*, 2326-2335.
242. Lucocq, J.M., Berger, E.G., and Warren, G. (1989). Mitotic Golgi fragments in HeLa cells and their role in the reassembly pathway. J Cell Biol *109*, 463-474.
243. Altan-Bonnet, N., Sougrat, R., Liu, W., Snapp, E.L., Ward, T., and Lippincott-Schwartz, J. (2006). Golgi Inheritance in Mammalian Cells Is Mediated through Endoplasmic Reticulum Export Activities. Mol Biol Cell *17*, 990-1005.
244. Colanzi, A., Suetterlin, C., and Malhotra, V. (2003). Cell-cycle-specific Golgi fragmentation: how and why? Curr Opin Cell Biol *15*, 462-467.
245. Altan-Bonnet, N., Phair, R.D., Polishchuk, R.S., Weigert, R., and Lippincott-Schwartz, J. (2003). A role for Arf1 in mitotic Golgi disassembly, chromosome segregation, and cytokinesis. Proc Natl Acad Sci U S A *100*, 13314-13319.
246. Litvak, V., Argov, R., Dahan, N., Ramachandran, S., Amarilio, R., Shainskaya, A., and Lev, S. (2004). Mitotic phosphorylation of the peripheral Golgi protein Nir2 by Cdk1 provides a docking mechanism for Plk1 and affects cytokinesis completion. Mol Cell *14*, 319-330.
247. Gromley, A., Yeaman, C., Rosa, J., Redick, S., Chen, C.T., Mirabelle, S., Guha, M., Sillibourne, J., and Doxsey, S.J. (2005). Centriolin anchoring of exocyst and SNARE complexes at the midbody is required for secretory-vesicle-mediated abscission. Cell *123*, 75-87.
248. Altan-Bonnet, N., Sougrat, R., and Lippincott-Schwartz, J.p. (2004). Molecular basis for Golgi maintenance and biogenesis. Curr Opin Cell Biol *16*, 364-372.
249. Misteli, T., and Warren, G. (1994). COP-coated vesicles are involved in the mitotic fragmentation of Golgi stacks in a cell-free system. J Cell Biol *125*, 269-282.
250. Nickel, W., Malsam, J., Gorgas, K., Ravazzola, M., Jenne, N., Helms, J.B., and Wieland, F.T. (1998). Uptake by COPI-coated vesicles of both anterograde and retrograde cargo is inhibited by GTPgammaS in vitro. J Cell Sci *111 (Pt 20)*, 3081-3090.
251. Serafini, T., and Rothman, J.E. (1992). Purification of Golgi cisternae-derived non-clathrin-coated vesicles. Methods Enzymol *219*, 286-299.
252. Dascher, C., and Balch, W.E. (1994). Dominant inhibitory mutants of ARF1 block endoplasmic reticulum to Golgi transport and trigger disassembly of the Golgi apparatus. J Biol Chem *269*, 1437-1448.
253. Randazzo, P.A., Weiss, O., and Kahn, R.A. (1995). Preparation of recombinant ADP-ribosylation factor. Methods Enzymol *257*, 128-135.
254. Lowe, M., Rabouille, C., Nakamura, N., Watson, R., Jackman, M., Jamsa, E., Rahman, D., Pappin, D.J., and Warren, G. (1998). Cdc2 kinase directly phosphorylates the cis-Golgi matrix protein GM130 and is required for Golgi fragmentation in mitosis. Cell *94*, 783-793.
255. D'Souza-Schorey, C., and Chavrier, P. (2006). ARF proteins: roles in membrane traffic and beyond. Nat Rev Mol Cell Biol *7*, 347-358.

256. Donaldson, J.G., Finazzi, D., and Klausner, R.D. (1992). Brefeldin A inhibits Golgi membrane-catalysed exchange of guanine nucleotide onto ARF protein. Nature *360*, 350-352.
257. Nickel, W., and Wieland, F.T. (1997). Biogenesis of COPI-coated transport vesicles. FEBS Lett *413*, 395-400.
258. Sheff, D., Lowe, M., Kreis, T.E., and Mellman, I. (1996). Biochemical heterogeneity and phosphorylation of coatomer subunits. J Biol Chem *271*, 7230-7236.
259. Futatsumori, M., Kasai, K., Takatsu, H., Shin, H.W., and Nakayama, K. (2000). Identification and characterization of novel isoforms of COP I subunits. J Biochem (Tokyo) *128*, 793-801.
260. Happe, S., and Weidman, P. (1998). Cell-free transport to distinct Golgi cisternae is compartment specific and ARF independent. J Cell Biol *140*, 511-523.
261. Keryer, G., Yassenko, M., Labbe, J.C., Castro, A., Lohmann, S.M., Evain-Brion, D., and Tasken, K. (1998). Mitosis-specific phosphorylation and subcellular redistribution of the RIIalpha regulatory subunit of cAMP-dependent protein kinase. J Biol Chem *273*, 34594-34602.
262. Sutterlin, C., Lin, C.Y., Feng, Y., Ferris, D.K., Erikson, R.L., and Malhotra, V. (2001). Polo-like kinase is required for the fragmentation of pericentriolar Golgi stacks during mitosis. Proc Natl Acad Sci U S A *98*, 9128-9132.
263. Randazzo, P.A., and Kahn, R.A. (1994). GTP hydrolysis by ADP-ribosylation factor is dependent on both an ADP-ribosylation factor GTPase-activating protein and acid phospholipids. J Biol Chem *269*, 10758-10763.
264. Antonny, B., Bigay, J., Casella, J.F., Drin, G., Mesmin, B., and Gounon, P. (2005). Membrane curvature and the control of GTP hydrolysis in Arf1 during COPI vesicle formation. Biochem Soc Trans *33*, 619-622.
265. Taguchi, T., Pypaert, M., and Warren, G. (2003). Biochemical sub-fractionation of the mammalian Golgi apparatus. Traffic *4*, 344-352.
266. Kuai, J., Boman, A.L., Arnold, R.S., Zhu, X., and Kahn, R.A. (2000). Effects of activated ADP-ribosylation factors on Golgi morphology require neither activation of phospholipase D1 nor recruitment of coatomer. J Biol Chem *275*, 4022-4032.
267. Pavel, J., Harter, C., and Wieland, F.T. (1998). Reversible dissociation of coatomer: functional characterization of a beta/delta-coat protein subcomplex. Proc Natl Acad Sci U S A *95*, 2140-2145.
268. Knehr, M., Poppe, M., Enulescu, M., Eickelbaum, W., Stoehr, M., Schroeter, D., and Paweletz, N. (1995). A critical appraisal of synchronization methods applied to achieve maximal enrichment of HeLa cells in specific cell cycle phases. Exp Cell Res *217*, 546-553.
269. Check, E. (2002). Cell biology: will the real Golgi please stand up. Nature *416*, 780-781.
270. Tang, D., Xiang, Y., and Wang, Y. (2010). Reconstitution of the cell cycle regulated Golgi disassembly and reassembly in a cell free system. Nature Protocols *5*, 758-772.

271. Acharya, U., Jacobs, R., Peters, J.M., Watson, N., Farquhar, M.G., and Malhotra, V. (1995). The formation of Golgi stacks from vesiculated Golgi membranes requires two distinct fusion events. Cell *82*, 895-904.
272. Kondo, H., Rabouille, C., Newman, R., Levine, T.P., Pappin, D., Freemont, P., and Warren, G. (1997). p47 is a cofactor for p97-mediated membrane fusion. Nature *388*, 75-78.
273. Meyer, H.H., Kondo, H., and Warren, G. (1998). The p47 co-factor regulates the ATPase activity of the membrane fusion protein, p97. FEBS Lett *437*, 255-257.
274. Meyer, H.H., Shorter, J.G., Seemann, J., Pappin, D., and Warren, G. (2000). A complex of mammalian ufd1 and npl4 links the AAA-ATPase, p97, to ubiquitin and nuclear transport pathways. Embo J *19*, 2181-2192.
275. Sagiv, Y., Legesse-Miller, A., Porat, A., and Elazar, Z. (2000). GATE-16, a membrane transport modulator, interacts with NSF and the Golgi v-SNARE GOS-28. Embo J *19*, 1494-1504.
276. Zerial, M., and McBride, H. (2001). Rab proteins as membrane organizers. Nat Rev Mol Cell Biol *2*, 107-117.
277. Christoforidis, S., and Zerial, M. (2000). Purification and identification of novel Rab effectors using affinity chromatography. Methods *20*, 403-410.
278. Anglesio, M.S., Evdokimova, V., Melnyk, N., Zhang, L., Fernandez, C.V., Grundy, P.E., Leach, S., Marra, M.A., Brooks-Wilson, A.R., Penninger, J., et al. (2004). Differential expression of a novel ankyrin containing E3 ubiquitin-protein ligase, Hace1, in sporadic Wilms' tumor versus normal kidney. Hum Mol Genet *13*, 2061-2074.
279. Zhang, L., Anglesio, M.S., O'Sullivan, M., Zhang, F., Yang, G., Sarao, R., Mai, P.N., Cronin, S., Hara, H., Melnyk, N., et al. (2007). The E3 ligase HACE1 is a critical chromosome 6q21 tumor suppressor involved in multiple cancers. Nat Med *13*, 1060-1069.
280. Satoh, A., Wang, Y., Malsam, J., Beard, M.B., and Warren, G. (2003). Golgin-84 is a rab1 binding partner involved in Golgi structure. Traffic *4*, 153-161.
281. de Wit, H., Lichtenstein, Y., Kelly, R.B., Geuze, H.J., Klumperman, J., and van der Sluijs, P. (2001). Rab4 regulates formation of synaptic-like microvesicles from early endosomes in PC12 cells. Mol Biol Cell *12*, 3703-3715.
282. de Graaf, P., Zwart, W.T., van Dijken, R.A., Deneka, M., Schulz, T.K., Geijsen, N., Coffer, P.J., Gadella, B.M., Verkleij, A.J., van der Sluijs, P., et al. (2004). Phosphatidylinositol 4-kinasebeta is critical for functional association of rab11 with the Golgi complex. Mol Biol Cell *15*, 2038-2047.
283. Chen, W., Feng, Y., Chen, D., and Wandinger-Ness, A. (1998). Rab11 is required for trans-golgi network-to-plasma membrane transport and a preferential target for GDP dissociation inhibitor. Mol Biol Cell *9*, 3241-3257.
284. White, J., Keller, P., and Stelzer, E.H. (2001). Spatial partitioning of secretory cargo from Golgi resident proteins in live cells. BMC Cell Biol *2*, 19.
285. Xu, Y., Martin, S., James, D.E., and Hong, W. (2002). GS15 forms a SNARE complex with syntaxin 5, GS28, and Ykt6 and is implicated in traffic in the early cisternae of the Golgi apparatus. Mol Biol Cell *13*, 3493-3507.

286. Tang, B.L., Low, S.H., Hauri, H.P., and Hong, W. (1995). Segregation of ERGIC53 and the mammalian KDEL receptor upon exit from the 15 degrees C compartment. Eur J Cell Biol *68*, 398-410.
287. Wilson, B.S., Nuoffer, C., Meinkoth, J.L., McCaffery, M., Feramisco, J.R., Balch, W.E., and Farquhar, M.G. (1994). A Rab1 mutant affecting guanine nucleotide exchange promotes disassembly of the Golgi apparatus. J Cell Biol *125*, 557-571.
288. Hui, N., Nakamura, N., Sonnichsen, B., Shima, D.T., Nilsson, T., and Warren, G. (1997). An isoform of the Golgi t-SNARE, syntaxin 5, with an endoplasmic reticulum retrieval signal. Mol Biol Cell *8*, 1777-1787.
289. Suga, K., Hattori, H., Saito, A., and Akagawa, K. (2005). RNA interference-mediated silencing of the syntaxin 5 gene induces Golgi fragmentation but capable of transporting vesicles. FEBS Lett *579*, 4226-4234.
290. Hibi, K., Sakata, M., Sakuraba, K., Shirahata, A., Goto, T., Mizukami, H., Saito, M., Ishibashi, K., Kigawa, G., Nemoto, H., et al. (2008). Aberrant methylation of the HACE1 gene is frequently detected in advanced colorectal cancer. Anticancer Res *28*, 1581-1584.
291. Diaz-Corrales, F.J., Asanuma, M., Miyazaki, I., and Ogawa, N. (2004). Rotenone induces disassembly of the Golgi apparatus in the rat dopaminergic neuroblastoma B65 cell line. Neurosci Lett *354*, 59-63.
292. Yoshimura, M., Ihara, Y., Matsuzawa, Y., and Taniguchi, N. (1996). Aberrant glycosylation of E-cadherin enhances cell-cell binding to suppress metastasis. J Biol Chem *271*, 13811-13815.
293. Roberts, J.D., Klein, J.L., Palmantier, R., Dhume, S.T., George, M.D., and Olden, K. (1998). The role of protein glycosylation inhibitors in the prevention of metastasis and therapy of cancer. Cancer Detect Prev *22*, 455-462.
294. Krishnan, V., Bane, S.M., Kawle, P.D., Naresh, K.N., and Kalraiya, R.D. (2005). Altered melanoma cell surface glycosylation mediates organ specific adhesion and metastasis via lectin receptors on the lung vascular endothelium. Clin Exp Metastasis *22*, 11-24.
295. Chen, X., Simon, E.S., Xiang, Y., Kachman, M., Andrews, P.C., and Wang, Y. (2010). Quantitative proteomics analysis of cell cycle regulated Golgi disassembly and reassembly. J Biol Chem *285*, 7197-7207.
296. Dong, X.P., Cheng, X., Mills, E., Delling, M., Wang, F., Kurz, T., and Xu, H. (2008). The type IV mucolipidosis-associated protein TRPML1 is an endolysosomal iron release channel. Nature *455*, 992-996.
297. Wang, Y., Taguchi, T., and Warren, G. (2005). Purification of Rat Liver Golgi Stacks. In Cell Biology: A Laboratory Handbook, 3rd Edition, J. Celis, ed. (San Diego: Elsevier Science (USA)), pp. 33-39.
298. Uchiyama, K., Jokitalo, E., Kano, F., Murata, M., Zhang, X., Canas, B., Newman, R., Rabouille, C., Pappin, D., Freemont, P., et al. (2002). VCIP135, a novel essential factor for p97/p47-mediated membrane fusion, is required for Golgi and ER assembly in vivo. J Cell Biol *159*, 855-866.